INVESTIGATING REGULATORY RELATIONSHIPS IN PLANT NITROGEN AND PHOSPHORUS NUTRITION



Fiona Jamieson

Corpus Christi College

University of Oxford

A thesis submitted for the degree of

Doctor of Philosophy

Michaelmas Term 2022

Acknowledgements

There are many people who contributed to my time at Oxford. I thank my supervisor Prof. Nick Harberd for his expertise, guidance and advice offered throughout the course of my research, and I am grateful to the BBSRC for providing the funding for this work.

I would like to thank the extended Harberd lab, in particular Eric and Luke, who were always happy to offer help and advice, and Ding, who provided genetic material for my work. To Julie, Lizzie and Rob, thanks for all your hard work to keep everything running behind the scenes, and to the extended members of the Harberd cake club family, thank you for creating such a friendly and well-fed environment.

My time at Oxford was made all the better by life outside the lab and the friends I made along the way. Chris and Jill – thank you for teaching me so much more than how to row, and to my teammates at OUWLRC, it was a privilege and a pleasure to train and race alongside you.

Finally, I thank my family for their love and support, and my partner Matt, who has provided encouragement, reassurance, and many a hug and cup of tea throughout the highs and lows of this degree.

Abstract

Modern crop varieties rely heavily on artificial fertiliser application, which is both unsustainable and detrimental to the environment. Understanding regulatory relationships underlying plant nutrition is therefore important to improve the nutrient use efficiency of modern crop varieties. This thesis identifies new regulators of Arabidopsis phosphorus and nitrogen nutrition using a combination of genetic and physiological approaches, achieved by investigating how nutrient metabolism is perturbed in Arabidopsis lines containing mutations in genes encoding proteins of interest.

This study identifies the Arabidopsis *constitutive triple response 1* (*ctr1*) mutant, which displays constitutive ethylene signalling, as having compromised nitrogen metabolism. *ctr1-1* is shown to have increased resistance to chlorate, a chemical analogue of nitrate, and utilises enzymatic assays to determine this is likely due to reduced nitrate reductase activity. A genetic screen identifies several mutagenized *ctr1-1* lines which uncouple the dwarfed and chlorate resistant phenotypes of the *ctr1-1* mutant, providing material that may uncover new regulators of ethylene-mediated nitrogen assimilation. This thesis also explores the interaction between the regulation of nitrate and phosphate metabolism, identifying that reduced phosphate availability alters Arabidopsis nitrogen metabolism, and that this is likely due to known genetic regulators of phosphate metabolism rather than shoot phosphate levels themselves. In particular, this study implicates known components of phosphate signalling, specifically PHOSPHATE STARVATION RESPONSE 1 (PHR1) and PHOSPHATE 2 (PHO2), as having additional roles in regulating nitrate assimilation. Finally, this thesis provides further evidence that the transcription factor HY5 modulates some, but not all, aspects of Arabidopsis phosphate metabolism. The *hy5* mutant is found to be partially deficient in phosphate uptake, as well as in a subset of phosphate-starvation responses. By utilising differing light regimes HY5 is identified as regulating Arabidopsis phosphate assimilation in response to shoot illumination.

Together, these findings further our understanding of regulatory relationships governing Arabidopsis nitrate and phosphate metabolism. Ultimately this research hopes to offer potential new targets to alter plant nutrient use efficiency in modern crops, reducing dependence on fertiliser application and furthering efforts to improve food security.

List of Abbreviations

Abbreviation	Definition
ABA	Abscisic acid
ABP	Active phyB binding
ACC	1-aminocyclopropane-1-carboxylic acid
ACCC	Australian Competition and Consumer Commission
ACE	ACGT-containing
ACO	ACC oxidase
ACS	ACC synthase
ANOVA	Analysis of variance
APA	Additional phyA-binding
APase	Acid phosphatase
BCIP	5-Bromo-4-chloro-3-indolyl phosphate
CBP	CAP BINDING PROTEIN
CC	Coiled-coil
CEND	C-terminus end of EIN2
ChIP	Chromatin immunoprecipitation
CLC	Chloride channel
CP3	CUPULIFORMIS 3
CPK	Calcium-dependent protein kinase
COP1	CONSITUTIVELY PHOTOMORPHOGENIC 1
CTR1	CONSTITUTIVE TRIPLE RESPONSE 1
DNA	Deoxyribonucleic acid
DTT	Dithiothreitol
DWF1	DWARF 1
EDTA	Ethylenediaminetetraacetic acid
EIL1	EIN3-LIKE 1
EIN	ETHYLENE INSENSITIVE
ER	Endoplasmic reticulum
ERF	ETHYLENE RESPONSE FACTOR
ETP	EIN2 TARGETING PROTEIN
ETR	ETHYLENE RESPONSE
FAO	Food and Agriculture Organization of the United Nations
FHL	FHY1-LIKE

FHY1	FAR-RED ELONGATED HYPOCOTYL 1
GFP	Green fluorescent protein
GOGAT	Glutamate synthase
GS	Glutamine synthetase
GUS	β-glucuronidase
HRS1	HYPERSENSITIVITY TO LOW PI-ELICITED PRIMARY ROOT SHORTENING 1
HY5	LONG HYPOCOTYL 5
HYH	HY5 HOMOLOGUE
MIN1	MINIATURE 1
MS	Murashige and Skoog medium
N	Nitrogen
NADH	Nicotinamide adenine dinucleotide
NADP	Nicotinamide adenine dinucleotide phosphate
NASC	Nottingham Arabidopsis Stock Centre
NIA	NITRATE REDUCTASE
NIGT1	NITRATE-INDUCIBLE GARP-TYPE TRANSCRIPTIONAL REPRESSOR 1
NiR	Nitrite Reductase
NLA	NITROGEN LIMITATION ADAPTATION
NLP	Nodulin Inception-like protein
NR	Nitrate Reductase
NRT	Nitrate transporter
P	Phosphorus
PCR	Polymerase chain reaction
PHF1	PHOSPHATE TRANSPORTER TRAFFIC FACILITATOR 1
PHO2	PHOSPHATE 2
PHR1	PHOSPHATE STARVATION RESPONSE 1
PHY	PHYTOCHROME
Pi	Inorganic phosphate
PIF	PHYTOCHROME INTERACTING FACTOR
Po	Organic phosphate
PSI	Phosphate-starvation-induced
PTR	Peptide transporter
PVA	Poly-vinyl alcohol
RNA	Ribonucleic acid

RSA	Root system architecture
RT-PCR	Reverse transcription polymerase chain reaction
S	Sulphur
SAIL	Syngenta Arabidopsis Insertion Library
SIS4	SUGAR INSENSTIIVE 4
SLAC1	SLOW ANION CHANNEL-ASSOCIATED 1
SLAH	SLOW ANION ASSOCIATED-ASSOCIATED 1 HOMOLOGUE
SNRK	SNF1 resembling kinase family
SPA1	SUPPRESSOR OF PHYA
SUC2	SUCROSE TRANSPORTER 2
SUMO	Small ubiquitin-related modifier
TPS1	TREHALOSE-6-PHOSPHATE SYNTHASE 1
Tukey-HSD	Tukey's honestly significant difference
UVR8	UV RESISTANCE LOCUS 8
WT	Wild type

Table of Contents

Acknowledgements 1
Abstract 2
List of Abbreviations 3
Table of Contents 6
List of Figures 11
List of Tables 14
Chapter 1: Introduction and literature review 15
1.1 The importance of understanding plant nutrient assimilation 15
1.1.1 Modern crop varieties are heavily dependent on fertiliser use 15
1.1.2 Phosphate fertiliser: production and concerns 15
1.1.3 Nitrogenous fertiliser: production and concerns 16
1.1.4 Consequences of excessive fertiliser application 17
1.1.5 Strategies to improve plant nutrient assimilation 18
1.2 Arabidopsis phosphate assimilation 19
1.2.1 Arabidopsis phosphate transporters 20
1.2.2 Transcriptional regulation of PHT1 phosphate transporters 22
1.2.3 Post-transcriptional regulation of PHT1 phosphate transporters 22
1.2.4 Plant Pi storage 23
1.2.5 Low phosphate signalling pathways 23
1.3 Arabidopsis nitrate assimilation 25
1.3.1 Arabidopsis root nitrate transporters 26
1.3.2 Shoot to root nitrate transport 27
1.3.3 Assimilation of nitrate into N-containing components 28
1.3.4 Nitrate reductase 28
1.3.5 Transcriptional control of genes encoding nitrate reductase 29
1.3.6 Post-translational regulation of nitrate reductase 30
1.3.7 Nitrogen signalling pathways 33
1.3.8 Chlorate is a structural analogue of nitrate 34
1.4 Regulation of nutrient assimilation 35
1.4.1 Links between phosphate and nitrate metabolism 35
1.4.2 Hormonal regulation of nutrient metabolism 38
1.5 The ethylene signalling pathway 41
1.5.1 Ethylene receptors 42
1.5.2 CTR1 43
1.5.3 EIN2 43

1.5.4 EIN3, EIL1 and downstream signalling targets 44
1.5.5 Negative feedback in the ethylene signalling pathway 45
1.5.6 Alternative ethylene signalling pathways: a cytoplasmic role for EIN2 45
1.5.7 Ethylene and Nitrogen metabolism 46
1.6 The role of Arabidopsis HY5 in nutrient acquisition 48
1.6.1 HY5 as a master regulator 48
1.6.2 HY5 and N assimilation 51
1.6.3 HY5 and S assimilation 53
1.6.4 HY5 and Pi assimilation 54
1.7 Objectives of Thesis 54
1.7.1 Objective 1: Understanding the role of CTR1 in modulating nitrogen metabolism 55
1.7.2 Objective 2: Exploring nitrogen metabolism in mutants lacking phosphate signalling components 55
1.7.3 Objective 3: Understanding the role of HY5 as a regulator of phosphate metabolism 56
Chapter 2: Materials and methods 57
2.1. Plant material and growth conditions 57
2.1.1 Compost 57
2.1.2 Agarose 57
2.1.3 Magenta Boxes 58
2.1.4 Plant material 58
2.2. Plant phenotypic analysis 59
2.2.1 Chlorate treatment on compost 59
2.2.2 Chlorate treatment on agarose 59
2.2.3 Quantifying the colour change of plant rosettes following chlorate treatment 60
2.2.4 Measurement of plant height 60
2.2.5 Root system architecture measurements 61
2.2.6 Quantification of plant inorganic phosphate content 61
2.2.7 Quantification of plant nitrate content 62
2.2.8 Quantification of plant chlorophyll content 62
2.2.9 Quantification of plant anthocyanin content 63
2.3. Protein extraction and measurements 63
2.3.1 Protein Extraction 63
2.3.2 Protein Quantification 64
2.3.3 Nitrate Reductase Activity Assay 64
2.3.4 Detection and quantification of root acid phosphatase activity 65
2.4. DNA isolation and analysis 66
2.4.1 DNA extraction 66

2.4.2 Confirmation of mutations 66
2.5. RNA isolation and cDNA synthesis 67
2.5.1 RNA extraction 67
2.5.2 DNAse treatment of RNA samples 68
2.5.3 cDNA synthesis 68
2.6. Semi-quantitative RT-PCR analysis of gene expression 68
2.7. In silico searches for DNA binding motifs 69
2.8. Mutant Screen 70
2.8.1 Mutagenesis 70
2.8.2 Screening lines of interest 70
2.9. Image capture 71
2.9.1 Photographs of plants on compost 71
2.9.2 Photographs of plants on plates 72
2.10. Statistical Analyses 72
2.11. Chemicals and Primers 72
2.12. Centrifugation 72
Chapter 3: Ethylene signalling modulates *Arabidopsis thaliana* nitrate metabolism 74
3.1 Introduction 74
3.2 Results and discussion 76
3.2.1 *ctr1-1* has increased resistance to chlorate treatment 76
3.2.2 *ctr1-1* has reduced Nitrate Reductase activity 78
3.2.3 *ctr1-1* has reduced NIA gene expression 79
3.2.4 *ctr1-1* does not have an altered shoot nitrate content 80
3.2.5 Despite being dwarfed, growth of *ctr1-1* is still altered by nitrogen availability 81
3.2.6 Altered nitrogen metabolism in mutants lacking components of ethylene biosynthesis and ethylene signalling 86
3.2.7 The *eto2* & *eto3* mutants show a slight increase in resistance to chlorate treatment, whilst *eto1, etr1* and *eto1 etr1* appear as susceptible as WT 87
3.2.8 Chlorate treatment of *ein2*, *ein3* and *ein3 Δ eil1* loss-of-function mutants 90
3.2.9 NR activity assay of mutants lacking components of ethylene signalling 92
3.2.10 Mutagenized *ctr1-1* lines with altered chlorate resistance were identified using a mutant screen 94
3.2.11 Nitrate metabolism in tall mutants displaying chlorate resistance 98
3.2.12 Growth characteristics of tall mutants displaying chlorate resistance 99
3.2.13 Mutagenized *ctr1-1* plants containing known mutations in the EIN2 locus differ in their chlorate sensitivity 101
3.2.14 The 6 mutagenized *ctr1-1* lines containing known mutations in the EIN2 locus have all lost the dwarfed phenotype conferred by the *ctr1-1* mutation 106

3.2.15 Mutagenized *ctr1-1* plants containing known mutations in the EIN2 locus differ in their nitrate content 107

3.2.16 The majority of mutagenized *ctr1-1* plants containing known mutations and with maintained chlorate resistance do not display a significant reduction in nitrate reductase activity 108

Chapter 4: The role of phosphate in regulating Arabidopsis nitrogen metabolism 112

4.1 Introduction 112

4.2 Results and discussion 113

4.2.1 Nitrate reductase activity is reduced in low phosphate conditions 113

4.2.2 Low phosphate conditions reduce Arabidopsis shoot nitrate content 114

4.2.3 Mutants impaired in the regulation of phosphate metabolism have altered nitrate reductase activity 116

4.2.4 Mutants impaired in the regulation of phosphate metabolism have altered shoot nitrate content 118

4.2.5 *phr1* shoot nitrate content is altered when phosphate availability is reduced 120

4.2.6 Potential PHR1 and NIGT1 binding sites are present in the promoters of genes encoding proteins involved in nitrate metabolism 122

4.2.7 The genotypes *phr1*, *pho2* and *pht1;1* Δ *pht1;4* do not have altered responses to chlorate treatment 124

4.2.8 Genotypes lacking regulatory components of phosphate metabolism maintain altered shoot and root nitrate content when nitrate availability is reduced 125

4.2.9 Genotypes lacking regulatory components of phosphate metabolism have no significant alteration in growth under reduced nitrate availability 127

4.2.10 Chlorate treatment causes toxicity on agarose plates 128

4.2.11 *nrt1.1* and *ctr1-1* have altered chlorate susceptibility when treated on agarose plates rather than on compost 131

4.2.12 Chlorate susceptibility of both WT and *ctr1-1* treated on agarose remains susceptible to the effects of light and sucrose provision 133

4.2.13 Transpiration may alter chlorate sensitivity 135

4.2.14 Nitrate reductase activity is not affected by growing plants in enclosed systems 136

Chapter 5: *hy5* has altered phosphate metabolism 139

5.1 Introduction 139

5.2 Results and discussion 140

5.2.1 Putative HY5 binding sites are present within the promoters of genes encoding PHT1 phosphate transporters 140

5.2.2 *hy5* has a reduced shoot phosphate content when grown on compost 143

5.2.3 *hy5* has reduced root system architecture changes in response to altered Pi availability 144

5.2.4 The *hy5* mutant has altered chlorophyll and anthocyanin content in high and low phosphate conditions 148

5.2.5 *hy5* plants have a reduced shoot phosphate content in both phosphate-replete and phosphate-deficient conditions 150

5.2.6 *hy5* seedlings have no significant difference in growth on different phosphate availabilities 153

5.2.7 *hy5* has no detectable difference in low phosphate induced Root Acid Phosphatase Activity 154

5.2.8 The *hy5* mutant may have altered expression of genes PHT transporters 156

5.2.9 *hy5* seedlings have a reduced seedling biomass on high sucrose concentrations of sucrose, regardless of phosphate concentration 157

5.2.10 The reduced phosphate content of *hy5* shoots is not altered by increasing concentrations of sucrose 160

5.2.11 *hy5* does not have altered root phosphate content on any concentration of sucrose 161

5.2.12 Sucrose does not impact *hy5* root acid phosphatase secretion 162

5.2.13 Altered root system architecture in response to phosphate deprivation in the *hy5* mutant is sustained under high sucrose concentrations 164

5.2.14 Anthocyanin content in *hy5* seedlings under phosphate deprivation in the presence of sucrose 166

5.2.15 Shoot illumination is necessary for HY5-dependent accumulation of shoot phosphate 168

5.2.16 *hy5* does not have altered root phosphate content, regardless of shoot and root illumination status 170

Chapter 6: Discussion 172

6.1 Understanding the role of CTR1 in regulating nitrogen metabolism 172

6.1.1 The *ctr1-1* mutation confers differences in nitrogen metabolism 172

6.1.2 Lack of EIN2 function correlates with suppression of chlorate resistance and NR activity reduction conferred by *ctr1* 176

6.2 Exploring phosphate as a regulator of nitrogen metabolism 179

6.2.1 Phosphate availability alters nitrogen metabolism in Arabidopsis 179

6.2.2 Mutations in regulatory components of phosphate signalling pathways confer differences in nitrogen metabolism 180

6.2.3 Chlorate resistance of genotypes can vary according to the growth media used 183

6.3 The role of HY5 in regulating phosphate metabolism 185

6.3.1 *hy5* has altered regulation of phosphate metabolism 186

6.3.2 Shoot illumination is required for HY5-mediated changes in shoot phosphate accumulation 188

6.3.3 HY5 does not affect sucrose-mediated phosphate metabolism 190

6.4 Conclusions and Implications 191

Appendix 1: Jamieson *et al.*, 2022 193

References 200

List of Figures

Figure 1: Simplified schematic of the whole-plant low phosphate signalling pathway. 24

Figure 2: Nitrate uptake and assimilation in plants. 28

Figure 3: Model of proposed NIGT1-centred transcriptional cascade that integrates both nitrate signalling and phosphate starvation signalling pathways. 38

Figure 4: Overview of the ethylene signalling pathway. 42

Figure 5: HY5 activity can be modulated by a range of light signalling pathways. 51

Figure 6: Schematic of mutant screen being used to search for new regulators of ethylene-mediated N metabolism. 71

Figure 7: ctr1 plants are strongly resistant to chlorate treatment compared to WT. 78

Figure 8: The ctr1 mutant has significantly reduced nitrate reductase activity compared to WT 79

Figure 9: ctr1 has significantly reduced expression of NIA2. 80

Figure 10: Nitrate content of WT, nrt1.1 and ctr1 plants. 81

Figure 11: WT and ctr1 plants grown on a variety of different nitrogen sources. 82

Figure 12: Effects of high and low nitrogen provision on primary root length of ctr1 plants. 84

Figure 13: Effects of high and low N provision on shoot: root ratio of WT and ctr1 plants 85

Figure 14: The eto2 and eto3 ethylene over-producing mutants have increased resistance to chlorate treatment; eto1, etr1 and eto1 etr1 are as sensitive to chlorate treatment as WT. 89

Figure 15: Height of various mutants lacking components of ethylene signalling 90

Figure 16 : The ein2, ein3 and ein3 Δ eil1 mutants are sensitive to chlorate treatment 92

Figure 17: Nitrate reductase activity of Arabidopsis lines containing mutations in the ethylene signalling pathway. 93

Figure 18: Lines of interest identified from ctr1 mutant screen displaying both chlorate-resistant and tall heritable phenotypes 97

Figure 19: Nitrate reductase activity of mutagenized ctr1 lines. 99

Figure 20: Height of selected mutagenized ctr1 lines characterised as both tall and resistant to chlorate treatment. 100

Figure 21: Position of point mutations in the EIN2 locus of EMS-treated ctr1 background plants with a tall phenotype. 102

Figure 22: Mutagenized ctr1 lines containing mutations in the EIN2 locus have altered responses to chlorate treatment. 106

Figure 23: Heights of mutagenized ctr1 lines containing mutations in the EIN2 locus. 106

Figure 24: Nitrate content of mutagenized ctr1 plants containing known mutations in the EIN2 locus. 108

Figure 25: Nitrate reductase activity of mutagenized ctr1 lines containing known mutations in the EIN2 locus. 109

Figure 26: Low phosphate reduces Arabidopsis shoot and root nitrate reductase activity. 114

Figure 27: Arabidopsis shoot nitrate content of WT plants grown on different phosphate concentrations 115

Figure 28: Nitrate reductase activity of mutants lacking regulatory components of phosphate metabolism. 117

Figure 29: Shoot nitrate content of soil-grown plants lacking regulatory components of phosphate metabolism. 119

Figure 30: Shoot nitrate and phosphate content of genotypes lacking regulatory components of phosphate metabolism. 120

Figure 31: Shoot nitrate content of plants lacking regulatory components of phosphate metabolism, grown on three different phosphate concentrations. 121

Figure 32: WT, phr1, pho2 and pht1;1 Δ pht1;4 lines all appear susceptible to chlorate treatment. 125

Figure 33: Average shoot nitrate of seedlings grown on replete and reduced nitrate concentrations. 126

Figure 34: Plant biomass and root: shoot ratio of phosphate mutants on high and low nitrate availability. 128

Figure 35: WT Arabidopsis grown on agarose plates and treated with 3 mL of chlorate solution. 130

Figure 36: Percentage of green tissue remaining in WT Arabidopsis shoots following treatment with different concentration of chlorate solution. 130

Figure 37: WT, nrt1.1 and ctr1 are all susceptible to chlorate treatment when treated on agarose. 131

Figure 38: Proportion of shoot tissue remaining green in WT, nrt1.1 and ctr1 genotypes following treatment with chlorate solution. 132

Figure 39: Chlorate resistance is increased when plants are grown in the absence of light. 134

Figure 40: Chlorate resistance is decreased by the presence of sucrose in the media of dark-grown plants 135

Figure 41: WT, nrt1.1 and ctr1 plants on soil treated with water or 2.5 mM chlorate solution in enclosed Magenta boxes. 136

Figure 42: Nitrate reductase activity of WT Arabidopsis grown in enclosed and open environments. 137

Figure 43: Pi content of soil-grown hy5, pht1;1 Δ pht1;4 and phr1 plants. 144

Figure 44: Root system architecture of WT and hy5 on high and low phosphate media. 146

Figure 45: hy5 seedlings have reduced shoot chlorophyll content and shoot anthocyanin content compared to WT in low phosphate conditions. 149

Figure 46: hy5 mutants have a reduced shoot phosphate content in both phosphate-replete and phosphate-deficient conditions. 152

Figure 47: hy5 seedlings have no significant difference in biomass compared to WT plants. 154

Figure 48: Analysis of APase activity in Arabidopsis seedlings of WT and hy5 mutants grown on 1000 µM, 100 µM and 10 µM Pi concentration. 156

Figure 49: Expression levels of PHT1;1, PHT1;4 and NRT2;1 in WT and hy5. 157

Figure 50: Seedling biomass of WT and hy5 grown on high and low phosphate in different sucrose conditions. 159

Figure 51: Shoot phosphate content of WT and hy5 grown on high and low phosphate in different sucrose conditions. 161

Figure 52: HY5 does not influence root phosphate content, regardless of sucrose concentration. 162

Figure 53: Detection of WT and hy5 root APase activity under different sucrose concentrations. 163

Figure 54: Root system architecture of WT and hy5 in 0% and 5% sucrose. 165

Figure 55: Sucrose does not affect the reduced anthocyanin content of hy5 plants in phosphate-deficient conditions. 167

Figure 56: Schematic demonstrating different shoot / root illumination regimes. 169

Figure 57: The reduced shoot phosphate content of hy5 is dependent on shoot illumination. 170

Figure 58: hy5 root phosphate content is unaffected by shoot illumination. 171

List of Tables

Table 1: *Arabidopsis* lines used in this study. 59

Table 2: Primers used for identification and verification of mutations 67

Table 3: Primer sequences for RT-PCR analysis of gene expression 69

Table 4: Categories of mutants of interest identified during mutant screen 96

Table 5: Position and type of point mutations in the EIN2 locus of selected mutagenised *ctr1-1* plants tested for altered N metabolism. 102

Table 6: List of key genes involved in the nitrate assimilation pathway and putative NIGT1 binding site presence within promoter regions. 124

Table 7: Presence of potential HY5 binding sites within the promoters of Arabidopsis *PHT1* phosphate transporters. 142

Chapter 1: Introduction and literature review

1.1 The importance of understanding plant nutrient assimilation

The 1996 World Food Summit defined food security as "when all people, at all times, have physical and economic access to sufficient, safe and nutritious food that meets dietary needs and food preferences for an active and healthy life" (FAO, 1996). With an increasing global population, and changing climate due to global warming, there is an urgent need to improve the efficiency of crop varieties if global food security is to be achieved (Godfray *et al.*, 2010). Improving our understanding of nutrient use efficiency, and how this relates to growth, is one area in which improvements could lead to increased crop yield (Veneklaas *et al.*, 2012). Two macronutrients essential for plant growth but often present in limiting quantities are nitrate and phosphate.

1.1.1 Modern crop varieties are heavily dependent on fertiliser use

Crop varieties require large application of fertiliser containing inorganic phosphate (Pi) and nitrogen (N) in order for yields to remain high; 2018 global fertiliser use was predicted to exceed 200 million tonnes (FAO, 2015). However, producing these macronutrients is energy intensive and costly, and excessive fertiliser application is environmentally damaging (Cordell *et al.*, 2009). Improving the efficiency by which plants use these nutrients is therefore important not just to alleviate environmental problems associated with widespread fertiliser use and high energy demands, but also has economic implications.

1.1.2 Phosphate fertiliser: production and concerns

Most commercial phosphate fertilisers are mined from phosphate rock using sulphuric acid. Phosphate rock is a geographically restricted, finite, and non-renewable resource.

Estimates of global reserves lifetime vary, with studies suggesting supplies may have only 50-200 years left (Baker *et al.*, 2015), and costs incurred to mine and produce rock phosphate fertiliser are expensive. Sustainable management of phosphate rock supplies are hindered by anthropogenic influences: an ever-growing demand, geopolitical restraints, excessive mining and increasing global prices. Over 90% of global rock phosphate is limited to a small number of countries: almost 75% of global reserves are restricted to Morocco alone (Cooper *et al.*, 2011). It has been predicted that by 2050 Morocco will account for 40% of global rock phosphate, which may increase to up to 80% by 2100 (Cooper *et al.*, 2011). Countries lacking strategic relationships with those that control the major supplies of rock phosphate may therefore suffer from geopolitical restraints as supply becomes more limited.

The importance of phosphate rock on global food security was demonstrated in 2007 - 2008, when increasing mineral fertilizer prices were amongst the causes of the global food price shock (FAO, 2008; FAO, 2011). A rapid rise in global demand for mined rock phosphate in 2007 caused prices to increase by 400% within a year, from US $50/tonne to US $200/tonne (Minemakers Limited, 2008). Similar increases were seen for global diammonium phosphate (DAP) prices, which went from US $265/tonne to US $1040/tonne within 14 months (ACCC, 2008). These sudden price rises in phosphate and other fertilizer sources led to riots and demonstrations across many developing countries (The Guardian, 2008), demonstrating the extent to which global agricultural production relies on this mineral.

1.1.3 Nitrogenous fertiliser: production and concerns

Although N constitutes over 78% of the Earth's atmosphere, the availability of N is one of the main limiting factors of terrestrial ecosystem productivity. The Haber-Bosch process enabled the industrial production of reactive N in the form of ammonia, synthesised by the reaction of atmospheric dinitrogen with hydrogen at high pressures and temperatures in the presence of iron (Erisman *et al.*, 2008). Oxidation of ammonia produces nitric acid, which is reacted with ammonia to produce ammonium nitrate, used worldwide as a cheap and effective nitrogenous fertiliser. The development of the Haber-Bosch process was hugely important in boosting modern agricultural yields (Erisman *et al.*, 2008). The Haber-Bosch process is energy intensive; in 2002 consuming 1% of global energy supplies (Smith *et al.*, 2002). The synthesis of fertilisers is also a significant contributor to greenhouse gas production; the largest single source of greenhouse gas emissions in arable agriculture is nitrogenous fertilisers (White and Brown, 2010).

1.1.4 Consequences of excessive fertiliser application

The environmental consequences of excessive fertiliser discharge are well documented. Excess nitrate and phosphate discharge has contributed to algal blooms and eutrophication of water bodies across the globe, including Lake Erie, USA (Michalak *et al.*, 2013; Bridgeman *et al.*, 2013), the Australian Great Barrier Reef Lagoon (Brodie *et al.*, 2011) and Lake Taihu, China (Xu *et al.*, 2010). A 37-year investigation into the effects of fertilising Lake-227 at the Experimental Lakes Area in Ontario, Canada demonstrated that P is an important contributor to freshwater eutrophication (Schindler *et al.*, 2008). Importantly, this study also showed that algal blooms are worsened if N inputs are decreased without simultaneously decreasing P input, demonstrating the need to devise strategies controlling both nutrients if the detrimental effects of eutrophication are to be reversed. These

environmental consequences have economic implications: it has been calculated that the cost of N pollution within the European Union ranges from €70 billion to €320 billion per annum, over twice the value N fertilisers add to EU farm income (Sutton *et al.*, 2011).

1.1.5 Strategies to improve plant nutrient assimilation

Fertiliser application is widespread as an insufficient supply of minerals in soil often limits crop production. However, there are environmental and economic consequences to this practice, and finite resources necessitate more efficient fertilisation strategies to be developed. This can be achieved agronomically, for example improving fertiliser-management practices, and/or by using genetic approaches to cultivate crop varieties that acquire or use minerals more efficiently, through either modern biotechnological approaches or conventional crop breeding strategies (White and Brown, 2010). By improving our understanding of how plants acquire and use mineral elements, ways in which we may be able to make this process more effective can be identified, reducing modern agriculture's reliance on intensive fertiliser application.

Understanding how plants acquire and subsequently metabolise two of the key components of agricultural fertiliser, N and P, is therefore important if we are to use genetic approaches to cultivate more efficient crop varieties. Understanding the regulatory networks and processes governing plant metabolism of these two nutrients, and how these both affect and are impacted by plant growth and carbon fixation, may identify new ways in which plant nutrient use efficiency may be altered, and the consequences of doing so. This thesis explores regulatory networks in plant phosphate and nitrate metabolism, and the interaction between them, in greater detail, focusing on the model organism *Arabidopsis thaliana* (Arabidopsis).

1.2 Arabidopsis phosphate assimilation

Phosphorus (P) is an essential plant nutrient. Within soil, P exists in various chemical forms, including organic (Po) and inorganic (Pi) sources; only Pi can be assimilated by plants (Abel, Ticconi and Delatorre, 2002).

Though P can be abundant in soil, it has low bioavailability – Po has to be mineralised before it can be absorbed by plants, whilst Pi is highly insoluble in most soils, owing to its high reactivity with cations such as aluminium and iron (acidic soils), and calcium and magnesium (calcareous soils), to form phosphate salts with low solubility (reviewed by Lopez-Arredondo *et al.*, 2014). The problem is particularly acute in acidic soils, with high P fixation by aluminium and iron (Penn and Camberato, 2019). The availability of P is therefore influenced by pH, soil organic matter, and exchangeable and soluble cations including aluminium, iron, and calcium (Smithson, 1999). The concentration of Pi in soil solution is often low (< 10 µM), and in addition Pi has low mobility, with a slow rate of diffusion (10^{-12} to 10^{-15} $m^2 s^{-1}$) (Schachtman, Reid and Ayling, 1998). Consequently, levels of Pi are commonly suboptimal for crop productivity, with approximately 70% of global cultivated land, including both acidic and calcareous soils, suffering from Pi deficiency (Lopez-Arredondo *et al.*, 2014).

In certain species, Pi acquisition can be enhanced by plant growth-promoting rhizobacteria, and relationships with arbuscular mycorrhizal fungi. Other microbial species, however, can have the opposite effect, through converting Pi into organic forms not readily available for plant uptake, or through competition with roots for available Pi (Lopez-Arredondo *et al.*, 2014).

With even a well-designed Pi fertilisation regime, plant roots have been calculated to acquire no more than 30% of applied Pi, with the rest lost due to rapid fixation within soil and microbial activity (Lopez-Arredondo *et al.*, 2014). Despite phosphate being relatively immobile, the remainder is prone to being washed from topsoil into water supplies via attachment to soil particles during erosion, where it can cause large environmental damage (Cordell *et al.*, 2009; Baker *et al.*, 2015).

Phosphate is taken up from the soil by Pi transporters. In cultivated soils Pi concentration tends to be low, with the median Pi concentration of most soil solutions < 10 µM (Abel, Ticconi and Delatorre, 2002), compared to plant internal concentrations in the millimolar range – the Pi concentration of plant tissues has been measured at 5 – 20 mM (Raghothama, 1999). Use of P^{33} and P^{32} Pi isotopes has identified both high- and low-affinity uptake systems (Nussaume *et al.*, 2011). Whilst a low-affinity transport system has been demonstrated to function at high Pi concentration, the low Pi availability in soil means it is generally thought that the high-affinity transport system operating at low external Pi concentrations is responsible for the majority of plant phosphate uptake (Chen *et al.*, 2008).

1.2.1 Arabidopsis phosphate transporters

In Arabidopsis there are four phosphate transporter families: PHT1, PHT2, PHT3 and PHT4 (Mudge *et al.*, 2002). Pi uptake from the soil is mediated by members of the PHT1 family. PHT1 transporters are H^+-Pi co-transporters, with 9 members identified in Arabidopsis (Mudge *et al.*, 2002), highly redundant in expression pattern and function. PHT1 transporter sequence analysis shows a conserved amino acid sequence from fungi to plants, with over 76% of the protein sequence conserved across various plant species, and

strong homology across plants and yeast (reviewed by Nussaume *et al.*, 2011). It has been suggested that the proteins may function as multimers, as western blots have shown higher molecular weight bands compatible with the presence of multimeric proteins, for example as also seen for the NO_3^- transporter NRT2.1 (Nussaume *et al.*, 2011). The suggestion of multimeric protein complexes is supported by the semi-dominant *pht1;1-3* phenotype, indicative of inactive subunits in multimeric pore complexes impairing the overall structure (Catarecha *et al.*, 2007).

Eight of the nine Arabidopsis PHT1 members are expressed in the roots, with PHT1;1 and PHT1;4 believed to be the most important transporters in coordinating Pi uptake from soil. The *pht1;1 pht1;4* double mutant displays a 50% reduction in Pi uptake in low phosphate conditions, and up to 75% reduced Pi uptake in phosphate – replete conditions (Shin *et al.*, 2004). In species which form mycorrhizal symbioses PHT1 transporters maintain an important role in Pi acquisition; genes encoding PHT1 transporters have been reported to be induced in specific response to mycorrhization (Loth-Pereda *et al.*, 2011). For example, the PHT1 transporter MtPT4 in *Medicago truncatula* is symbiosis-specific: detected only in cells containing arbuscules (hyphal structures developed by the mycorrhizal fungus within the cortex of the root system, that are believed to be the site of nutrient exchange between the plant and fungus), and only located on the plasma membrane surrounding arbuscule branches (Pumplin and Harrison, 2009).

Genes encoding PHT1 transporters are also expressed in other organs indicating a wide-ranging role in transporting phosphate through the plant, as well as soil-phosphate assimilation. For example, *AtPHT1;6* is highly expressed in pollen, suggesting a role for

PHT1 transporters in flower development, and *AtPHT1;5* has been shown to have a role in senescing leaves, promoting source-to-sink Pi mobilisation (Nussaume *et al.*, 2011).

1.2.2 Transcriptional regulation of PHT1 phosphate transporters

Assorted transcriptomic experiments and reporter gene studies have demonstrated the role of internal cell Pi concentration in regulating *PHT1* expression (reviewed by Nussaume *et al.*, 2011). Plants adjust *PHT1* expression in response to a wide range of Pi concentrations beyond the typical range of soil Pi, and basal levels of gene expression are typically observed when external Pi is supplied at a concentration greater than that of 250 µM (Nussaume *et al.*, 2011).

1.2.3 Post-transcriptional regulation of PHT1 phosphate transporters

Multiple steps of post-translational regulation exist to control PHT1 targeting and accumulation at the plasma membrane. The loss of function mutant *phosphate transporter traffic facilitator1* (*phf1*) has a severe decrease in Pi influx (González *et al.*, 2005), with up to a 80% reduction of Pi uptake occurring in low Pi conditions compared to WT. PHF1 resides in the endoplasmic reticulum (ER) and the *phf1* mutant displays abnormal accumulation of PHT1;1 PHT1;2 and PHT1;4 in the ER, suggesting PHF1 is involved in co-ordinating intracellular trafficking of a variety of PHT1 family members (González *et al.*, 2005; Bayle *et al.*, 2011). Protein modification via phosphorylation is also important; mutagenesis of PHT1;1 at Ser514 mimics phosphorylation and results in accumulation of PHT1;1 at the ER, a mechanism likely conserved among different members of the PHT1 family transporters (Bayle *et al.*, 2011). The same study identified a mechanism by which PHT1 proteins present in the plasma membrane were degraded in response to the

presence of phosphate, which occurs via endocytosis and subsequent degradation in the vacuole.

1.2.4 Plant Pi storage

The vacuole is the major storage compartment for excess Pi: under phosphate-replete conditions Pi is stored in the vacuole (to prevent toxicity in the cytoplasm) (Mimura *et al.*, 1990), whilst during times of Pi starvation, Pi is exported from the vacuole to the cytosol (Shane *et al.*, 2004).

1.2.5 Low phosphate signalling pathways

Phosphate depletion induces a range of developmental responses in plants. For example, changes in root system architecture include inhibition of primary root growth, increased numbers of lateral roots and an increase in root hair growth, increasing the surface area with which plants can transport Pi from the soil (Lopez-Bucio *et al.*, 2002). There are also biochemical and metabolic changes: a common feature of phosphate-starved plants is dark-green or purple leaves due to the accumulation of anthocyanins as a result of phosphate-starvation-induced (*PSI*) expression of anthocyanin biosynthetic enzymes, which produce anthocyanins that subsequently protect against photoinhibition (Rubio *et al.*, 2001). Also up-regulated are phosphate-starvation-induced hydrolases that scavenge Pi from intra and extra-cellular organic P compounds: growing Arabidopsis on RNA as the sole source of P produces the same amount of growth as Pi-fertilised controls, whereas a mutant defective in inducing *PSI* genes requires additional Pi supplementation (Ticconi and Abel, 2004). Another metabolic response is to replace membrane phospholipids with galactolipids and sulpholipids (Andersson *et al.*, 2003; Essigmann *et al.*, 1998) and to upregulate intra- and extra-cellular APases which hydrolyse Pi from a broad range of

substrates with an acidic pH optimum (Duff *et al.*, 1991). Plants therefore respond to low phosphate at both a whole-plant systemic level, but also at the local level, with separate signalling mechanisms involved to regulate Pi metabolism.

PHR1 – miR399 – PHO2 pathway

The phosphate sensor has not been identified, however, whole-plant signalling pathways that are activated in response to phosphate starvation have been well studied. MicroRNAs are important in nutrient status signalling between root and shoot, and several miRNAs have been demonstrated to be strongly induced by phosphate starvation (Hsieh *et al.*, 2009). Of these, the best understood is miR399. Grafting experiments show that miR399 is transported in the phloem from the shoot to the root, where it targets the E2 conjugase PHOSPHATE 2 (PHO2) (Pant *et al.*, 2008; Lin *et al.*, 2008). The *pho2* mutant expresses many phosphate starvation genes at levels expected in WT during Pi deprivation, and over-expression of miR399 can reduce *PHO2* transcripts, and increases leaf Pi levels to as high as in *pho2* mutants (Bari *et al.*, 2006).

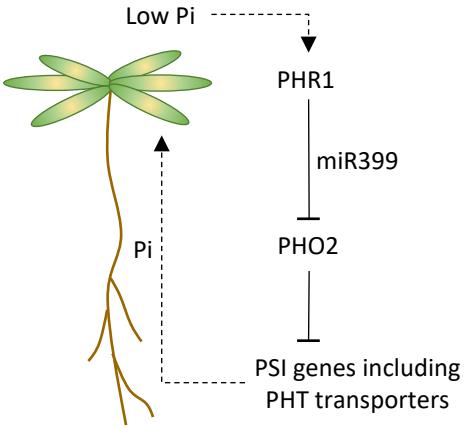


Figure 1: Simplified schematic of the whole-plant low phosphate signalling pathway. Low phosphate conditions cause increased expression of PHR1, which in turn promotes expression of the mobile microRNA miR399. miR399 travels from shoot to root through the phloem, where it targets the E2 conjugase PHO2. This prevents PHO2 repressive action on phosphate starvation induced (*PSI*) genes, which include PHT phosphate transporters. Relieving this repression allows expression of *PSI* genes, resulting in increased phosphate uptake.

Arabidopsis PHOSPHATE STARVATION RESPONSE 1 (PHR1) coordinates the phosphate signalling response. *AtPHR1* encodes a MYB-CC transcription factor, and in the *phr1* loss-of-function mutant the majority of phosphate starvation responses are impaired, including accumulation of anthocyanins, Pi content levels, and changes in root: shoot ratios (Rubio *et al.*, 2001). The *phr1* mutant has reduced expression of many PSI genes, and notably lacks the accumulation of miR399 upon Pi limitation seen in WT plants, placing *phr1* upstream of miR399 in the signalling pathway (Bari *et al.*, 2006) [**Figure 1**].

1.3 Arabidopsis nitrate assimilation

N is critical for plant growth, necessary for the production of proteins and a wide range of other N-containing molecules. In soil, N is found in both inorganic (NO_3^- and NH_4^+), and organic (amino acids, proteins and other N-containing substances e.g. urea) forms. The relative abundance of NO_3^- and NH_4^+ ions is highly variable, often depending on the relative rates of nitrification (the conversion of ammonium to nitrate) and mineralisation (release of ammonium from organic N sources) (Marschner, 1995). Many plants can use either source, although exceptions have been identified (Kronzucker *et al.*, 1997), and additionally some plants, such as legumes, form symbiotic relationships with rhizobacteria that can fix atmospheric dinitrogen directly (Wagner *et al.*, 2011).

In well aerated soils, nitrification is rapid, so NO_3^- is the main N source since ammonium concentrations are low (Crawford and Forde, 2002). In natural habitats soil NO_3^- concentrations are typically < 1 mM, increasing to up to 70 mM in fertilised agricultural land (Reisenauer, 1966). NO_3^- readily dissolves in soil solutions, and this mobility can cause large variations in NO_3^- availability across arable fields – up to a 100-fold difference in NO_3^- concentration (Lark *et al.*, 2004). Plants therefore need to possess adaptive mechanisms

that allow them to handle large fluctuations in NO_3^- availability, and detect when this availability changes, in order to optimise their N acquisition.

1.3.1 Arabidopsis root nitrate transporters

Under varying NO_3^- concentrations, plants need to acquire NO_3^- from the soil, distribute it throughout the plant, and additionally regulate N metabolism at the cellular level. Analysing NO_3^- uptake kinetics indicates that plants have constitutive high-affinity transport systems, inducible high-affinity transport systems, and both constitutive and inducible low-affinity transport systems (Forde, 2000). A diverse range of NO_3^- transporters and channels are used to achieve this, with different affinities and specificities.

Four gene families encode proteins that function as NO_3^- transporters in Arabidopsis. The largest of these is the PTR (peptide transporter) family, with 53 members, of which at least 16 have been shown to have NO_3^- transport activity. The other three families are the NRT2 and CLC families (each containing 7 members), and the SLAC1/SLAH (slow anion channel-associated 1 homologues) with 5 members (reviewed by Krapp *et al.*, 2014).

The first NO_3^- transporter to be identified in plants was NRT1.1 (CHL1) (Tsay *et al.*, 1993). A member of the Arabidopsis PTR family of transporters, it was initially characterised as a low-affinity transport system but later shown to have dual-affinity dependent on the phosphorylation state of the Thr101 residue (Ho *et al.*, 2009). Phosphorylation gives NRT1.1 high-affinity for nitrate, whilst the non-phosphorylated form acts as a low-affinity transporter. Mutants deficient in NRT1.1 have been shown to have reduced NO_3^- uptake in both low and high concentration ranges (Tsay *et al.*, 1993; Muños *et al.*, 2004), although since the contribution of NRT1.1 to root NO_3^- acquisition appears to vary heavily according

to environmental conditions the extent to which NRT1.1 co-ordinates plant NO_3^- supplies is hard to precisely determine (Krapp *et al.*, 2014).

1.3.2 Shoot to root nitrate transport

Once in the root, NO_3^- can either be assimilated in the root tissue or transported to the shoot tissue. In NO_3^- replete conditions, the majority of NO_3^- assimilation occurs in shoot tissue (Krapp *et al.*, 2011). This requires root NO_3^- to be loaded into root xylem vessels by transporters such as the bi-directional NRT1.5 transporter. Whilst root to shoot nutrient status mainly depends on the transpiration stream moving nutrients through the xylem, it can also be regulated by interactions between the xylem and phloem. The genes encoding low-affinity NO_3^- transporters NRT1.8 and NRT1.9 are expressed in root companion cells and xylem parenchyma cells, and negatively impact root to shoot NO_3^- transport (Li *et al.*, 2010; Wang and Tsaya, 2011). In *nrt1.9* mutants, shoot NO_3^- concentration is elevated compared to WT, whilst root NO_3^- content is decreased (Wang and Tsaya, 2011). Functional disruption of NRT1.8, meanwhile, has been shown to significantly increase the NO_3^- concentration in xylem sap, with *in situ* hybridisation showing that *NRT1.8* is predominantly expressed in xylem parenchyma cells (Li *et al.*, 2010). The spatial expression pattern of NRT1.9 (identified using GUS and GFP reporter assays), together with identified NRT1.9 NO_3^- transport activity, suggests that this protein is responsible for loading NO_3^- into root phloem – the authors suggest this may fine-tune local NO_3^- redistribution (Wang and Tsaya, 2011). NO_3^- transport in the phloem is also important in remobilisation from source to sink tissue. In mature leaves NRT1.7 is involved in remobilising NO_3^- to younger tissue (Hornitschek *et al.*, 2009), and *NRT2.4*, which encodes a high-affinity transporter and is

expressed in phloem parenchyma cells, has also been implicated: the loss of function mutant has decreased NO_3^- concentration in phloem sap (Kiba *et al.*, 2012).

1.3.3 Assimilation of nitrate into N-containing components

Once taken up by the plant and transported to various tissues, NO_3^- can either be stored in cell vacuoles or reduced to nitrite (NO_2^-) by nitrate reductase (NR), and then ammonium (NH_4^+) by nitrite reductase (NiR). Ammonium is converted by glutamine synthetase (GS) and glutamate synthase (GOGAT) into glutamine via the GS-GOGAT cycle, from which it can be assimilated into other amino acids [**Figure 2**]. NO_3^- assimilation can therefore be regulated at each step of the pathway, with the reduction of NO_3^- to NO_2^- by NR forming the rate-limiting step of the pathway (Campbell, 1999).

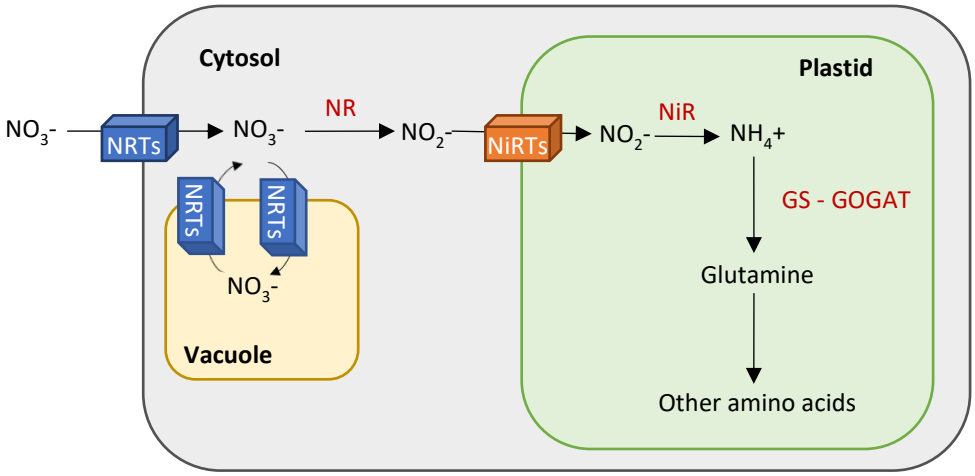


Figure 2: Nitrate uptake and assimilation in plants. Nitrate ions (NO_3^-) are transported into the plant via nitrate transporters (NRTs), where they are reduced to nitrite (NO_2^-) by nitrate reductase (NR). Nitrite is then transported by nitrite transporters (NiRTs) into the plastid, where nitrite is further reduced to ammonium ions (NH_4^+) by the enzyme nitrite reductase (NiR). Ammonium is incorporated into glutamine via the GS (glutamine synthetase) /GOGAT (glutamate synthase) cycle, from which it can be incorporated into other amino acids and organic N-containing compounds.

1.3.4 Nitrate reductase

Eukaryotic NR catalyses the reaction:

$$NO_3^- + NAD(P)H \rightarrow NO_2^- + NAD(P)^+ + OH^-$$

$$\Delta G = -34.2 \text{ kcal/mol}$$

Under standard conditions the large negative free energy means that to all intents and purposes this reduction of NO_3^- to NO_2^- nitrite is irreversible (Campbell, 1999). In the majority of cases this reaction is the rate-limiting step of nitrogen acquisition; understanding the role of NR is therefore of particular importance to understanding plant nitrogen nutrition.

In plants both nitrite and ammonia are toxic at high concentrations: in normal conditions leaf nitrite concentrations rarely exceed 15 nmol g^{-1} FW (Kaiser and Huber, 2001). It is therefore not surprising that a variety of regulatory mechanisms exist to control nitrite production. The capacity of a plant to reduce NO_3^- depends on three things: the availability of NO_3^- and NAD(P)H in the cytoplasm, the amount of NR protein and its cofactors and metal ions, and the activity level of the NR present. Each of these factors can be controlled to affect the NO_3^- reduction capacity of a plant.

1.3.5 Transcriptional control of genes encoding nitrate reductase

Arabidopsis has two genes encoding NR: *NIA1* and *NIA2*. Of these two genes, *NIA2* encodes the majority of NR protein, as the Arabidopsis *nia2* mutant retains only 10% of WT NR activity (Wilkinson and Crawford, 1991). NODULIN INCEPTION-like proteins (NLPs) have been identified as important transcription factors responsible for nitrate-inducible expression of a number of different genes including those that encode the NR enzyme. Arabidopsis contains nine copies of *NLP* genes (*NLP1* – *NLP9*); the *nlp7* loss-of-function mutant displays several features of nitrogen-starved plants, and reduced expression of the NO_3^- transporter genes *NRT2.1* and *NRT2.2* and NR genes *NIA1* and *NIA2* following NO_3^- re-supply after starvation (Castaings *et al.*, 2009). Numerous studies have since demonstrated

the role of NLPs in regulating nitrate-inducible gene expression, including that of *NIA1* and *NIA2*.

In addition to nitrate, *NIA* expression can be modulated by a range of other environmental factors, and so additional transcription factors are believed to control the expression levels of these genes. The bZIP transcription factors LONG HYPOCOTYL 5 (HY5) and HY5 HOMOLOGUE (HYH) have been suggested to have a role: the double loss-of-function mutant *hy5 Δ hyh* lacks light-dependent activation of *NIA2* (although light-dependent activation of *NIA1* is unaffected), and the bHLH *phytochrome interacting factor 4* (*pif4*) mutant has higher expression levels of *NIA2*, consistent with the fact these transcription factors often act antagonistically to each other (Jonassen *et al.*, 2009).

NIA genes display a diurnal expression pattern, and whilst the circadian clock generally regulates circadian gene expression, diurnal oscillation of *NIA* mRNAs may also be regulated by oscillating nitrate or glutamine contents since NR activity is regulated by light (reviewed by Yanagisawa, 2014).

1.3.6 Post-translational regulation of nitrate reductase

Transcriptional control of genes encoding NR mediate slow and/or long-term changes in metabolism; rapid changes in enzyme activity are regulated on a post-translational level. In *Nicotiana plumbaginifolia* de-regulating *NR* transcription by placing the *NR* gene under the control of the cauliflower mosaic virus 35S promoter had little influence on metabolite levels (Lea *et al.*, 2006). Nitrogen metabolite levels were significantly altered, however, when post-translational control was deregulated - by either a deletion mutation in the N-terminus or by mutating the important regulatory phosphorylation site serine-521 (Lea *et al.*, 2006), indicating the importance of post-translational mechanisms of regulation.

NR activity can be altered by three mechanisms of post-translational control. Inhibition of the NR enzyme can be achieved by the binding of a 14-3-3 protein to a phosphorylated serine residue (Ser534 in *Arabidopsis thaliana*) (Lambeck *et al.*, 2010)., irreversible inhibition of the enzyme by degradation (Lambeck *et al.*, 2010), and thirdly by a mechanism using the non-conserved N-terminus which has not been well described. In plants, 14-3-3 binding is believed to be the most important mode of regulation (Lambeck *et al.*, 2010).

Phosphorylation

NR is a homodimeric enzyme, containing three cofactors, each bound to separate domains to form an electron transfer chain. Each domain is connected by a hinge region. Arabidopsis Ser534 phosphorylation in hinge 1 can be catalysed by both members of the calcium-independent SNF1 resembling kinase family (SNRK1) and the calcium-dependent protein kinase family (CPK), suggesting it is under the control of different regulatory circuits (Campbell, 1999). The canonical binding motifs for both CPKs and SNRK1s is found in hinge 1, and both have overlapping substrate specificities. Both free (NR) and phosphorylated (pNR) forms of the enzyme are active (Campbell, 1999).

14-3-3 proteins

After Ser534 phosphorylation, phosphorylated NR (pNR) can be bound by 14-3-3 proteins causing inhibition. 14-3-3 proteins are binding proteins, demonstrated to interact with numerous enzymes involved in metabolism and biosynthesis in plants, and to be of particular importance in regulating C and N metabolism (Huber *et al.*, 2002). They bind consensus motifs and operate by either enabling/disabling the interaction of their target with other molecules, or by inducing a conformational change within the target protein (Oecking and Jaspert, 2009).

14-3-3 binding has been shown to reduce NR activity by slowing the rate of transfer of electrons from the heme domain to the molybdenum cofactor, and it is suggested this is achieved by 14-3-3 binding inducing a conformational change that increases the distance between these two redox-active sites (Lambeck *et al.*, 2010). Kinetic studies showed that this achieved an 18-fold reduction in k_{cat}, halving the $K_M^{nitrate}$ relative to the pNR form with no 14-3-3 binding (Lambeck *et al.*, 2010). This mechanism of 14-3-3 inhibition can be influenced by NO_3^- availability: 14-3-3 proteins preferentially bind to NR in the substrate-bound state, with an increased rate of release of 14-3-3 proteins at low substrate concentrations (Lambeck *et al.*, 2010).

Sumoylation

The small ubiquitin-related modifier (SUMO) polypeptide is an important regulator of biological processes, capable of altering protein activity and regulating hormone signalling in addition to responses to abiotic and biotic factors. SUMO can be covalently conjugated to a substrate protein via a lysine residue; this post-translational modification is reversible and facilitated by E3 sumo ligases (Wilkinson and Henley, 2010). It was observed that mutations in *AtSiz1*, which encodes an E3 sumo ligase in Arabidopsis, resulted in dwarfed plants - a phenotype recovered when plants were supplied with exogenous NH_4^+ but not with NO_3^- (Park *et al.*, 2011). Subsequent yeast two-hybrid and pull-down assays showed strong interactions between AtSIZ1 and NIA1 or NIA2, and further work showed that both NIA1 and NIA2 are sumoylated, which depends on the AtSiz1 E3 SUMO ligase activity (Park *et al.*, 2011). This is the first report of SUMO conjugation modulating the catalytic activity of plant enzymes, and suggests that sumoylation may be a further important post-

translational mechanism by which NR activity is modulated in Arabidopsis (Park *et al.*, 2011).

Degradation

NR has a relatively short half-life of several hours; NR amount is therefore not only affected by *NIA* transcription and translation, but also by NR protein degradation. A number of experiments have indicated that the inactive, 14-3-3 bound pNR form can undergo specific proteolysis, however, the role of 14-3-3 proteins is not entirely understood as other studies have suggested they may protect proteins from degradation (Kaiser and Huber, 2001). Controlling NR degradation is therefore likely to be another aspect by which plants can regulate NR activity.

1.3.7 Nitrogen signalling pathways

Similar to phosphate, sustained nitrogen deficiency results in a variety of adaptive responses, including alterations to root architecture, upregulation of genes encoding transporters, and alterations to flowering time (Nguyen *et al.*, 2015; Chen *et al.*, 2008). Low N availability is signalled in response to both nitrogen-satiety status in the shoot via systemic signalling and by direct NO_3^- signalling in the roots (reviewed by Krapp *et al.*, 2014). NR null mutants retain many nitrate-induced effects (Wang *et al.*, 2004), indicating that NO_3^- itself is an important signalling molecule, that controls a wide range of metabolic and developmental processes.

NO_3^- is an important regulator of transcription, with nitrate-responsive genes suggested to account for up to 10% of the Arabidopsis transcriptome (Krouk *et al.*, 2010). The so-called "primary nitrate response" refers to the rapid up-regulation of gene expression by NO_3^-, including those encoding many of the proteins required for N assimilation (Krapp *et al.*,

2014). Many of these responses are dependent on NRT1.1. The role of NRT1.1 in NO_3^- signalling was first demonstrated by the finding that *nrt1.1* null-mutants have significantly reduced *NRT2.1* expression (Muños *et al.*, 2004). Analysis of point mutations in the NRT1.1 protein that uncouple NO_3^- signalling and NO_3^- transport activity has provided further evidence of the dual function of NRT1.1. The P492L point mutation does not affect the NRT1.1-dependent *NRT2.1* induction by nitrate, but does prevent NO_3^- transport (Ho *et al.*, 2009), whilst the T101A mutation (preventing Thr101 phosphorylation by a CIP23 kinase) does not abolish NO_3^- transport, but does suppress nitrate-regulated root system architecture changes in response to L-glutamate application (Walch-Liu and Forde, 2008).

Downstream components of NO_3^- signalling include NIN-like proteins (NLPs), transcription factors that are master regulators of the NO_3^- response. NO_3^- triggers calcium signalling, activating calcium sensor kinases (CPKs) which phosphorylate NLPs at a conserved serine residue, promoting their accumulation in the nucleus and activation of target genes. Arabidopsis NLP7 has been shown by ChIP-chip approaches to bind 851 genes in response to NO_3^- (Marchive *et al.*, 2013), including those involved in N metabolism, carbon metabolism, and regulatory proteins such as transcription factors.

1.3.8 Chlorate is a structural analogue of nitrate

Chlorate (ClO_3^-) has been used extensively as a herbicide; plants treated with chlorate display visible chlorosis – leaves yellow and die. Chlorate is a structural analogue of nitrate, and is reduced by NR to chlorite, which is toxic to plants (Åberg, 1947). Many chlorate resistant mutants have been isolated and characterised across bacteria, plants and fungi; most of these are impaired in nitrate reduction (Wray and Kinghorn, 1989).

Chlorate acts as a competitive inhibitor of NR (Solomonson and Vennesland, 1972). The toxicity of chlorate depends on other nutrients present – plants grown on ammonium as the sole N source are much more sensitive to chlorate than plants grown on NO_3^- also (Steingrover and Feenstra, 1981), despite NO_3^- being a positive regulator of NR activity. Although levels of Arabidopsis mRNA encoding leaf NR increase following chlorate treatment, NR activity decreases – suggested due to the chlorite inactivating NR, and the inactivated NR being prone to rapid degradation (LaBrie *et al.*, 1991). This study raised the possibility of chlorate acting as a signalling molecule (like nitrate) in itself – although the NR affinity for chlorate is lower than for nitrate, and so it is suggested that responses would be weaker (LaBrie *et al.*, 1991).

By screening for mutants that are resistant to chlorate, plants defective in the assimilation of nitrate, and the mutations responsible for these phenotypes, have been identified (Braaksma and Feenstra, 1982; Wilkinson and Crawford, 1993). Similarly, this thesis uses chlorate to identify mutants with altered resistance to the herbicide, with the aim of identifying further mutations which alter Arabidopsis chlorate resistance, and therefore Arabidopsis N metabolism.

1.4 Regulation of nutrient assimilation

1.4.1 Links between phosphate and nitrate metabolism

Plants are sessile and must therefore integrate a variety of environmental and internal signals to produce a growth output most suited to current growth conditions. Consequently, inputs from different nutrient status signalling pathways must be integrated, as well as information regarding carbon assimilation, to produce a growth output that is appropriate to the environmental conditions. Plants must balance their

acquisition of different nutrients, as deficiency in one nutrient may cause excess accumulation of others, or over-accumulation of certain nutrients may result in deficiencies of others.

It is therefore expected that there will be extensive crosstalk between different environmental signalling pathways, and physiological studies have indicated that regulation of P and N metabolism is linked. Phosphate deficiency has been shown to reduce NO_3^- uptake in barley (Lee, 1982) maize (De Magalhães *et al.*, 1998) and tobacco (Rufty *et al.*, 1990), and to enhance accumulation of amino acids due to increased rates of protein degradation (Rufty *et al.*, 1990; Schlüter *et al.*, 2013).

Whilst the interaction of nitrate and phosphate signalling pathways is not well understood, more recent studies have identified some genetic components of crosstalk that regulate both NO_3^- and Pi metabolism. NITROGEN LIMITATION ADAPTATION (NLA) is a ring-type ubiquitin ligase that positively regulates the response of Arabidopsis to N deprivation; *nla* null-mutants are defective in developing nitrogen limitation adaptive responses, and display early senescence in low N conditions (Peng *et al.*, 2007). NLA has also been implicated in regulating phosphate metabolism: NLA expression is regulated by the microRNA miR827, induced under low-phosphate conditions (Kant *et al.*, 2011). This study showed that the early senescence phenotype of *nla* plants in low NO_3^- was due to Pi toxicity occurring in a nitrate-dependent manner, with mutants accumulating over five times the Pi content in shoots under low N and high Pi (but not high N and high Pi) (Kant *et al.*, 2011). Further studies have identified NLA as responsible for directing the ubiquitination of plasma-membrane located PHT1 phosphate transporters, targeting them for endocytosis and subsequent vacuolar degradation (Lin *et al.*, 2013). NLA is suggested to act co-

operatively with PHO2 to regulate PHT1 transporter abundance in different subcellular compartments: when phosphate levels are depleted, upregulation of miRNAs miR399 (targeting PHO2) and miR827 (targeting NLA) reduces expression of these proteins, alleviating PHT1 removal from plasma membranes (Lin *et al.*, 2013).

A more recent study identified a nitrate-inducible transcription factor, HYPERSENSITIVITY TO LOW PI-ELICITED PRIMARY ROOT SHORTENING 1 (HRS1), which represses primary root growth in response to low phosphate conditions when NO_3^- is present (Medici *et al.*, 2015). HRS1 expression is positively regulated by NO_3^- availability, a process dependent on NRT1.1, and HRS1 can be bound by NLP7 (Medici *et al.*, 2015). HRS1 is also regulated post-transcriptionally by phosphate provision, with phosphate deprivation reducing accumulation of the protein. This study suggests that HRS1 can integrate both NO_3^- and phosphate signals at the Arabidopsis root tip, where it is involved in the control of primary root growth (Medici *et al.*, 2015).

The highly conserved NIN-LIKE PROTEIN (NLP) transcription factors act as the primary regulators of the plant nitrate response (Konishi and Yanagisawa, 2013). These proteins are phosphorylated by calcium sensor kinases (CPKs) following nitrate-triggered Ca^{2+} signalling, where they activate target genes (Liu *et al.*, 2017). NITRATE-INDUCIBLE GARP-TYPE TRANCRIPTIONAL REPRESSOR1 (NIGT1) are nitrate-inducible transcriptional repressors, and rice OsNIGT1 has been suggested to form part of a negative feedback loop regulating NO_3^- metabolism, as transgenic rice lines overexpressing *OsNIGT1* have reduced nitrate-induced *NIGT1* expression (Sawaki *et al.*, 2013). A 2018 study proposed a model for a NIGT1-centred transcriptional cascade that integrates Pi and NO_3^- signalling (Maeda *et al.*, 2018). The authors propose that nitrate-induced expression of NLP transcription factors

upregulates both *NRT2.1* (encoding a NO_3^- transporter), and *NIGT1*-clade gene promoters. The expression level of *NRT2.1* is modulated by the balance of positive and negative regulatory feedback loops: NLPs directly upregulate *NRT2.1* expression, whilst NLP-induced *NIGT1* genes act to repress *NRT2.1* transcription. The authors found that Pi starvation upregulated *NIGT1*-clade genes, whilst downregulating *NRT2.1* expression, but that this phosphate-starvation-induced *NIGT1* upregulation and *NRT2.1* downregulation was compromised in the *phr1* Δ *phl1* mutant (Maeda *et al.*, 2018). PHR1 is therefore proposed to upregulate *NIGT1* genes, enhancing expression of these negative regulators of *NRT2.1* expression, inducing Pi-starvation induced downregulation of NO_3^- uptake (Maeda *et al.*, 2018) [**Figure 3**].

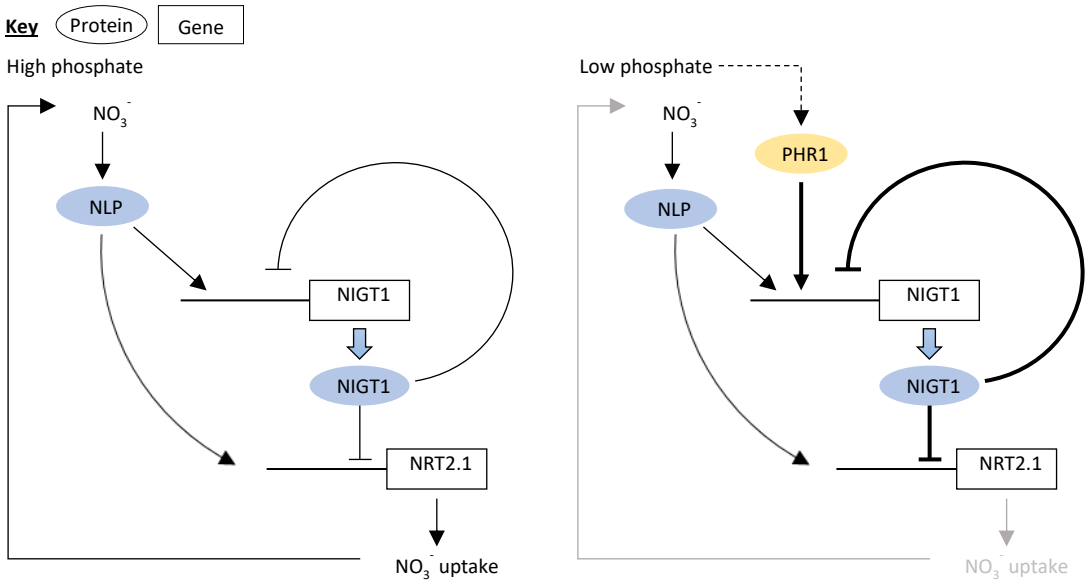


Figure 3: Model of proposed NIGT1-centred transcriptional cascade that integrates both nitrate signalling (blue) and phosphate starvation signalling (yellow) pathways. In phosphate replete conditions (left panel) NLP proteins initiate positive and negative feedback loops: upregulating expression of *NRT2.1* which encodes a nitrate transporter (a positive feedback loop that increases nitrate uptake), whilst also upregulating expression of the *NIGT1* negative regulators, establishing a negative feedback loop. Phosphate starvation (right panel) causes an accumulation of PHR1 protein, which alters this pathway by increasing expression of *NIGT1*-clade genes, reducing *NRT2.1* expression and therefore lowering nitrate uptake when phosphate supply is limited. Figure adapted from Maeda *et al.*, 2018.

1.4.2 Hormonal regulation of nutrient metabolism

Nutrient availability in soil varies both spatially and temporally. When a nutrient supply is limited, plants trigger both physiological and developmental responses to increase nutrient acquisition, thereby improving their nutrient status. When a particular nutrient is limited, expression of high-affinity ion transporters may increase, there may be secretion of enzymes that facilitate remobilisation of the nutrient from organic and inorganic sources in soil, and the growth of organs directly involved in nutrient acquisition may be stimulated (Hermans *et al.*, 2006; Reymond *et al.*, 2006). For example, lateral root growth increases in plants grown under low supplies of sulphur or phosphorus, increasing the surface area available for ion absorption (López-Bucio *et al.*, 2003). Other responses cause adaptations to lower nutrient supplies within the plant, such as alternative metabolic pathways (Plaxton and Tran, 2011) or accumulation of anthocyanins to protect from photoinhibition that can be caused by low P or N availability (Trull *et al.*, 1997).

Switching *Nicotiana tabacum* (tobacco) from pure NO_3^- to pure NH_4^+ triggers, within hours, a decrease in shoot growth, despite there being no modification of shoot N content within this time frame. Plant growth can therefore be controlled by signalling pathways in response to nutritional cues, rather than purely as a result of a change in actual nutrition status of plant organs (Walch-Liu *et al.*, 2000). Since plant development is influenced by hormonal signals, it is not surprising that plant hormones can regulate nutrient metabolism, and vice versa.

Multiple roles for plant hormones in the control of nutrient metabolism have been identified. Cytokinins, for example, are proposed to play a key role in controlling long-distance signalling of plant N status. NO_3^- availability alters the expression of the genes encoding isopentenyl transferase enzymes IPT3 and IPT5, which catalyse the rate-limiting

step of cytokinin biosynthesis, resulting in increased cytokinin accumulation when NO_3^- is present (Takei *et al.*, 2004). Adding cytokinin to plants induces leaf expression of genes that regulate NO_3^- and carbon metabolism, mimicking the response induced by increasing NO_3^- supply to plant roots (Brenner *et al.*, 2005; Scheible *et al.*, 2004). When NO_3^- levels rise, production of cytokinins therefore increases, which act as a long-distance signalling mechanism to induce transcription changes in the shoot to maintain the C: N balance.

Arabidopsis mutants impaired in the biosynthesis of the plant hormone abscisic acid (ABA) have impaired inhibition of lateral root formation following NO_3^- application (Signora *et al.*, 2001), impaired phosphate starvation-induced gene expression and anthocyanin accumulation when grown in phosphate-deficient conditions (Trull *et al.*, 1997), and treating phosphate deprived WT Arabidopsis with ABA represses expression of several low-phosphate-induced *At4* genes (Shin *et al.*, 2006). However, mutants lacking components of ABA signalling do not have altered low-phosphate-induced acid phosphatase activity, or changes in their root: shoot ratio (Trull *et al.*, 1997). ABA is therefore a plant hormone implicated to control a subset of both nitrate and phosphate signalling, demonstrating the multifaceted control exhibited by plant hormones with regard to plant nutrition.

Ethylene, another plant hormone, has been implicated in the regulation of plant phosphate metabolism. In plants grown under phosphate deficient conditions, ethylene induces primary root elongation, whilst adding an ethylene inhibitor reduces root elongation (Ma *et al.*, 2003). Ethylene is also implicated in biochemical responses to phosphate deprivation, as ethylene signalling is involved in up-regulating expression of both intracellular and secreted acid phosphatases (Lei *et al.*, 2011). Applying the ethylene precursor 1-aminocyclopropane-1-carboxylic acid (ACC) to several plant species

(Arabidopsis, tomato, cucumber) increases expression of genes encoding iron transporters, ferric reductases and H^+-ATPases, which increase iron uptake when availability is reduced (Lucena *et al.*, 2006). Ethylene has also been implicated in the regulation of potassium metabolism: low potassium supply almost doubles ethylene biosynthesis (Shin and Schachtman, 2004). This thesis explores further the role of ethylene in regulating plant nitrogen status.

1.5 The ethylene signalling pathway

Ethylene, C_2H_4, is a gaseous plant hormone. It is produced in response to a wide range of stimuli, both internal and external, triggering a range of developmental and physiological responses (Bleeker and Kender, 2000). Growing 3-day-old etiolated seedlings under ethylene treatment produces a characteristic 'triple response': short hypocotyls, exaggerated apical hooks and short roots (Bleeker and Kender, 2000). Screening for mutants that either lack this triple response phenotype, or produce it in the absence of ethylene, has identified several ethylene signalling components, building an understanding of the ethylene signalling pathway [**Figure 4**].

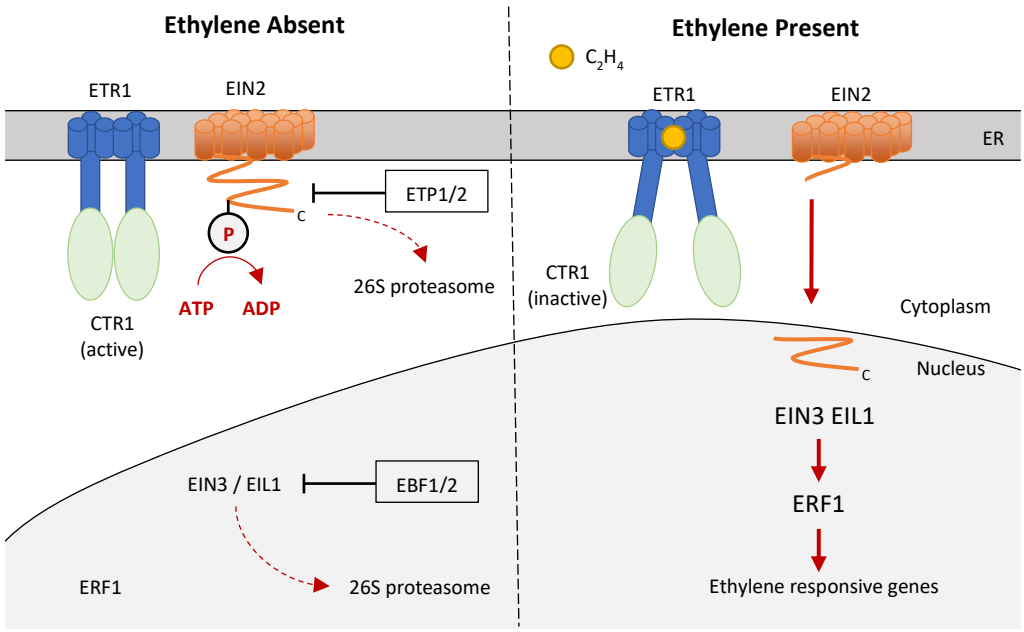


Figure 4: Overview of the ethylene signalling pathway. In the absence of ethylene (left panel), CTR1 is active, and phosphorylates the EIN2 C-terminus, targeting it for degradation via the 26S proteasome. Within the nucleus EBF1 and EBF2 target EIN3 and EIL1 for degradation. When ethylene is present (right panel), it binds to ethylene receptors, resulting in de-activation of CTR1. This leaves the EIN2 C-terminus free to be cleaved and translocated into the nucleus, where it causes the stabilisation of EIN3 and EIL1, leading to downstream transcriptional cascades of ethylene responsive genes. Figure adapted from Ju *et al.*, 2012**.**

1.5.1 Ethylene receptors

Ethylene binds with high affinity to ER-localised receptor proteins (Chang and Stadler, 2001). Five ethylene receptors have been identified in Arabidopsis: ETR1, ERS1, ETR2, ERS2 and EIN4. These receptors function as homodimers but share a common modular structure, consisting of an N-terminal transmembrane domain that facilitates ethylene binding, a C-terminus domain that interacts with downstream signalling components, and a GAF domain through which receptors can interact to form higher-order complexes (reviewed by Merchante *et al.*, 2013). Whilst a significant amount of redundancy exists in the different receptors control of ethylene responses, several studies have identified specificity amongst the different receptor isoforms (Binder *et al.*, 2012; McDaniel and Binder, 2012; Dong *et al.*, 2010; Kim *et al.*, 2011). The differential composition that higher-

order complexes of multiple receptor types could take on may explain the broad range of ethylene sensitivity in different plant tissues.

1.5.2 CTR1

The 5 Arabidopsis ethylene receptors are negative regulators of the ethylene signalling pathway: in the absence of ethylene they repress the ethylene response. When ethylene is absent, the hormone-free receptors activate the Ser-Thr protein kinase CONSTITUTIVE TRIPLE RESPONSE 1 (CTR1) (Mayerhofer *et al.*, 2012). The *ctr1* loss-of-function mutant displays a constitutive ethylene signalling response: CTR1 is therefore a key member of the ethylene signalling pathway. Despite lacking any predicted transmembrane domains, CTR1 physically interacts with ethylene receptors to reside in the ER membrane (Gao *et al.*, 2003). When activated by these receptors, CTR1 dimerizes and suppresses the ethylene response by phosphorylating the C-terminus of another ER-localised membrane protein, ETHYLENE INSENSITIVE 2 (EIN2) (Ju *et al.*, 2012). This targets EIN2 for degradation through the proteasome via the two F-box proteins ETP1 and ETP2 (Qiao *et al.*, 2009). Binding of ethylene to the N-terminal transmembrane domain inactivates the receptors, resulting in de-activation of CTR1 (Schaller and Bleecker, 1995). In addition to this well understood signalling pathway, recent research suggests an additional role for CTR1 - with the finding that ethylene can trigger the translocation of CTR1 from the ER to the nucleus, where it stabilises EIN3 through inhibition of EBF proteins (Park et al., 2023).

1.5.3 EIN2

The *ethylene insensitive 2* (*ein2)* loss-of-function mutant has a completely ethylene-insensitive phenotype, lacking all examined ethylene responses (Ji and Guo, 2013). The single-copy gene encoding EIN2 in Arabidopsis is conserved from charophyte green algae

to land plants (Ju *et al.*, 2015). The EIN2 protein consists of a hydrophobic N-terminus region with 12 predicted transmembrane domains (the function of which is not clear); the C-terminus end of EIN2 (CEND) is hydrophilic and contains a conserved nuclear localisation sequence. CEND is thought to be critical to signalling output, as inducing overexpression of this domain in light grown plants can constitutively activate ethylene responses, although in loss-of-function *ein2* mutants this does not restore full ethylene sensitivity (Wen *et al.*, 2012).

Like CTR1, EIN2 is located in the ER membrane and physically interacts with ethylene receptor kinase domains. In the absence of ethylene, receptor activated CTR1 directly phosphorylates the CEND domain of EIN2, and this phosphorylation prevents signalling to downstream components EIN3 and EILs. This phosphorylation state is abolished by ethylene application and the subsequent inactivation of receptors and CTR1 (Ju *et al.*, 2012; Qiao *et al.*, 2012). EIN2, in the presence of ethylene, lacks phosphorylation at multiple Ser and Thr residues, enabling the CEND to be cleaved from the ER-tethered N terminus, and shuttled into the nucleus via the nuclear localisation sequence (Qiao *et al.*, 2012).

1.5.4 EIN3, EIL1 and downstream signalling targets

Within the nucleus, the EIN2 CEND causes the stabilisation of EIN3, permitting downstream activation of EIN3-EIL dependent transcriptional cascades (Wen *et al.*, 2012). EIN3 and EIL1 are two major transcription factors responsible for generating the primary output of ethylene responses. They have been shown as both necessary and sufficient for the regulation of ethylene - responsive gene expression (Solano *et al.*, 1998). EIN3 and EIL1 function as dimers to induce expression of ethylene target genes, such as the transcription factor ERF1. EIN3 has been shown to act in a ‘four-wave manner’, regulating downstream

transcription by cumulatively controlling a number of downstream transcriptional cascades that lead to the activation and repression of hundreds of ethylene-regulated genes (Chang *et al.*, 2013). Some of the targets downstream of EIN3 regulation include components of other hormone signalling pathways, demonstrating the complex crosstalk of interactions between the many different plant hormone signalling networks.

1.5.5 Negative feedback in the ethylene signalling pathway

A negative feedback loop acts to dampen the ethylene signalling pathway, ensuring the signal reduces once ethylene is no longer present. Key to this negative feedback loop is proteasome-mediated protein degradation, which acts at all levels of the ethylene signalling pathway.

Ethylene induces degradation of the ethylene receptor ETR2 via the 26S proteasome (Chen *et al.*, 2007), whilst also activating *ETR2*, *ERS1* and *ERS2* transcription. Newly synthesised receptors are not bound by ethylene and therefore active, inhibiting the downstream signalling steps via phosphorylation of CTR1 as soon as ethylene levels decrease. Further down the pathway, EIN2, EIN3 and EIL1 protein levels are under tight regulation: in the absence of ethylene specific F-box proteins target these proteins to degradation via the 26S proteasome. EIN2 is regulated via the F-box proteins ETP1 and ETP2 (Qiao *et al.*, 2009) whilst EIN3 is targeted by EBF1 and EBF2 (Guo and Ecker, 2003). *EBF2* is also a target of EIN3, with transcription induced by ethylene (Maeda *et al.*, 2018; Konishi and Yanagisawa, 2008), there are therefore multiple steps of regulation to this pathway, providing a mechanism by which plant responsiveness to this hormone can be dynamically modulated.

1.5.6 Alternative ethylene signalling pathways: a cytoplasmic role for EIN2

Although the “cleave and shuttle” mechanism of EIN2 signalling via the CTR1-regulated C terminus is well understood, a number of studies have suggested alternative ethylene signalling pathways may exist, bypassing one or multiple components of the traditional ethylene signalling pathway outlined above. For example, it has been suggested the ETR1 N-terminus may work together with RTE1 to mediate ethylene signalling via a CTR1-independent pathway (Qiu *et al.*, 2012), and analysing the ethylene-mediated growth inhibition of etiolated Arabidopsis seedling hypocotyls has suggested the existence of a ‘first phase’ fast-response signalling pathway, which whilst requiring EIN2 is independent of the key regulators EIN3 and EIL1 (Binder *et al.*, 2004).

The suggestion of a signalling role for EIN2 independent of EIN3 and EIL1 is further supported by the observation that induced nuclear localisation of CEND has been shown to only partially activate the full ethylene signalling pathway (Ji and Guo, 2013; Wen *et al.*, 2012), and that cleaved CEND, in addition to entering the nucleus, also form discrete foci in the cytoplasm (Wen *et al.*, 2012; Qiao *et al.*, 2012). It has been reported that a cytoplasmic mode of EIN2-mediated ethylene signalling exists, with EIN2 repressing translation of EBF1 and EBF2 mRNA in P-body compartments within the cytosol (Li *et al.*, 2015). These authors demonstrated that the cytoplasmic function of EIN2 is responsible for quickly halting protein synthesis of EBF1/2, rapidly depleting EBF1/2 proteins due to proteasomal degradation. EIN2 therefore has an additional role in regulating translation of ethylene signalling components, acting in the cytoplasm either in parallel or prior to the EIN2-regulated nuclear signalling cascade.

1.5.7 Ethylene and Nitrogen metabolism

Ethylene signalling has been implicated to affect plant development and adaptations in response to a change in NO_3^- availability. Transferring seedlings from low NO_3^- to high NO_3^- conditions causes a rapid burst in root ethylene production, accompanied by a short-term increase in ACC synthase (ACS) and ACC oxidase (ACO) transcripts (Tian *et al.*, 2009). This NO_3^- -dependent ethylene production regulates lateral root (LR) development, inhibiting growth of immature LRs. The *etr1-3* and *ein2-1* mutants both have reduced ethylene responses, and the root system architecture of these mutants is less responsive to external NO_3^- levels, with a reduced inhibition of lateral root development (both lateral root numbers and lateral root length) on transfer of seedlings from low to high NO_3^- conditions compared to WT (Tian *et al.*, 2009). The same study showed that ethylene was also shown as important in modulating expression of the *NRT1.1* and *NRT2.1* nitrate transporters. Seedlings transferred to high NO_3^- concentrations had a strong induction of *the NRT1.1* transporter, whilst expression of the *NRT2.1* transporter was reduced, with effects stronger at 6 h rather than 24 h after transfer. Treating low-nitrate-grown plants with the ethylene precursor ACC increased *NRT1.1* transcription whilst reducing that of *NRT2.1* to a similar level seen in plants transferred to high NO_3^- conditions, further supporting the role of ethylene in controlling these changes (Tian *et al.*, 2009).

Ethephon (2-chloroethyl phosphoric acid) induces ethylene release in plant tissues, and is widely used commercially to promote fruit development, including maturation, abscission, and colour development (Shulman *et al.*, 1985). A study measuring NR activity in mustard (*Brassica juncea* L.) treated with different concentrations of ethephon found that in high soil N conditions (200 mg kg^{-1} soil), ethephon application increased NR activity for all ethephon concentrations tested, and intermediate levels of ethephon (100 µl and 200 µl L^-

^{1}) also increased leaf N concentration, although leaf N concentration was decreased following treatment with the highest ethephon concentration tested (400 µl L^{-1}). In low soil N conditions (100 mg kg^{-1} soil) however, ethephon application decreased NR activity at all concentrations tested, whilst the effects on resulting leaf N concentration follow no specific trend: decreasing at 100 µl and 400 µl L^{-1} but increasing after treatment with 200 µl L^{-1} (Khan *et al.*, 2008).

Whilst these studies have identified a role for ethylene signalling in regulating plant nitrogen nutrition, they have either focussed on short term effects on NO_3^- re-supply (Tian *et al.*, 2009), or are limited in their restriction to physiological observations which are at times difficult to interpret (Khan *et al.*, 2008). This leaves scope to further investigate the role of ethylene signalling in regulating N metabolism.

1.6 The role of Arabidopsis HY5 in nutrient acquisition

1.6.1 HY5 as a master regulator

Photosynthetically active radiation is used for photosynthesis, and therefore directly affects the carbohydrate supply available to plants. A broad wavelength range of light can be perceived by plants by a variety of photoreceptors, which allow wavelength-specific responses to be induced. Blue light and UV-A light (380-500 nm and 320-380 nm respectively) are perceived by the cryptochrome photoreceptor, involved in the regulation of growth, development and the circadian clock; another receptor, phototropin, can perceive blue light and modulates phototropisms, chloroplast repositioning and stomatal opening (Lin, 2000). The UV RESISTANCE LOCUS 8 (UVR8) receptor has been identified as perceiving UV-B radiation (Rizzini *et al.*, 2011), whilst red light is perceived by

phytochromes which primarily absorb red light and far-red light, regulating a varied range of physiological processes including seed germination, flowering, and shade avoidance.

Phytochromes are encoded by 5 genes in Arabidopsis, with phyB – phyE controlling the reversible red/far-red low fluence response – of these four phytochromes, phyB is present in by far the highest abundance in Arabidopsis (reviewed by Sakuraba and Yanagisawa, 2018). On exposure to red light, inactive Pr phytochromes are converted to the biologically active Pfr form and translocated to the nucleus, where they modulate the activity of a variety of downstream transcription factors. Unlike phytochromes B – E, phyA is rapidly degraded in red light, but in response to far-red light is translocated into the nucleus together with FAR-RED ELONGATED HYPOCOTYL 1 (FHY1) and FHY1-LIKE (FHL). This activates far-red light signalling (Sakuraba and Yanagisawa, 2018).

The PHYTOCHROME INTERACTING FACTOR (PIF) family of proteins are members of the basic helix-loop-helix family of transcriptional regulators that can interact with the active phytochromes, and act as negative regulators in most phytochrome signalling pathways (Leivar and Quail, 2011). In Arabidopsis, all PIFs contain an active phyB binding (APB) motif necessary for interaction with PHYB, and two PIFs (PIF1 and PIF3) contain an additional phyA-binding (APA) domain (Khanna *et al.*, 2004). In the absence of phytochrome activation, inactive phytochrome (in the Pr form) is located in the cytosol, allowing the accumulation of PIF proteins in the nucleus. On exposure to light, inactive Pr phytochromes are converted to the biologically active Pfr form, translocated to the nucleus, and physically interact with PIF proteins (Al-Sady *et al.*, 2006). Interaction with phyA or phyB induces phosphorylation and subsequent ubiquitylation of PIFs, targeting the proteins for destruction via the 26S proteasome (Al-Sady *et al.*, 2006).

HY5 was first identified for its role in regulating plant growth in response to light (Osterlund *et al.*, 2000). LONG HYPOCOTYL 5 (HY5) and its functional homolog HY5 HOMOLOG (HYH) are bZIP transcription factors that act as positive regulators of phytochrome-regulated light signalling. Activity of HY5 and HYH proteins is controlled by the CONSITUTIVELY PHOTOMORPHOGENIC 1 (COP1) and SUPPRESSOR OF PHYA 1 (SPA1) complex (Osterlund *et al.*, 2000). The COP1-SPA1 complex destabilises HY5 and HYH via the E3 ligase activity of COP1, which causes ubiquitination of HY5 and HYH, targeting the proteins for degradation via the 26S proteasome (Saitjo *et al.*, 2003). Red-light activated PHYB prevents the COP1-SPA1 complex from forming, preventing degradation via the 26S proteasome - therefore under red light, the actions of PHYB enhance the activity of HY5 and HYH (Xu *et al.*, 2014).

HY5 activity has been shown to be controlled by multiple light signalling pathways. COP1-dependent HY5 degradation is affected by red, far-red and blue light (Osterlund *et al.*, 2000), and in addition PIF1 has been shown to regulate HY5 activity by physically interacting with the COP1-SPA1 complex, presumably to regulate HY5 and HYH activity in response to red light (Xu *et al.*, 2014). HY5 expression is also promoted by UV-B receptor UVR8, forming part of a positive feedback loop involved in the regulation of UV-B responses although the exact mechanism is not well understood (Huang *et al.*, 2012). HY5 activity is therefore altered by a range of light responses [**Figure 5**].

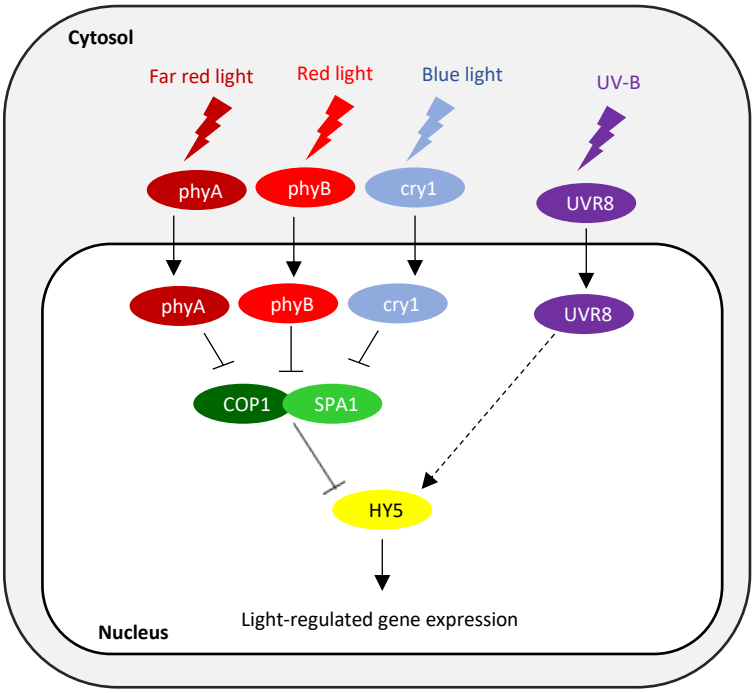


Figure 5: **HY5 activity can be modulated by a range of light signalling pathways.** Far-red, red and blue wavelengths of light convert specific photoreceptors (phyA, phyB and cry1 respectively) to their active forms, which can be translocated from the cytosol into the nucleus. Within the nucleus these activated photoreceptors interact with the SPA1-COP1 complex, preventing its activity and accumulation. The COP1-SPA1 complex targets HY5 for degradation via the 26S proteasome, relieving this inhibition therefore enhances activity of HY5 and downstream light-regulated gene expression. Diagram adapted from Sakuraba and Yanagisawa, 2018.

1.6.2 HY5 and N assimilation

Light is known to affect nutrient acquisition, and this is perhaps best understood with respect to nitrogen. Exposing 5 different plant species (wheat, soybean, tobacco, sunflower and maize) to light increases uptake of stable isotope-labelled nitrate ($^{15}NO_3^-$) and nitrite ($^{15}NO_2^-$) (Reed *et al.*, 1983). Similarly, in Arabidopsis NO_3^- and NH_4^+ uptake is higher in seedlings exposed to light than in the dark, and moving plants from darkness to continuous light has been shown to significantly increase the transcription of genes encoding root ion transporters, including those for nitrate, ammonium, phosphate, sulphate and potassium (Lejay *et al.*, 2003).

The first step of NO_3^- assimilation, the reduction of NO_3^- to NO_2^-, is catalysed by the NR enzyme. Light has been shown to regulate NR activity, with NR activity in etiolated terminal

pea buds induced by both white and red light. Induction was reversibly controlled by red and far red light, suggesting the involvement of phytochromes in regulating NR activity (Jones and Sheard, 1972). NR activity is strongly reduced in *hy5* Δ *hyh* seedlings under continuous red or far-red light, whilst *cop1* has a relatively high NR activity (Jonassen *et al.*, 2008). Expression of *NIA2*, the gene responsible for encoding the majority of Arabidopsis NR protein, was significantly reduced in the *hy5* Δ *hyh* mutant although expression of other nitrate-assimilation related genes, including *NIA1* and *GS2* genes encoding nitrite reductase and glutamine synthetase had no significant difference in expression levels compared to WT (Jonassen *et al.*, 2009). ChIP-chip assays have demonstrated HY5 can specifically bind to a putative HY5-binding site in the *NIA2* promoter, suggesting HY5 can directly regulate *NIA2* expression (Lee *et al.*, 2007).

Photosynthesis results in carbon fixation, and fixed carbon is primarily transported within plants as sucrose, produced in mesophyll cells and imported into the phloem for translocation throughout the plant. Using optical sensors, a subfamily of SWEET sucrose exporters has been identified, with AtSWEET11 and AtSWEET12 shown to localise to the phloem plasma membrane. These transporters mediate sucrose export from parenchyma cells, therefore controlling loading of sucrose to the phloem (Chen *et al.*, 2012). Leaf-derived sucrose promotes root development (Kircher and Schopfer, 2012) and root NO_3^- uptake (Lejay *et al.*, 2003), and providing plants with an exogenous source of sucrose upregulates expression of genes encoding the dual-affinity NO_3^- transporter NRT1.1, the high affinity NO_3^- transporter NRT2.1, and low affinity NO_3^- transporters NRT2.4 and NRT1.5 (Lejay *et al.*, 2008). The *hy5* mutant has reduced expression of *TPS1* (a gene encoding trehalose-6-phosphate synthase), *SWEET11* and *SWEET12*, with further ChIP

experiments indicating HY5 can bind to the promoters of *TPS1*, *SWEET11* and *SWEET12* directly (Chen *et al.*, 2016). HY5 therefore regulates both initial carbon fixation, and the subsequent loading of sucrose into the phloem for translocation from shoot to root.

HY5 is therefore suggested to be involved in the regulation of N acquisition at a variety of stages: promoting uptake in the roots, and promoting increased production of NR in the leaves, through both light and sucrose-mediated signalling (Chen *et al.*, 2016; Jonassen *et al.*, 2008). HY5 has also been shown to be involved in the regulation of both sucrose metabolism and transport. This sucrose-mediated pathway can therefore be considered an additional mechanism of light signalling-induced regulation of N uptake. HY5 is therefore a coordinator of growth and carbon assimilation, with roles in light signalling, sucrose transport and metabolism, and N acquisition (Chen *et al.*, 2016). HY5 is also mobile, linking shoot carbon assimilation with root NO_3^- acquisition: shoot-derived HY5 has been shown to act as a mobile signal, auto-activating root *HY5* expression, and upregulating expression of the *NRT2.1* nitrate transporter (Chen *et al.*, 2016). By regulating the carbon – nitrogen balance, HY5 therefore acts as a coordinator by which plants can balance their acquisition of nutrients with growth.

1.6.3 HY5 and S assimilation

In addition to regulating N acquisition, HY5 has been implicated in co-ordinating the metabolism of a range of other nutrients. Plants predominantly acquire sulphur (S) in the form of sulphate in soil, which is subsequently reduced and assimilated into cysteine. ChIP-seq suggested HY5 can bind to the promoter of the sulphate transporter gene *SULTR1;2* (Lee *et al.*, 2007), a subsequent ChIP assay with dissected regions of the *SULTR1;2* promoter confirmed selective binding of HY5 to a putative HY5-binding site (Lee *et al.*, 2011).

Additionally, the *hy5* mutant has reduced expression of *APR1* and *APR2*, two genes that encode a key enzyme of sulphate assimilation, adenosine 5'-phosphosulphate reductase.

Acquisition and assimilation of N and S need to be coordinated to optimise growth: substantial proportions of assimilated N and S are required for protein biosynthesis, and O-acetylserine, an essential metabolite for S assimilation, is supplied from N metabolism. In N-deficient conditions expression of *SULTR1;2* is significantly reduced, and APR activity lowered. Similarly, in conditions of S starvation, expression of the two genes encoding NR (*NIA1* and *NIA2*) was reduced also (Lee *et al.*, 2011). The HY5-mediated regulation of both pathways therefore contributes to the regulatory system that balances N and S assimilation in response to carbon fixation.

1.6.4 HY5 and Pi assimilation

In 2017 the *hy5-215* mutant was identified as having increased *PHR1* expression, suggesting that HY5 negatively regulates PHR1 expression, and therefore Pi starvation responses (Liu *et al.*, 2017). *hy5-215* seedlings were shown to have enhanced total Pi content and altered root-shoot ratios in response to phosphate starvation. This suggestion that HY5 may have a role in regulating plant phosphate metabolism was supported by the 2018 finding that *hy5* has reduced levels of root phosphate uptake, and that HY5 could directly bind the promoter of *PHT1;1*, which encodes one of the major root phosphate transporters in Arabidopsis (Sakuraba *et al.*, 2018). Together these studies provide the first published evidence that HY5 is also a regulator of phosphate metabolism, indicating HY5 may have a broad role in coordinating Arabidopsis nutrition.

1.7 Objectives of Thesis

This thesis aims to further understand the regulatory relationships coordinating plant N and P nutrition. I had three main objectives:

1.7.1 Objective 1: Understanding the role of CTR1 in modulating nitrogen metabolism

The ethylene signalling pathway is reasonably well understood, and ethylene signalling is known to have a role in regulating some aspects of nutrient metabolism. This thesis aimed to further explore the role of ethylene signalling in regulating nitrogen metabolism in Arabidopsis, in particular investigating the role of CTR1 and EIN2 in regulating NO_3^- acquisition. Whilst some studies have identified a limited role for ethylene signalling altering N metabolism, I aimed to explore this further through analysis of the *ctr1-1* mutant, using chlorate treatment and subsequent analysis of NO_3^- metabolism. The *ctr1* mutant is also dwarfed, and therefore has reduced growth. I identified mutagenized *ctr1* plants that retain chlorate resistance whilst losing their dwarfed phenotype, investigating further the interaction between nutrient metabolism and growth.

1.7.2 Objective 2: Exploring nitrogen metabolism in mutants lacking phosphate signalling components

Building on the previous observation that in bean plants reduced Pi availability causes a reduction in root NR activity (Gniazdowska and Rychter, 2000), I explored the role of Pi in regulating Arabidopsis nitrate metabolism. By utilising genetics approaches, using a range of mutants which have altered low-phosphate signalling pathways in addition to differing phosphate contents, I explored the role of known components of low-phosphate signalling on plant nitrate metabolism. I also explored the effects of different growth mediums on Arabidopsis chlorate resistance.

1.7.3 Objective 3: Understanding the role of HY5 as a regulator of phosphate metabolism

HY5 is a known regulator of some aspects of plant nutrition: coordinating NO_3^- uptake in response to carbon fixation, and subsequent regulation of nitrate metabolism via transcriptional control of the *NIA2* gene which encodes the majority of Arabidopsis NR. The presence of putative HY5 binding sites in the promoters of *PHT1* phosphate transporter genes suggests a role for HY5 in regulating Pi metabolism. I aimed to explore the potential role of HY5 in regulating P nutrition by examining Pi metabolism in a *hy5* mutant which does not produce a functional copy of the HY5 protein, and the role of HY5 in coordinating Pi metabolism with carbon fixation.

Overall, this thesis seeks to further our understanding of the regulatory relationships governing plant N and P nutrition and explore possible mechanisms behind this regulation.

Chapter 2: Materials and methods

2.1. Plant material and growth conditions

2.1.1 Compost

Seeds to be grown on compost were surface sterilised with 70% (v/v) ethanol and left to dry on filter paper. Seeds were sown on the surface of sieved compost (ICL Levington Advanced F2 compost, 144N 73P 239K, particles < 1 cm) and subsequently stratified in the dark at 4 °C for 2 – 4 days. After stratification plants were moved to controlled environment rooms (CERs) with a long-day photoperiod (16 h light/ 8 h dark) at 22 °C, irradiance 120 µmol of photons m^{-2} s^{-1}.

2.1.2 Agarose

Seeds to be grown on agarose (Merck Life Science, Dorset, UK) were surface sterilised with 70% (v/v) ethanol and left to dry on sterile filter paper. Agarose was used instead of agar to reduce the amount of residual Pi in the growth medium, since agarose generally contains less elemental contaminants than agar (Gruber *et al.*, 2013). The seeds were sown on the surface of half-strength Murashige and Skoog (½ MS) medium, pH 5.8, solidified with 0.8% (w/v) agarose (Murashige and Skoog, 1962). Seeds were sown at 10 mm intervals following a template on plates 120 mm square. The seeds were stratified at 4°C for 2 –4 days in the dark. After 5 – 7 days of growth, seedlings were transferred to plates of varying nutrient conditions for further experiments, seedlings were placed at 10 mm intervals following a template on plates 120 mm square, with 75 ml of media per plate.

Plates containing high / low phosphate consisted of adjusted ½ MS medium, pH 5.8 (0.055 µM $CoCl_2$, 0.05 µM $CuSO_4$, 50 µM FeNaEDTA, 50 µM H_3BO_3, 2.5 µM KI, 50 µM $MnSO_4$, 0.5 µM Na_2MoO_4, 15 µM $ZnSO_4$, 0.75mM $MgSO_4$, 1.5 mM $CaCl_2$, 10.3 mM NH_4NO_3 and 9.4 mM

KNO_3), with phosphate added in the form of K_2HPO_4 at the stated concentrations, and an appropriate amount of K_2SO_4 added to ensure the amount of K^+ ions remained constant. No sucrose was added to the media, unless stated otherwise.

2.1.3 Magenta Boxes

Plants grown on compost plugs within Magenta boxes were first grown on agarose as described in [**2.1.2**]. At 10 days old seedlings were transferred to hydrated Jiffy compost pellets, and enclosed within Magenta boxes sealed with 2 layers micropore tape.

2.1.4 Plant material

Arabidopsis seeds used in this study are listed in were all of the *Columbia* (Col-0) ecotype. T-DNA knock-out lines were obtained from the European Arabidopsis Stock Centre (NASC, UK, www.arabidopsis.info) and belonged to either the SALK or SAIL collection, the Noble Foundation (https://www.noble.org), or as otherwise listed [**Table 1**]. Seeds from external stocks were genotyped by PCR to confirm mutations were homozygous.

Genotype	Ecotype	Source	Stock ID
WT	Col	Lab stock	n/a
ctr1	Col	Lab stock	n/a
ein2	Col	Lab stock	n/a
ein3	Col	Lab stock	n/a
ein 3 Δ eil1	Col	Lab stock	n/a
etr1	Col	Lab stock	n/a
eto1	Col	Lab stock	n/a
eto2	Col	Lab stock	n/a
eto3	Col	Lab stock	n/a
eto1 etr1	Col	Lab stock	n/a
pho2-1	Col	NASC	N8508
phr1	Col	NASC	N686175
pht1;1 Δ pht1;4	Col	Noble Foundation	*pht1;1 Δ pht1;4*
hy5-526	Col	Lab stock	n/a
Mutagenized *ctr1* lines	Col	Lab stock (Zhong Jie Ding, unpublished data)	n/a

Table 1: *Arabidopsis* lines used in this study.

2.2. Plant phenotypic analysis

2.2.1 Chlorate treatment on compost

Chlorate treatment was applied to 4-5-week-old plants. Compost was allowed to dry (approx. 7 days without watering) and 1 L of 2.5 mM potassium chlorate solution applied to trays. After 2 h any solution not absorbed into the compost was discarded. Control plants were treated with water. Chlorate treatment was repeated up to 3 times total depending on severity of symptoms observed, with irrigation occurring when the compost surface was visibly dry.

2.2.2 Chlorate treatment on agarose

Chlorate treatment of plants on agarose was applied when plants were 4-5 weeks old. In order to mimic the treatment of plants on compost, concentrated chlorate solution was

applied to agarose plates under sterile flow hoods and plates left open for 3 h whilst the solution was absorbed.

2.2.3 Quantifying the colour change of plant rosettes following chlorate treatment

To gain a quantitative measure of how much susceptible plants were to chlorate treatment, photos of trays of chlorate-treated plants were analysed in imageJ (http://www.imagej.nih.gov/ij/) to determine the proportion of each rosette falling under green vs yellow hues. Images of individual rosettes were cropped and any leaves falling into the frame from other plants manually removed by selecting and clearing that area. Using the Image > Adjust > Color Threshold command, all areas of plant tissue in the image containing green hues was selected by setting the following parameters: Hue 41 - 90; Saturation 0 - 255 and Brightness 60 - 255. This area was measured (Analyse > Measure), and compared to the area of plant tissue occupied by yellow hues, measured by setting the parameters: Hue 1 - 40; Saturation 0 - 255; and Brightness 60 - 255. If necessary the brightness threshold was adjusted to ensure no background, and all plant tissue, was captured. The proportion of the total area measured occupied by green hues gave a visual indication of plant resistance to chlorate treatment and was calculated as follows:

$$\%\ rosette\ tissue\ remaining\ green = \frac{Area\ of\ green\ tissue}{Area\ of\ green\ tissue + Area\ of\ yellow\ tissue}\ x\ 100$$

2.2.4 Measurement of plant height

Plant height was measured from seven-week-old Arabidopsis plants, with a minimum of 12 plants analysed for each genotype. The maximal extension between the base of the rosette and the tips of the shoots were measured with a ruler, with the total length recorded to the nearest mm.

2.2.5 Root system architecture measurements

To determine the effects of phosphate on primary root elongation, following 8 days of growth at a 90° angle on ½ MS media solidified with 0.8% agarose, seedlings were transferred to media containing differing nutrient conditions, and the position of the root tip marked on the back of the plates. Plates were returned to the tissue culture room for a further 7 days and kept at a 90° angle. After 6 days the backs of the plates were imaged using a flatbed scanner (CanoScan 5600F, Canon) and the images analysed using ImageJ software (http://www.imagej.nih.gov/ij/). The neuronJ software plugin (http://www.imagescience.org/meijering/software/neuronj/) was used to measure the root length, from the position of the mark indicating root length at time of transfer to the root tip.

All emerged secondary roots that were clearly visible were counted to determine the number of lateral roots on individual plants.

2.2.6 Quantification of plant inorganic phosphate content

Plant inorganic phosphate content was measured using the malachite green method. Arabidopsis shoot tissue was collected, weighed, and ground to fine powder in liquid nitrogen and re-suspended in 10 µL mg^{-1} MES buffer (0.17 M MES, 100 mM DTT, pH 5.8). Samples were centrifuged at 17,115 x g. and supernatant recovered. 10 - 100 µL aliquots of each solution (700 µL final volume) were mixed with 120 µL of acid molybdate solution (17.55 g L^{-1} ammonium molybdate in 3 M H_2SO_4) and incubated for 10 minutes at room temperature. Then 120 µL of green malachite solution (3.5 g L^{-1} poly-vinyl alcohol (PVA), 0.35 g L^{-1} malachite green) was added and the samples mixed by inverting the tubes several times. After 2 h staining at room temperature the absorbance was measured at 600 nm

(OD_{600}) using the Evolution 260 Bio UV-Visible Spectrophotometer. Plant phosphate content was calculated by comparing to a standard curve created using serial dilutions of H_2PO_4.

2.2.7 Quantification of plant nitrate content

Fresh shoots and roots were excised, weighed and frozen in liquid N_2. Samples were ground in liquid nitrogen and 10 volumes ultrapure water added, and the sample incubated at 100°C for 60 minutes and vortexed at 10-minute intervals. Samples were then centrifuged at 4 °C at 20,400 x g for 10 minutes.

To determine nitrate content 40 µL of 0.5% (w/v) salicylic acid in sulphuric acid was added to 10 µL supernatant and mixed thoroughly, then incubated at room temperature for 20 minutes. 1 mL of 8% (w/v) NaOH in ultrapure water was added and vortexed until the contents was clear. Absorbance was measured using the Evolution 260 Bio UV-Visible Spectrophotometer at 410 nm (OD_{410}). Nitrate content was determined against a standard curve created using serial dilutions of $NaNO_3$.

2.2.8 Quantification of plant chlorophyll content

Chlorophyll was extracted according to Kim *et al.* (2003). Extraction took place at by immersing seedling shoot tissue in 95% ethanol (w/v) for 24 h in the dark at 4 °C. The mixture was then centrifuged and supernatant transferred to a cuvette. The absorbance of the supernatant was measured at 663 nm (OD_{663}) and 645 nm (OD_{645}) using the Evolution 260 Bio UV-Visible Spectrophotometer. The total of chlorophyll *a* and *b* was calculated using Arnon's equation:

$$\text{Total chlorophyll } a \text{ and } b \text{ (µg / mL)} = 20.2\ (A_{663}) + 8.02\ (A_{645})$$

Chlorophyll content was expressed relative to sample fresh weight for a minimum of 4 independent samples.

2.2.9 Quantification of plant anthocyanin content

Anthocyanins were extracted according to Jeong *et al.* (2010). Seedlings were grown on ½ MS solidified with 0.8% agarose for 4 days, and then transferred to media containing either 1000 µM, 100 µM or 10 µM phosphate concentration. After 12 days of further growth, shoot tissue was harvested for anthocyanin extraction. Shoots from 4-8 seedlings were harvested, weighed, and placed in 600 µL of 1% HCl in methanol (v/v) and then incubated overnight in the dark at 4 °C with gentle shaking. After extraction, 400 mL of water and 400 mL of chloroform were added to the extract and the sample mixed. After centrifugation at 14,674 x g for 2 min, the absorbance of the supernatant was measured at 530 and 657 nm, and the concentration of anthocyanin was calculated as follows:

$$\text{Total anthocyanin} = A_{530} - 0.25 \times A_{657}\, g^{-1}\ (FW)$$

Anthocyanin content was expressed relative to sample fresh weight for a minimum of 4 independent samples.

2.3. Protein extraction and measurements

2.3.1 Protein Extraction

Plant tissue (0.5 g of Arabidopsis rosette leaf) was harvested, ground to fine powder in liquid nitrogen and homogenised in 5 mL/ g extraction buffer (50 mM Potassium Phosphate (KH_2PO_4 pH 7.6), 1 mM Ethylenediaminetetraacetic acid (EDTA), 5 mM 1,4-Dithiothreitol (DTT), 0.5% Triton and 1x HALT™ Protease Inhibitor Cocktail (ThermoFisher) until thawed. 2 mL of protein extract was transferred to a separate Eppendorf tube and centrifuged at

17,115 x g for 15 minutes, before supernatant was collected and centrifugation repeated. 1 mL of protein extract was collected and kept on ice for further experiments.

2.3.2 Protein Quantification

Protein extract was quantified using the Bio-Rad DC colorimetric protein assay kit (Bio-Rad). Protein extracts from 2.3.1 were diluted five-fold with dH_2O and the assay performed according to manufacturer's instructions. Before quantification, the necessary solutions were prepared: both Solution A (alkaline copper tartrate solution) and Solution B (dilute folin reagent) were brought to room temperature, and 20 µL of Solution S (sodium dodecyl sulphate) added per mL of Solution A to create Solution A'. 25 µL of protein extract was mixed with 125 µL Solution A and 1 mL of Solution B, and mixed by vortexing. The reaction was incubated at room temperature for 30 minutes before being transferred to a cuvette and the absorbance measured at 750 nm (OD_{750}) using the Evolution 260 Bio UV-Visible Spectrophotometer (Thermo Scientific). The OD_{750} value was compared to a standard curve created using serial dilutions of bovine serum albumin (BSA) to calculate the protein content of the extract (expressed as mg protein mL^{-1}).

2.3.3 Nitrate Reductase Activity Assay

NR activity was measured using a modified protocol from Park *et al.*, 2011. 200 µL protein extract from 2.3.1 was added to 800 µL reaction buffer (50 mM KH_2PO_4 (pH 7.6), 5 mM EDTA, 10 mM KNO_3 and 0.2 mM NADH). The reaction was allowed to proceed for 30 minutes in the dark at room temperature. The reaction was stopped by adding 1 ml of 0.36 M Zinc Acetate (ZnAc), followed by centrifugation at 14,674 x g for 5 minutes. 500 µL of supernatant was transferred to a new tube, to which 1 mL of colour developer reagent (made up of equal volumes of 1% sulphanilamide in 3 M HCl and 0.02% N-(1-naphthyl)

ethylenediamine dihydrocholoride) was added. The reaction mixture was left in the dark for 30 minutes to allow colour development.

The concentration of nitrite was determined by measuring the absorbance at 540 nm (OD_{540}) on an Evolution 260 BIO UV-Visible Spectrophotometer. NR activity was expressed as the absorbance of the reaction mixture at 540 nm (A540) relative to the sample protein concentration.

2.3.4 Detection and quantification of root acid phosphatase activity

Seedlings were germinated on ½ MS media solidified with 0.8% agarose, and 4-day old plants transferred to either high (1000 µM), medium (100 µM) or low (10 µM) phosphate media. 7 days after transfer roots were stained for acid phosphatase activity. Roots were overlaid evenly with 0.5% (w/v) agar solution containing 0.01% (w/v) 5-Bromo-4-chloro-3-indolyl phosphate (BCIP). Plants were incubated at 24 h to allow blue colour development, before being imaged using a camera attached to a stereo-microscope.

Root APase activity was quantified using a protocol adapted from Wang and Liu, 2017. 4-day old plants were transferred to either high (1000 µM), medium (100 µM) or low (10 µM) phosphate media. 7 days after transfer portions of primary root were excised using a razor blade, measured, and immersed into 650 µL pre-warmed reaction buffer (10 mM $MgCl_2$, 50 mM NaAc, pH 4.9). 50 µl of *p*NPP solution (1 mg mL^{-1} *p*NPP dissolved in reaction buffer) was added and the mixture incubated at 37 °C for 1 h. The reaction was stopped by adding 100 µL of 0.4 N NaOH and shaking. APase activity was calculated from the production of *p*-nitrophenol, as determined by absorbance at 405 nm (OD_{405}) measured on using the Evolution 260 Bio UV-Visible Spectrophotometer.

2.4. DNA isolation and analysis

2.4.1 DNA extraction

Genomic DNA was extracted from leaf tissue using a Plant DNeasy Mini kit (Qiagen) according to the manufacturer's instructions. Once extracted, genomic DNA was flash-frozen and stored in aliquots at -20 °C until further use.

2.4.2 Confirmation of mutations

PCR amplification of sequences to confirm mutations used 5 units of Mango*Taq*™ polymerase (Meridian Bioscience) in a 47 µl reaction mixture (2 µl 5 µM primers [Table 2], 0.1 mM dNTPs, 10 µl 10 x Mango*Taq*™ Buffer, 1.5 µL 50 mM $MgCl_2$, and 1 µL 5 µM DNA). The PCR program used was as follows: A 2 minute initial denaturation at 94 °C was followed by 35 cycles of [60 seconds at 94 °C, 60 seconds at 59 °C and 2 minutes at 72 °C] finishing with a 10 minute extension at 72 °C. The size of products was determined by electrophoresis, running on a 1% agarose-gel, to determine if bands of expected size were produced. For any mutant lines containing point mutations, if a band of the expected size produced the product was purified using a PCR product purification kit (Qiagen). Purified PCR products were analysed on a spectrophotometer to check for DNA content, and then together with 5 µM sequencing oligo were sent for Sanger sequencing.

Sanger sequencing data were viewed in Chromas (http://technelysium.com.au/wp/chromas), and the sequence data copied and pasted into Clustal Omega (http://www.ebi.ac.uk/Tools/msa/clustalo) in FASTA format together with the TAIR 10 Col-0 reference sequence of that particular site (if the sequencing oligo was on the reverse strand, the reverse complement was used). Clustal Omega alignment of the two sequences enabled the location of any mutations to be determined.

Primer Name	Primer sequence (5' to 3')
pho2_genotyping_Fw	ACTGCTCGGACCATCATTTC
pho2_genotyping_Rv	ACTGGTGGCTCATGAGGATATTG
pho2_genotyping_Seq	TGGCTAGGAAATCAACAGAGAAT
phr1_genotyping_Fw	CAAATTCCGCAACCTCAGATTG
phr1_genotyping_Rv	GGCGAACCTGTAGTGATCAAAG
pht1;1_genotyping_Fw	TTCAAAATTTTGGCCATTGAG
pht1;1_genotyping_Rv	CCAAACATCGCACTCCAAATAAC
pht1;4_genotyping_Fw	CAGATCAGATCCCACATAAACTTTC
pht1;4_genotyping_Rv	ATGTCCGAAAGAGAGACCAGAG
T-DNA Lb-b1	TGGAACAACACTCAACCCTATC
T-DNA JL202	CATTTTATAATAACGCTGCGGACATCTAC

Table 2: Primers used for identification and verification of mutations

2.5. RNA isolation and cDNA synthesis

2.5.1 RNA extraction

Approximately 250 - 500 mg of Arabidopsis rosette leaf tissue was ground to fine powder in liquid nitrogen. 1 mL of TRIzol™ reagent (ThermoFisher) was added to each sample, mixed and incubated at 56 °C For 5 minutes. Following incubation, a centrifugation step of 12,000 g at 4 °C for 10 minutes occurred, the supernatant collected and mixed with 200 µL of chloroform, mixed and briefly left at room temperature, before being centrifuged at 4 °C for 15 minutes. The clear top layer of supernatant was collected and transferred to a new tube, with equal volumes of isopropanol added, and the samples left for 20 minutes on ice whilst the RNA precipitated. After precipitation the sample was spun at 4 °C at 12,000 g, the supernatant discarded and the pellet washed with 75% ice-cold ethanol. The sample was further centrifuged at 7,500 g for 5 minutes, the ethanol removed and the sample air-dried at 37 °C for 2 minutes. The RNA was dissolved in 50 µL dH_2O and stored at –80 °C.

2.5.2 DNAse treatment of RNA samples

RNA concentration was quantified with the Nanodrop ND-1000 Spectrophotometer (Thermo Scientific) and diluted to 200 µg/mL. 8 µL (1.6 µg) of RNA from 2.5.1 was transferred to a PCR tube, and 1 µL of 10 x reaction buffer and 1 µL of DNAse (Sigma-Aldrich, 1 unit / µL) added to the sample, mixed, and incubated at 37 °C for 30 minutes. The reaction was terminated by the addition of 1 µL of DNase stop solution (Sigma-Aldrich), followed by incubation at 65 °C for 10 minutes.

2.5.3 cDNA synthesis

Annealed RNA was prepared by adding 1 µL of 10 mM dNTPs (final concentration 0.5 mM) and 1 µL of 50 µM oligo d(T)20 to 11 µL (1.6 µg) of DNAse-treated RNA from 2.5.2. The sample was mixed and briefly centrifuged, incubated at 65 °C for 5 minutes, and then transferred to ice for at least 1 hour. A reverse-transcriptase reaction mix was prepared by vortexing and briefly spinning 5 x SSIV buffer, and mixing 4 µL of 5 x SuperScript^{TM} IV buffer with 1 µL of 100 mM DTT, 1 µL of Ribonuclease inhibitor and 200 units of Superscript reverse transcriptase (Invitrogen).

To synthesise cDNA, the reverse-transcriptase reaction mix was added to the annealed RNA, and incubated at 55°C for 10 minutes, followed by incubating at 80°C for 10 minutes. The resulting cDNA was stored at -20 °C until future use.

2.6. Semi-quantitative RT-PCR analysis of gene expression

For semi-quantitative analysis of gene expression, RT-PCR reactions were set up using 1 µL of cDNA and 5 µM of intron-spanning primers for genes of interest [Table 3] in a 47 µl reaction mixture [2.4.2]. Primers for *ACTIN2* and *CAP BINDING PROTEIN 20* (*CBP20*) were used as an internal normalisation and cDNA loading control. Titration of cycles determined

that the PCR amplification of *NIA1* and *NIA2* was within the linear range at 26 cycles using the following conditions: [94°C for 60 seconds, 56 °C for 60 seconds, 72°C for 2 minutes], and *ACTIN2* and *CBP20* at 26 cycles [94°C for 60 seconds, 59 °C for 60 seconds, 72°C for 2 minutes]. Similarly, PCR of *PHT1;1* and *PHT1;4* was performed under non-saturating conditions within the linear range (28 cycles at [94 °C for 60 seconds, 56 °C for 60 seconds, 72 °C for 2 minutes]), as was *NRT2.1* (28 cycles at [94 °C for 60 seconds, 59 °C for 60 seconds, 72 °C for 2 minutes]). The amount of PCR products was quantified by measuring band intensities on 1% agarose gels stained with ethidium bromide and analysed using VisionWorksLS software.

Primer Name	Primer sequence (5' to 3')
AtActin2_Fw	GGTACCGGTATGGTGAAGGCTG
AtActin2_Rv	GGCCTTTGGGTTAAGAGGAGCC
AtCBP20_Fw	GAAGGAAGACAATGGGGCCG
AtCBP20_Rv	GAAGGAAGACAATGGGGCCG
NIA1_Fw	AAACTCATCTGGAACCTCATG
NIA1_Rv	GAGGCACCATGAACTGAGAC
NIA2_Fw	GGGTTACGCATATTCCGGAG
NIA2_Rv	GCTTCTTGACCTCGGACATC
PHT1;1_Fw	TGGTCTCTCTTTTGGCCACG
PHT1;1_Rv	GAATTCCTTGGAGAACAAGCC
PHT1;4_Fw	TTGGACCCAATGCTACAACC
PHT1;4_Rv	TGAGTTGCTAGAGACAAGGAG
NRT2.1_Fw	TGAGAGGGAGGTTGTGGACG
NRT2.1_Rv	TGTTGGGTGTGTTCTCAGGC

Table 3: Primer sequences for RT-PCR analysis of gene expression

2.7. In silico searches for DNA binding motifs

The genomic DNA sequences for Arabidopsis thaliana (*Columbia* ecotype, *Col*) were obtained for genes of interest from The Arabidopsis Information Resource (TAIR,

https://www.arabidopsis.org/), and viewed by copying and pasting into SnapGene software (from GSL Biotech; available at snapgene.com). Putative binding sequences previously identified for PHR1, NIGT1 and HY5 were identified in the promoter region of genes of interest by searching using the SnapGene software. Unless otherwise stated, the DNA sequence up to 3000 bp prior to the ATG start codon for each gene of interest was searched.

2.8. Mutant Screen

2.8.1 Mutagenesis

Mutagenised *ctr1* lines used in this study were created by Ethyl Methane Sulfonate (EMS) mutagenesis by Zhong Jie Ding (unpublished data). Approximately 12,500 *ctr1-1* progenitor seeds were transferred to a falcon tube and washed with 0.1% Tween-20 for 15 minutes, this solution was removed and the seeds rinsed three times with dH_2O prior to adding 50 ml of 0.4% EMS solution. The seeds in EMS solution were mixed on a benchtop shaker for 8 hours in darkness, after which seeds were rigorously washed with dH_2O 10 times. The seeds were then soaked in 50 ml dH_2O, and the tube agitated on a benchtop shaker for 1 hour to allow any residue EMS to diffuse out of the seeds. The seeds were subsequently left to dry overnight on filter paper.

Following EMS treatment, seeds were mixed with approximately 130 g of sand, and 10 g of sand/ seed mixture sown on trays of Levington's F2 compost mix. Seeds were grown under standard conditions [2.1.1], allowed to self-fertilise and the M2 bulked seeds harvested to screen for phenotypes of interest.

2.8.2 Screening lines of interest

M2 seeds from 30 families were screened for chlorate resistance by sowing approximately 10,000 seeds on Levington's F2 compost mix and irrigated with water until 4 weeks post-germination. At 4 weeks compost was allowed to dry and plants irrigated with 2.5 mM $KClO_3$ solution. Trays were soaked in this solution for 2 h after which any remaining solution was drained. Irrigation with 2.5 mM $KClO_3$ solution was repeated 5 weeks post-germination also.

Plants displaying increased phenotypes of interest [**Figure 6**] were identified and rescued by transplanting to fresh compost. M3 plants were characterised further by testing chlorate resistance, NR activity and growth compared to the *ctr1-1* parental line and WT Col-0 background.

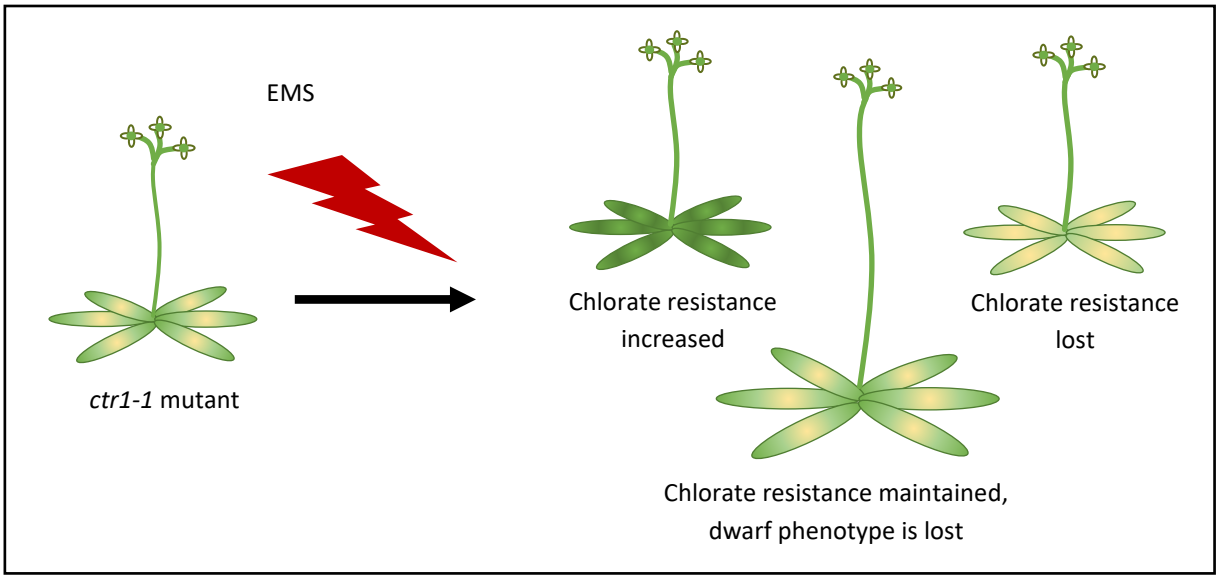


Figure 6: Schematic of mutant screen being used to search for new regulators of ethylene-mediated N metabolism. Screening ~10,000 mutagenised *ctr1-1* plants with chlorate treatment identified three phenotypes of interest. Lines were identified which retained the dwarfed phenotype of *ctr1-1*, but with either increased or reduced resistance, and lines were identified which maintained the chlorate resistance of *ctr1-1*, whilst losing the dwarfed stature characteristic of the *ctr1-1* mutant.

2.9. Image capture

2.9.1 Photographs of plants on compost

An Honor 10 smartphone with digital camera (model COL-L29) captured images which were subsequently stored in jpeg format. Settings for the digital camera were the following: aperture = f/1.8, shutter speed = 1/100 s, ISO = 400, exposure compensation = 0, AF type = AF-C.

2.9.2 Photographs of plants on plates

Plates were scanned using a flatbed scanner (CanoScan 5600F; Canon).

2.10. Statistical Analyses

Student's t-test and R^2 values of linear regression models were calculated in Microsoft Excel. For comparison across multiple groups, the statistical package R was used: ANOVA followed by TukeyHSD was used to determine statistical significance.

2.11. Chemicals and Primers

Chemicals used in this study were purchased from Duchefa Biochemie (www.duchefa-biochemie.com), Fisher Scientific (www.fishersci.co.uk) or Sigma-Aldrich (www.sigmaaldrich.com) unless specified otherwise. Chemical solutions were prepared with de-ionised water (dH_2O) and sterilised before use. Sterilisation was performed by autoclaving for 20 minutes at 121 °C under 100 kPa pressure. Chemicals that were heat unstable were sterilised by passing through 0.2 µm syringe filters (VWR, www.uk.vwr.com). Primers used for PCR reactions and Sanger sequencing were purchased from Sigma-Aldrich.

2.12. Centrifugation

Centrifugation was carried out using a MiniSpin plus centrifuge machine (Eppendorf), at room temperature unless otherwise specified.

Chapter 3: Ethylene signalling modulates *Arabidopsis thaliana* nitrate metabolism

This chapter reports several results subsequently published in Jamieson *et al.*, 2022 – contained within Appendix 1.

3.1 Introduction

Whilst there have been some studies investigating the role of ethylene in regulating N metabolism, there is scope to understand the role of this hormone in plant N nutrition further.

As discussed in **Chapter 1**, ethylene has been identified as playing a role in plant adaptation to increased NO_3^- availability, with a burst of ethylene inducing altered LR development, and changes in nitrate transporter expression levels, in seedlings transferred from low to high NO_3^- concentrations (Tian *et al.*, 2009). In this study, ethylene was shown to increase expression of the *NRT1.1* transporter, whilst reducing *NRT2.1* expression, and *etr1* and *ein2* mutants with reduced ethylene responses were less responsive to external NO_3^- levels in terms of changing their root system architecture. Another study in mustard suggested that when NO_3^- concentration is high, ethephon application (which induces ethylene release in plant tissues) increased NR activity, although the role of ethylene when NO_3^- concentration was low was less clear, with no obvious trend observed (Khan *et al.*, 2008). There is therefore evidence that ethylene can regulate plant N nutrition, however, these studies both focus on the short-term regulation of N metabolism via bursts of ethylene production. This leaves considerable scope to understand the role of ethylene signalling in regulating plant N nutrition at a whole-plant level.

Previous work has focussed on ethylene-mediated regulation of N metabolism in specific plant tissues. To investigate the role of ethylene signalling at the whole-plant level, and over longer time scales, I examined mutants impaired in the production of ethylene signalling components to determine the long-term effects of alterations in ethylene signalling pathways on plant N metabolism.

An important method previously used to identify differences in N metabolism is applying potassium chlorate solution ($KClO_3$) to plants. Chlorate is a structural analogue of nitrate. This structural similarity allows the NR enzyme of bacteria, fungi, algae (Cove, 1976) and higher plants (Murphy and Imbrie, 1981) to readily convert chlorate to chlorite. Chlorate can be taken up through nitrate transport systems where it is transported to the leaves and reduced to chlorite by NR. Unlike nitrite, chlorite is toxic to plants, and Arabidopsis plants grown on compost treated with chlorate solution display toxicity – noticeably visible chlorosis of leaves. Resistance to chlorate can therefore be used as a proxy measure to identify potentially altered NO_3^- metabolism. Several components involved in NO_3^- metabolism have been identified by treating mutagenized populations of Arabidopsis with chlorate and screening for plants showing increased resistance, for example the chlorate-resistant mutant *chl1*, subsequently identified as containing a loss of function mutation in the *nrt1.1* NO_3^- transporter (Tsay *et al.*, 1993).

In this chapter I specifically investigated the role of CTR1 in regulating Arabidopsis N metabolism; CTR1 is a negative regulator of ethylene signal transduction (see **Chapter 1**). The *ctr1-1* loss-of-function mutant maintains constitutive ethylene signalling and has a characteristic phenotype. Seedlings display a constitutive triple response, even in the absence of ethylene: a short root, short and thick hypocotyls, and exaggerated apical hook.

Mature plants are noticeably dwarfed, with small rosette leaves, short stems, and have delayed flowering compared to WT (Achard *et al.*, 2007). Plant lines containing loss-of-function mutations in *CTR1* are particularly interesting because they are dwarfed. If the characteristics of being dwarfed and having altered nutrient metabolism can be separated, this may identify new targets to improve crop nutrient efficiency without impairing crop growth and subsequently crop yield.

3.2 Results and discussion

3.2.1 *ctr1-1* has increased resistance to chlorate treatment

As discussed in **3.1**, treating plants with chlorate solution enables potential differences in nitrate metabolism to be visually observed. Treating 6-week-old WT Arabidopsis with 2.5 mM chlorate solution causes clear visual chlorosis of leaves, whilst the *nrt1.1* mutant (which lacks a nitrate transporter, and therefore has greatly reduced chlorate uptake) has a strong chlorate-resistance phenotype (Ho *et al.*, 2009) [**Figure 7A**]. Treating 6-week old *ctr1-1* lines with 2.5 mM potassium chlorate solution indicates that *ctr1-1* is also strongly resistant to chlorate treatment compared to WT [**Figure 7A**]. Like *nrt1.1*, the rosette tissue of *ctr1-1* plants is visibly still green following chlorate treatment, unlike that of chlorate-treated WT plants [**Figure 7A**].

The resistance of plants to chlorate treatment can be quantified by using imageJ to measure the area of leaf rosette tissue containing green hues, and expressing this as a percentage of the total leaf rosette area. Comparing the percentage of leaf rosette tissue remaining green following chlorate treatment, and comparing this to control-treated plants, gives a quantitative measure of chlorate resistance. Analysing the percentage of green shoot tissue indicates that there is no significant difference in the percentage of

green tissue between control-treated WT, *ctr1-1* and *nrt1.1* plants [**Figure 7B**]. However, following chlorate treatment only 25% of WT rosette tissue remains green, whilst *nrt1.1* has no significant difference between the percentage of green rosette tissue in control-treated and chlorate-treated plants. Approximately 80% of *ctr1-1* rosette tissue remains green following chlorate treatment, indicating that this genotype is strongly resistant to chlorate treatment, albeit not quite to the same level as *nrt1.1* [**Figure 7B**].

There are two potential hypotheses that could explain why *ctr1-1* could have increased chlorate resistance if this resistance is caused by perturbed N metabolism. Either the amount of chlorate entering the plant is reduced, and so fewer chlorate ions are reduced to toxic chlorite ions, or, if the amount of chlorate entering the plant is unchanged, altered metabolic processes in the *ctr1-1* mutant could provide greater resistance to the toxic effects of chlorate treatment – for example, the amount of chlorite being produced by the NR enzyme could be reduced. It is also possible that chlorate resistance could be altered due to changed metabolic processes unrelated to N metabolism. However, given that chlorate is a structural analogue of nitrate, it is plausible that since chlorate metabolism is altered in *ctr1-1*, nitrate metabolism could be altered too, since both nitrate and chlorate use some of the same metabolic machinery (nitrate transporters and the NR enzyme). This result therefore suggests that CTR1, and the ethylene signalling pathway that this protein is a crucial part of, may modulate Arabidopsis nitrate metabolism in some as yet unknown capacity.

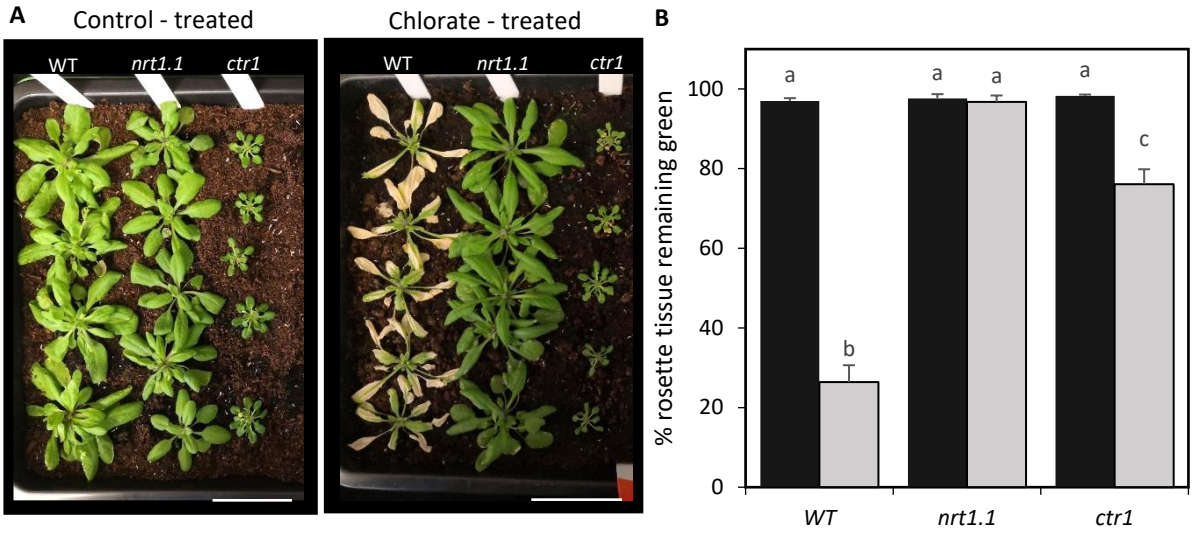


Figure 7: *ctr1-1* plants are strongly resistant to chlorate treatment compared to WT. [**A**] 6-week-old WT (Col) and *ctr1-1* plants following treatment with either water (control) or 2.5 mM chlorate solution (chlorate-treated) applied to the soil. 8 days after treatment plants were photographed, image shows plants with stems removed. Whilst WT plants display visible chlorosis following chlorate treatment, *nrt1.1* and *ctr1-1* plants are strongly resistant with leaves remaining green. Scale bars = 50 mm. [**B**] Individual rosettes were analysed in imageJ to determine the proportion of rosette tissue that remained green following treatment with either control or chlorate solution. Dark bars denote control plants (treated with water), lighter bars denote chlorate treated plants. Values are means ± S.D. Different letters denote statistically significant differences (one-way ANOVA/Tukey HSD post hoc test, $p < 0.05$, $n = 4$). The experiment was repeated independently 3 times with similar results.

3.2.2 *ctr1-1* has reduced Nitrate Reductase activity

To investigate the mechanism of *ctr1-1* chlorate resistance further, NR activity of *ctr1-1* and WT leaf extracts were measured *in vitro*. Leaves from 5-week old *ctr1-1* plants had a significantly reduced NR activity compared to WT, retaining approximately 50% of WT enzyme activity [**Figure 8**]. Since 50% of activity remains it is unclear whether the reduction in enzyme activity alone is sufficient to account for all of the strong chlorate resistant phenotype of the *ctr1-1* mutant.

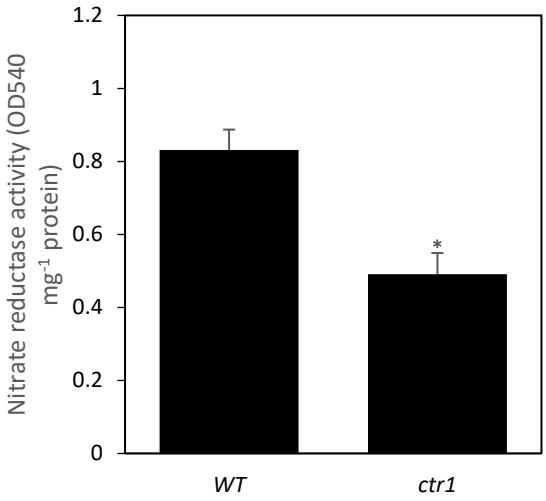


Figure 8: The *ctr1-1* mutant has significantly reduced nitrate reductase activity compared to WT. The NR activity of 5-week-old WT and *ctr1-1* shoot tissue was measured relative to leaf protein content. *ctr1-1* has significantly reduced NR activity compared to WT (* denotes statistically significant difference, student's t-test, $p < 0.05$, $n = 4$). The experiment was repeated independently 4 times with similar results.

3.2.3 *ctr1-1* has reduced NIA gene expression

The NR enzyme is encoded by two genes in Arabidopsis, *NIA1* and *NIA2*. To determine if the difference in NR activity was likely due to changes at the transcriptional or post-transcriptional level, I measured the relative expression of the *NIA1* and *NIA2* genes that encode NR in WT and *ctr1-1*.

As expected, in WT plants *NIA2* was expressed at a much greater level than *NIA1*, this was the same for *ctr1-1* also [**Figure 9**]. There was no observable difference in expression of *NIA1*, however, *ctr1-1* has slightly reduced expression of *NIA2*, which is believed to encode approximately 90% of NR in Arabidopsis. In the *ctr1-1* line expression was reduced by approximately 15% compared to WT, it is therefore uncertain whether this change in transcription is sufficient to account for the difference in altered NR activity and strong chlorate-resistant *ctr1-1* phenotype [**Figure 9**].

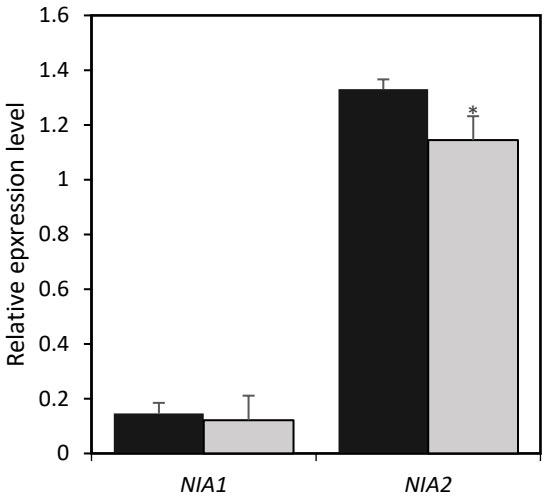


Figure 9: *ctr1-1* has reduced expression of *NIA2*. The expression levels of *NIA1* and *NIA2* were measured relative to the control gene *CAP BINDING PROTEIN 20* (*CBP20*) in WT (dark bars) and *ctr1-1* (light bars) using semi-quantitative RT-PCR. The experiment was repeated independently 3 times with similar results.

3.2.4 *ctr1-1* does not have an altered shoot nitrate content

In addition to lowered NR activity, it is also possible that the strong chlorate-resistance phenotype of *ctr1-1* is due to a reduction in shoot chlorate content caused by altered uptake and/or transport of chlorate ions. If this is the case, then it might be expected *ctr1-1* plants would have a reduced shoot nitrate content. Measuring the shoot nitrate content of WT, *nrt1.1* and *ctr1-1* plants, relative to fresh weight of shoot tissue, indicated that whilst the shoot nitrate content of the *nrt1.1* mutant, which lacks a major nitrate transporter, was significantly reduced compared to WT, there was no significant difference in the shoot nitrate content of WT and *ctr1-1* [**Figure 10**]. This suggests that the chlorate-resistant phenotype of *ctr1-1* is not due to differences in shoot chlorate content, and is instead due to the reduced NR activity [**Figure 8**]. These results are consistent with previous observations of the reduced nitrate content of *nrt1.1* (Wang *et al.*, 2009), although further replication would be desirable.

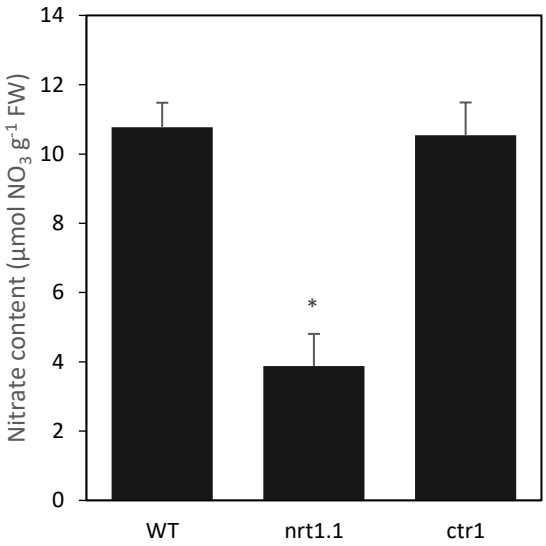


Figure 10: Nitrate content of WT, *nrt1.1* and *ctr1-1* plants. The shoot nitrate content of 4-week-old WT, *nrt1.1* and *ctr1-1* plants was measured relative to fresh weight. Error bars denote S.D, n = 5. * denotes statistical difference to WT (student's t-test, $p < 0.05$).

3.2.5 Despite being dwarfed, growth of *ctr1-1* is still altered by nitrogen availability

Since *ctr1-1* appears to have altered nitrate metabolism, it is conceivable that *ctr1-1* would have altered growth in response to lowered N provision. It might be argued that dwarfed genotypes, such as *ctr1*, are more likely to have resistance to chlorate treatment due to a presumably lower N demand, since less growth is occurring in dwarfed lines. However, a colleague (Zhe Ji) has shown that other dwarfed lines can retain susceptibility to chlorate treatment (Jamieson *et al.*, 2022), and so the presence of a dwarfed phenotype does not necessarily confer enhanced resistance to chlorate treatment. To investigate this idea further, I grew WT and *ctr1-1* plants on different concentrations of different N sources, to see if *ctr1-1* was more resistant to growth-inhibiting effects of nutrient depletion compared to WT, or indeed more susceptible to toxicity caused by high N concentrations. If this was the case, it would lend support to the idea that the chlorate-resistant phenotype of *ctr1-1*

is in part due to its dwarfed stature reducing nutrient demands, as well as indicating whether root developmental responses to N are altered in *ctr1*.

WT and *ctr1-1* plants were therefore grown on ½ MS media and at 4 days old transferred to media containing either high (20 mM) or intermediate (2 mM) N [**Figure 11**]. Previous work has demonstrated that 2 mM nitrate concentrations are sufficient to restrict growth of Arabidopsis (Loudet *et al.*, 2003; Lemaître *et al.*, 2008), whilst 20 mM provides N-replete conditions when provided in the form of NO_3^- without causing NO_3^- toxicity (Verly *et al.*, 2020). In addition, N was provided in the form of ammonium nitrate and ammonium only (NH_4) at the same N concentrations [**Figure 11**].

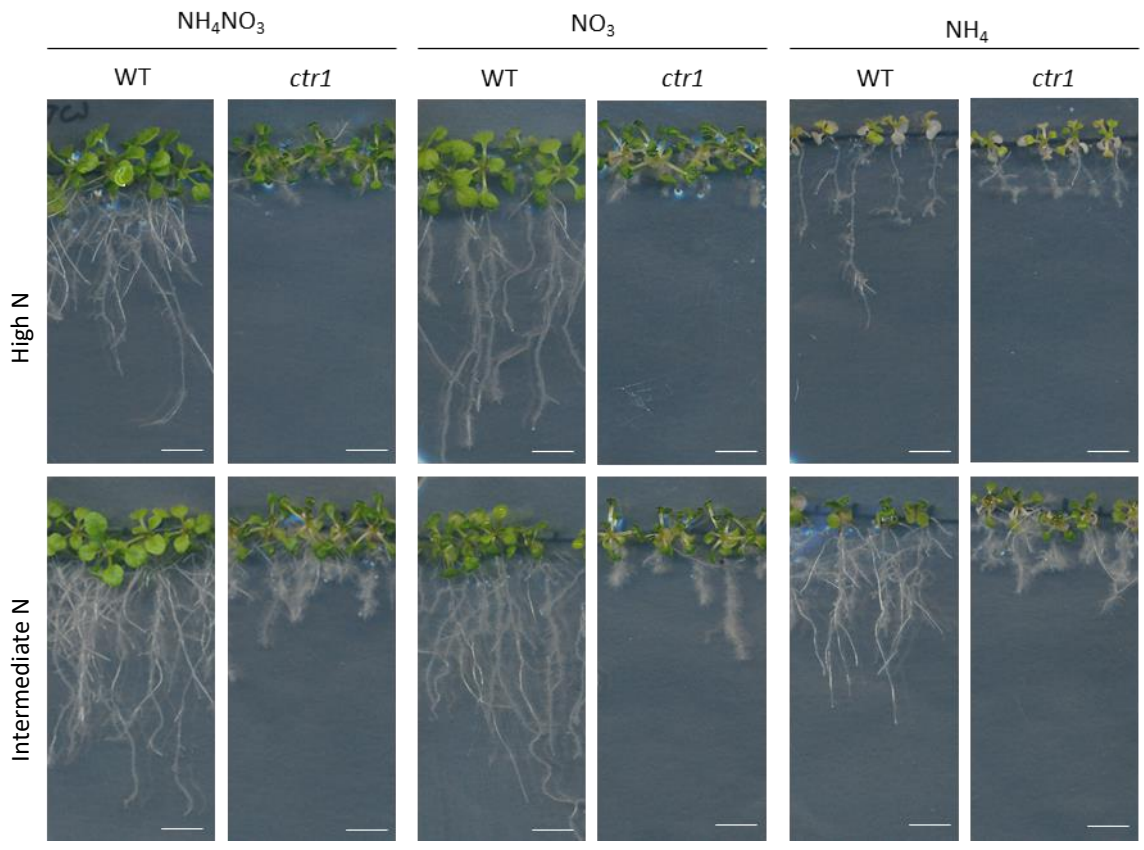


Figure 11: WT and *ctr1-1* plants grown on a variety of different nitrogen sources. WT and *ctr1-1* seedlings were grown on ½ MS solidified with 0.8% (w/v) agarose before being moved to agarose containing either high (20 mM) or intermediate (2 mM) N, in the form of NH_4NO_3 (provided at 10 mM and 1 mM concentrations), NO_3^- or NH_4^+. Plants were imaged 2 weeks after transfer; representative seedlings shown.

A common developmental adaptation to changes in N supply is a change in primary root growth. I therefore measured primary root growth of WT and *ctr1-1* seedlings grown on different N sources, to determine whether *ctr1-1* root growth responses were altered in response to low N provision, which might indicate a difference in sensitivity to N depletion.

When N was provided in the form of ammonium nitrate (NH_4NO_3), primary root length of WT plants increased in intermediate (1 mM) relative to high (10 mM) conditions [**Figure 12**]. This was true for *ctr1-1* also, which like WT had significantly longer roots in seedlings grown on 1 mM NH_4NO_3 from 4 days after transfer [**Figure 12**], despite seedlings root growth being significantly reduced compared to WT in all conditions, as would be expected for a genotype that is significantly dwarfed. This suggests that *ctr1-1* responds to lowered availability of NH_4NO_3, at least in terms of primary root development, in the same way as WT and that 1 mM NH_4NO_3 is sufficient for low N- induced changes in root development to occur in the *ctr1-1* mutant.

As has been previously reported, providing N solely in the form of NO_3 at high and low concentrations caused no difference in primary root elongation in WT plants. This was also seen in *ctr1-1* plants, with no significant difference in primary root length seedlings transferred to either 2 mM or 20 mM NO_3 provision at any of the stages measured [**Figure 12**].

Providing N solely as ammonium causes toxicity at high concentrations, which can be seen by the leaves of both WT and *ctr1-1* plants showing visible yellowing in 20 mM NH_4 conditions compared to leaves of seedlings grown in 2 mM NH_4 or on alternative N sources [**Figure 11**]. High NH_4 conditions are well known to inhibit growth of primary roots (Britto and Kronzucker, 2002), this is seen in both WT and *ctr1-1* plants [**Figure 12**]. Both

genotypes have significantly shorter primary roots in seedlings grown on 20 mM NH_4 compared to seedlings grown on 2 mM NH_4 when measured 10 days after transfer [**Figure 12**].

ctr1-1 seedling root growth, despite being reduced compared to WT plants, is therefore still responsive to changes in external N concentration for different N sources. When provided in the form of NH_4 or NH_4NO_3, reduced concentrations of N cause increased root growth compared to higher N concentrations, suggesting the *ctr1-1* mutant is still susceptible to lowered N availability, at least in terms of primary root growth responses, despite being dwarfed.

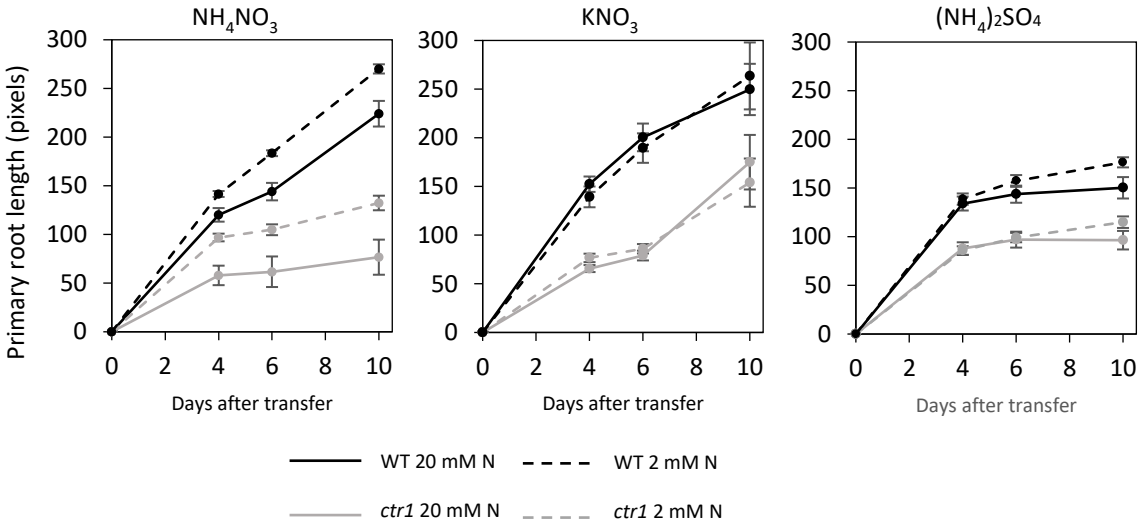


Figure 12: Effects of high and low nitrogen provision on primary root length of *ctr1-1* plants. WT and *ctr1* seedlings were grown on ½ MS solidified with 0.8% (w/v) agarose before being moved at 4-days-old to agarose containing either 20 mM or 2 mM N, in the form of NH_4NO_3 (provided at 10 mM and 1 mM concentrations), NO_3^- or NH_4^+. The position of plant primary roots was recorded at the time of transplant and further primary root growth measured and analysed using Image J. The experiment was repeated independently 3 times with similar results.

Another common developmental response to changing nutrient availability is a changing ratio of shoot: root biomass. Lowered nutrient availability encourages a greater proportion of plant biomass to be invested in the roots relative to shoots, in order to scavenge

nutrients from a greater area of soil. This results in a decrease in the shoot: root biomass ratio as a lowered proportion of resources goes to shoot growth. I therefore measured the shoot: root biomass WT and *ctr1-1* seedlings three weeks after transfer to different nutrient conditions to determine whether *ctr1-1* displayed significant changes in biomass allocation in response to nutrient deprivation, despite being dwarfed.

As expected, WT seedlings transferred to 1 mM NH_4NO_3 display a significant reduction in their shoot: root biomass ratio compared to those transferred to 10 mM NH_4NO_3 [**Figure 13**]. This is true for *ctr1-1* also. The same trend is observed in seedlings transferred to 2 mM and 20 mM NH_4; both WT and *ctr1-1* have a significant reduction in shoot: root biomass in seedlings transferred to 2 mM NH_4 rather than 20 mM NH_4 [**Figure 13**]. Neither WT nor *ctr1-1* displayed a significant difference in the shoot: root biomass ratio of plants transferred to 2 or 20 mM NO_3, perhaps not surprising given that 2 mM NO_3^- did not cause a difference in primary root growth for either genotype [**Figure 12**]. Overall, these results indicate that *ctr1-1* is as susceptible as WT to change in biomass allocation in response to N deprivation, despite the dwarfed phenotype of this genotype.

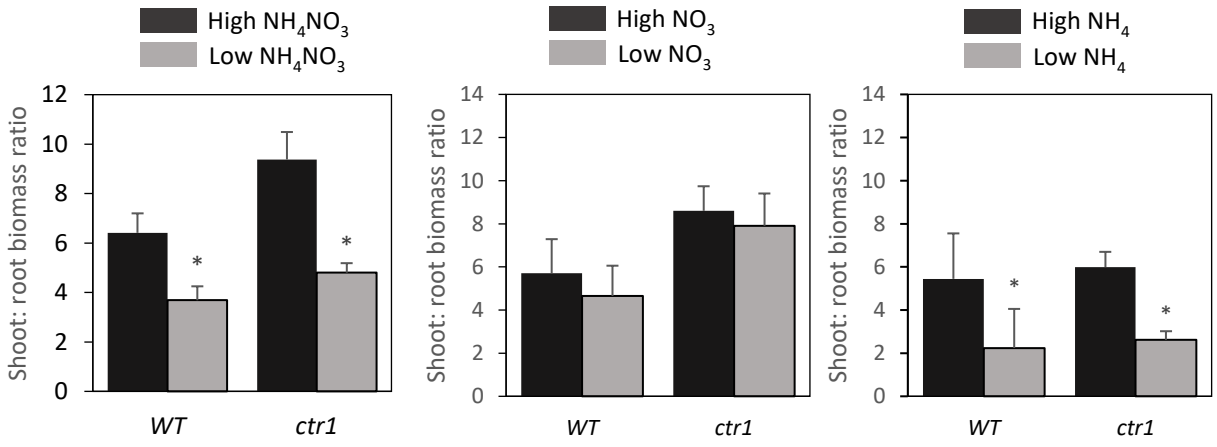


Figure 13: Effects of high and low N provision on shoot: root ratio of WT and *ctr1-1* plants. WT and *ctr1-1* seedlings were grown on ½ MS solidified with 0.8% (w/v) agarose before being moved to agarose containing either high (20 mM) or low (2 mM) nitrogen, in the form of NH_4NO_3 (provided at 10 mM and 1 mM

concentrations), NO_3^- or NH_4^+. At 3 weeks old plants were harvested and the root and shoot biomass recorded, allowing the shoot: root ratio to be calculated. * denotes statistically significant difference between high and low N within the same genotype (WT or *ctr1*), $p < 0.05$, student's T-Test. n = 5 pools of seedlings, error bars denote SD. The experiment was repeated independently 3 times with similar results.

3.2.6 Altered nitrogen metabolism in mutants lacking components of ethylene biosynthesis and ethylene signalling

ctr1-1 therefore has a strongly chlorate resistant phenotype, likely due to reduced NR activity, and despite being dwarfed still displays altered growth when N availability is reduced. In the *ctr1-1* mutant the ethylene signalling pathway is constitutively active, indicating that the ethylene signalling pathway could be implicated in regulating chlorate susceptibility, and NR activity, in Arabidopsis.

To further investigate the contribution of the ethylene signalling pathway to regulation of Arabidopsis N metabolism, I analysed the chlorate susceptibility and NR activity of several Arabidopsis lines containing mutations in genes encoding other proteins involved in the ethylene signalling pathway.

The precursor of ethylene is *S*-adenosylmethionine (*S*-AdoMet), which is converted to 1-aminocyclopropane-1-carboxylic acid (ACC) by the enzyme ACC synthase (ACS). ACC is in turn oxidised by ACC oxidase (ACO) to form ethylene, CO_2 and cyanide. The ethylene over-producing mutants *eto2* and *eto3* contain mutations in *ACS5* and *ACS9* respectively, with *eto2* containing a dominant mutation in the *ACS5* C-terminus, which normally has negative regulatory function (Vogel *et al.*, 1998). This is analogous to the mutation in *ACS9* of *eto3*, which contains a missense mutation in the C-terminus of this gene, resulting in both lines having enhanced ethylene production (Chae *et al.*, 2003). ETO1 negatively regulates ethylene production via a dual mechanism, both directly inhibiting the enzyme activity of

ACS and additionally targeting ACS for degradation (Wang *et al.*, 2004); the *eto1* mutant has enhanced ACS activity, also resulting in ethylene over-production.

The *eto1*, *eto2* and *eto3* lines therefore have enhanced ethylene production. In addition to lines with enhanced ethylene production, mutant lines with reduced ethylene sensitivity were also analysed. The *ein2* mutant lacks EIN2, which mediates an essential step between CTR1 and EIN3 in the ethylene signalling pathway (see **Chapter 1**), *ein2* loss-of-function mutations cause an ethylene-insensitive phenotype. Loss-of-function mutations in the genes encoding EIN3 and EIN3-LIKE (EIL1) mutations cause partial ethylene insensitivity, and therefore have an opposing phenotype to *ctr1*. The *etr1-1* mutant was also investigated, containing a mutation in the gene encoding ETR1 which confers dominant ethylene insensitivity (Gamble *et al.*, 2002). Analysing these mutants with reduced ethylene signalling allows the effects of reduced ethylene signalling on chlorate sensitivity and NR activity to be analysed, and compared to the results of the *ctr1-1* mutant.

3.2.7 The *eto2* & *eto3* mutants show a slight increase in resistance to chlorate treatment, whilst *eto1, etr1* and *eto1 etr1* appear as susceptible as WT

To determine further the role of the ethylene signalling pathway in modulating chlorate sensitivity, the chlorate susceptibility of a number of mutants impaired in either ethylene biosynthesis, or ethylene signalling, was tested.

The ethylene over-producing mutants *eto1*, *eto2* and *eto3* displayed varying sensitivity to treatment with chlorate solution [**Figure 14A**]. None of the lines tested appeared as resistant to chlorate treatment as either *nrt1.1* or *ctr1*. Whilst *eto1* appears very similar to WT, with visible widespread yellowing of the majority of leaves, *eto2* and *eto3* appear more resistant to chlorate treatment than WT and *eto1*, with younger rosette leaves having a

greener appearance, although not to the same extent as *ctr1-1* or the *nrt1.1* control [**Figure 14A**]. Neither the *etr1* mutant nor the *eto1 etr1* double mutant displayed a significant difference in chlorate sensitivity compared to WT, with widespread yellowing of leaves present in both genotypes following chlorate treatment [**Figure 14A**].

Using ImageJ to quantify the proportion of visible rosette tissue that remains green following treatment supports these observations: *eto1*, *etr1* and *eto1 etr1* have no significant difference in the percentage of green rosette tissue compared to WT (approximately 17% of leaf tissue remains green), whilst both *eto2* and *eto3* rosettes have approximately 40% green leaf tissue, therefore higher than WT but lower than *ctr1-1* (62%) and *nrt1*.1 (98%) [**Figure 14B**].

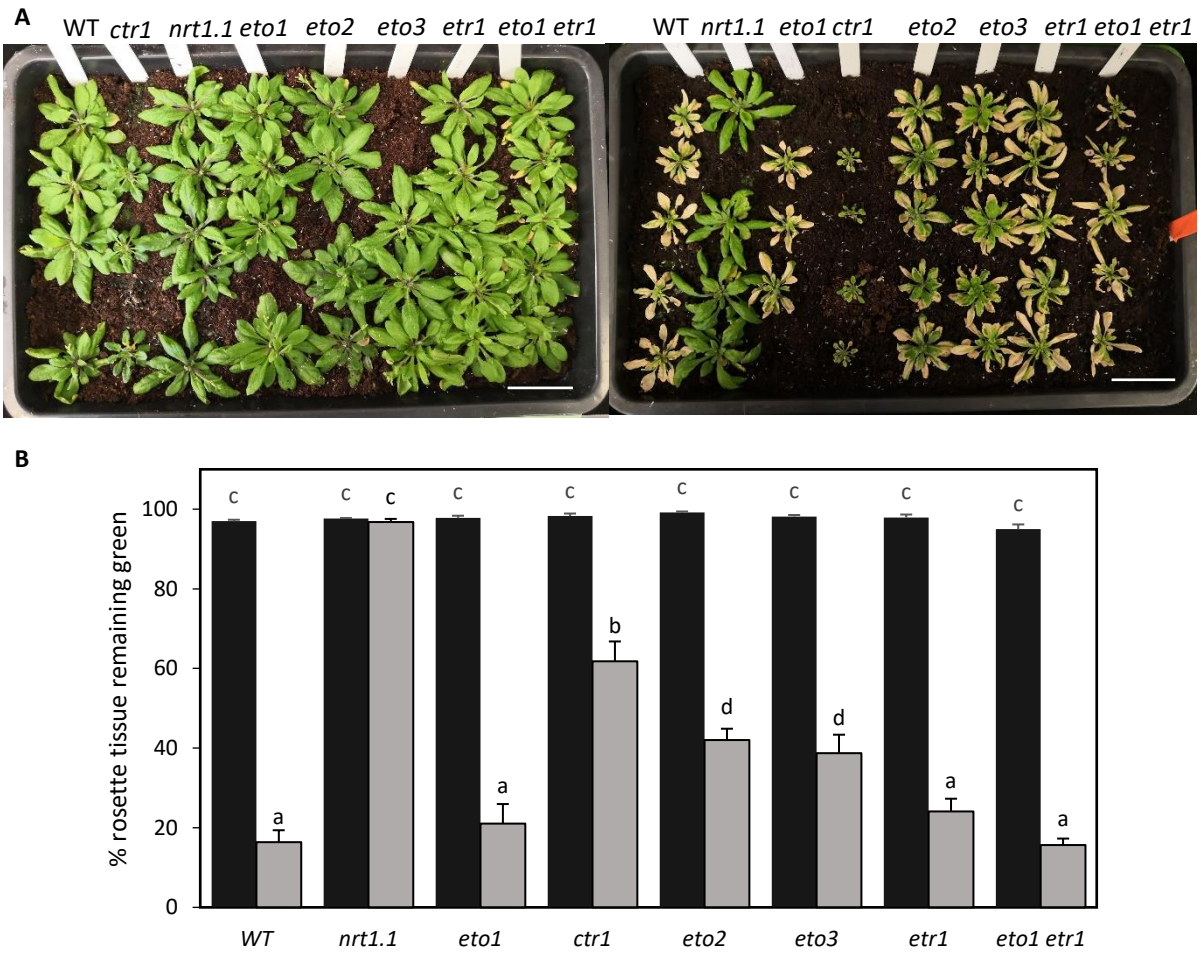


Figure 14: The *eto2* and *eto3* ethylene over-producing mutants have increased resistance to chlorate treatment; *eto1*, *etr1* and *eto1 etr1* are as sensitive to chlorate treatment as WT. [**A**] 5-week-old WT, *ctr1*, *eto1*, *eto2*, *eto3*, *etr1* and *eto1 etr1* plants were treated with either water (left panel) or 2.5 mM chlorate solution (right panel). Plants were photographed 11 days after the first chlorate treatment. Scale bars = 50 mm. [**B**] Individual rosettes were analysed in imageJ to determine the proportion of rosette tissue that remained green following treatment with control or chlorate solution. Dark bars denote control plants (treated with water), lighter bars denote chlorate treated plants. Values are means ± SD, n = 5. Different letters denote statistically significant differences (one-way ANOVA/Tukey HSD post hoc test, $p < 0.05$). The experiment was repeated independently 3 times with similar results.

The *ctr1-1* mutant displays constitutive ethylene responses, and it may therefore be expected that if this constitutive ethylene signalling is providing the *ctr1-1* mutant with a strongly chlorate resistant phenotype, that ethylene over-producing mutants may have a strongly chlorate resistant phenotype also. This is not seen, although plants do appear to be greener than WT, producing an intermediate phenotype. This can perhaps be explained by the fact that ethylene over-production has been reported to occur predominantly in the

early seedling stage and not during adulthood (Woeste *et al.*, 1999). Treating plants at 5 weeks old, as undertaken in this study is therefore possibly too late a stage to observe any differences in chlorate resistance conferred by these mutations. Indeed, it is clear that ethylene over-producing mutants do not have the same dwarfed phenotype seen in adult *ctr1-1* plants; measuring the height of 5-week-old plants indicated that none of the ethylene-over-producing mutants were significantly different to WT, only *ctr1-1* was significantly shorter [**Figure 15**].

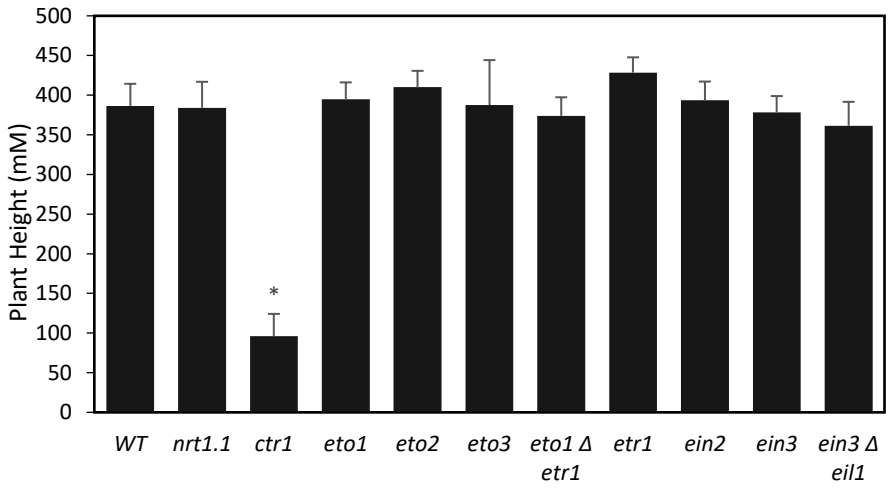


Figure 15: Height of various mutants lacking components of ethylene signalling. The height of 5-week-old WT plants and genotypes lacking components of the ethylene signalling pathway was measured to determine the effects of these mutations on growth. Height was determined by measuring the maximal extension between the base of the rosette and the tips of the shoots. Error bars denote S.D, n = 10. * denotes statistical difference to WT (student's t-test, $p < 0.05$). The experiment was repeated independently 3 times with similar results.

3.2.8 Chlorate treatment of *ein2*, *ein3* and *ein3 Δ eil1* loss-of-function mutants

The ethylene signalling mutants *ein2*, *ein3* and *ein3* Δ *eil1* all lack downstream components of the ethylene signalling pathway, and therefore have reduced responses to ethylene signalling (Ji and Guo, 2013), (Solano *et al.*, 1998). Since the *ctr1-1* loss of function mutation confers resistance to chlorate treatment, and the *ctr1-1* mutant has constitutive ethylene

signalling responses, I therefore hypothesised that mutants with reduced ethylene signalling capabilities would be at least as susceptible to chlorate treatment as WT plants.

Treating *ein2*, *ein3* and *ein3* Δ *eil1* lines with 2.5 mM chlorate solution indicated that these lines are all susceptible to chlorate treatment, with leaves showing clear visible chlorosis unlike the *ctr1-1* and *nrt1.1* controls which have shoot tissue that remains green [**Figure 16A**]. Quantitative analysis of the proportion of green shoot tissue following treatment with either chlorate or control solution indicates that there is no statistical difference between any of the lines in control conditions [**Figure 16B**]. Following chlorate treatment only *nrt1.1* and *ctr1-1* have a significantly greater proportion of rosette tissue remaining green compared to WT, whilst WT plants have no significant difference compared to *ein2*, *ein3* and *ein3* Δ *eil1* lines.

In addition to having no significant difference in chlorate resistance compared to WT, like the ethylene over-producing mutants, the *ein2*, *ein3* and *ein3* Δ *eil1* genotypes also have no significant difference in height compared to WT [**Figure 15**]. This suggests that ethylene-insensitivity, as is seen in these mutants, does not enhance susceptibility to chlorate treatment. In future, it would be interesting to treat these lines with chlorate whilst exposing plants to exogenous ethylene; this may allow differences between WT and ethylene-insensitive lines to be identified. This would determine if low endogenous ethylene levels in WT plants are masking any differences in nitrate metabolism caused by reduced ethylene sensitivity in the *ein2*, *ein3* and *ein3* Δ *eil1* mutants.

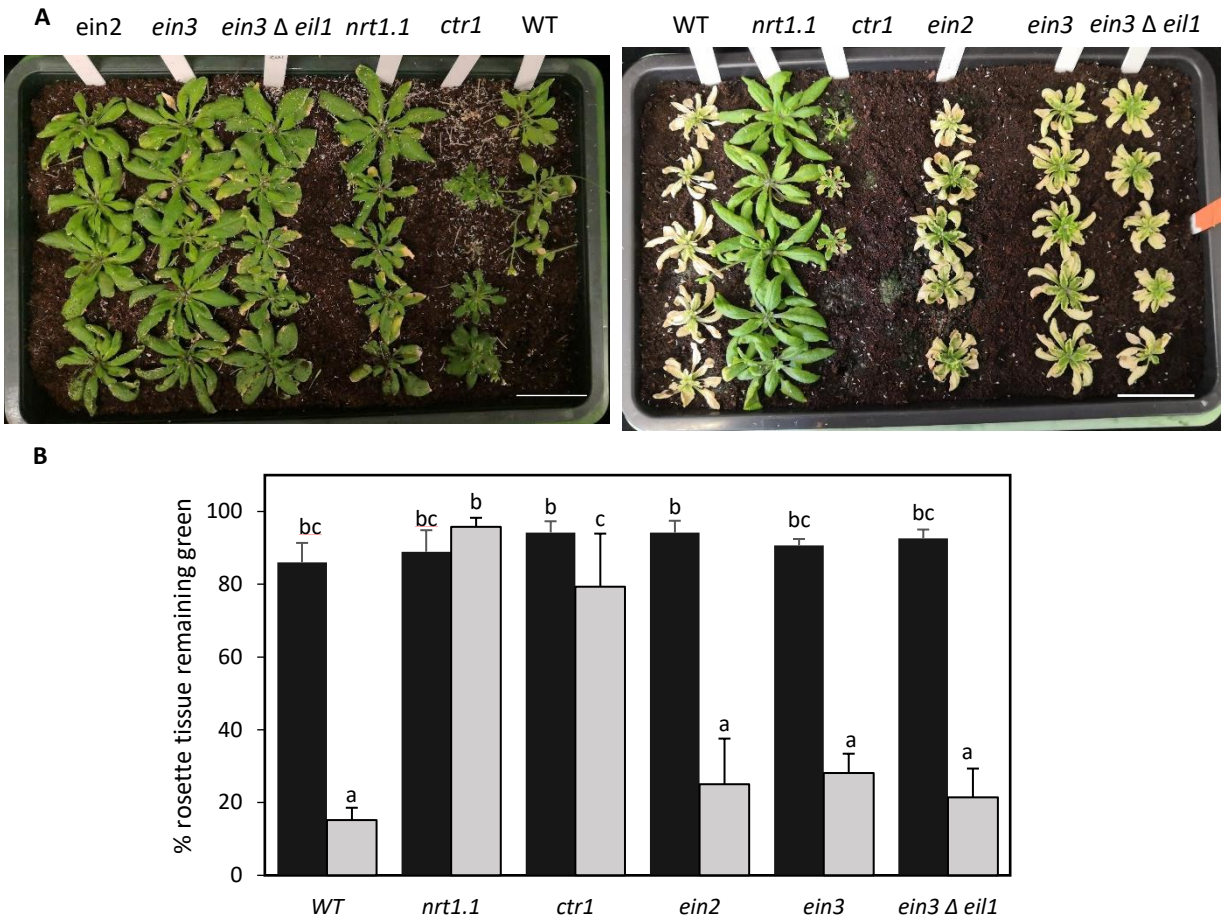


Figure 16 : The *ein2*, *ein3* and *ein3 Δ eil1* mutants are sensitive to chlorate treatment. [**A**] 5-week-old WT (Col), *ctr1*, *ein2*, *ein3*, and *ein3* Δ *eil1* plants were treated with either water (left panel) or 2.5 mM chlorate solution (right panel). Plants were photographed 11 days after the first chlorate treatment. Scale bars = 50 mm. [**B**] Individual rosettes were analysed in imageJ to determine the proportion of rosette tissue that remained green following chlorate treatment. Dark bars denote control plants (treated with water), lighter bars denote chlorate treated plants. Error bars denote S.D, n = 5. Different letters denote statistically significant differences (one-way ANOVA/Tukey HSD post hoc test, $p < 0.05$). The experiment was repeated independently 3 times with similar results.

3.2.9 NR activity assay of mutants lacking components of ethylene signalling

As discussed previously, increased resistance to chlorate treatment may be due to a reduction in chlorate uptake, and/or a reduction in NR activity that leads to reduced amounts of chlorite being produced. Since *ctr1-1* had reduced NR activity, I wanted to determine whether *eto2* and *eto3* genotypes, which displayed partially increased resistance to chlorate treatment, had altered NR activity, and whether this was altered in any of the other ethylene signalling mutants also.

Measuring shoot NR activity from *eto1*, *eto2*, *eto3*, *ein2*, *ein3* and *etr1* genotypes indicated that only *ctr1-1* had a significantly reduced shoot NR activity compared to WT. None of the other lines containing mutations in genes encoding components of the ethylene signalling pathway had a significant difference in NR activity to WT [**Figure 17**].

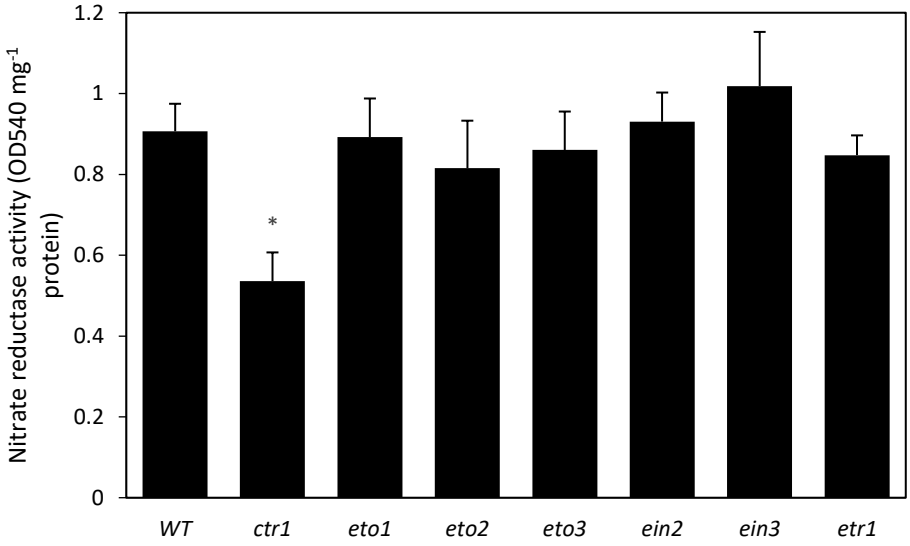


Figure 17: Nitrate reductase activity of Arabidopsis lines containing mutations in the ethylene signalling pathway. Shoot tissue was harvested from 4-week-old plants and protein extracted. The NR activity of protein extract was assayed and expressed relative to protein concentration. *ctr1-1* was the only ethylene signalling mutant tested to have significantly reduced NR activity compared to WT (* denotes statistically significant difference, student's t-test, $p < 0.05$, $n = 4$). The experiment was repeated independently 4 times with similar results.

Therefore, whilst *eto2* and *eto3* display a partial increase in chlorate resistance compared to WT, this is not reflected in significantly reduced NR activity [**Figure 17**]. It would be interesting in future work to explore nitrate metabolism in these lines at a younger stage, since the ethylene over-production effect that these mutations cause is most pronounced at the seedling stage.

Interestingly, the lack of significant changes in NR activity in the *ein2*, *ein3* and *etr1* lines indicates that NR activity is not enhanced in these lines. If constitutive ethylene signalling is causing reduced NR activity, it may be expected that impaired ethylene signalling (as

would be expected in the *etr1*, *ein2* and *ein3* mutant lines) may cause an increase in NR activity, if NR activity is reduced by constitutive ethylene signalling. The lack of difference in these lines to WT suggests that either WT plants used in this study have minimal ethylene signalling, and are therefore physiologically not very different to *etr1, ein2* and *ein3* in terms of ethylene signalling levels, or, whilst constitute ethylene signalling responses caused by the *ctr1-1* mutation inhibit NR activity, mutations causing an opposite phenotype (resulting in inhibition of the ethylene signalling pathway) do not cause an increase in NR activity. Further studies could distinguish between the two by measuring NR activity following exogenous application of ethylene, or ethephon, to these lines in addition to WT.

3.2.10 Mutagenized *ctr1-1* lines with altered chlorate resistance were identified using a mutant screen

To understand how CTR1 may regulate Arabidopsis chlorate resistance, and therefore potentially regulate N metabolism, further, I screened an EMS- mutagenized population of *ctr1-1* following chlorate treatment to identify mutants with altered chlorate responses.

Plants were screened by sowing approximately 10,000 F2 seeds on trays of compost, and at four weeks treating trays with 2.5 mM $KClO_3^-$ solution (see **Chapter 2**). This treatment was repeated after seven days, enabling plant lines showing differences in chlorate toxicity to be visually identified, and therefore mutagenized *ctr1-1* lines with potentially altered NO_3^- metabolism to be isolated. Lines of interest were rescued by transferring plants to trays of compost that had not been subjected to chlorate treatment, where they were allowed to self-fertilise and seed collected for further experiments.

Following chlorate treatment, four categories of mutants of interest were identified [**Table 4**]. The first and smallest category was plants that retained the *ctr1-1* dwarfed phenotype

but had increased sensitivity to chlorate treatment, of which 2 plants were identified. The second category consisted of plants retaining the *ctr1-1* dwarfed phenotype but displaying increased resistance to chlorate treatment – 27 such plants were identified although since *ctr1-1* has a strongly chlorate resistant phenotype whether these were truly more chlorate resistant was unclear. It was also notable that a number of plants had lost the dwarfed phenotype of *ctr1*, reverting to being 'tall'. Of these, the majority (72) were in the third category of interest: those that were tall and appeared to revert to WT- levels of chlorate sensitivity, whilst a minority (15) were in the fourth category of interest: 'tall' mutants that appeared to retain the chlorate resistant phenotype of the *ctr1-1* mutant.

Neither of the short mutants with increased chlorate sensitivity produced seed and so were unable to be tested further. Of the remaining categories it was decided to focus on the fourth category of mutants (those that were tall yet appeared to retain chlorate resistance) in future work. This category is particularly interesting because the limitation on growth that the *ctr1-1* mutation confers has been overcome, whilst the resistance to chlorate treatment has not been lost in parallel. This suggests that these plants contain mutations that allow them to retain the altered nitrate metabolism seen in *ctr1-1* whilst escaping this mutation's constraints on growth.

Category	1	2	3	4
Height	Dwarfed	Dwarfed	Tall	Tall
Response to chlorate treatment	Increased sensitivity	Increased resistance	Increased sensitivity	Retained or increased resistance
Number of mutants of interest identified	2	17	72	15
Number of plants that produced seed	0	10	57	15
Number of mutants with heritable phenotype	-	Not tested	10/10 tested	14/15 tested

Table 4: Categories of mutants of interest identified during mutant screen

As discussed in 3.2.1, *ctr1-1* is strongly resistant to chlorate treatment compared to WT, and this suggests that N metabolism is altered in the *ctr1-1* mutant in some way. I therefore aimed to identify *ctr1-1* lines containing additional mutations that altered their phenotype in some way. I chose to focus on lines that retained the chlorate resistance seen in *ctr1*, but no longer had a dwarfed phenotype, with the aim to further explore whether the correlation between altered nitrate metabolism and reduced growth could be disrupted.

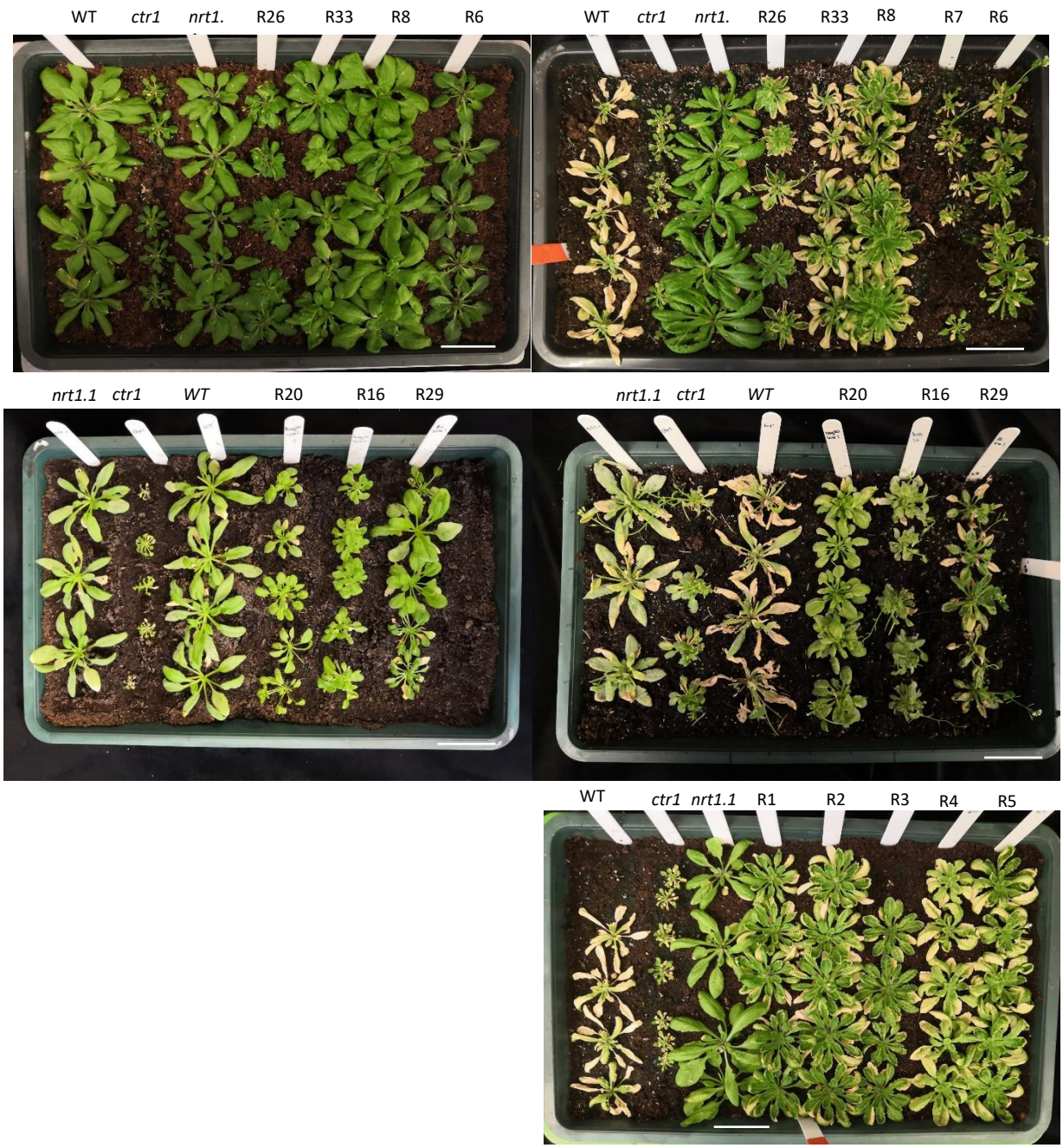


Figure 18: Lines of interest identified from *ctr1-1* mutant screen displaying a heritable chlorate-resistant heritable phenotype. 5-week-old WT, *nrt1.1*, *ctr1*, and mutagenized *ctr1-1* lines were treated with either water (left panel) or 2.5 mM chlorate solution (right panel). The third tray shown does not have a photo of plants in control conditions, but lines behaved as expected. Plants were photographed 10 days after the first chlorate treatment with stems removed. Scale bars = 50 mm.

A number of different mutants were identified that retained some level of chlorate resistance, whilst no longer having a dwarfed phenotype. 12 of these lines of interest had heritable phenotypes for both chlorate resistance and a tall plant height [**Figure 18, 22**]. Of

these, there was some variation in the degree of chlorate resistance retained, although all were more resistant to treatment than WT [**Figure 18**]. All lines were additionally tested under control conditions and behaved as expected, with no yellowing of leaves [**Figure 18**] (the third tray shown does not have a photo of plants in control conditions, but lines behaved as expected).

3.2.11 Nitrate metabolism in tall mutants displaying chlorate resistance

In order to better understand the chlorate resistance phenotype of these *ctr1-1* lines containing additional unknown mutations, I investigated the characteristics of these lines in greater detail. Since I was interested in the fact that these mutants were no longer dwarfed, whilst retaining some degree of chlorate resistance, I analysed both changes in nitrate metabolism and the growth characteristics of these lines. Since the chlorate-resistance of *ctr1-1* appears to be due, at least in part, to a reduction in NR activity, I analysed the NR activity of six lines chosen for further analysis, which all displayed high levels of chlorate resistance, to determine whether the reduced NR activity seen in the *ctr1-1* mutant was present in these lines also. To further understand the degree to which the dwarfed trait had been lost I measured plant height to determine the extent to which growth was altered compared to both WT and *ctr1*.

Since *ctr1-1* has significantly reduced NR activity, and this is likely to contribute to the genotype's chlorate-resistant phenotype, I analysed the shoot NR activity of some of the lines of interest I had identified to determine if reduced NR activity had been maintained in these lines. Six lines with a particularly strong chlorate-resistant phenotype were chosen for analysis: R1, R2, R3, R6, R16 and R20, alongside *ctr1*.

As expected, the *ctr1-1* mutant had significantly reduced NR activity compared to WT [**Figure 19**]. Two of the chlorate-resistant mutants tested also had significantly reduced NR activity compared to WT: R16 and R20. Analysing the NR activity of lines R1, R2, R3 and R6 found no significant difference to WT, suggesting that the strongly chlorate-resistant phenotype of these lines is not due to altered NR activity, and is therefore likely due to alternative factors that alter chlorate toxicity, for example differences in chlorate uptake.

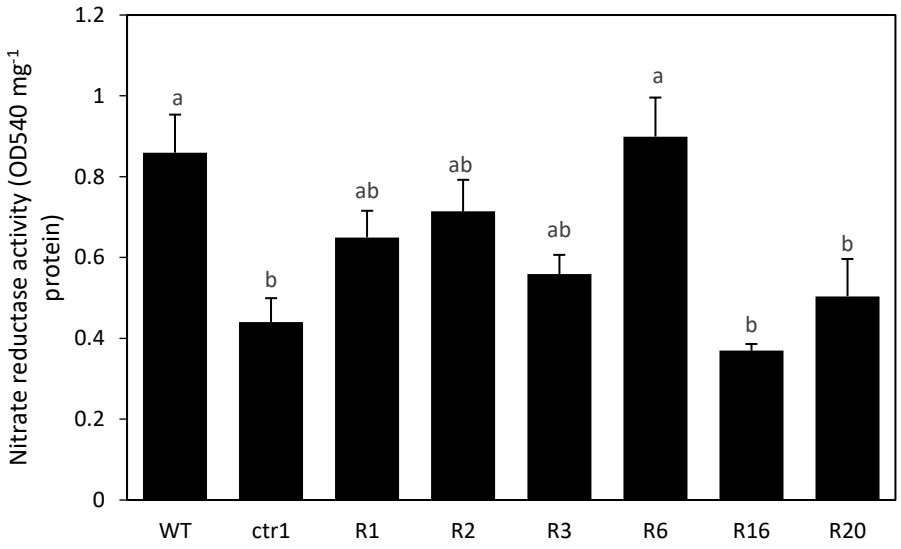


Figure 19: Nitrate reductase activity of mutagenized *ctr1-1* lines. Shoot tissue was harvested from 4-week-old plants and protein extracted. The NR activity of protein extract was assayed and expressed relative to protein concentration. *ctr1*, and mutagenized *ctr1-1* lines named R16 and R20 had significantly reduced NR activity compared to WT (* denotes statistically significant difference, student's t-test, $p < 0.05$, $n = 4$). The experiment was repeated independently 3 times with similar results.

3.2.12 Growth characteristics of tall mutants displaying chlorate resistance

Compared to WT, *ctr1-1* is dwarfed, with both reduced height and visibly smaller rosettes. The average height of the six mutants selected for further analysis that were both "tall" and chlorate resistant was measured to determine if plants had reverted to a fully WT height phenotype, or if lines displayed an intermediate height between that of WT and *ctr1*. I was particularly interested in determining whether changes in NR activity correlated with height. Results indicated that lines display a range of different heights: all are

significantly taller than *ctr1*, with R3, R6, R16 and R20, having heights that are intermediate between WT and *ctr1*, whilst lines R1 and R2 have no significant difference to WT and, in terms of height, have reverted back to a fully WT phenotype [**Figure 20**].

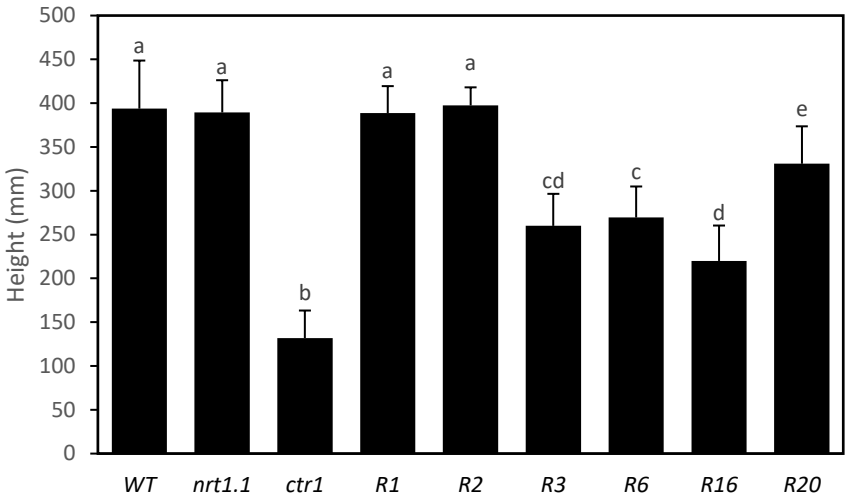


Figure 20: Height of selected mutagenized *ctr1-1* lines characterised as both tall and resistant to chlorate treatment. The height of the six mutagenized *ctr1-1* lines selected for further analysis, and identified as being tall and having retained resistance to chlorate treatment was measured. Error bars denote S.D, n = 14. Different letters denote statistically significant differences (one-way ANOVA/Tukey HSD post hoc test, $p < 0.05$). The experiment was repeated independently 3 times with similar results.

I have therefore identified two mutagenized ctr1-1 lines that have significantly reduced NR activity (R16 and R20), but have lost a degree of their dwarfed trait. Interestingly both lines are still shorter than WT plants, however, all are also significantly taller than the *ctr1-1* mutant. It would be interesting to characterise the remaining 6 lines identified as both tall and chlorate-resistant to determine if any of these other lines maintain significantly reduced NR activity, and if so whether they are also still shorter than WT or have reverted back to WT height, to see if a correlation between NR activity and height exists.

Further investigation is required to understand the nature of the mutations in these lines, in particular to understand whether a single mutation, or separate mutations, are causing the plants to revert back towards WT height whilst retaining significantly reduced NR

activity. Whole-genome sequencing of these lines, and the *ctr1-1* progenitor, would enable the location of all mutations present in the mutagenized lines, but not the progenitor plant, to be identified, following which further analysis could pinpoint mutations that are likely to be causal, potentially identifying new regulators of ethylene-mediated regulation of N metabolism.

3.2.13 Mutagenized *ctr1-1* plants containing known mutations in the EIN2 locus differ in their chlorate sensitivity

A previous screen isolating tall mutants from a *ctr1-1* population carrying additional EMS-induced mutations identified the majority of isolated lines as containing mutations in EIN2 (Zhong Jie Ding, unpublished data). This finding suggests that it is likely the majority of the lines I have isolated would contain mutations in EIN2 also.

To further investigate whether mutations in EIN2 were likely responsible for changes in chlorate sensitivity, in addition to changes in plant height, I obtained a number of the mutagenized *ctr1-1* lines identified in the earlier screen for tall plants; these had subsequently been confirmed to contain mutations in the EIN2 locus (Zhong Jie Ding, unpublished data).

Six lines were successfully bulked up for seed to allow further study. Five of these lines (named 9-11, 12-9, 16-3, 20-15 and 24-39) contained G → A point mutations, one line (22-10) contained a C → T mutation, all were non-synonymous mutations [**Table 5**]. These mutations were distributed across the EIN2 coding sequence, one each in exons 1 (20-15) and 7 (12-9) with 4 lines containing mutations located in exon 6 (9-11, 16-3, 22-10 and 27-23) [**Figure 21**].

Line name	Mutation in EIN2 DNA sequence			Mutation in mRNA sequence			Mutation in amino acid sequence		
	Position	Original	Mutated	Position	Original	Mutated	Position	Original	Mutated
9-11	1725	G	A	1209	GGA	AGA	404	G	T
12-9	4155	G	A	3561	TGC	TAC	1188	C	A
16-3	2584	G	A	2067	GGG	GAG	690	G	E
20-15	105	G	A	105	GGG	AGG	36	G	R
22-10	3979	C	T	3462	CCT	CTT	1155	P	L
24-39	4023	G	A	3507	GGA	AGA	1170	G	R

Table 5: Position and type of point mutations in the EIN2 locus of selected mutagenised *ctr1-1* plants (Zhong Jie Ding, unpublished data), tested for altered N metabolism.

The EIN2 CEND is located between amino acids 459 – 1294, with the minimal functional fragment of EIN2 identified as being amino acids 654 – 1272 (Li *et al.*, 2015). The mutations in lines 20-15 and 9-11 were all located in the EIN2 N-terminus transmembrane domain, whilst the mutations in lines 16-3, 22-10, 24-39 and 12-9 were located in the EIN2 CEND; none of the EIN2 mutations were located in the predicted nuclear translocation sequence [**Figure 21**]. Three of the lines had mutations that were not within the minimal functional fragment of EIN2 (20-15, 27-23 and 9-11) (Zhong Jie Ding, unpublished data).

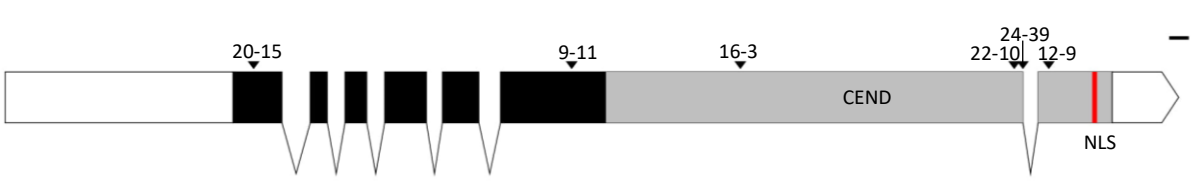


Figure 21: Position of point mutations in the EIN2 locus of EMS-treated *ctr1-1* background plants with a tall phenotype. Diagram shows EIN2 gene structure: shaded bars denote exons, lines denote introns, unshaded bars denote untranslated regions. The grey region indicates the position of the EIN2 CEND domain, the red bar indicates the position of the predicted nuclear translocation sequence, and the black region the EIN2 N-terminus transmembrane domain. The position of point mutations in the EIN2 locus of obtained *ctr1-1* mutants are indicated by arrow heads. Scale bar = 100 base pairs.

Since *ctr1-1* is dwarfed, and these plants, subsequently found to contain mutations in EIN2, were tall, it is hypothesised that the mutations in the EIN2 locus are resulting in defective

signalling of the CTR1- EIN2 ethylene signalling pathway (although the possibility that this phenotype is caused by other mutations unrelated to the CTR1- EIN2 signalling pathway cannot be ruled out). The *ctr1-1* mutant has constitutive ethylene signalling, as in the absence of ethylene there is no functional CTR1 protein to phosphorylate the EIN2 CEND and target the protein for degradation. The *ctr1-1* mutant therefore has constitutively active EIN2 activity in the nucleus. In order for dwarfed *ctr1-1* to revert to a tall WT phenotype, it is therefore presumed that these additional mutations in the EIN2 locus of these lines are preventing this downstream signalling pathway from occurring.

Since I had obtained lines that were tall, but differed in their response to chlorate treatment, I wanted to determine if differing mutations in EIN2 could be responsible for causing this difference, and therefore offer a way to separate the different phenotypes of altered height and altered N metabolism. I therefore analysed the response of these six obtained lines to chlorate treatment.

Of the six lines tested, a range of responses to chlorate treatment were visible [**Figure 22**]. Both 24-39 and 20-15 display enhanced chlorate resistance relative to WT, though these lines appear slightly more susceptible to treatment than *ctr1*. The 22-10 line appears to be as susceptible to chlorate treatment as WT, and has therefore lost the resistance conferred by the *ctr1-1* mutation [**Figure 22A**]. Lines 9-11, 12-9 and 16-10 all appear to have lost the chlorate resistant phenotype of *ctr1-1* [**Figure 22B**].

Analysing the proportion of rosette tissue remaining green after chlorate treatment confirms these observations. As expected, WT plants are significantly less green than either *nrt1.1* or *ctr1-1* genotypes. Both the 24-39 and 20-15 lines remain significantly greener than WT plants following treatment, with line 24-39 showing no significant difference in

'greenness' to *ctr1*, whilst 20-15 has an intermediate value between WT and *ctr1*. 22-10 is significantly less green than even WT plants, indicating this line may contains mutation(s) that cause chlorate susceptibility to increase beyond that of WT Col-0 plants [**Figure 22A**]. Lines 9-11, 12-9 and 16-10 all had significantly less green rosette tissue than *ctr1-1* and *nrt1.1* plants, with no significant difference compared to WT, suggesting that these lines have reverted back to WT levels of chlorate resistance [**Figure 22B**].

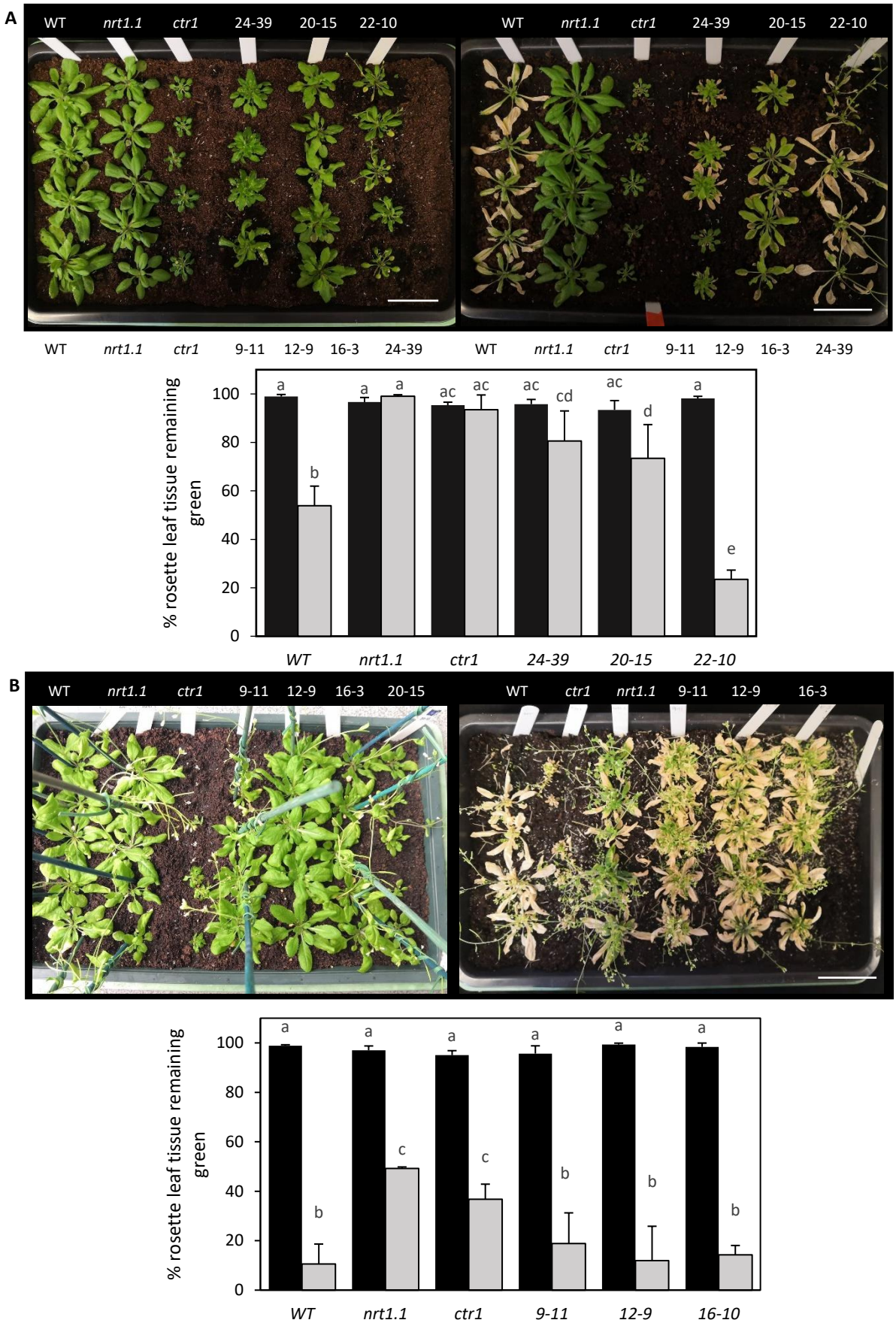

A
WT
nrt1.1
ctr1
24-39
20-15
22-10
WT
nrt1.1
ctr1
24-39
20-15
22-10
WT
nrt1.1
ctr1
9-11
12-9
16-3
24-39
WT
nrt1.1
ctr1
9-11
12-9
16-3
24-39
% rosette leaf tissue remaining green
0
20
40
60
80
100
a
b
a
a
ac
ac
ac
cd
ac
d
a
e
WT
nrt1.1
ctr1
24-39
20-15
22-10
B
WT
nrt1.1
ctr1
9-11
12-9
16-3
20-15
WT
ctr1
nrt1.1
9-11
12-9
16-3
% rosette leaf tissue remaining green
0
20
40
60
80
100
a
b
a
c
a
c
a
b
a
b
a
b
WT
nrt1.1
ctr1
9-11
12-9
16-10

Figure 22: Mutagenized *ctr1-1* lines containing mutations in the EIN2 locus have altered responses to chlorate treatment. 5-week-old WT (Col), *nrt1*.1, *ctr1-1* and mutagenised *ctr1-1* lines containing known mutations in the EIN2 locus were treated with either water (left panel) or 2.5 mM chlorate solution (right panel). Plants were imaged either 7 days (**A**) or 14 days (**B**) after treatment. Scale bar = 50mm. Different letters denote statistically significant differences (one-way ANOVA/Tukey HSD post hoc test, $p < 0.05$). The experiment was repeated independently 3 times with similar results.

3.2.14 The 6 mutagenized *ctr1-1* lines containing known mutations in the EIN2 locus have all lost the dwarfed phenotype conferred by the *ctr1-1* mutation

Measuring the terminal height reached of mutagenized *ctr1-1* lines containing mutations in the EIN2 locus indicated that whilst all of these lines were significantly taller than *ctr1*, a spectrum of heights was reached. Lines 9-11, 12-9, 16-3, 20-15, 22-10 and 24-39 all had no significant difference in terminal plant height compared to WT, although there was some variation within the lines, with 22-10 significantly shorter than lines 9-11 and 12-9 [**Figure 23**].

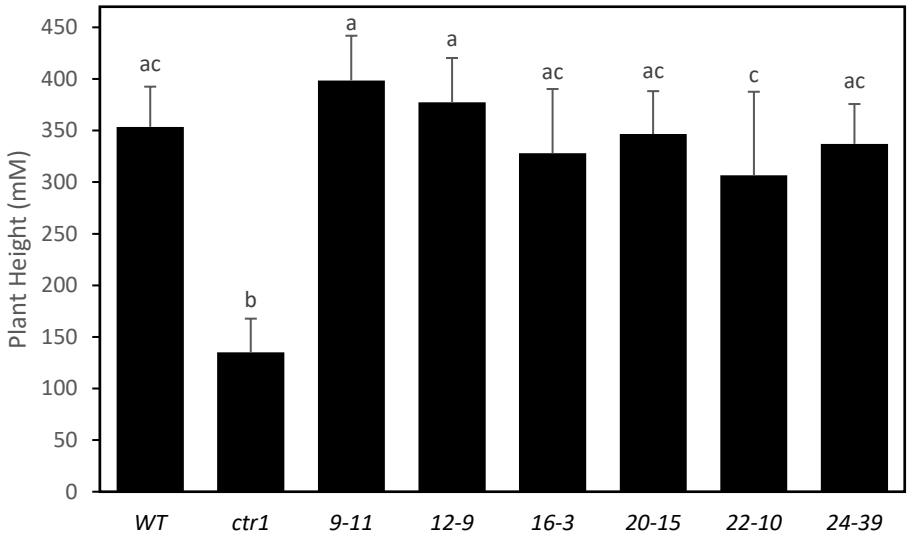


Figure 23: Heights of mutagenized *ctr1-1* lines containing mutations in the EIN2 locus. The height of 5-week-old WT plants and *ctr1-1* lines containing additional mutations, including those in EIN2, was measured to determine the effects of these mutations on growth. Error bars denote S.D, n = 10. Different letters denote statistically significant differences (one-way ANOVA/Tukey HSD post hoc test, $p < 0.05$). The experiment was repeated independently 3 times with similar results.

The variation in chlorate resistance seen in these lines [**Figure 22**] does not therefore correlate with plant height, with the two chlorate-resistance lines (24-39 and 20-15)

reverted back to WT height, with no significant difference in height compared to the chlorate-susceptible lines (9-11, 12-9, 16-3 and 22-10).

3.2.15 Mutagenized *ctr1-1* plants containing known mutations in the EIN2 locus differ in their nitrate content

Since chlorate resistance can be altered by changes in nitrate uptake, I analysed the nitrate content of the 6 mutagenized *ctr1-1* lines containing known mutations in the EIN2 locus. In addition to mutations causing a possible difference in NR activity, it is also possible that mutations reduce NO_3^- uptake, and therefore are responsible for the altered chlorate resistance observed. Measuring NO_3^- content would therefore help to indicate whether this was likely.

Measuring the shoot NO_3^- content of 4-week-old plants indicated that, as has previously been reported, *nrt1.1* had a significantly reduced shoot NO_3^- content compared to WT (Wang *et al.*, 2009). There was no difference in shoot nitrate content between WT and *ctr1-1* [**Figure 24**]. Of all *ctr1-1* lines containing additional mutations tested, none had a statistically significant alteration in shoot nitrate content relative to WT; line 12-9 had no significant difference from *nrt1.1* also [**Figure 24**]. It is unlikely this result is biologically significant since this line did not display any increase in resistance to chlorate treatment [**Figure 22**]. Therefore, the altered chlorate resistance in lines 24-39 and 20-15 are unlikely to be due to mutations causing reduced nitrate uptake in these plants since shoot nitrate content is unaffected. This suggests that, like in *ctr1*, the maintained chlorate resistance of these two lines may be due to alterations in NR activity.

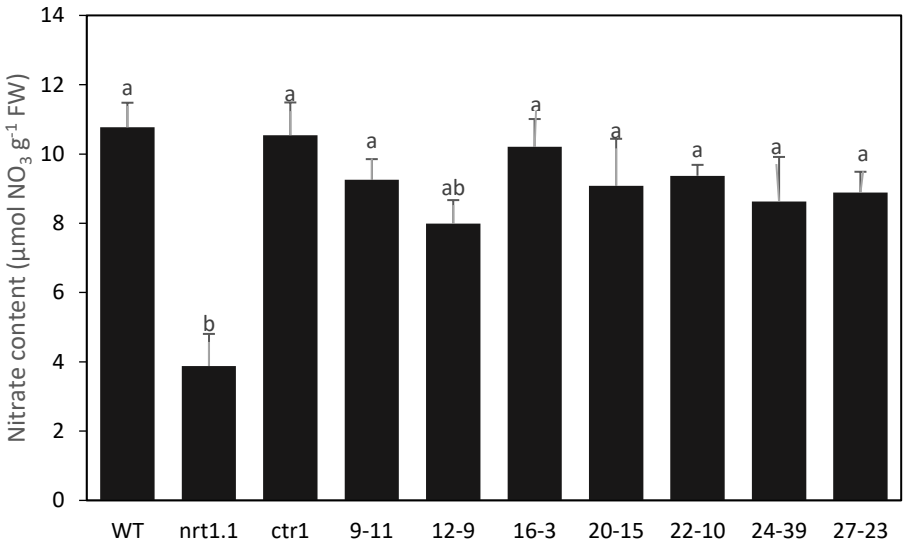


Figure 24: Nitrate content of mutagenized *ctr1-1* plants containing known mutations in the EIN2 locus. The shoot nitrate content of 4-week-old WT, *nrt1.1*, *ctr1-1* and mutagenized *ctr1-1* plants containing mutations in the EIN2 locus was measured. Error bars denote S.E.M, n = 5. Different letters denote statistically significant differences (one-way ANOVA/Tukey HSD post hoc test, $p < 0.05$)

3.2.16 The majority of mutagenized *ctr1-1* plants containing known mutations and with maintained chlorate resistance do not display a significant reduction in nitrate reductase activity

Since shoot nitrate content is unaffected, I also measured the NR activity of these lines. It may be expected that for chlorate resistance to be altered, and if shoot nitrate content is no different to WT, the difference in chlorate sensitivity could be due to alterations in NR activity so that a lower amount of chlorite, which is toxic, is produced in the chlorate-resistant lines.

Assaying shoot NR activity, relative to leaf protein content, revealed that whilst *ctr1-1* has significantly reduced NR activity compared to WT plants, only one of the mutagenized *ctr1-1* lines tested was significantly different to WT, line 20-15 [**Figure 25**].

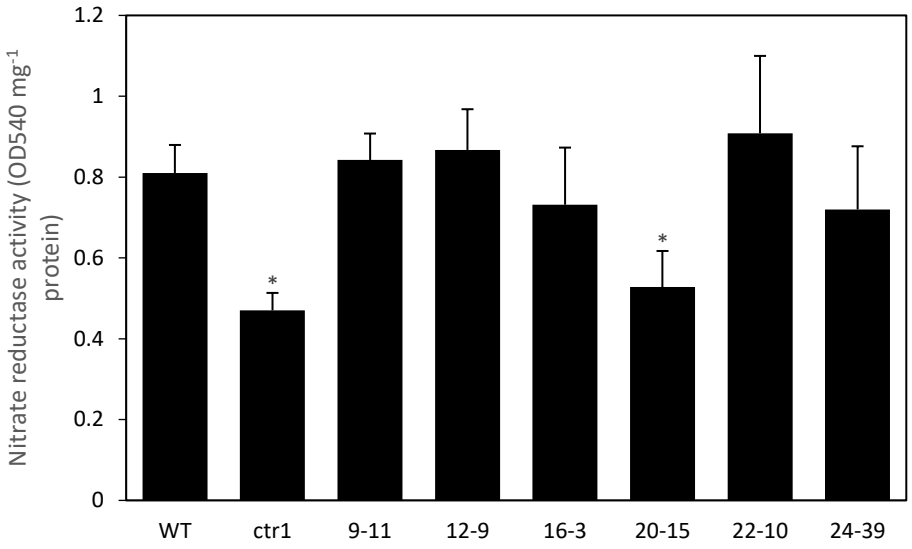


Figure 25: Nitrate reductase activity of mutagenized *ctr1-1* lines containing known mutations in the EIN2 locus. Shoot tissue from 4-week-old WT, *ctr1-1* and mutagenized *ctr1-1* lines was harvested and the NR activity assayed and expressed relative to leaf protein content. *ctr1-1* has significantly reduced NR activity compared to WT, as did line 20-15 (* denotes statistically significant difference, student's t-test, $p < 0.05$, $n = 4$). Error bars denote S.E.M. The experiment was repeated independently 3 times with similar results.

Whilst this result is not unexpected for lines 9-11, 12-9, 16-3 and 22-10 given the susceptibility of these lines to chlorate treatment, it is unexpected that line 24-39 did not show any significant difference in NR activity compared to WT, given shoot nitrate content appeared unaffected in this mutant and yet it still displays chlorate resistance [**Figure 25**]. Although not statistically significant, the mean values of this line were the second lowest of all six mutagenized *ctr1-1* lines tested, and it is possible that the degree of replication was insufficient to reveal real differences (a type II error). Replicating this experiment with larger sample sizes may reveal differences in the nitrate metabolism of this line. Alternatively, this line may provide a good candidate to understand mechanisms of chlorate resistance that are independent of NO_3^- metabolism.

By utilising a mutant screen, I have therefore identified a number of mutagenized *ctr1-1* lines that have lost the dwarfed phenotype of *ctr1*, whilst maintaining the strongly chlorate-resistant phenotype of this mutant. Further work is now required to understand

the mutations causing the separation of these two traits, and in particular to understand whether it is separate or single mutations causing these differences.

EMS- treated *ctr1-1* seeds may contain a large number of additional mutations located throughout the genome. Without collecting and analysing whole-genome sequencing data for these lines, it is impossible to rule out the possibility of the presence of additional mutations, unrelated to the ethylene signalling pathway, affecting N metabolism in these lines. It is therefore possible, that the chlorate resistance phenotype seen in the mutagenized *ctr1-1* lines of interest identified in this chapter, could be due to additional mutations elsewhere in the genome and not due to additional mutations in the ethylene signalling pathway. Until this possibility is ruled out by whole-genome sequencing of these lines, these results must therefore be treated with caution. Line 20-15 is particularly interesting however, as it has reverted to a fully WT height, is strongly chlorate resistant, and has reduced NR activity whilst shoot nitrate content is unaffected. Additionally, 24-39 offers further opportunity to understand the mechanistic basis of chlorate resistance, since whilst chlorate resistance was high, neither nitrate content nor NR activity were altered compared to WT. Of key importance is identifying whether the mutations these lines carry in the EIN2 locus are responsible for the altered NR activity; obtaining lines containing these mutations only, in a WT background, and measuring NR activity and chlorate resistance will determine whether this is the case or not. If so, this would suggest that EIN2 is of particular importance in regulating Arabidopsis N nutrition.

This chapter therefore identifies that ethylene signalling modulates nitrate metabolism in Arabidopsis. I show that *ctr1-1* has a strong chlorate-resistant phenotype likely caused by a reduction in NR activity. Other lines containing mutations in genes encoding proteins

involved in ethylene signalling appear unaltered in NR activity, suggesting that either there is little physiological difference in mutants displaying reduced ethylene signalling and WT in the growth conditions used in this study, or the effects of ethylene-mediated regulation of N metabolism in Arabidopsis are limited caused by constitutive ethylene signalling only, and are not reversed in mutants where ethylene signalling is impaired. I have additionally identified a number of mutagenized *ctr1-1* lines that separate the dwarfed phenotype of *ctr1*, and the chlorate-resistant phenotype of *ctr1*, which in future work may allow components of CTR1-mediated nitrate metabolism to be identified and characterised further.

Chapter 4: The role of phosphate in regulating Arabidopsis nitrogen metabolism

4.1 Introduction

Plants must integrate different signalling pathways, including those regarding nutrient status, for appropriate growth and development to occur. It is therefore expected that there will be extensive cross-talk between signalling pathways controlling the uptake and metabolism of N and P, two important nutrients for plant growth. However, the mechanisms behind this integration are not well understood. As discussed in **1.4.1**, there are some known links between different nutrient pathways, including those of N and P, but there is still scope to understand this further.

In particular, there is scope to utilise genetics approaches to investigate how signalling components involved in the regulation of P metabolism affect the regulation of N metabolism. Several studies have identified components regulating N metabolism as having a role in regulating Pi metabolism; the ubiquitin ligase NLA controls nitrogen limitation adaptive responses, and can also affect targeting of PHT1 Pi transporters (Peng *et al.*, 2007; Liu *et al.*, 2014). Another study identified the transcription factor HRS1 as influencing low-Pi induced changes in primary root growth, but only when nitrate is present (Medici *et al.*, 2015).

In this chapter I set out to investigate how components regulating P metabolism may also impact the regulation of N metabolism. I aimed to first determine how lowered P conditions alter N metabolism in WT Arabidopsis, and then to use loss-of-function mutants which differ in their Pi accumulation to determine the involvement of known components of the Arabidopsis low phosphate signalling pathway. I also explored how different growth conditions alter chlorate resistance, and suggest possible mechanisms behind this.

4.2 Results and discussion

4.2.1 Nitrate reductase activity is reduced in low phosphate conditions

In 2000, a study was published that showed growing bean (*Phaseolus vulgaris L*.) on Pi-deficient media caused reduced root NR activity compared to plants grown on Pi-replete media (Gniazdowska and Rychter, 2000). Plants grown on Pi-deficient media had a reduced nitrate content, but a greater proportion of nitrate distributed in root tissue (rather than shoot tissue), compared to plants grown in Pi-replete conditions. The authors suggested that reduced NR activity could be causing the increased nitrate accumulation in root tissue. To investigate how the regulation of N and P metabolism interact in Arabidopsis, I first investigated if low Pi causes an alteration in Arabidopsis NR activity, as has been reported in bean.

Whilst the study in bean was done on root tissue, it has previously been reported that the majority of Arabidopsis NR activity occurs in the shoot tissue (Krapp *et al.*, 2011). I measured the NR activity of WT Arabidopsis plants grown on ½ MS agarose plates with either high or low Pi concentrations, in order to investigate whether low Pi reduces shoot and / or root NR activity, as has previously been reported to be the case in bean roots (Gniazdowska and Rychter, 2000). 1000 µM Pi has been used as phosphate-replete conditions and concentrations between 1 µM and 50 µM used as low phosphate conditions in previous Arabidopsis studies (e.g. Sánchez-Calderón *et al.*, 2005; Janes *et al.*, 2018).

The elevated NR activity of shoot tissue compared to root tissue suggests that the majority of Arabidopsis NR activity occurs in shoots, with shoot tissue having an almost 10-fold higher NR activity than roots [**Figure 26**]. When plants were grown on low phosphate (20 µM), rather than high phosphate (1000 µM), NR activity was reduced in both shoots and

roots. Shoot tissue had an approximately 41% reduction in NR activity under low Pi, whilst in roots NR activity was reduced by approximately 49% [**Figure 26**]. Therefore, the majority of Arabidopsis NR activity occurs in the shoots, in both high and low Pi conditions, and low Pi reduces NR activity in both shoot and root tissues.

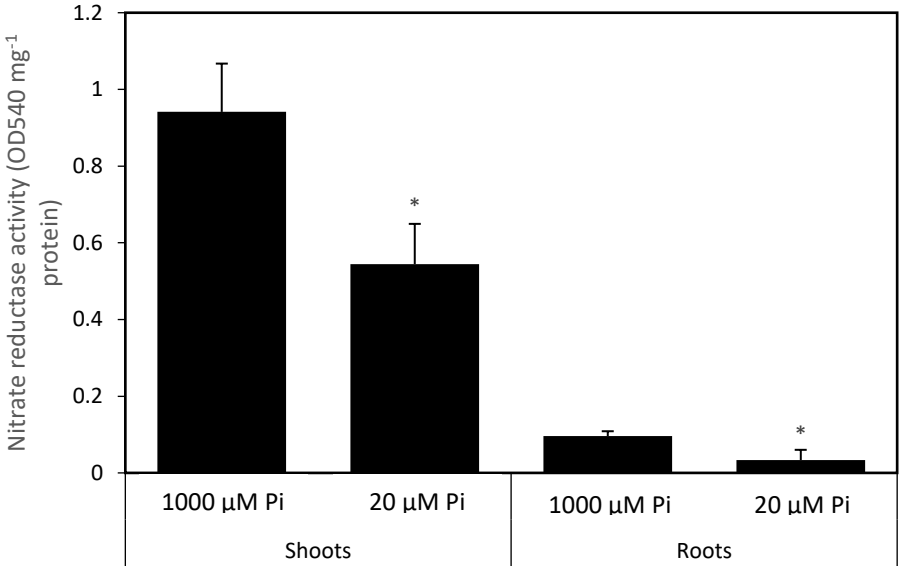


Figure 26: Low phosphate reduces Arabidopsis shoot and root nitrate reductase activity. 14-day-old WT Arabidopsis seedlings grown on ½ MS agarose plates were transferred to agarose containing modified ½ MS with either high Pi (1000 µM) or low Pi (20 µM) availability. Seedlings were grown for a further 3 weeks before shoot and root tissue was harvested. The NR activity was assayed by measuring the reduction of nitrate to nitrite by shoot protein extract and compared to the tissue protein content. * denotes statistical difference to the same tissue type in full phosphate (Student's t-test, $p < 0.05$), error bars denote S.D, n = 4 pools of 8-12 plants. The experiment was repeated independently 3 times with similar results.

4.2.2 Low phosphate conditions reduce Arabidopsis shoot nitrate content

Since Arabidopsis NR activity is reduced in low Pi conditions, I wanted to determine if plant root and shoot NO_3^- content was affected by low Pi also. Gniazdowska and Rychter (2000) suggested that the lowered root NR activity in bean was responsible for the observed increase in root NO_3^- content. It was therefore possible that Arabidopsis grown in low Pi would have an increased shoot NO_3^- content, due to reduced use of NO_3^- as a substrate by shoot NR. It was also possible that the opposite might be true: lowered Pi conditions may induce regulatory changes that reduce N metabolism at a broader level, and this may

extend to mechanisms coordinating NO_3^- uptake as well as NR enzyme activity. I therefore measured the shoot NO_3^- content of plants grown on three different phosphate concentrations, testing plants grown in high (1000 µM), intermediate (100 µM) and low (10 µM) Pi.

Measuring the shoot NO_3^- content of plants grown on different levels of Pi indicated that reducing Pi availability reduces Arabidopsis shoot NO_3^- content [**Figure 27**]. A 10-fold reduction in Pi availability from 1000 µM to 100 µM reduced shoot NO_3^- content by approximately 91%, and a further 10-fold reduction of Pi availability from 100 µM to 10 µM reduced shoot NO_3^- content by a further 50% [**Figure 27**].

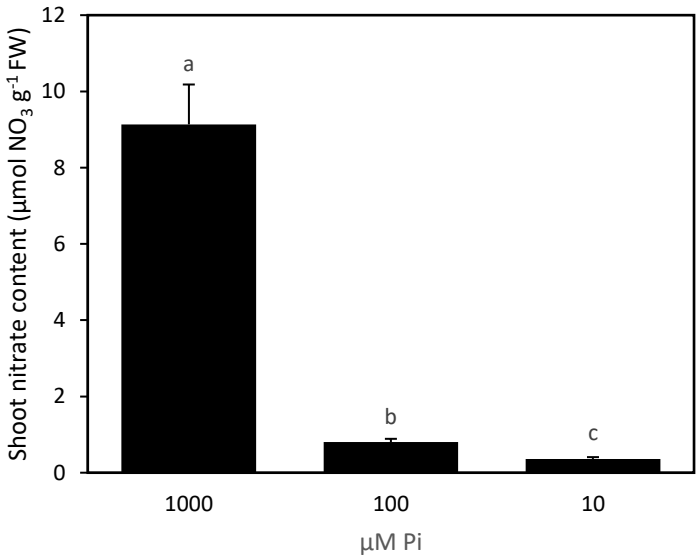


Figure 27: Arabidopsis shoot nitrate content of WT plants grown on different phosphate concentrations. 14-day-old WT Arabidopsis seedlings grown on ½ MS agarose plates were transferred to agarose containing modified ½ MS with either high (1000 µM), medium (100 µM) or low (10 µM) phosphate concentrations. Seedlings were grown for a further 3 weeks before shoot and root tissue was harvested. The shoot nitrate content was determined relative to tissue fresh weight (FW). Different letters denote statistically significant difference (Student's t-test, $p < 0.05$), error bars denote S.D, n = 4-5. The experiment was repeated independently 3 times with similar results.

4.2.3 Mutants impaired in the regulation of phosphate metabolism have altered nitrate reductase activity

The lack of studies utilising genetics approaches to investigate the interaction between the regulation of N and P metabolism in Arabidopsis offers scope to understand this further. By investigating how N metabolism is altered in plants containing mutations in the Pi signalling pathway, it is possible to distinguish whether it is a reduction in actual Pi content within a plant, or genetic regulation by signalling pathways controlling Pi metabolism, that alters N metabolism.

I therefore investigated how N metabolism is altered in mutants containing specific mutations in the low-phosphate signalling pathway. The *phr1* loss-of-function mutant cannot produce the PHR1 MYB transcription factor expressed during Pi starvation, responsible for inducing many low-phosphate-signalling pathways. As well as directly altering expression of phosphate-starvation-induced (*PSI*) genes, PHR1 also initiates transcription of miR399, a mobile RNA that enables long-distance signalling of plant Pi status from shoot to root tissues. The *phr1* mutant therefore has impaired Pi starvation responses (Rubio *et al.*, 2001). The second Pi signalling mutant studied was *pho2*, PHO2 is the target of miR399. Under Pi-replete conditions PHO2 represses the transcription of *PSI* genes, the *pho2* loss-of-function mutant has enhanced expression of these genes, even when Pi availability is plentiful (Bari *et al.*, 2006). The *pho2* mutant therefore has enhanced Pi accumulation, due to increased expression of e.g. *PHT1* Pi transporters that would normally occur when Pi is limiting. The final loss-of-function mutant studied was *pht1;1* Δ *pht1;4*, a double mutant lacking two of the major Pi transporters. In Pi-replete conditions

this double mutant has up to a 75% reduction of Pi uptake; in low Pi conditions Pi uptake is reduced by 50% (Shin *et al.*, 2004).

Since I had found that the majority of Arabidopsis NR activity occurs in shoots [**Figure 26**], I focussed only on shoot tissue in further NR assays. This allowed plants to be grown on compost and therefore more biologically relevant conditions. I have shown that reduced Pi availability causes a reduction in shoot NR activity [**Figure 26**], and also a reduction in shoot NO_3^- content [**Figure 27**]. To determine whether plant Pi accumulation, or low Pi signalling pathways, are responsible for this alteration in NR enzyme activity, I analysed the NR activity of WT, *pho2*, *phr1* and *pht1;1* Δ *pht1;4* plants.

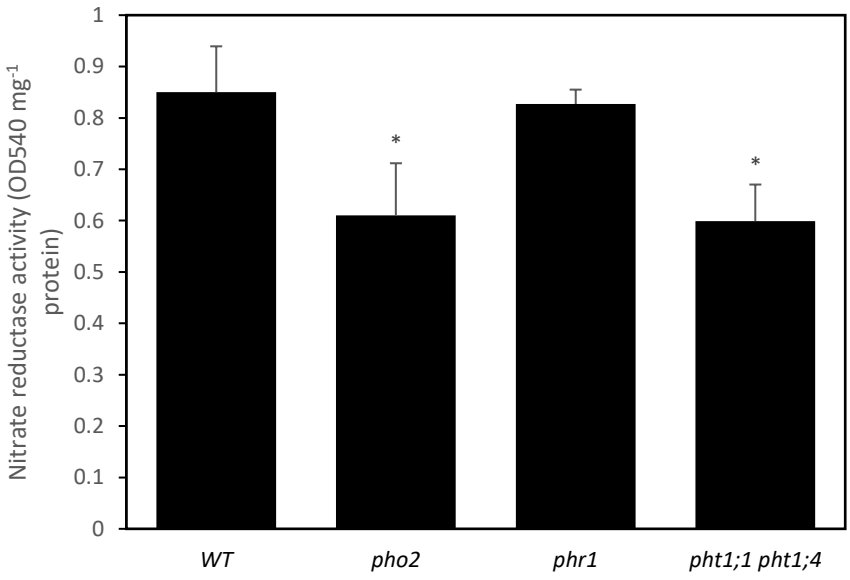


Figure 28: Nitrate reductase activity of mutants lacking regulatory components of phosphate metabolism. The NR activity of 5-week-old plant shoot tissue was assayed and compared to shoot protein content. * denotes statistical significance compared to WT (student's t-test, $p < 0.05$), n = 3, error bars denote S.E.M. The experiment was repeated independently 4 times with similar results.

Measuring the NR activity of 5-week-old *phr1*, *pht1;1* Δ *pht1;4* and *pho2* plants identified *pht1;1* Δ *pht1;4* and *pho2* as having significantly reduced NR activity compared to WT and *phr1*. The *phr1* mutant had no statistical difference in NR activity compared to WT [**Figure 28**]. Since both *pht1;1* Δ *pht1;4* and *pho2* plants had reduced NR activity, this suggests that

low Pi signalling pathways, rather than an absolute reduction of Pi content, are responsible for the reduced NR activity in plants grown on reduced Pi conditions. This is because whilst *pht1;1* Δ *pht1;4* plants have been reported to have a lowered shoot Pi content, *pho2* does not – indeed it is a known Pi over-accumulator due to increased expression of phosphate-starvation-induced genes encoding components that act to increase Pi uptake from the environment. The finding that *pho2* has reduced NR activity therefore suggests that it is genetic regulation, rather than absolute Pi content, affecting NR activity.

4.2.4 Mutants impaired in the regulation of phosphate metabolism have altered shoot nitrate content

To determine if altered regulation of Pi metabolism in the *phr1*, *pht1;1* Δ *pht1;4* and *pho2* plants was affecting NO_3^- uptake, as well as the regulation of NO_3^- metabolism, I measured the shoot NO_3^- content of these plants grown on compost. It is possible that the reduced NR activity observed in *pht1;1* Δ *pht1;4* and *pho2* plants could cause an increase in shoot NO_3^- concentration, since if NO_3^- uptake rates were not also altered then there would be a reduction in the quantity of shoot NO_3^- being reduced to NO_2^- via the NR enzyme, which could result in an accumulation of NO_3^- within shoot tissue. Alternatively, the changes in NO_3^- metabolism may be more widespread, and NO_3^- uptake mechanisms could also have lowered activity, causing no change or a reduction in shoot NO_3^- content.

Whilst *phr1* has no significant difference in NO_3^- content compared to WT, both *pho2* and *pht1;1* Δ *pht1;4* have significantly reduced levels of shoot NO_3^- [**Figure 29**]. This suggests that changes in N metabolism are more widespread than just alteration of NR activity.

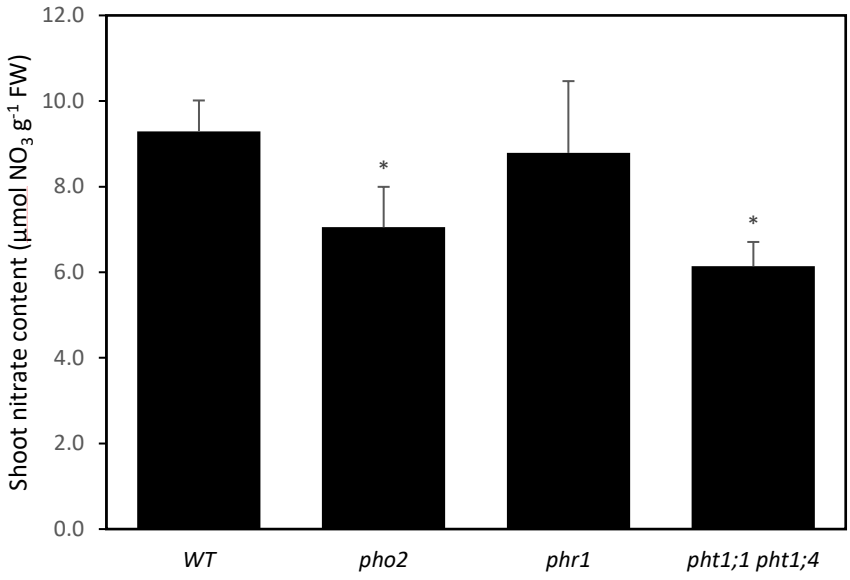


Figure 29: Shoot nitrate content of compost-grown plants lacking regulatory components of phosphate metabolism. 21-day-old shoot tissue was harvested, ground to a fine powder using liquid N_2 and assayed to determine nitrate, relative to fresh weight (FW) of shoot tissue. * denotes statistically significant difference compared to WT (Student's t-test, $p < 0.05$), error bars denote S.D, n = 5. The experiment was repeated independently 3 times with similar results.

To confirm whether these alterations in shoot NO_3^- content and shoot NR activity were independent of actual Pi levels within the plant, I additionally measured shoot Pi content to determine whether there was any correlation between NO_3^- and Pi content across different Arabidopsis genotypes. If shoot Pi content had a correlation with shoot NO_3^- content, this would suggest that the inherent Pi availability within a plant was regulating NO_3^- uptake, whereas if the two did not corelate, this would suggest that genetic mechanisms were responsible for this change in the regulation of NO_3^- metabolism. Although different Pi and NO_3^- contents were measured for different genotypes, there was no overall significant correlation between the shoot NO_3^- and Pi content of individual plants ($R^2 = 0.0395$) [**Figure 30**]. This suggests that genetic mechanisms are responsible for altered NO_3^- metabolism when Pi content is reduced, rather than a reduction in actual Pi content within a plant.

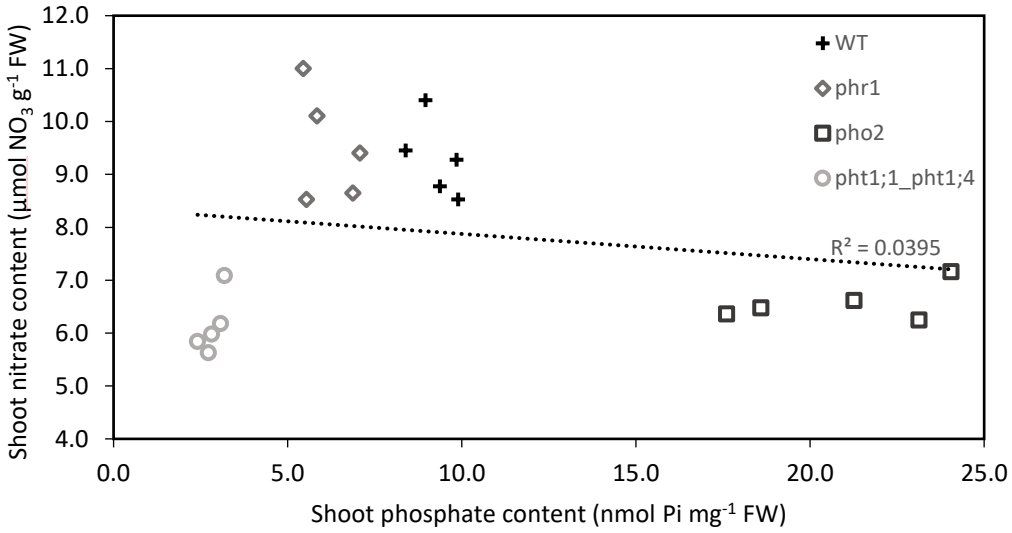


Figure 30: Shoot nitrate and phosphate content of genotypes lacking regulatory components of phosphate metabolism grown on compost. 21-day-old shoot tissue was harvested, ground to a fine powder using liquid N_2 and half of each sample assayed to determine nitrate or phosphate content, relative to the fresh weight (FW) of powdered shoot tissue. Shoot NO_3^- and Pi content varied according to genotype, but there was no significant linear correlation between shoot NO_3^- and shoot Pi content (R^2 = 0.0.0395).

4.2.5 *phr1* shoot nitrate content is altered when phosphate availability is reduced

On compost, I have found that both *pht1;1* Δ *pht1;4* and *pho2* plants have reduced NO_3^- content. In these conditions Pi is considered abundant, and therefore the lack of difference between *phr1* and WT is not unexpected. If PHR1 is responsible for inducing changes in N metabolism, then differences between WT and *phr1* could be expected only under reduced Pi levels, when in WT plants PHR1 would upregulate phosphate-starvation induced genes. To determine further the involvement of *phr1*, I therefore measured the shoot NO_3^- content of these genotypes under differing availability of Pi, to determine whether lowered Pi reduced or exacerbated the differences observed between these genotypes.

Measuring the shoot NO_3^- content of plants grown on different levels of Pi indicated that in high Pi conditions (1000 µM), there was no significant difference in shoot NO_3^- content between WT and *phr1* genotypes, however, both *pho2* and *pht1;1* Δ *pht1;4* had significantly reduced shoot NO_3^- levels relative to WT, a similar trend to that observed in

plants grown on compost [**Figure 31**]. All genotypes had reduced shoot NO_3^- content when grown on 100 µM Pi compared to 1000 µM Pi, however, there was no significant difference between WT and *pho2* or *pht1;1* Δ *pht1;4* on this Pi concentration, and unlike on 1000 µM Pi, *phr1* had a significantly increased NO_3^- content compared to WT [**Figure 31**]. This trend was repeated on 10 µM Pi: there was no significant difference in shoot NO_3^- content observed between WT and *pho2* and *pht1;1* Δ *pht1;4* genotypes, however, *phr1* had a significantly higher shoot NO_3^- content than WT [**Figure 31**]. This indicates that the reduced NO_3^- content in response to Pi starvation is at least partially PHR1-dependent, and the failure to reduce shoot NO_3^- content in response to low Pi is another facet of the failed phosphate starvation phenotype of *phr1* mutants.

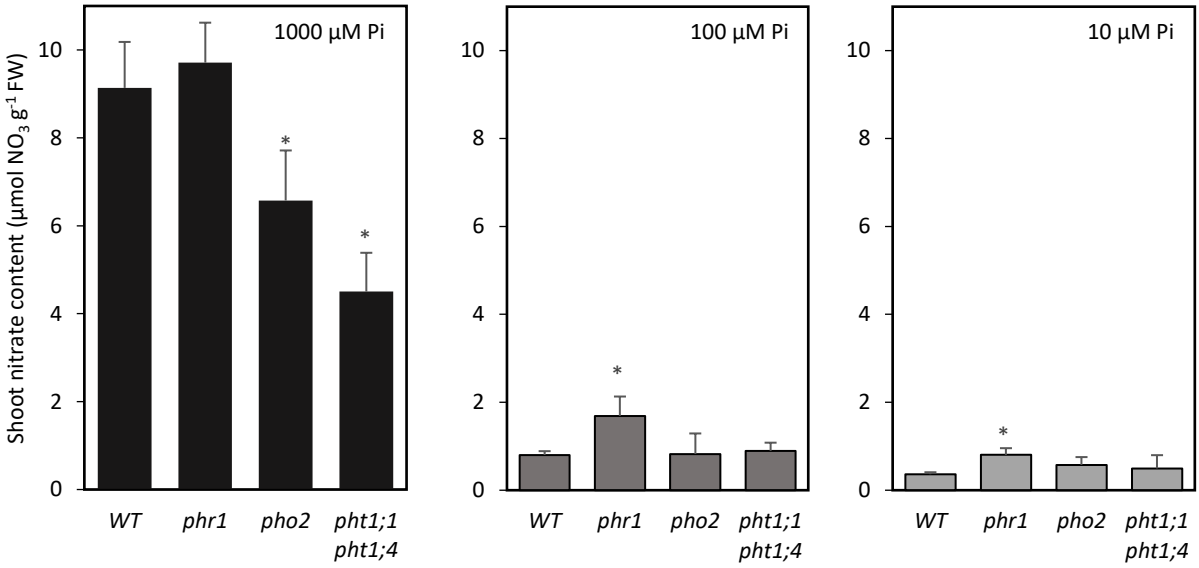


Figure 31: Shoot nitrate content of plants lacking regulatory components of phosphate metabolism, grown on three different phosphate concentrations. 14-day-old WT Arabidopsis seedlings were transferred to high (1000 µM), medium (100 µM) or low (10 µM) phosphate conditions and grown for a further two weeks before shoot tissue was harvested. The shoot nitrate content was determined relative to tissue fresh weight. * denotes statistically significant difference compared to WT (Student's t-test, $p < 0.05$), error bars denote S.D., n = 4-5. The experiment was repeated independently 3 times with similar results.

4.2.6 Potential PHR1 and NIGT1 binding sites are present in the promoters of genes encoding proteins involved in nitrate metabolism

PHR1 and PHR1-like (PHL1) are key transcriptional activators responsible for inducing expression of a range of phosphate-starvation genes, binding the 5'-GNATATNC-3' PHR1 binding sequence (*P1BS*) located in target gene promoters. Since genetic regulation by components of the phosphate-starvation-induced signalling pathway appears to alter NO_3^- metabolism, I searched the promoter sequences of genes encoding key components of NO_3^- metabolism to identify whether putative *P1BS* PHR1/ PHL1 binding sequences were present. The presence of putative binding sequences does not confirm binding of a transcription factor to a promoter sequence (there will be likely false positives), however, it does indicate whether candidate genes may be worthy of further analysis or not.

Analysing the promoter sequences of key genes regulating NO_3^- metabolism indicates that potential *P1BS* sequences are contained in the promoters of the *NRT1.1* and *NRT2.1* genes encoding NO_3^- transporters, the *NIA1* gene encoding NR and the *NIR1* gene NiR, although not within 1000 bp of the transcriptional start sequence for any of these genes. However, this sequence is not contained within the promoter regions of either *NIA2* or *GLN2* [**Table 6**]. Therefore, whilst one of the genes encoding NR (*NIA1*) does contain a potential *P1BS* element, this gene is suggested to encode a minority of Arabidopsis NR, as *NIA2* (which contains no *P1BS* elements within its promoter) has been reported to encode up to 90% of the enzyme in Arabidopsis.

Gene	Function of encoded protein	*P1BS* sequence within promoter	Number of *P1BS* elements	Position of *P1BS* element relative to start codon (bp)
NRT1.1	Nitrate transporter	Yes	1	-2362
NRT2.1	Nitrate transporter	Yes	1	-2899
NIA1	Nitrate reductase enzyme	Yes	2	-1267 -1540
NIA2	Nitrate reductase enzyme	No	0	N/A
NIR1	Nitrite reductase enzyme	Yes	1	-1585
GLN2	Glutamine synthetase enzyme	No	0	N/A

NR activity is strongly regulated by NO_3^- (described in **Chapter 1**), and so it is possible that NO_3^- transporters, which do contain potential *P1BS* sequences within their gene promoters, may impact the amount of NO_3^- entering the plant which in turn can regulate NR activity. Recent research demonstrated that PHR1 can regulate a negative regulator of several N metabolism-associated genes, NITRATE-INDUCIBLE GARP-TYPE TRANSCRIPTIONAL REPRESSOR1 (NIGT1) (Maeda *et al.*, 2018). In times of Pi starvation, accumulation of PHR1 protein upregulates *NIGT1* expression, which in turn reduces expression of *NRT2.1* which encodes a NO_3^- transporter. I therefore searched the promoters (the 1000 bp prior to the start codon, in line with the authors of this study) of these key nitrate metabolism genes for the presence of putative NIGT1 binding sites (5'-GAATC-3').

All gene promoters examined contained at least one putative NIGT1 binding sequence within 1000 bp of the start codon [**Table 7**]. Whilst the presence of putative promoter binding sites is insufficient to determine whether PHR1, PHL1 and NIGT1 regulate transcription of these genes, it does suggest these genes are potential candidates for

nitrate-responsive regulation, and if regulated by NIGT1 they could be under downstream regulation of PHR1-induced NIGT1 expression. Analysing supplementary datasets from Maeda *et al*., 2018 indicates that expression of *NRT1.1, NRT2.1, NIA1, NIR1* and *GLN2* is repressed by *NIGT1.2* overexpression, supporting this hypothesis.

These genes are excellent candidates for future work to determine the significance of these findings - including whether PHR1, PHL1 and NIGT1 bind the promoter sequences directly, and whether these genes are differentially expressed in the *phr1*, *pho2* and *pht1;1* Δ *pht1;4* lines.

Gene	NIGT1 binding site within promoter	Number of (5'-GAATC-3') elements	Position of NIGT1 binding site relative to start codon (bp)	Expression repressed by NIGT1.2 overexpression
NRT1.1	Yes	1	-428	Yes
NRT2.1	Yes	3	-41, -138, -181	Yes
NIA1	Yes	1	-328	Yes
NIA2	Yes	1	-164	No
NIR1	Yes	1	-212	Yes
GLN2	Yes	7	-52, -80, -112, -122, -373, -510, -576	Yes

Table 6: List of key genes involved in the nitrate assimilation pathway and putative NIGT1 binding site presence within promoter regions. The promoter sequences (defined as 1000 bp upstream of the ATG start codon) were searched to determine if they contained the NIGT1 (5'-GAATC-3') binding sequence, and if so, their position relative to the ATG start codon. Datasets from Maeda *et al.* (2018) were analysed to determine whether there is evidence these genes are repressed by NIGT1.2 overexpression.

4.2.7 The genotypes *phr1*, *pho2* and *pht1;1* Δ *pht1;4* do not have altered responses to chlorate treatment

Since two of the genotypes tested, *pho2* and *pht1;1* Δ *pht1;4*, had reduced shoot NR activity, and reduced shoot NO_3^- content, it was plausible that these genotypes would have increased resistance to chlorate treatment, since reduced NR activity and/or chlorate uptake would reduce the amount of ClO_2^-, which is toxic, being produced within the plant.

I treated 4-week-old *phr1*, *pht1;1* Δ *pht1;4* and *pho2* plants with 2.5 mM chlorate solution for two weeks to observe whether this is the case.

As expected, the *nrt1.1* control was strongly resistant to chlorate treatment (shown by leaves that remained green), whilst WT plants were susceptible, with clear yellowing of leaves [**Figure 32**]. Also susceptible were all three Pi signalling mutants, with no apparent difference in chlorate resistance between *phr1*, *pht1;1* Δ *pht1;4* and *pho2* plants and the WT control [**Figure 32**]. Although not pictured, all lines tested had green leaves with no abnormal colouring under control conditions. This suggests that under laboratory compost conditions, the previously observed difference in NR activity in the shoots of *pht1;1* Δ *pht1;4* and *pho2* plants is not sufficient to confer a reduction in the chlorate susceptibility of these genotypes.

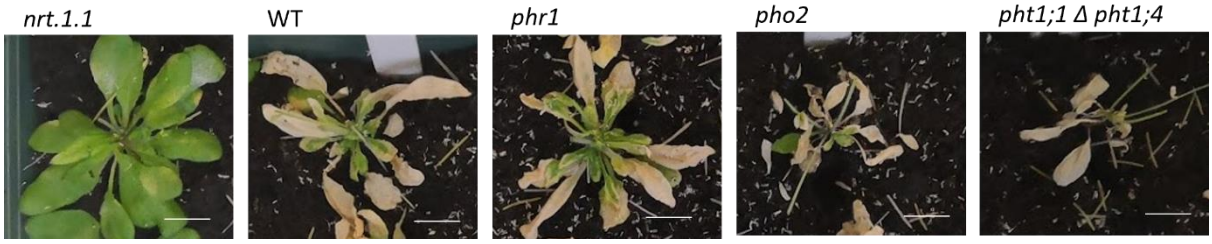


Figure 32: WT, *phr1*, *pho2* and *pht1;1* Δ *pht1;4* lines all appear susceptible to chlorate treatment. 4-week-old plants were treated with 2.5 mM chlorate solution and imaged 10 days after being treated. Image shows plants with stems removed. Whilst *nrt1.1* shows strong resistance to chlorate treatment, with leaves remaining green, WT, *phr1*, *pho2* and *pht1;1* Δ *pht1;4* genotypes display visible chlorosis of leaves. Scale bars = 10 mm.

4.2.8 Genotypes lacking regulatory components of phosphate metabolism maintain altered shoot and root nitrate content when nitrate availability is reduced

Since up to 10% of the transcriptome has been reported to be nitrate-responsive, and low N availability causes a variety of adaptive responses, including upregulation of genes encoding NO_3^- transporters (Chen *et al.*, 2008), I wanted to determine how NO_3^-

metabolism was altered in mutants lacking Pi signalling components when NO_3^- availability was decreased. It might be expected that low-nitrate signalling pathways may override the observed effects in *pho2* and *pht1;1* Δ *pht1;4* mutants, and so I wanted to understand the contribution of these genes to the regulation of N metabolism, specifically shoot NO_3^- content, when N was present in more limiting concentrations.

The shoot and root NO_3^- content of plants grown on media with either 20 mM or 2 mM NO_3^- was determined. As expected, on NO_3^--replete conditions (20 mM), shoot NO_3^- content was reduced in *pho2* and *pht1;1* Δ *pht1;4*, and root NO_3^- content was reduced in these genotypes also [**Figure 33**]. In intermediate NO_3^- conditions (2 mM NO_3^-, selected for reasons described in **Chapter 3**), both *pho2* and *pht1;1* Δ *pht1;4* had significantly lower shoot and root NO_3^- concentrations than WT plants [**Figure 33**].

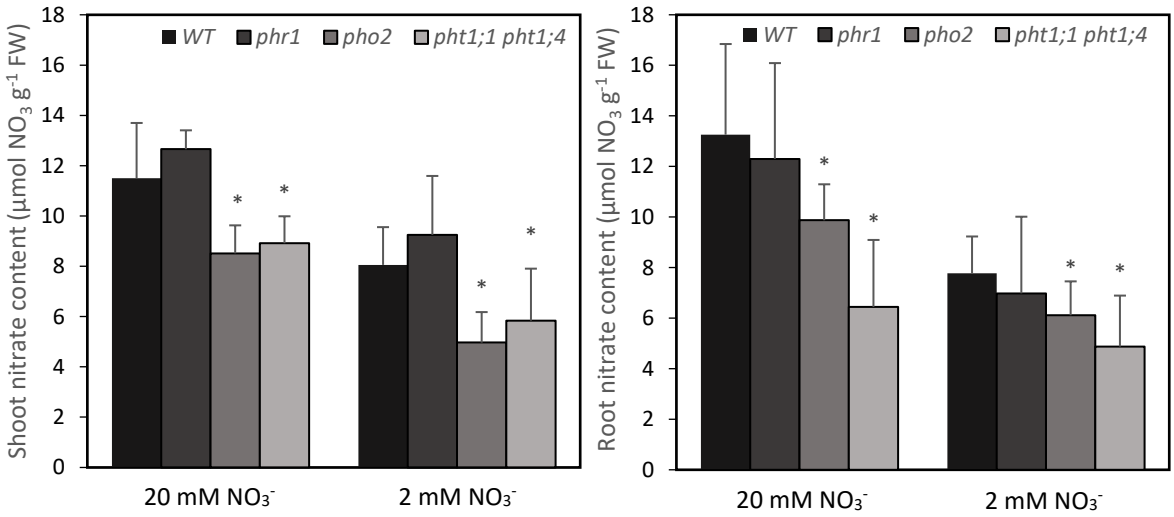


Figure 33: Average shoot nitrate of seedlings grown on replete and reduced nitrate concentrations. 8-day-old seedlings were transferred to agarose media containing either high (20 mM) or intermediate (2 mM) concentrations of nitrate as the sole nitrogen source. After a further 12 days of growth seedlings were weighed and the shoot nitrate concentration (left panel) and root nitrate concentration (right panel) determined relative to fresh weight (FW). * denotes statistical difference compared to WT (student's t-test, $p < 0.05$, n = 5-7 pools of plants), error bars denote S.D. The experiment was repeated independently 3 times with similar results.

4.2.9 Genotypes lacking regulatory components of phosphate metabolism have no significant alteration in growth under reduced nitrate availability

When nutrient availability is limiting, plant growth is typically reduced. In addition to a reduction in overall growth, a common adaptation is to invest a greater proportion of growth into root tissue, rather than shoot tissue, so that there is greater growth of the tissue responsible for nutrient uptake (roots) relative to the tissue which is the site of carbon fixation (shoots) (Lopez-Bucio *et al.*, 2003).

Since I had found NO_3^- metabolism is altered in the *phr1*, *pht1;1* Δ *pht1;4* and *pho2* genotypes, I wanted to determine the effect of altered NO_3^- availability on the growth and biomass allocation of these genotypes. As discussed in **4.2.8**, a possible hypothesis was that low-nitrate signalling pathways may override Pi signalling-induced changes in NO_3^- metabolism, although the observation that reductions in NO_3^- content persist in *pht1;1* Δ *pht1;4* and *pho2* even when NO_3^- availability is reduced 10-fold suggests this may not be the case. It was possible that these genotypes would be more affected by reduced NO_3^- availability, since NO_3^- metabolism was already reduced in these lines, or alternatively these genotypes may be able to sustain more growth under reduced NO_3^- conditions compared to WT if their altered NO_3^- metabolism caused an increase in nitrate use efficiency.

To determine the effect of N availability on the growth and biomass allocation of mutants lacking components of phosphate metabolism, 10-day-old seedlings were transferred to nitrate-replete (20 mM) and reduced nitrate (2 mM) media. After a further 10 days of growth, the mass of shoot and root tissue of the seedlings was measured, and the ratio between the two calculated, to determine if any of the mutants lacking components of Pi

metabolism have altered growth (in terms of biomass), and allocation of shoot: root tissue, when NO_3^- availability is reduced.

In WT plants, as expected, reduced NO_3^- availability causes a reduction in the overall biomass of seedlings [**Figure 34**]. When grown on either 20 mM or 2 mM NO_3^-, with no other N source present, there is no significant difference between the biomass of WT and *phr1*, *pho2* or *pht1;1* Δ *pht1;4* genotypes. When NO_3^- availability is reduced, WT plants invest a greater proportion of growth into roots, reflected by a decrease in the shoot: root biomass ratio [**Figure 34**]. In high NO_3^- conditions, neither *phr1*, *pho2* or *pht1;1* Δ *pht1;4* genotypes have a significant difference in their shoot: root biomass ratio, this is the same in low NO_3^- conditions also [**Figure 34**]. This result suggests that despite the reduced nitrate content and NR activity in *pho2* or *pht1;1* Δ *pht1;4*, growth, at least at the stage measured in this study, is not significantly affected.

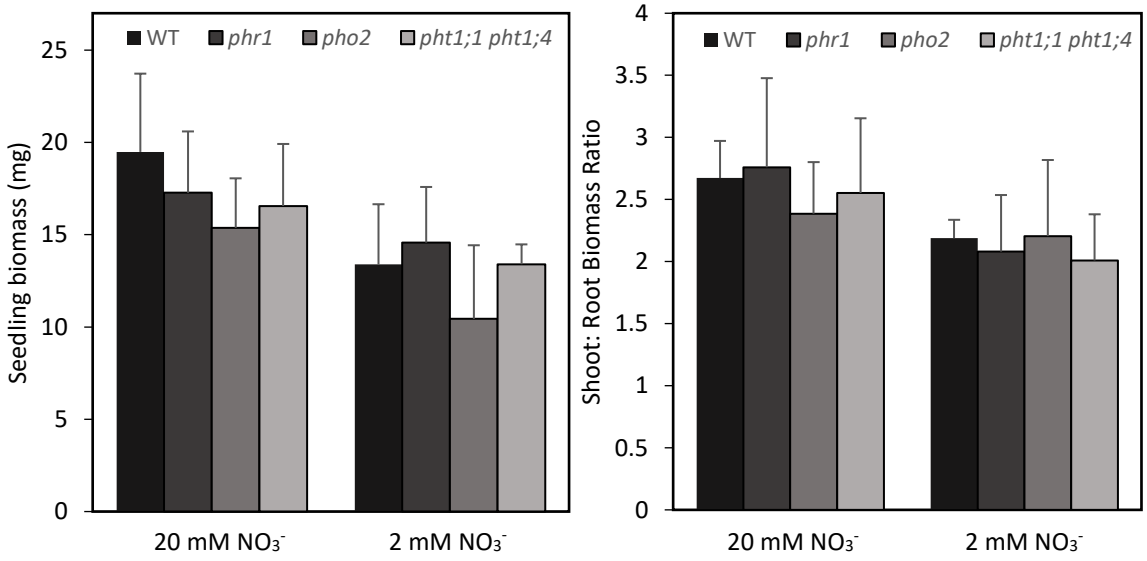


Figure 34: Plant biomass and root: shoot ratio of phosphate mutants on high and low nitrate availability. 10-day-old seedlings were transferred to media containing either 20 mM or 2 mM nitrate. After a further 10 days of growth, seedlings were pooled and the plant biomass measured and the root: shoot biomass ratio determined. No significant difference between WT and any of the genotypes tested was observed (student's t-test, $p < 0.05$, $n = 7$), error bars denote S.D. The experiment was repeated independently 3 times with similar results.

4.2.10 Chlorate treatment causes toxicity on agarose plates

Since mutants lacking components of Pi metabolism did not appear to have a significantly altered response to chlorate treatment on compost, I wanted to determine if this would change when Pi availability was lowered, which could enhance the difference between the four genotypes. *phr1*, for instance, lacks the full response to low Pi availability, so when Pi levels are replete this mutation can cause little difference in responses to Pi compared to WT, but it would be expected that this mutant is significantly impaired compared to WT when Pi availability is lowered. I therefore wanted to develop an experimental system where I could both manipulate nutrient availability and subject plants to chlorate treatment.

In order to manipulate nutrient levels, I wanted to determine if it was possible to treat plants grown on agarose plates with chlorate solution. I grew WT Arabidopsis on agarose plates, using serial dilutions of $KClO_3^-$ to determine an optimal concentration to use, with water applied as a control [**Figure 35**]. This demonstrates that, as on laboratory compost conditions, applying chlorate solution to plants grown on agarose plates results in toxicity: at high concentrations plants die, at lower concentrations plants have visible chlorosis of leaves, and when control solution (dH_2O) is applied plant rosette tissue remains fully green.

To determine the best concentration of chlorate solution to use in further experiments I quantified the proportion of shoot tissue remaining green following treatment, which indicated that plants treated with a final concentration of 2.5 mM and 5 mM chlorate solution had a significantly lower proportion of green shoot tissue than those treated with 0 mM chlorate solution, whilst still surviving unlike those treated with 20 mM, 15 mM or 10 mM chlorate solution [**Figure 36**]. I therefore used final concentrations of between 2 and 5 mM for future experiments.

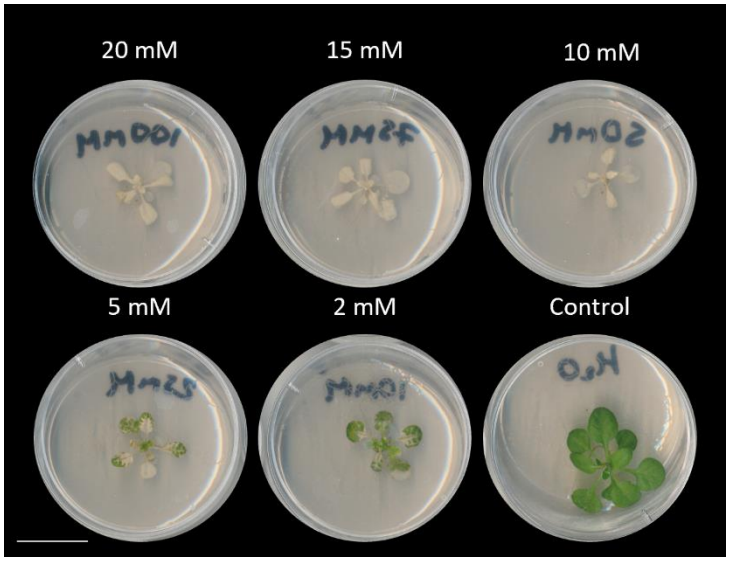


Figure 35: WT Arabidopsis grown on agarose plates and treated with 3 mL of chlorate solution. 3-week-old WT Arabidopsis plants grown on agarose plates were treated with chlorate by adding 3 mL of chlorate solution to 15 mL of ½ MS solidified with 0.8% agarose. This solution was absorbed into the media to give a final concentration (shown in figure) of 20% that of the solution added. Scale bar = 10 mm. For each concentration, n = 3, representative samples are shown. The experiment was repeated independently 3 times with similar results.

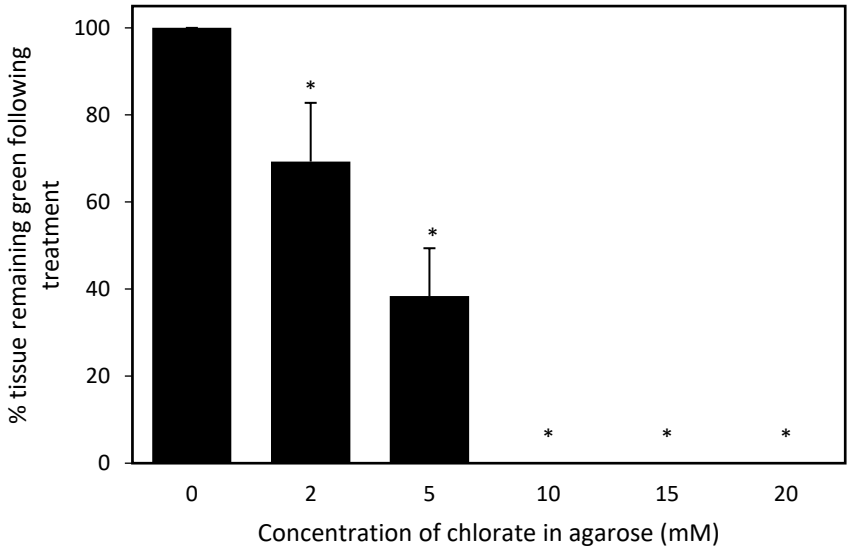


Figure 36: Percentage of green tissue remaining in WT Arabidopsis shoots following treatment with different concentration of chlorate solution. 3-week-old Arabidopsis plants grown on agarose plates were treated with chlorate by adding 3 mL of chlorate solution to 15 mL of agarose. The percentage of shoot tissue remaining green following chlorate treatment was quantified using imageJ. Error bars denote S.D, * denotes statistical difference to plants treated with 0 mM chlorate solution (student's t-test, $p < 0.05$, n = 3). The experiment was repeated independently 3 times with similar results.

4.2.11 *nrt1.1* and *ctr1-1* have altered chlorate susceptibility when treated on agarose plates rather than on compost

Once a suitable concentration of chlorate solution to add had been identified, I treated *nrt1.1* and *ctr1-1* lines grown on agarose with 2 mM and 4 mM chlorate solution. As shown in Chapter 3, both genotypes are strongly chlorate resistant on laboratory compost conditions, so I used these as controls to determine if this system was working as expected. Plants were treated at 4 weeks old to mimic the conditions of previous treatment on compost. The results were surprising: whilst WT had slight yellowing of leaves, *nrt1.1* and *ctr1-1* both had clear and widespread yellowing of leaves, indicating that although these genotypes were strongly resistant to chlorate treatment on compost, this is not the case when treated on agarose [**Figure 37**].

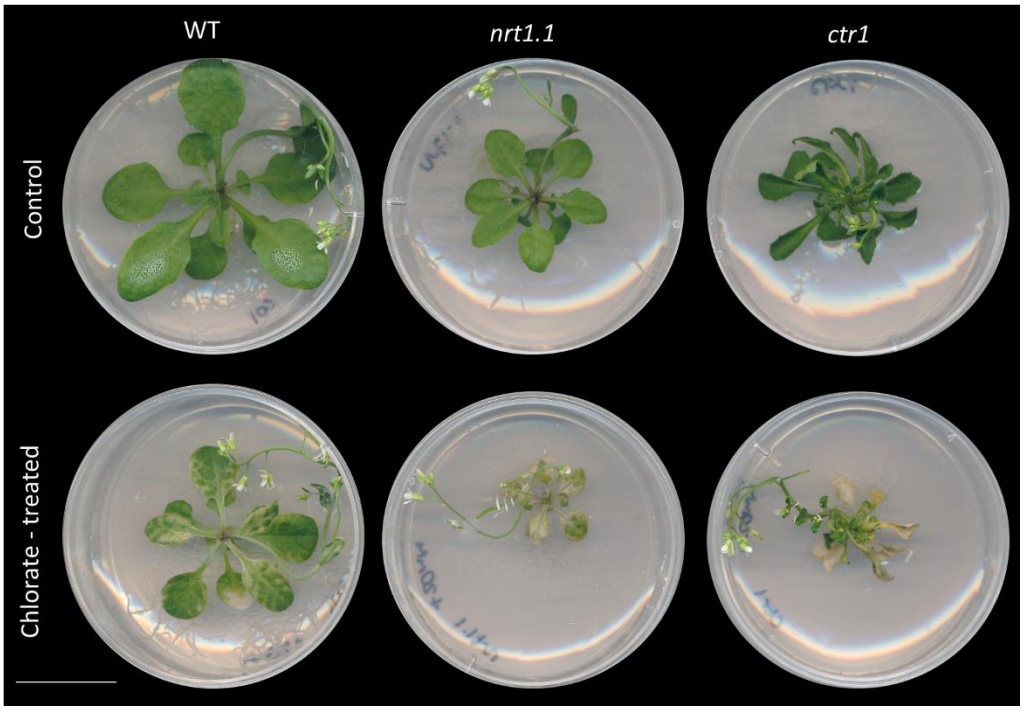


Figure 37: WT, *nrt1.1* and *ctr1-1* are all susceptible to chlorate treatment when treated on agarose. WT, *nrt1.1* and *ctr1-1* plants were grown on 15 ml of agarose, and after four weeks, treated with chlorate solution to give a final concentration of 4 mm 1 week after treatment plants were imaged: all three genotypes have visible yellowing of leaves in response to increased chlorate treatment. Scale bar = 10 mm. For each concentration n = 3, representative samples are shown. The experiment was repeated independently 3 times with similar results.

Quantifying this result by analysing the proportion of green shoot tissue remaining following treatment indicated that all three genotypes were susceptible to chlorate treatment, with a significant reduction in the proportion of green tissue following treatment with concentrations of both 2 mM and 4 mM chlorate solution in all genotypes analysed [**Figure 38**].

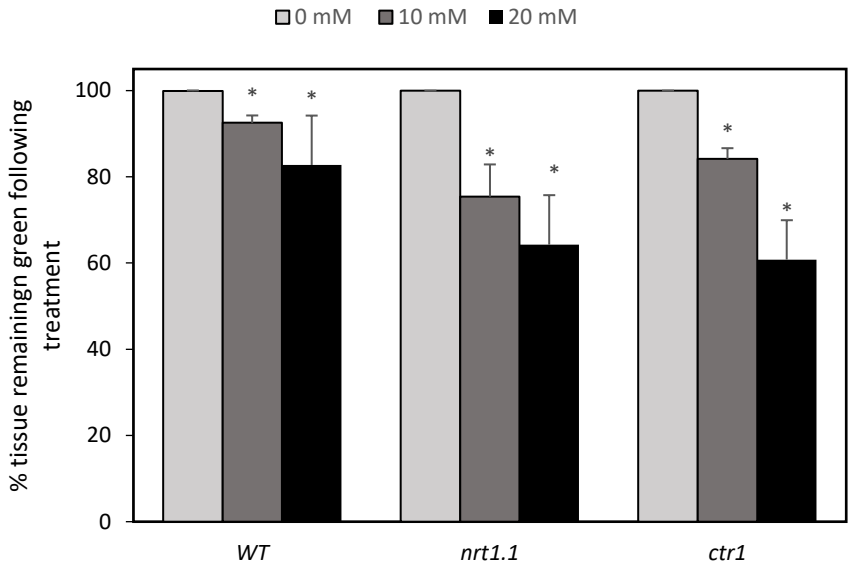


Figure 38: Proportion of shoot tissue remaining green in WT, *nrt1.1* and *ctr1-1* genotypes following treatment with chlorate solution. 4 – week old plants were treated with control (0 mM chlorate, light bars) or chlorate solution to give a final concentration of 2 mM (medium grey bars) or 4 mM (dark grey bars). 1 week after treatment plates were imaged and the proportion of shoot tissue remaining green analysed using imageJ. Error bars denote S.D, * denotes statistical difference compared to control (0 mM) treatment (student's t-test, $p < 0.05$, $n = 3$). The experiment was repeated independently 3 times with similar results.

This result is particularly surprising for *nrt1.1*, which has an extremely strong chlorate resistance phenotype compared to WT when grown on compost. The basis of the *nrt1.1* mutant's chlorate resistance is hypothesised to be due to decreased uptake of chlorate ions due to the absence of the NRT1.1 nitrate transporter. The *nrt1.1* loss-of-function mutant has reduced high-affinity and low-affinity uptake of NO_3^- ions (Wang *et al.*, 1998) and so regardless of the concentration of NO_3^- and chlorate ions in the media it would be

expected that the *nrt1.1* mutant would still have reduced chlorate uptake relative to WT. Without measuring rates of NO_3^- uptake, it is difficult to understand if NO_3^- transport is significantly altered in *nrt1.1* plants grown on agarose compared to those grown on compost, but since the severity of NO_3^- toxicity is still strongly dose-dependent [**4.2.11**] it is unlikely the concentrations applied in this experiment were simply too large for 'normal' metabolic processes to occur. It is possible that chlorate solution is instead entering through leaves in this system, however, leaves were not touching the surface of the agarose, and newer leaves appear more affected than older leaves, and these are furthest from the media and therefore least likely to come into contact with the solution. This explanation is therefore unlikely.

4.2.12 Chlorate susceptibility of both WT and *ctr1-1* treated on agarose remains susceptible to the effects of light and sucrose provision

To further investigate why treating plants grown on agarose with chlorate solution was producing results in contrast to those expected, I investigated the effects of light and sucrose presence on resistance to chlorate treatment. NR activity is known to be strongly regulated in response to carbon fixation (reviewed by Yanagisawa, 2014) and so I wanted to determine if plants would always show signs of chlorate toxicity when grown on agarose, or if this was still dependent on fixed carbon acquisition.

To determine whether chlorate toxicity was altered by photosynthesis, I treated plants with control or chlorate solution and moved them to either long-day conditions or continuous darkness. In plants kept in long-day conditions (16 h light / 8 h dark) 100% of shoot tissue remained green following treatment with control solution, but no tissue remained green following chlorate treatment in either genotype [**Figure 39**]. In plants

treated with control solution and kept in continuous darkness, 90-100% of tissue remained green in WT and *ctr1-1* plants, with no significant difference in the proportion of tissue remaining green for the plants treated with chlorate solution [**Figure 39**]. The toxic effects of chlorate treatment on agarose plates are therefore dependent on the presence of light.

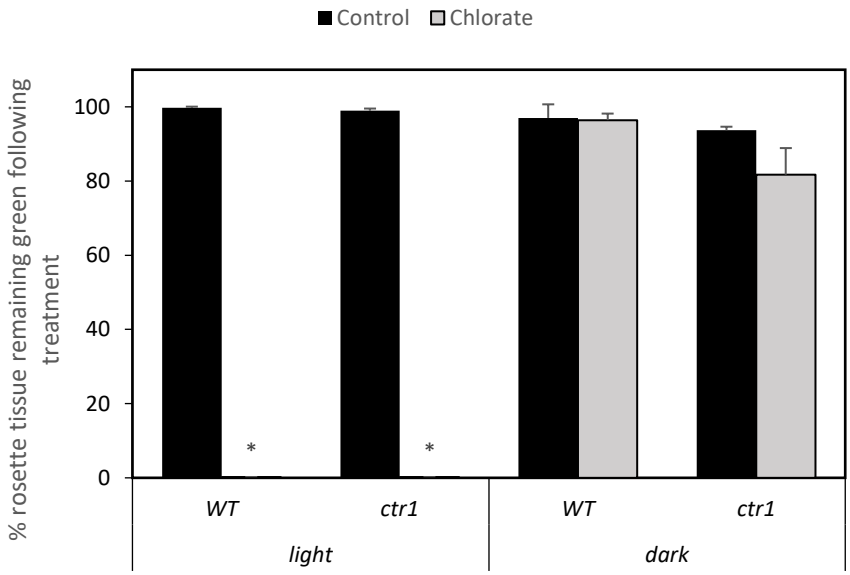


Figure 39: Chlorate resistance is increased when plants are grown in the absence of light. 4-week-old plants grown on agarose plates were treated with 5 mM chlorate solution and either kept in long-day or covered to create continuous-darkness conditions. * denotes significant difference between control and chlorate-treated plants of the same genotype (student's t-test, $p < 0.05$). Error bars denote S.D, n = 3. The experiment was repeated independently 3 times with similar results.

In the absence of light plants cannot photosynthesise, however, fixed carbon can be acquired by plants if sugars are provided externally in the media. I therefore investigated the effects of sucrose provision on chlorate toxicity in dark-grown plants. Whilst in 0% sucrose there was no significant difference in the proportion of green shoot tissue following either control or chlorate treatment, in 3% sucrose chlorate -treated WT and *ctr1-1* plants had significantly less rosette tissue remaining green [**Figure 40**]. Chlorate resistance is therefore decreased by the presence of sucrose in the medium.

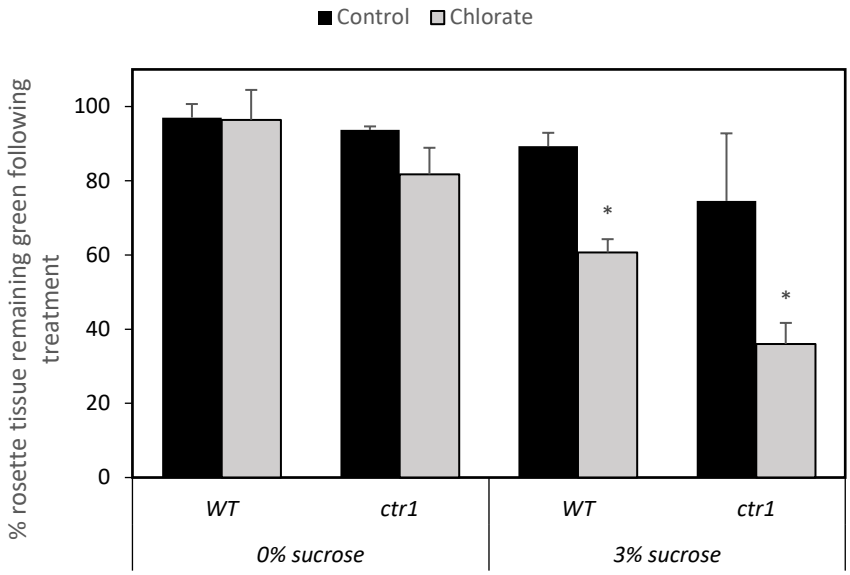


Figure 40: Chlorate resistance is decreased by the presence of sucrose in the media of dark-grown plants. 4-week-old plants grown on agarose plates were treated with 5 mM chlorate solution and moved to either long-day or continuous-darkness conditions. * denotes significant difference between control and chlorate-treated plants of the same genotype (student's t-test, $p < 0.05$). Error bars denote S.D, n = 3. The experiment was repeated independently 3 times with similar results.

These results therefore suggest that chlorate toxicity is regulated by light and sucrose, and therefore despite the fact that the *ctr1-1* genotype does not have the expected chlorate resistance in this system as is observed on compost, this is not due to all genotypes in all conditions losing resistance to treatment due to the media used.

One of the differences between this growth environment and that on compost is that plants grown on agarose plates are enclosed, and therefore likely have very little transpiration due to high humidity levels. Although reduced transpiration might suggest that there would be reduced chlorate uptake due to reduced movement of the transpiration stream, it is possible that transpiration is responsible for these observed differences in chlorate sensitivity; the effects of transpiration on chlorate resistance were therefore investigated further.

4.2.13 Transpiration may alter chlorate sensitivity

To determine the effects of transpiration on chlorate resistance in the WT, *nrt1.1* and *ctr1-1* genotypes, I grew plants on compost in enclosed Magenta boxes, replicating the sealed environment of plants grown on agarose plates. Similar to plants grown on agarose, plants flower earlier, suggesting this environment is more stressful than on compost. At four weeks old plants were treated with either water or 2.5 mM $KClO_3^-$ solution. The results showed that whilst plants treated with water (the control) are flowering early, they remain green. Plants treated with chlorate are also flowering early and appear visibly more stressed than controls: WT leaves were completely yellowed, whilst both *nrt1.1* and *ctr1-1* have visible yellowing of leaves in addition to probable anthocyanin accumulation due to the purple colour also seen on leaves [**Figure 41**].

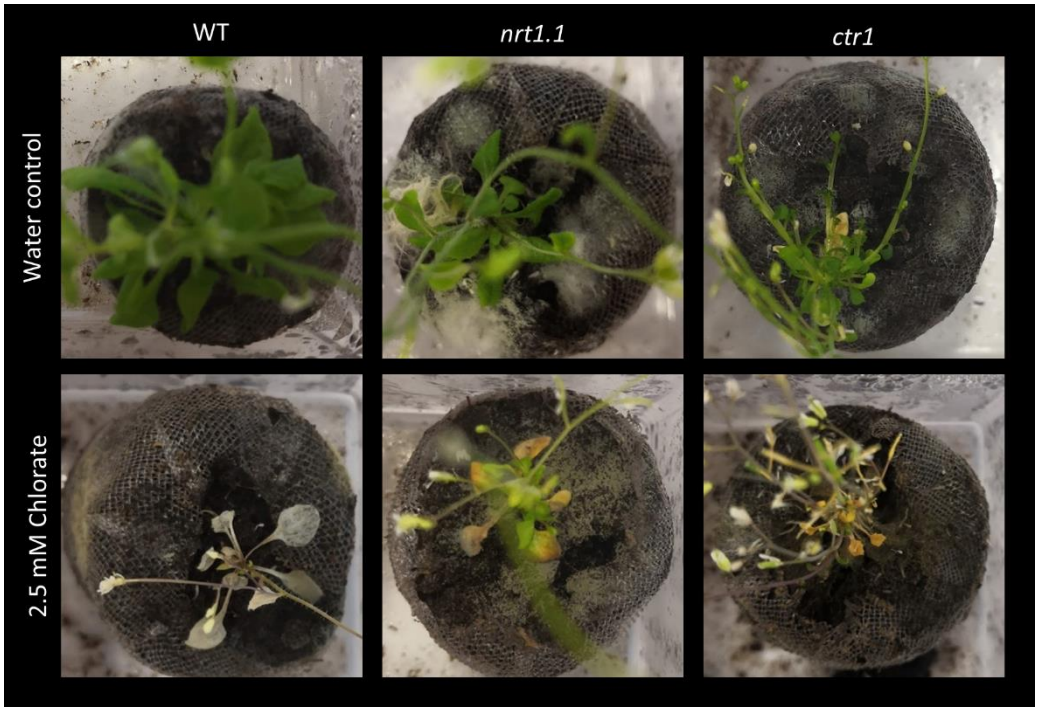


Figure 41: WT, *nrt1.1* and *ctr1-1* plants on Jiffy compost pellets treated with water or 2.5 mM chlorate solution in enclosed Magenta boxes. 4-week-old plants were treated with either water (controls) or 2.5mM chlorate solution and imaged 10 days after treatment. All genotypes show yellowing of leaves following chlorate treatment, with WT plants most affected. N = 3, representative samples are shown.

4.2.14 Nitrate reductase activity is not affected by growing plants in enclosed systems

Since chlorate resistance was altered in plants grown in enclosed systems, I investigated whether plants grown in enclosed Magenta boxes had altered NR activity which could explain the difference in chlorate susceptibility. I therefore compared the NR activity of WT plants grown in Magenta boxes with no lid, and therefore presumably the same levels of transpiration as plants grown in regular laboratory compost conditions, with that of plants grown in sealed Magenta boxes where transpiration is presumed to be significantly lowered.

Measuring the NR activity of Arabidopsis shoot tissue from plants grown in the two environments indicated that growing plants in enclosed vs open systems did not alter NR activity [**Figure 42**].

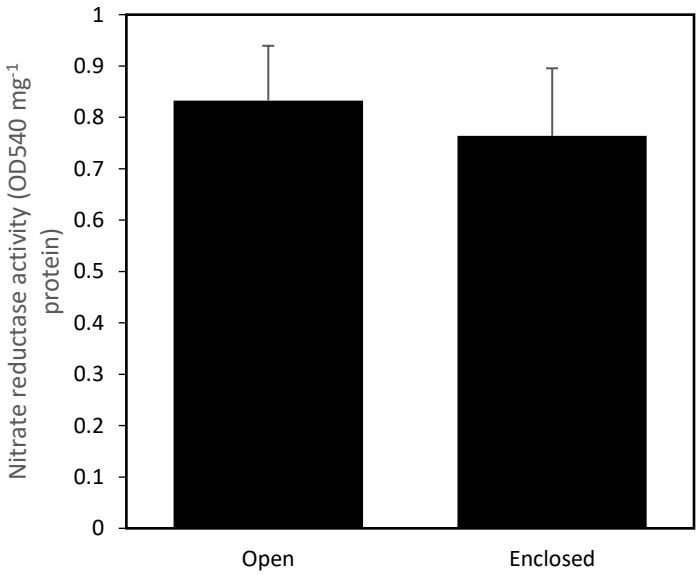


Figure 42: Nitrate reductase activity of WT Arabidopsis grown in enclosed and open environments. WT Arabidopsis was grown on Jiffy compost pellets in Magenta boxes, either with no lid ("open") or with a lid on and sealed shut ("enclosed"). Shoot tissue was harvested from 4-week-old plants and protein extracted. The NR activity of protein extract was assayed and expressed relative to protein concentration. There was no significant difference in NR activity of plants grown in either enclosed or open environments (student's t-test, $p < 0.05$, $n = 5$). Error bars denote S.D. The experiment was repeated independently 4 times with similar results.

This suggests that transpiration does not alter this aspect of nitrate metabolism. It is possible that transpiration alters other aspects of chlorate metabolism; and worth noting

that plants grown on Jiffy compost pellets in enclosed boxes appear stressed so other regulatory processes may be at play. At this stage, there is no satisfactory explanation to interpret these findings, although they are interesting given that a large number of experiments investigating Arabidopsis nutrient use are performed using ½ MS media solidified with either agarose or agar, and these results indicate that the biology of plants on agarose vs compost may be more different than may be initially assumed. Given these findings, the chlorate resistance of mutants lacking components of Pi metabolism in high and low Pi conditions was not investigated, as it would be difficult to interpret any results given controls are not behaving as expected. However, it may be worth exploring chlorate treatment in other experimental systems, such as hydroponics, to investigate this further.

Chapter 5: *hy5* has altered phosphate metabolism

5.1 Introduction

HY5 is a master regulator, known to coordinate a wide range of plant functions in response to light (Osterlund *et al.*, 2000). As discussed in **1.6.2** and **1.6.3**, HY5 has subsequently been identified as coordinating whole-plant carbon – nitrogen metabolism (Chen *et al.*, 2016), as well as having roles in sulphur acquisition (Sakuraba and Yanagisawa, 2018). Up to one third of Arabidopsis genes are subject to HY5-mediated regulation of expression, with approximately 3000 genes suggested to be regulated directly via HY5 binding (Lee *et al.*, 2007; Zhang *et al.*, 2011a). HY5 binds promoters containing ACE (ACGT-containing) elements, for example the G-box (CACGTG), C-box (GACGTC), Z-box (ATACGGT) and A-box (TACGTA), and can act as both a transcriptional up-regulator and a transcriptional repressor (Zhang *et al.*, 2011a).

The *hy5-526* loss-of-function mutant has previously been identified as having altered N metabolism, and contains a splice-site nucleotide substitution mutation that results in a product lacking the HY5 C-terminal domain (Chen *et al.*, 2016). This mutation caused indistinguishable responses from the *hy5* null mutant when investigating the regulation of nitrate metabolism (Chen *et al.*, 2016). HY5 regulates nitrate metabolism in conjunction with carbon fixation by, in part, mobile shoot HY5 acting to upregulate expression of root *HY5* and of the *NRT2.1* gene encoding a root nitrate transporter (Chen *et al.*, 2016).

Putative HY5 binding sites have been identified in the promoters of a number of genes encoding Arabidopsis phosphate transporters, including *PHT1;1* and *PHT1;4*. Since evidence suggests these are two of the main root Pi transporters (Shin *et al.*, 2004), HY5 is therefore implicated as a potential regulator of phosphate transport, and in turn,

phosphate metabolism. The *hy5-526* line was used to investigate the role of functional HY5 protein in regulating Arabidopsis phosphate metabolism, and additionally, whether this was coordinated with respect to carbon acquisition.

5.2 Results and discussion

5.2.1 Putative HY5 binding sites are present within the promoters of genes encoding PHT1 phosphate transporters

It had been suggested that the promoters of some Pi transporter genes may contain HY5 binding sites (Zhe Ji, unpublished data). To determine the presence of HY5 binding sites, I therefore searched the promoter sequences (defined as 3000 bp upstream of the ATG start codon) of genes encoding the nine Arabidopsis PHT1 phosphate transporters for the presence of eight common putative HY5 binding motifs: the A-box (TACGTA), C-box (GACGTC), G-box (CACGTG), Z-box (ATACGGT), C/A box (TACGTC), C/G box (GACGTG), C/T box (AACGTC) and stand-alone ACE elements (ACGT) (Song *et al.*, 2008). Whilst the presence of a putative binding sequence does not confirm binding of a transcription factor to a promoter sequence (for example, there will be likely false positives), it can suggest whether candidate genes may be worthy of further analysis or not.

All nine *PHT1* gene promoters analysed contained at least one of these eight putative HY5 binding motifs. Not surprisingly, the promoter region of all nine genes contained at least one ACE element [**Table 8**]. In addition, at least one A-box was present in the gene promoters of *PHT1;1*, *PHT1;2* and *PHT1;7*, C-boxes were present in the promoter regions of *PHT1;2*, *PHT1;4* and *PHT1;7*, G-boxes in the promoter regions of *PHT1;8* and *PHT1;9* and Z-boxes in *PHT1;2* and *PHT1;4*. C/A boxes were found in *PHT1;*5 and *PHT1;7*, C/G boxes in *PHT1;7*, *PHT1;8* and *PHT1;9*, and six of the promoter regions of genes encoding PHT1

phosphate transporters contained C/T boxes (*PHT1;1*, *PHT1;2*, *PHT1;3*, *PHT1;4*, *PHT1;5* and *PHT1;7*) [**Table 8**]. The distance between putative HY5 binding sites and the ATG start codon of each gene varied from 89 base pairs to 2972 base pairs [**Table 8**].

The presence of multiple putative HY5 binding sites within the promoters all nine PHT1 phosphate transporters suggests that these are strong candidates for HY5-mediated regulation of gene expression, and HY5 may therefore be involved in the regulation of phosphate metabolism. This is supported by experimental evidence that HY5 binds the promoter of *PHT1;6*, although the promoters of other PHT1 phosphate transporters were not identified in this study (Lee *et al.*, 2007).

Since HY5 can act to both up-regulate and repress gene expression, I wanted to determine how the regulation of phosphate metabolism was altered in the *hy5* mutant to determine whether HY5 is a potential new regulator of phosphate metabolism, and if so, further investigate the role that this protein plays.

Gene	Number	A-box TACGTA	C-box GACGTC	G-box CACGTG	Z-box ATACGGT	C/A box TACGTC	C/G box GACGTG	C/T box AACGTC	ACE ACGT
PHT1;1	AT5G43350	-2114	-	-	-	-	-	-851, -2788, -2822	-360, -411, -657, -1487
PHT1;2	AT5G43370	-978, -1621	-2310	-	-1931	-	-	-1916	-723, -1289
PHT1;3	AT5G43360	-	-	-	-	-	-	-1876	-892
PHT1;4	AT2G38940	-	-671	-	-2267	-	-	-1043, -2767	-477 , -884, -2981
PHT1;5	AT2G32830	-	-	-	-	-1457, -2686	-	-982	-249, -281, -634
PHT1;6	AT5G43340	-	-	-	-	-	-	-	-89, -134, -712, -1745,
PHT1;7	AT3G54700	-958	-1018	-	-	-1608	-1671	-2935	-94, -1393, -1648
PHT1;8	AT1G20860	-	-	-2908, -2917, -2972	-	-	-485, -1616	-	-1483
PHT1;9	AT1G76430	-	-	-1953	-	-	-837	-	-610

Table 7: Presence of potential HY5 binding sites within the promoters of Arabidopsis *PHT1* phosphate transporters. The promoter sequences (defined as 3000 bp upstream of the ATG start codon) were searched to determine whether any eight potential HY5 binding sites were present, and if so, their position relative to the ATG start codon of each gene.

5.2.2 *hy5* has a reduced shoot phosphate content when grown on compost

A number of mutants with altered regulation of phosphate metabolism have been reported to have altered shoot Pi content. For example, the *pht1;1* Δ *pht1;4* double mutant lacks functional copies of genes encoding two of the major root Pi transporters (PHT1;1 and PHT1;4), and has previously been reported to have a 75% reduction in Pi uptake capacity relative to WT Arabidopsis, and a 70% reduction in shoot Pi content (Shin *et al.*, 2004). To investigate whether regulation of Pi metabolism was altered in *hy5*, the shoot Pi content of compost-grown *hy5* plants was measured, alongside *pht1;1* Δ *pht1;4* and *phr1* (lacking *PHR1*, encoding an important component of low-phosphate signalling). As has previously been reported (Shin *et al.*, 2004), the shoot Pi content of the *pht1;1* Δ *pht1;4* double mutant was reduced by 70% compared to WT, and the *phr1* mutant displayed a 35% reduction in shoot Pi content [**Figure 43**]. *hy5* plants were found to have a significantly reduced shoot Pi content compared to WT also, with a shoot Pi content 26% lower than WT [**Figure 43**]. This suggests that the *hy5* mutant does indeed have altered regulation of Pi metabolism. Compared to the mutants impaired in Pi metabolism investigated, *hy5* had a significantly higher shoot Pi content than *pht1;1* Δ *pht1;4*, and there was no significant difference in shoot Pi content between *hy5* and *phr1* mutant [**Figure 43**].

Interestingly, these findings contradict that of Liu *et al.*, 2017, but support those of Yeh *et al.*, 2020, published during the course of, and after, this research. Liu *et al.* demonstrated that the total Pi content of ten day old seedlings grown on ½ MS media solidified with agar and supplemented with 2% sucrose was significantly higher for the *hy5-215* mutant; *hy5-215* is considered a null allele (Oyama *et al.*, 1997), contradicting both the findings here and those

of Yeh *et al.*, who reported a reduced shoot phosphate content in *hy5-215* seedlings in phosphate-replete (625 µM Pi) conditions.

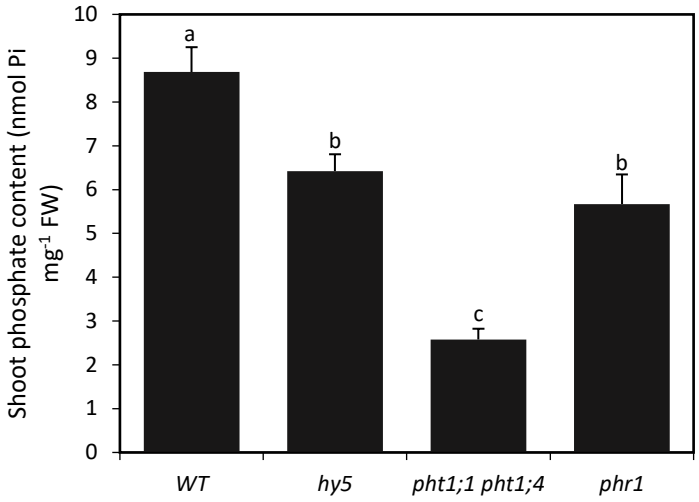


Figure 43: Pi content of compost-grown *hy5*, *pht1;1* Δ *pht1;4* and *phr1* plants. The phosphate content of rosette leaves of 4-week old plants growing on compost was measured using the malachite green method and compared to shoot fresh weight (FW). Plants were grown under a long day photoperiod (16 h light / 8 h dark) with irradiance of 120 µmol of photons m^{-2} s^{-1}. Values are means ± SD, n = 3. Different letters denote statistically significant differences (one-way ANOVA/Tukey HSD post hoc test, $p < 0.05$). The experiment was repeated independently 3 times with similar results.

5.2.3 hy5 has reduced root system architecture changes in response to altered Pi availability

Since *hy5* plants have reduced shoot Pi contents when grown on compost, I examined the phosphate starvation responses of *hy5* plants grown on ½ MS media, solidified with agarose, where the external Pi concentration could be easily manipulated. Since *hy5* plants have a reduced Pi content on compost, I hypothesised that phosphate starvation responses in this mutant would likely be altered. If *hy5* plants are able to sustain normal growth with a lower shoot Pi content, then it is possible plants would be less sensitive to reduced Pi availability. Alternatively, phosphate starvation symptoms might be exacerbated, if plants are further compromised in their ability to take up Pi from their environment when it is present in very limiting quantities.

Altered Pi availability induces well documented changes in Arabidopsis root system architecture (RSA), that act to increase the surface area available for Pi uptake. Primary root growth is inhibited, whilst there is increased lateral root growth and root hair formation (Péret *et al.*, 2011). The RSA responses of *hy5* plants in low Pi was therefore investigated by measuring differences in primary root elongation, and number of lateral roots, of seedlings transferred from Pi-replete ½ MS media, to media containing concentrations of 1000 µM, 100 µM, or 10 µM Pi [**Figure 44A**]. These concentrations were used for reasons described in **Chapter 4**.

As expected, reduced Pi availability (100 µM or 10 µM) resulted in a significant decrease in the length of primary roots [**Figure 44A, 44B**]. Roots of WT seedlings transferred to 100 µM Pi were on average 23% shorter than those transferred to 1000 µM Pi, and roots of seedlings transferred to 10 µM Pi were on average 50% shorter than those transferred to 1000 µM Pi, and significantly shorter than those grown on 100 µM Pi. On 1000 µM Pi, *hy5* seedlings had significantly shorter primary root lengths than WT, whilst there was no significant difference in the primary root length of WT and *hy5* seedlings transferred to 100 µM or 10 µM Pi. Altering Pi availability from 1000 µM to 10 µM still caused a significant reduction in primary root length however; although seedlings transferred to 100 µM Pi did not have a significant reduction in root length compared to those on 1000 µM Pi, seedlings transferred to 10 µM Pi did, with root lengths on average 31% shorter than those grown on 1000 µM Pi [**Figure 44B**].

These results appear to contradict those of Yeh *et al.*, and Liu *et al.*, who indicated that whilst *hy5* root lengths were shorter than WT in Pi- replete conditions, there appeared to be little reduction in the root length of *hy5* plants under Pi- starvation conditions relative to Pi-replete

conditions. However, growth and experimental conditions differ so it harder to make a true comparison.

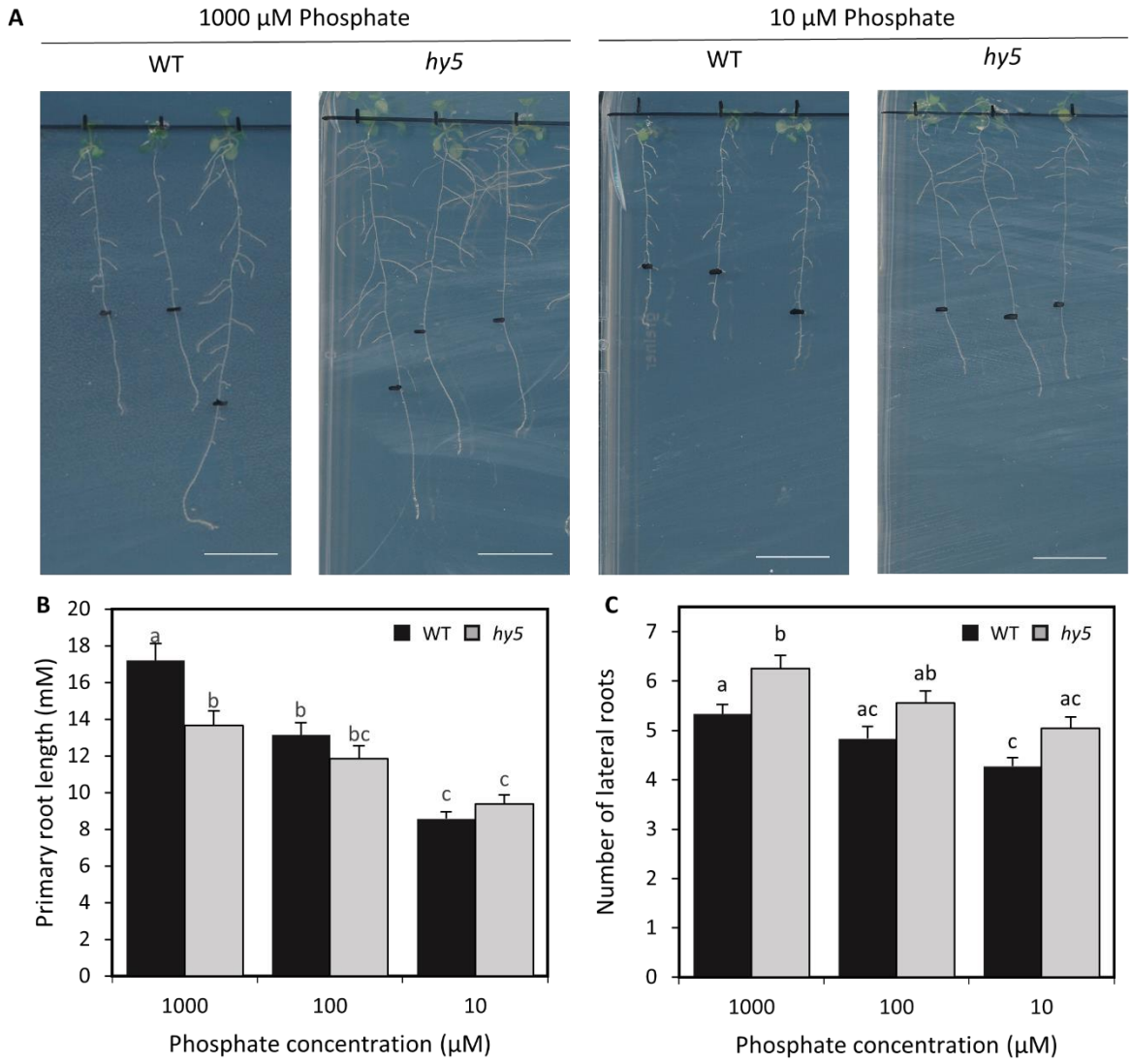


Figure 44: Root system architecture of WT and *hy5* on high and low phosphate media. Arabidopsis seedlings were grown on ½ MS solidified with 0.8% agarose, at four days old transferred to modified ½ MS solidified with 0.8% agarose, containing either 1000 µM, 100 µM or 10 µM phosphate, and the position of the primary root tip marked on the back of the plates. [**A**] WT and *hy5* plants grown on 1000 µM and 10 µM phosphate. Scale bar = 1 cm. [**B**] 7 days after transfer plates were scanned and primary root elongation determined by measuring the distance along the root between the mark indicating the length of root at the time of transfer, and the root tip. [**C**] 7 days after transfer to different phosphate concentrations the number of lateral roots present in seedlings was counted by viewing seedlings under a stereomicroscope and counting all lateral roots > 1 mM in length. Different letters denote statistically significant differences (one-way ANOVA/Tukey HSD post hoc test, $p < 0.05$). Error bars denote S.E.M, n = 35-44. The experiment was repeated independently 3 times with similar results.

Although reduced Pi availability is widely reported to increase the number of lateral roots in seedlings, this was not observed in this experiment, in which WT plants had significantly fewer numbers of lateral roots on seedlings transferred to 10 µM Pi compared to seedlings transferred to 1000 µM Pi [**Figure 44C**]. There was no significant difference in the number of lateral roots between seedlings grown on 1000 µM or 100 µM Pi. In 1000 µM Pi *hy5* seedlings had significantly greater numbers of lateral roots than WT, and like WT plants, transferring seedlings to 10 µM, but not 100 µM Pi, caused a significant reduction in the number of lateral roots present [**Figure 44C**]. At both 100 µM and 10 µM Pi concentrations there was no significant difference in the number of lateral roots in *hy5* and WT seedlings [**Figure 44C**].

10 µM Pi is therefore sufficient to cause a significant reduction in primary root growth in both WT and *hy5* genotypes. However, the response in *hy5* plants is not as large as that of WT plants: primary root lengths are reduced by 31% rather than 50%, and 100 µM Pi is not sufficient to cause a significant reduction in *hy5* primary root length when measured at 7 days after transfer, unlike WT plants. It is surprising that reduced phosphate availability did not cause an increase in the number of lateral roots; one possible explanation is the absence of sucrose in the media. Indeed, in this study 10 µM Pi was found to significantly reduce the number of lateral roots in both WT and *hy5* seedlings. Similar to the results for primary root length, *hy5* plants transferred to 1000 µM Pi had significantly different numbers of lateral roots (and primary root lengths) compared to WT, whilst there was no significant difference in these parameters in seedlings transferred to reduced (100 µM or 10 µM) Pi concentrations. Reduced Pi availability therefore appears to diminish the difference in root system architecture between WT and *hy5* plants that is observed in phosphate-replete conditions.

5.2.4 The *hy5* mutant has altered chlorophyll and anthocyanin content in high and low phosphate conditions

A well characterised adaptation to low-phosphate conditions in Arabidopsis is the accumulation of shoot anthocyanin pigments. HY5 is known to directly bind anthocyanin biosynthetic genes, and the *hy5* loss-of-function mutant has defects in anthocyanin accumulation when grown under continuous far-red or blue light conditions (Shin *et al.*, 2007; Shin *et al.*, 2013), and deficiencies in low temperature-induced anthocyanin accumulation when grown in the presence of light (Zhang *et al.*, 2011b). I wanted to determine if *hy5* is deficient in low phosphate-induced accumulation of anthocyanin pigments. I therefore analysed the shoot anthocyanin content of WT and *hy5* in response to a range of different phosphate concentrations. I also observed that *hy5* seedlings grown on low external Pi concentrations appeared to have a lighter green appearance than WT seedlings on plates containing low levels of phosphate, I therefore quantified shoot chlorophyll content of seedlings also to determine if this was altered in the *hy5* mutant.

Both WT and *hy5* seedlings transferred to 1000 µM Pi had low levels of anthocyanin, as would be expected given anthocyanins are produced primarily as a response to stress [**Figure 45B**]. WT seedlings transferred to 100 µM Pi had significantly increased shoot anthocyanin levels, with a significantly greater anthocyanin content than *hy5* seedlings. Transferring seedlings to 10 µM Pi caused significant accumulation of anthocyanin pigments in both genotypes, although the anthocyanin content of *hy5* was again significantly less than that of WT [**Figure 45B**]. This is similar to the results subsequently published by Yeh *et al.*, 2020, who reported a reduced anthocyanin content in *hy5-215* seedlings grown on 10 µM Pi, but not 625 µM Pi, compared to WT.

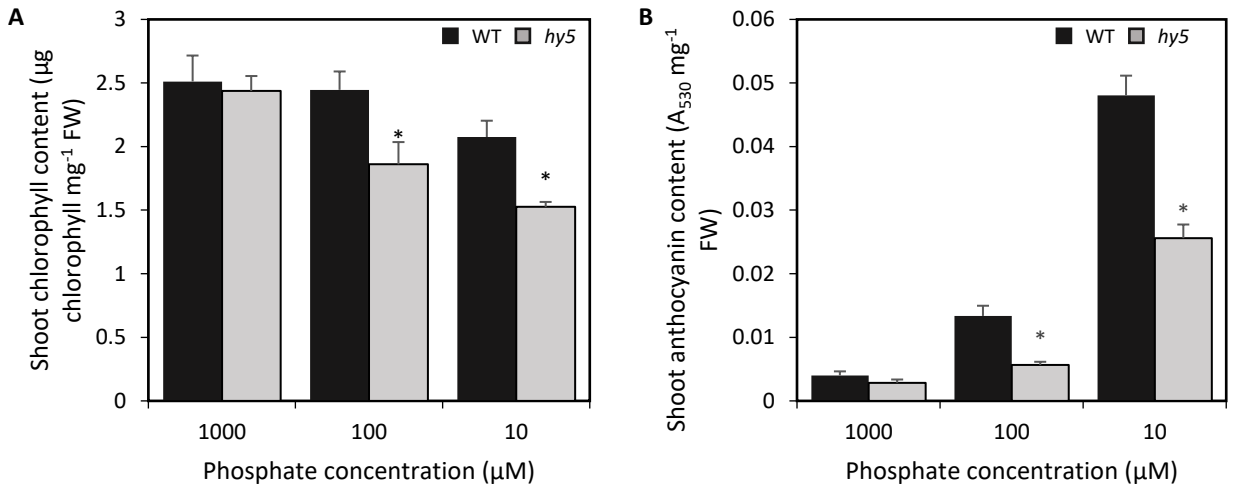


Figure 45: *hy5* seedlings have reduced shoot chlorophyll content and shoot anthocyanin content compared to WT in low phosphate conditions. 4-day-old seedlings grown on phosphate replete agarose media were transferred to agarose media containing either high (1000 µM), medium (100 µM) or low (10 µM) phosphate concentrations. Seedlings were grown for a further 10 days before shoot tissue was harvested for analysis. [**A**] Shoot chlorophyll was extracted in 95% ethanol and total chlorophyll *a* and *b* quantified using a spectrophotometer. * denotes statistical difference compared to WT plants grown on the same phosphate concentration (student's t-test, $p < 0.05$, $n = 4$) Error bars denote S.E.M. [**B**] Shoot anthocyanins were extracted in 1% HCl in methanol, and quantified using a spectrophotometer after separation from chlorophyll pigments. * denotes statistical difference compared to WT plants grown on the same phosphate concentration (student's t-test, $p < 0.05$, $n = 6$) Error bars denote S.E.M. The experiment was repeated independently 3 times with similar results.

WT and *hy5* seedlings transferred to 1000 µM Pi displayed no significant difference in chlorophyll content [**Figure 45A**]. However, for seedlings transferred 100 µM and 10 µM Pi, *hy5* seedlings had a significant reduction in chlorophyll content compared to their WT seedlings on the same concentrations [**Figure 45A**].

hy5 seedlings are therefore deficient in maintaining WT-levels of shoot chlorophyll under phosphate-deficient conditions. This suggests that functional HY5 protein may play a role in maintaining shoot chlorophyll content under reduced Pi availability – although the mechanistic basis for this observation is unclear, as later results published by Yeh *et al.*, 2020 suggest no difference in photosynthetic gene expression in shoots between WT and *hy5-215* under Pi-deficient conditions (although growth conditions differ).

The *hy5* mutant also displayed deficiencies in anthocyanin accumulation under reduced phosphate conditions. Anthocyanin is a well characterised response to low Pi availability, with WT seedlings showing increasing anthocyanin accumulation under reduced phosphate concentrations. Although *hy5* seedlings had significantly greater anthocyanin accumulation when grown on 10 µM Pi than 100 µM or 1000 µM Pi, this was significantly less than the anthocyanin levels of WT plants. Therefore, whilst the functional HY5 protein does not appear to be absolutely required for low-phosphate induced anthocyanin accumulation, it does appear necessary to achieve the full response displayed in WT plants.

5.2.5 *hy5* plants have a reduced shoot phosphate content in both phosphate-replete and phosphate-deficient conditions

Plants under phosphate starvation induce a range of mechanisms aimed at increasing phosphate uptake from the environment, for example increasing expression of *PHT* phosphate transporters, secreting acid phosphatase proteins (APases) to mobilise Pi from the soil, and altering root system architecture to increase root surface area (Zhang *et al.*, 2014). In addition, plants also induce metabolic changes that reduce Pi demand. For instance, membrane phospholipids are replaced with sulpholipids and galactolipids, and alternative metabolic pathways can be utilised that reduce requirements for adenylates or Pi as cosubstrates for enzymes (Plaxton and Tran, 2011).

I have shown that *hy5* plants appear deficient in inducing some adaptations to phosphate starvation: primary root lengths are not decreased to the same extent as WT and anthocyanin accumulation under phosphate deprivation is reduced. I have also shown that on laboratory compost conditions, where Pi levels are presumed replete, the *hy5* mutant has a reduced shoot Pi content compared to WT [**Figure 43**]. Since a range of low phosphate signalling

pathways act to increase phosphate uptake in conditions of phosphate starvation, it is possible that these may override the effects of the *hy5* mutation causing a depleted shoot Pi content in plants grown on compost. However, given that the *hy5* mutant appears partially deficient in inducing some characteristic phosphate starvation responses **[Figure 44, Figure 45**], it would appear likely that *hy5* has altered regulation of phosphate metabolism under conditions of Pi limitation also. I therefore measured how *hy5* seedling Pi content was altered in conditions of Pi limitation, in addition to conditions where phosphate is abundant. In order to manipulate the phosphate content of growth media accurately, I grew WT and *hy5* seedlings on ½ MS media solidified with 0.8% agarose, and at 4 days old transferred seedlings to modified ½ MS media, solidified with 0.8% agarose, with a concentration of either 1000 µM, 100 µM or 10 µM Pi. After a further 14 days of growth, seedlings were harvested, and the Pi content of pools of seedlings determined using the malachite green method.

Transferring seedlings to a lower (100 µM or 10 µM) Pi concentration caused a significant reduction in the phosphate content of seedlings compared to those transferred to 1000 µM Pi, in both WT and *hy5* genotypes [**Figure 46**]. This is to be expected, as plants induce metabolic changes to reduce their Pi requirements. Both genotypes exhibited an approximate reduction in shoot Pi content of 70% in seedlings transferred to 10 µM as opposed to 1000 µM Pi. In plants grown on phosphate-replete conditions (1000 µM Pi), like the results from plants grown on compost, *hy5* seedlings have a significantly lower Pi content than WT, with a reduction of approximately 33%. This is also true for seedlings transferred to low Pi conditions, with *hy5* shoot Pi content significantly lower than WT on both 100 µM and 10 µM Pi, a reduction of approximately 15% and 25% respectively [**Figure 46**].

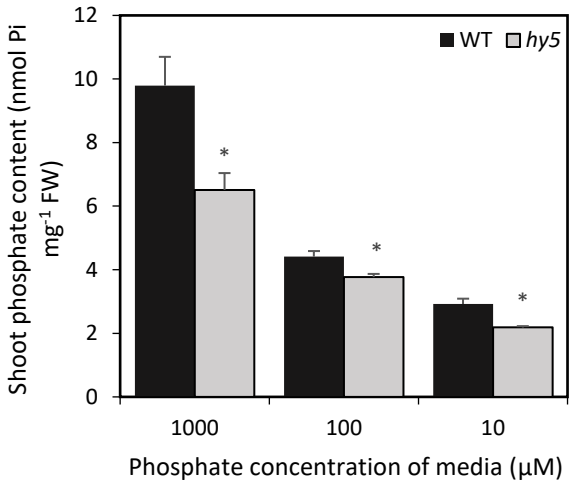


Figure 46: *hy5* mutants have a reduced shoot phosphate content in both phosphate-replete and phosphate-deficient conditions. Arabidopsis seedlings were grown on ½ MS solidified with 0.8% agarose, at four days old transferred to modified ½ MS solidified with 0.8% agarose, containing either 1000 µM, 100 µM or 10 µM phosphate, and grown for a further 14 days. After 14 days seedlings were harvested and the phosphate content determined relative to fresh weight (FW), using the malachite green method. * denotes statistically significant difference to WT (student's t-test, $p < 0.05$). Error bars denote S.E.M., n = 4. The experiment was repeated independently 3 times with similar results.

Therefore, *hy5* has perturbed regulation of phosphate metabolism in both phosphate-replete and phosphate-deficient conditions. This indicates that the HY5 protein is necessary for normal Pi metabolism in Arabidopsis in both high and low Pi availability, and the difference in shoot Pi content observed in phosphate-replete conditions cannot be overridden by the low phosphate signalling pathway. These findings continue to contradict those of Liu *et al.* who identified *hy5* seedlings as having an elevated total Pi content compared to WT, although they do align with previous findings of plants grown on laboratory compost conditions [**Figure 43**] These results support the subsequent finding of Yeh *et al.*, that shoot *hy5* content is reduced, although the authors did not report a reduction in shoot Pi content on low Pi, unlike the findings presented here. Only shoot Pi content is measured here; whilst Liu *et al.* looked at total seedling content – it is possible either the difference in tissue type, age of seedlings, or presence of sucrose in the media used by Liu *et al.* may explain these differences in results – similarly the age of seedlings differs to Yeh *et al.*

5.2.6 *hy5* seedlings have no significant difference in growth on different phosphate availabilities

To determine if overall plant growth was altered in plants lacking a functional copy of the HY5 protein, and whether this was further altered by external Pi availability, the biomass of seedlings grown on different Pi concentrations was recorded. Lowered nutrient availability causes a reduction in plant growth, due to decreased availability of resources. It would therefore be expected that lowering Pi availability would reduce plant growth, and that since *hy5* has altered regulation of Pi metabolism, this may be either impaired (due to insufficient ability to adapt to low Pi availability), or not impaired as much (if altered metabolism allowed growth to be continued whilst acquiring less Pi).

As expected, significantly greater plant growth (reflected in terms of average plant biomass) is seen in plant growing on increased phosphate concentrations, with WT plants having an approximately 14-fold greater biomass on 1000 µM Pi relative to 10 µM Pi [**Figure 47**]. This was the same for *hy5* seedlings also, with no significant difference in the average biomass of WT and *hy5* plants on any of the Pi concentrations tested [**Figure 47**]. This suggested that despite the differences in shoot Pi content observed in these plants, the *hy5* mutant is still able to produce the same amount of growth as WT plants, at least at the stage measured in this study.

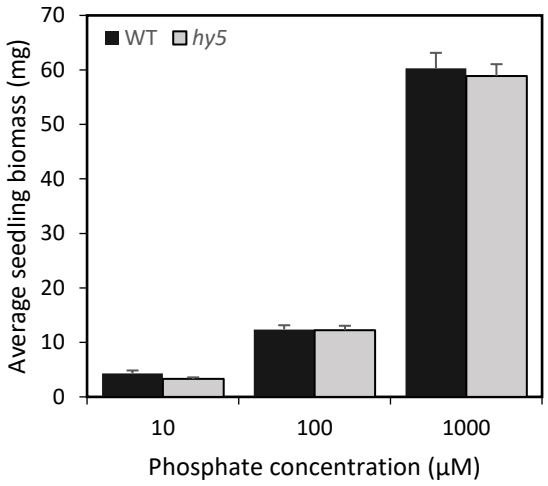


Figure 47: *hy5* seedlings have no significant difference in biomass compared to WT plants. 8-day-old seedlings were transferred to media containing either high (1000 µM), medium (100 µM) or low (10 µM) phosphate concentrations. After 21 days of further growth pools of seedlings were weighed and the biomass recorded. Dark bars denote WT plants, light bars *hy5*. * denotes statistical difference compared to WT in the same concentration (student's t-test, $p < 0.05$, $n = 6$) Error bars denote S.E.M. The experiment was repeated independently 3 times with similar results.

5.2.7 hy5 has no detectable difference in low phosphate induced Root Acid Phosphatase Activity

Induction and secretion of acid phosphatases enables plants to scavenge Pi from their environment, and is a long recognised hallmark of plant phosphate starvation (Duff *et al.*, 1994). Extracellular acid phosphatases are secreted from roots of phosphate-depleted plants; these enzymes catalyse the hydrolysis of phosphate from soil organophosphates, which can contain up to 80% of soil phosphate (Tran *et al.*, 2010). Root-secreted acid phosphatase (APase) activity has been widely used to evaluate the extent of plant responses to Pi starvation (Wang and Liu, 2017), therefore I investigated whether *hy5* had altered root APase activity in response to Pi deprivation. To determine whether *hy5* has impaired root APase activity, roots of seedlings transferred to 1000 µM, 100 µM, or 10 µM Pi were stained by overlaying roots with agarose containing 5-bromo-4-chloro-3-indolyl phosphate (BCIP), which can be cleaved by secreted APases on the root surface to produce a blue precipitate. APase activity is therefore visible as a blue stain on the root surface. APase activity was then

quantified by measuring the production of *p*-nitrophenol by root samples using a colorimetric assay.

Using the BCIP staining method allowed root APase activity to be visually detected, demonstrating that seedlings grown on 1000 µM Pi had very little visibly detectable APase activity, as would be expected in phosphate-replete conditions [**Figure 48A**]. Both WT and *hy5* seedlings transferred to 100 µM Pi or 10 µM Pi had visibly increased blue staining of root tissue, indicating increased APase activity, and in both genotypes root APase activity appears higher in seedlings grown on 10 µM Pi compared to 100 µM Pi, as the blue staining of roots appears darker. There is no obvious difference between WT and *hy5* root APase activity, as detected by BCIP staining of seedlings transferred to 100 µM or 10 µM Pi [**Figure 48A**].

Root samples from plants grown on 10 µM Pi had the highest levels of BCIP staining, and so roots grown on this condition were therefore selected for quantification of root APase activity. As expected given the visible blue staining of roots, both WT and *hy5* had detectable APase activity when quantified using a colorimetric assay, and there was no significant difference between the WT and *hy5* genotypes [**Figure 48B**]. This suggests that HY5 is not required for the induction and secretion of root acid phosphatases in response to low Pi conditions in Arabidopsis.

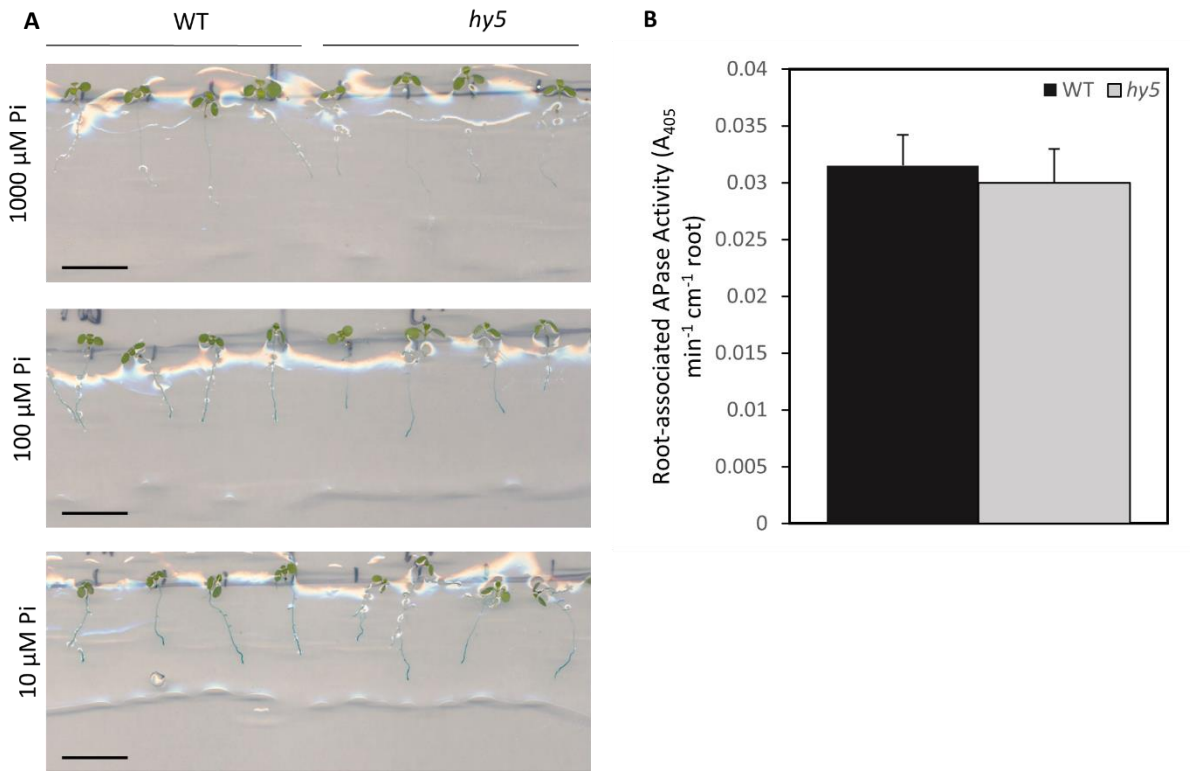


Figure 48: Analysis of APase activity in Arabidopsis seedlings of WT and *hy5* mutants grown on 1000 µM, 100 µM and 10 µM Pi concentration. 6-day-old seedlings were transferred from phosphate-sufficient agarose medium to agarose medium containing 1000 µM, 100 µM or 10 µM Pi. [**A**] After a further 4 days of growth, seedlings were stained with 0.01% BCIP, and imaged using a flatbed scanner. Scale bar = 10 mm. [**B**] APase activity was quantified by measuring the production of *p*-nitrophenol by root samples taken from WT and *hy5* plants growing on low (10 µM) Pi. No statistically significant difference was detected between WT and *hy5* (student's t-test, $p < 0.05$). Error bars denote S.E.M, n = 3. The experiment was repeated independently 3 times with similar results.

5.2.8 The *hy5* mutant may have altered expression of genes PHT transporters

Multiple putative HY5 binding sites can be found in the promoters of all nine genes encoding Arabidopsis PHT1 phosphate transporters [**Table 8**]. I therefore investigated the root expression levels of two of these genes, *PHT1;1* and *PHT1;4*, which have been previously identified as encoding transporters responsible for the majority of Arabidopsis phosphate uptake in the roots (Shin *et al.*, 2004). I also measured expression of *NRT2.1*, previously identified as being expressed at lower levels in the *hy5* null mutant (Chen *et al.*, 2016).

As previously reported (Chen *et al.*, 2016), expression levels of *NRT2;1* were significantly reduced in the roots of the *hy5* mutant [**Figure 49**]. Expression values of *PHT1;1* and *PHT1;4*

phosphate transporters may also be reduced, although this was not statistically significant (student's t-test, p = 0.15 and p = 0.13 respectively) [**Figure 49**]. Whilst not statistically significant, these results do provide some support for the 2018 finding that *PHT1;1* expression is significantly reduced in the *hy5* mutant (Sakuraba *et al.*, 2018), and further experiments with an increased sample size would help to confirm whether this is the case also for *PHT1;4* (in which case the lack of significance presented here may be a type II error).

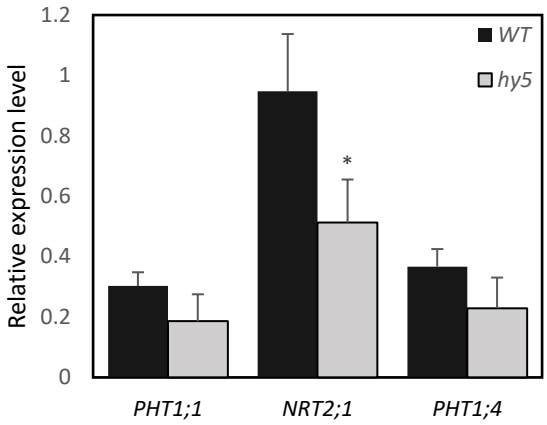


Figure 49: Expression levels of *PHT1;1*, *PHT1;4* and *NRT2;1* in WT and *hy5*. RNA was extracted from roots of 21-day-old plants grown on ½ MS media supplemented with 0.8% agarose. Semi-quantitative RT-PCR was used to determine relative expression levels of the *PHT1;1*, *NRT2;1*, and *PHT1;4* genes relative to Arabidopsis *CAP BINDING PROTEIN 20* (*CBP20*). Error bars denote S.D, * denotes statistically significant difference to WT (student's t-test, $p < 0.05$, n = 3). The experiment was repeated independently 3 times with similar results.

5.2.9 *hy5* seedlings have a reduced seedling biomass on high sucrose concentrations of sucrose, regardless of phosphate concentration

Sucrose is known to affect plant Pi responses, and is suggested to be a global regulator of plant responses to Pi starvation (Lei, Liu, *et al.*, 2011). The expression levels of PSI genes positively correlate with elevated sucrose concentration in growth media (Karthikeyan *et al.*, 2007), and the *hps1* mutation, which causes overexpression of *SUCROSE TRANSPORTER 2* (*SUC2*) and increased sucrose concentrations in root and shoot tissues, also causes enhanced sensitivity to phosphate starvation, with 73% of PSI genes induced in the *hps1* mutant when grown in phosphate-replete conditions. The *hps1* mutation causes a shift in Pi allocation

between the roots and shoots, with plants having a significantly reduced shoot Pi content and a significantly increased root Pi content relative to WT, in both Pi-replete and Pi-deficient conditions (Lei, Liu, *et al.*, 2011).

HY5 promotes expression of *TPS1*, which encodes a trehalose-6-phosphate synthase, and also *SWEET11* and *SWEET12*, which encode sucrose efflux transporters; HY5 therefore affects both sucrose metabolism and shoot-to-root sucrose transport (Chen *et al.*, 2016). The same study showed that although HY5-GFP abundance or mobility was not increased by sucrose, sucrose did promote light-activated binding of myc-HY5 to the *NRT2.1* promoter, an effect that was absent in the sugar insensitive mutant *sis4* (Chen *et al.*, 2016). This suggests that sucrose is an important regulator of HY5-mediated regulation of gene expression, and therefore that HY5 may be a strong candidate for playing a role in mediating sucrose-dependent regulation of phosphate metabolism. I therefore investigated whether the HY5 protein could be involved in co-ordinating sucrose-mediated changes in the severity of Pi starvation symptoms, by determining how the presence of sucrose affects previously measured Pi starvation responses in the *hy5* loss-of-function mutant.

Nutrient deficiencies limit plant growth, however, previous experiments suggested that *hy5* plant growth, as measured by recording seedling biomass, was no different to that of WT in phosphate-deficient environments [**Figure 47**]. Since sucrose can exacerbate Pi starvation symptoms, and HY5 regulates sucrose metabolism and transport, it is possible that HY5 is involved in mediating these changes. If HY5 is involved in sucrose-mediated changes in Pi starvation severity, it would be expected that the *hy5* mutant may have altered growth during Pi starvation when sucrose is present. I therefore measured average seedling biomass of 20-

day-old WT and *hy5* seedlings, which at 6 days old were transferred to either high or low Pi concentrations (1000 µM or 10 µM), supplemented with 1%, 3% or 5% sucrose.

As expected, seedlings transferred to 10 µM Pi had a significantly reduced biomass compared to seedlings transferred to 1000 µM Pi, for both WT and *hy5* genotypes [**Figure 50**]. *hy5* seedlings transferred to media supplemented with 1% sucrose had no significant difference in biomass to WT, for either 1000 µM or 10 µM Pi concentrations. Seedlings transferred to high Pi conditions supplemented with 3% or 5% sucrose, however, had a significantly lower biomass than WT seedlings [**Figure 50**]. The same was true for seedlings transferred to low phosphate concentrations supplemented with 3% or 5% sucrose, with *hy5* seedling biomass in the region of 20-25% lower than that of WT [**Figure 50**].

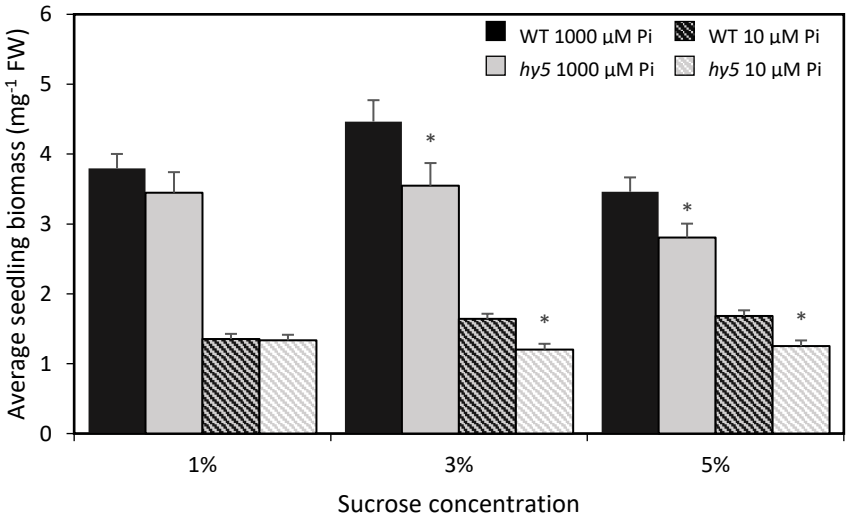


Figure 50: Seedling biomass of WT and *hy5* grown on high and low phosphate in different sucrose conditions. 6-day-old seedlings were transferred to either media containing high concentrations of phosphate ("HP", 1000 µM) or low concentrations of phosphate ("LP", 10 µM) supplemented with 1%, 3% or 5% sucrose. 14 days after transfer seedlings were weighed and the biomass recorded. Values are means ± SEM, n = 20. * denotes statistically significant differences to WT seedlings in the same conditions (student's T-test, $p < 0.05$). The experiment was repeated independently 3 times with similar results.

These results demonstrate that *hy5* has reduced growth compared to WT on high sucrose concentrations, perhaps due to the altered expression of sucrose transporter genes documented in previous studies (Chen *et al.*, 2016). However, this does not provide evidence

that HY5 is specifically involved in maintaining growth under Pi-deficient conditions in the presence of high sucrose concentrations, since the reduction in seedling biomass was observed regardless of the Pi concentration of the growth media.

5.2.10 The reduced phosphate content of *hy5* shoots is not altered by increasing concentrations of sucrose

In Arabidopsis, under Pi starvation leaf sucrose levels increase, this sucrose is transported from shoot to root via the action of SUC2 (Lei *et al.*, 2011). The transported sucrose (and specifically sucrose, rather than the glucose and fructose molecules that sucrose is broken down into) acts as a signal to trigger the root Pi starvation response (Lei, Liu, *et al.*, 2011), which includes increased expression of genes encoding Pi transporters, amongst others. The *hy5* mutant has altered sucrose metabolism and transport; I therefore wanted to determine the effects of exogenous sucrose on the accumulation of shoot Pi in the *hy5* mutant.

As expected given the results on 0% sucrose [**Figure 46**], both WT and *hy5* plants transferred to low (10 µM) Pi had significantly lower shoot Pi content than plants transferred to high (1000 µM) Pi, on all sucrose concentrations tested [**Figure 51**]. As in previous experiments, *hy5* also had a significantly lower shoot Pi content than WT plants in both Pi-replete and Pi-deficient conditions, a reduction of approximately 20%; this was unaltered by increasing sucrose concentrations [**Figure 51**].

Sucrose does not, therefore, exacerbate the difference in shoot Pi content seen between WT and *hy5* plants, and under low Pi concentrations, both WT and *hy5* plants accumulate greater shoot Pi when grown on 5% sucrose, compared to 1% sucrose. This indicates that *hy5* plants still respond to sucrose-induced changes in shoot Pi content during Pi starvation, and that HY5 is not involved in mediating these changes.

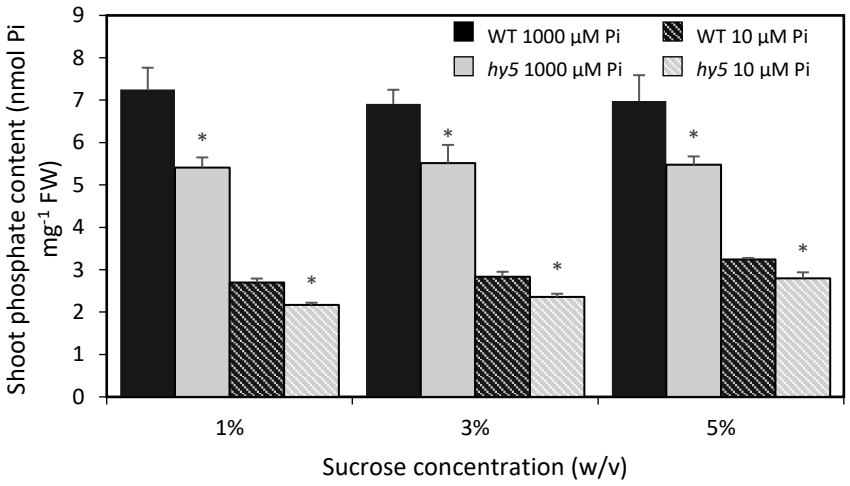


Figure 51: Shoot phosphate content of WT and *hy5* grown on high and low phosphate in different sucrose conditions. 6-day-old seedlings were transferred to either media containing high concentrations of phosphate ("HP", 1000 µM) or low concentrations of phosphate ("LP", 10 µM) supplemented with 1%, 3% or 5% sucrose. 14 days after transfer shoot tissue was harvested and phosphate content determined via the malachite green method. Values are means ± SEM, n = 5. * denotes statistically significant differences to WT (student's T-test, $p < 0.05$). The experiment was repeated independently 3 times with similar results.

5.2.11 *hy5* does not have altered root phosphate content on any concentration of sucrose

I also measured root phosphate content of WT and *hy5* plants grown on different sucrose concentrations, in Pi-replete and Pi-deficient conditions. As seen for shoot tissue, both genotypes displayed a lower root Pi content in plants grown on Pi-deficient conditions (10 µM Pi) compared to plants grown on Pi-replete (1000 µM Pi) conditions [**Figure 52**]. However, there was no significant different in root Pi content between WT and *hy5* on either Pi-replete or Pi-deficient conditions, regardless of sucrose concentration in the media [**Figure 52**]. This suggests that HY5 does not influence root Pi content, and further supports the fact that HY5 does not play a role in sucrose-mediated Pi uptake. Interestingly these results continue to contradict that of Liu *et al.* 2017, who reported elevated Pi content of 10 day old seedlings grown in Pi-replete conditions in the presence of sucrose, although these plants were younger, and grown under the presence of continuous white light rather than long-day conditions used in this study (see **Materials and Methods**). Since I have shown that root Pi

content is unaltered in *hy5*, in the presence of sucrose, one possible explanation is that differences in root Pi content at a younger seedling stage may mask the differences I have observed in *hy5* shoot Pi content. The lack of difference in root phosphate content between WT and *hy5* is also reported by Yeh *et al*., 2020, supporting these results, although they did not investigate the effects of sucrose addition to growth media.

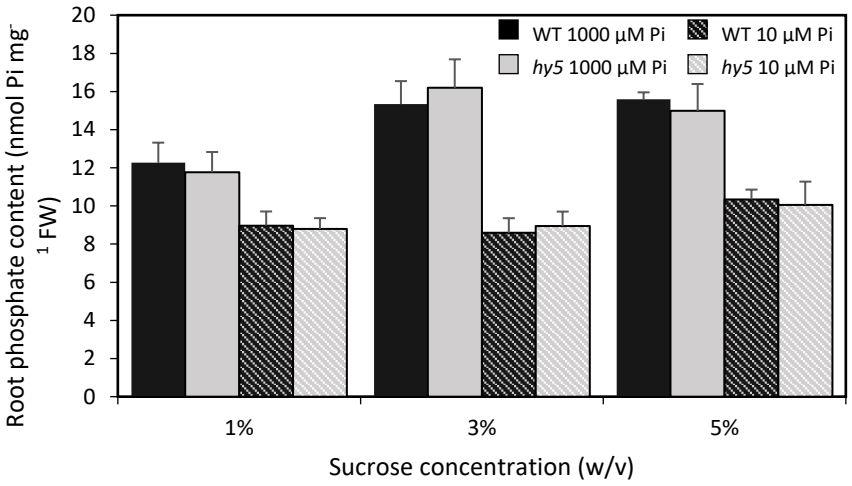


Figure 52: HY5 does not influence root phosphate content, regardless of sucrose concentration. 6-day-old seedlings were transferred to either media containing high concentrations of phosphate ("HP", 1000 µM) or low concentrations of phosphate ("LP", 10 µM) supplemented with 1%, 3% or 5% sucrose. 14 days after transfer shoot tissue was harvested and phosphate content determined via the malachite green method. Values are means ± SEM, n = 5. Different letters denote statistically significant differences to WT (student's T-test, $p < 0.05$). The experiment was repeated independently 3 times with similar results.

5.2.12 Sucrose does not impact *hy5* root acid phosphatase secretion

I have shown that low external Pi availability significantly increases acid phosphatase activity in both WT and *hy5* seedlings [**Figure 48**]. The presence of sucrose is known to exacerbate APase activity; the *hps1* mutant has an enhanced production of the major Arabidopsis isoform of APase in both Pi-replete and Pi-deficient conditions (Lei, Liu, *et al.*, 2011). Since HY5 can alter sucrose metabolism and transport, I wanted to determine if *hy5* had altered APase activity in conditions of low Pi and the presence of sucrose. Seedlings were grown on ½ MS media solidified with 0.8% agarose for six days, and then transferred to modified media containing either high (1000 µM) or low (10 µM) Pi concentrations, supplemented with 1%,

3% or 5% sucrose. After seven days on the new media, roots were stained using BCIP to visualise APase activity, which was quantified by measuring the production of *p*-nitrophenol by root samples using a colorimetric assay.

As in seedlings grown on 0% sucrose [**Figure 48**], transferring seedlings to 10 µM Pi supplemented with 1%, 3% or 5% sucrose caused noticeable BCIP staining of roots in both WT and *hy5* plants, indicating both genotypes have reasonable APase activity [**Figure 53A**]. There was no obvious visual difference in the root staining between WT and *hy5* on either 1%, 3% or 5% sucrose, which would suggest that sucrose does not impact *hy5* root APase secretion.

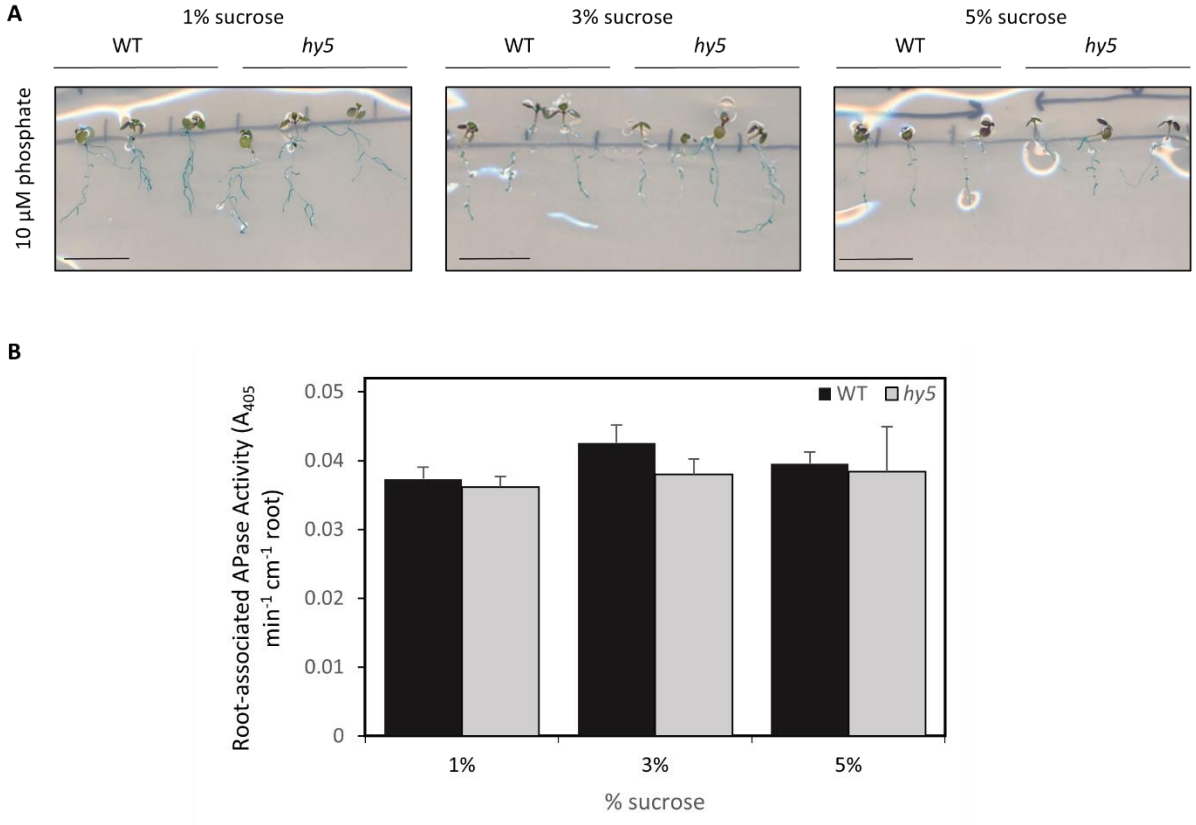


Figure 53: Detection of WT and *hy5* root APase activity under different sucrose concentrations. Seedlings were grown on ½ MS media solidified with 0.8% agarose, and at 6 days old transferred to 10 µM Pi with different sucrose concentrations. [**A**] Four days after transfer seedlings were stained for acid phosphatase activity using BCIP. Scale bar = 1 cm. [**B**] Root acid phosphatase activity was quantified by measuring production of *p*-nitrophenol from WT and *hy5* root samples by measuring absorbance at 405 nm. No significant difference between WT and *hy5* roots on either 1%, 3% or 5% sucrose was observed (student's t-test, $p < 0.05$, $n = 3$). The experiment was repeated independently 3 times with similar results.

Quantifying root APase activity indicated that there was no significant difference in the root acid phosphatase activity of either WT or *hy5* plants, on any sucrose concentration tested [**Figure 53B**]. This suggests that in the conditions of this study, sucrose does not affect root APase activity under low Pi conditions, and Arabidopsis root APase activity is not dependent on functional HY5 protein.

5.2.13 Altered root system architecture in response to phosphate deprivation in the *hy5* mutant is sustained under high sucrose concentrations

Previous work in this chapter identified the *hy5* mutant as having reduced primary root growth in response to low Pi conditions, although primary root growth was not reduced to the same proportion as for WT plants roots [**Figure 44A**]. I therefore measured primary root growth in plants grown on 0% and 5% sucrose, to determine the effect of sucrose on the low-Pi induced reduction of primary root growth in the *hy5* mutant.

In 0% sucrose conditions, both WT and *hy5* had a significant reduction in primary root growth in response to transfer to low Pi, with *hy5* displaying a smaller, but still significant, reduction in root length compared to WT. WT seedlings grown on low Pi were approximately 50% shorter than those on high Pi; whilst *hy5* seedlings grown on low Pi were approximately 18% shorter than those on high Pi. Transferring plants to high (1000 µM) or low (10 µM) Pi conditions containing 5% sucrose caused a difference in root length responses [**Figure 54A, 54B**]. Both WT and *hy5* plant roots were considerably shorter in full Pi conditions compared to plants grown on 0% sucrose, and a reduction in phosphate availability again caused a significant reduction in primary root elongation for both WT and *hy5* plants [**Figure 54B**]. WT plants in 5% sucrose and low Pi conditions displayed an approximate 40% reduction in growth relative to plants on 5% sucrose and full Pi, whilst *hy5* plants on 5% sucrose showed an

approximate 28% reduction in primary root elongation. Therefore, as seen in 0% sucrose, *hy5* has a smaller reduction in primary root growth in response to low Pi, although the difference between WT and *hy5* does appear to be smaller (with each genotype reduced by 40% and 28% respectively, rather than the 50% and 18% reductions seen on 0% sucrose).

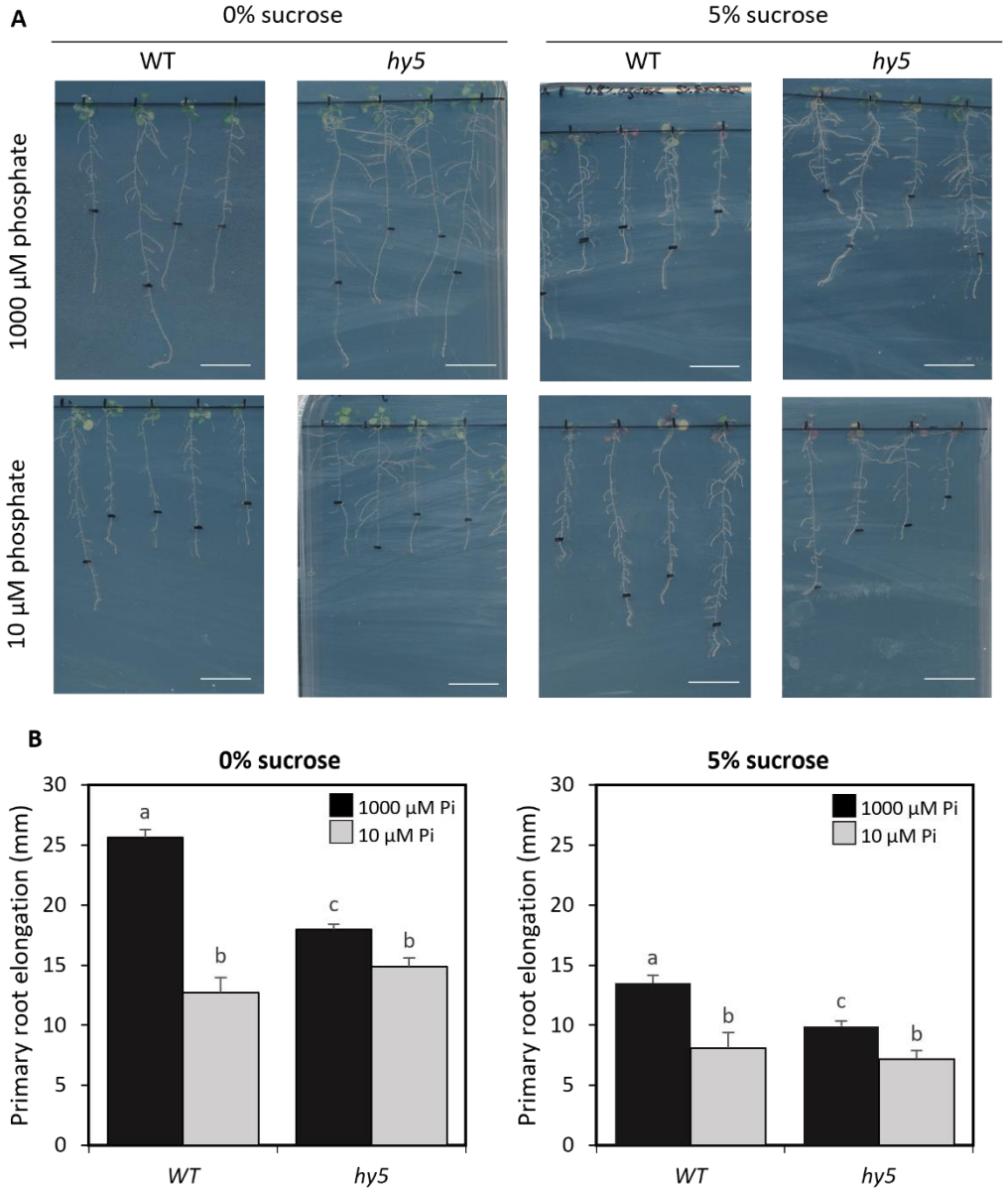


Figure 54: Root system architecture of WT and *hy5* in 0% and 5% sucrose. [**A**] 8-day-old seedlings grown on high phosphate conditions were transferred to high phosphate (1000 µM KH_2PO_4) or low phosphate media (10 µM KH_2PO_4) with 0% or 5% sucrose, and the position of root tips marked on the back of plates. [**B**] 6 days after transfer plates were scanned and primary root elongation determined by measuring the distance along the root between the mark indicating the length of root at the time of transfer, and the root tip. Values are means ± SEM, n = 24-32. Different letters denote statistically significant differences (one-way ANOVA/Tukey HSD post hoc test, $p < 0.05$). The experiment was repeated independently 3 times with similar results.

5.2.14 Anthocyanin content in *hy5* seedlings under phosphate deprivation in the presence of sucrose

Accumulation of leaf anthocyanins is a common response to Pi starvation. Measuring shoot anthocyanin content of WT and *hy5* grown in high and low Pi showed that low Pi conditions increased anthocyanin content, and this is impaired in the *hy5* mutant which has significantly lower anthocyanin content compared to WT in seedlings grown on 100 µM and 10 µM Pi concentrations. The *hps1* mutant, which contains a mutation that causes an overaccumulation of sucrose and increased sensitivity to Pi starvation, has significantly greater anthocyanin content when grown in Pi-deficient conditions (Lei, Liu, *et al.*, 2011). I therefore also measured *hy5* anthocyanin content under Pi-deficient conditions, with different concentrations of sucrose present. If HY5 is necessary for increased levels of low- Pi induced shoot anthocyanin accumulation that occurs in the presence of sucrose, it would be expected that the reduced anthocyanin accumulation seen during Pi starvation in the *hy5* mutant would be further exacerbated under high sucrose concentrations.

I therefore transferred *hy5* and WT seedlings to modified ½ MS agarose plates containing either 1000 µM, 100 µM or 10 µM Pi concentrations, supplemented with 1%, 3% or 5% (w/v) sucrose. Seedlings were grown for a further 14 days before shoot tissue harvested and anthocyanin content determined. In phosphate-replete (1000 µM) Pi conditions, supplementing media with 5% sucrose caused a significant increase in anthocyanin content of both WT and *hy5* seedlings compared to shoot anthocyanin content of plants grown on 1% or 3% sucrose, but no significant difference between WT and *hy5* seedlings was detected for any sucrose concentration [**Figure 55**]. In low (10 µM) Pi conditions, shoot anthocyanin content was over 10-fold higher than for shoots of plants grown on high phosphate, this was

true for both WT and *hy5*. As observed on 0% sucrose [**Figure 45**], *hy5* plants had a significantly reduced shoot Pi content compared to WT in low Pi, and this was true for plants grown on media supplemented with all (1%, 3% and 5%) sucrose concentrations [**Figure 55**]. As in Pi-replete conditions, supplementing media with 5% sucrose caused a significant increase in shoot anthocyanin accumulation compared to plants grown on 1% sucrose, and this was true for both WT and *hy5* [**Figure 55**].

Therefore, whilst *hy5* plants are deficient in accumulating WT-levels of shoot anthocyanins in response to low Pi, this is unaffected by the presence of sucrose in the media. *hy5* mutants still respond to increased sucrose concentrations by accumulating greater levels of anthocyanin, and so HY5 does not appear to be required for anthocyanin accumulation in the presence of sucrose, in either Pi-replete or Pi-deficient conditions.

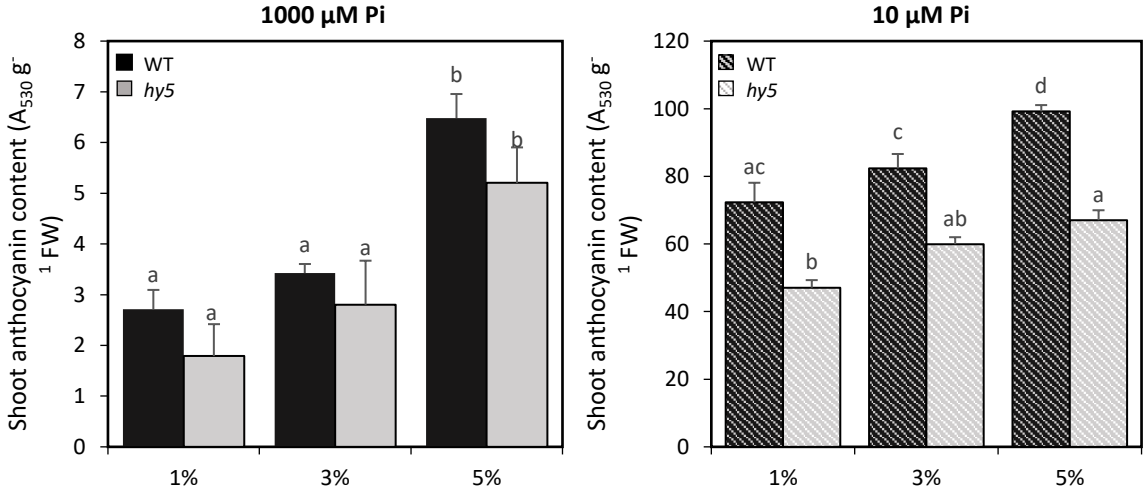


Figure 55: Sucrose does not affect the reduced anthocyanin content of *hy5* plants in phosphate-deficient conditions. 4-day-old seedlings grown on phosphate replete agarose media were transferred to agarose media containing either 1000 µM or 10 µM Pi, supplemented with 1%, 3% or 5% sucrose. Seedlings were grown for a further 14 days before shoot tissue was harvested and pooled for analysis. Shoot anthocyanins were extracted in 1% HCl in methanol, and quantified using a spectrophotometer after separation from chlorophyll pigments. * denotes statistical difference compared to WT plants grown on the same phosphate concentration (one-way ANOVA/TukeyHSD post hoc test, $p < 0.05$, $n = 5$) Error bars denote S.E.M. The experiment was repeated independently 3 times with similar results.

5.2.15 Shoot illumination is necessary for HY5-dependent accumulation of shoot phosphate

In addition to sucrose, light is also known to affect Pi responses. For example, moving common bean plants grown on Pi-replete media to Pi-deficient conditions strongly induces miR399 expression in both shoot and root tissues, for plants in a 16-hour light / 8-hour dark photoperiod (Liu *et al.*, 2010). However in plants moved to phosphate-deficient conditions but kept in continuous darkness, miR399 was not detected in either shoot or root tissues (Liu *et al.*, 2010).

The HY5 protein is controlled by multiple light signalling pathways [**Chapter 1**]. HY5 protein levels decline upon transfer from illuminated to dark conditions, via a COP1-dependent degradation mechanism (Osterlund *et al.*, 2000), and similarly increase upon transfer from dark to illuminated conditions. In addition, shoot-derived HY5 is mobile, and can travel to the roots where, for instance, it promotes expression of root *HY5* in addition to HY5-regulated genes such as the NRT2.1 nitrate transporter (Chen *et al.*, 2016). It is therefore feasible that HY5 may regulate phosphate metabolism in a light-dependent manner, and that shoot illumination may be of particular importance as has been previously identified in HY5-mediated regulation of nitrate metabolism.

I therefore investigated the role of HY5 in light-mediated regulation of Pi metabolism. Experiments focussed on both investigating the effects of different light intensities, and also shoot vs root illumination in WT and *hy5* seedlings.

Both *hy5* plants grown on compost, and *hy5* plants grown on agarose, have a reduced shoot Pi content [**Figure 43, Figure 46**]. Since HY5 is a positive regulator of phytochrome-regulated light signalling, and HY5 protein in the absence of light is targeted for degradation via a COP1-

dependent mechanism, I wanted to determine whether the reduction in shoot phosphate in the *hy5* mutant is dependent on shoot illumination.

Growing plants on agarose plates allowed WT and *hy5* plants to be grown in altered shoot / root illumination regimes [**Figure 56**], allowing the role of shoot vs root illumination on HY5-dependent maintenance of shoot Pi content to be determined. 10-day-old seedlings grown on Pi-replete ½ MS agarose media were transferred to different shoot/root illumination regimes, and grown for a further 14 days before shoot and root samples were harvested and the Pi content measured using the malachite green method.

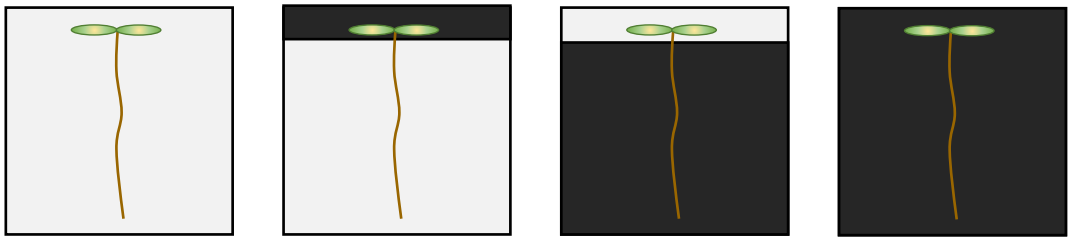


Figure 56: Schematic demonstrating different shoot / root illumination regimes. 10-day-old seedlings were transferred to plates with different light treatments. Shoots were either in light [S(L)] or dark [S(D)] conditions, and roots were either in light [R(L)] or dark [R(D)] conditions also. Sterile foil was used to cover plant roots and / or shoots to prevent light reaching these tissues.

Measuring the shoot Pi content of plants in the different shoot / root illumination regimes [**Figure 56**] indicated that *hy5* shoot Pi content was significantly reduced compared to WT in all conditions where shoots were illuminated, regardless of whether roots were illuminated also [**Figure 57**]. When shoots were kept in continuous darkness, there was no significant difference between the shoot Pi content of WT and *hy5* plants, regardless of whether roots were illuminated also [**Figure 57**].

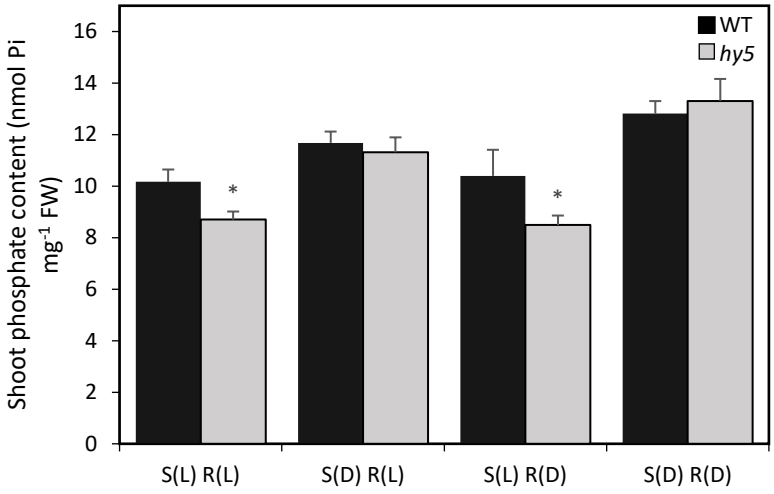


Figure 57: The reduced shoot phosphate content of *hy5* is dependent on shoot illumination. 10-day-old seedlings grown on ½ MS agarose media were transferred to different shoot/ root illumination regimes and grown for a further 14 days. Shoots were either in light [S(L)] or dark [S(D)] conditions, and roots were either in light [R(L)] or dark [R(D)] conditions also. Shoot tissue was harvested and the shoot phosphate content quantified using the malachite green method. * denotes statistical difference relative to WT ($p < 0.05$, student's t-test), error bars denote S.E.M, n = 6. The experiment was repeated independently 3 times with similar results.

5.2.16 *hy5* does not have altered root phosphate content, regardless of shoot and root illumination status

Measuring root Pi content of the plants grown on different illumination regimes indicated that as seen previously, *hy5* root tissue does not have a significantly different Pi content compared to WT, regardless of shoot/ root illumination regime [**Figure 58**].

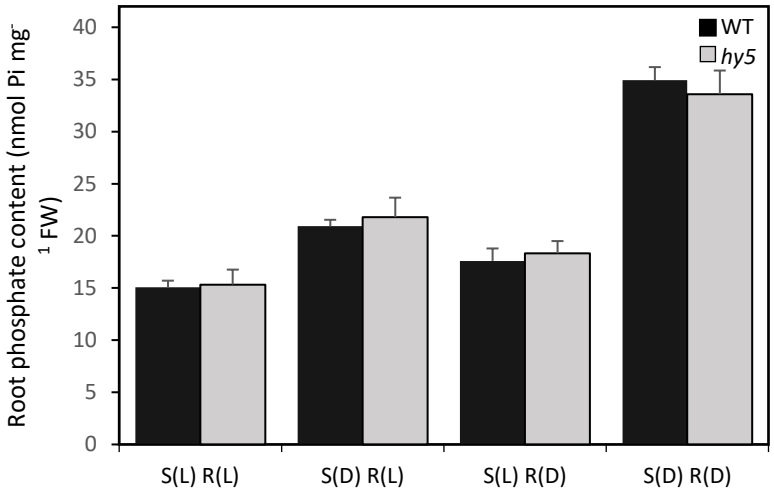


Figure 58: *hy5* root phosphate content is unaffected by shoot illumination. 10-day-old seedlings grown on ½ MS agarose media were transferred to different shoot/ root illumination regimes and grown for a further 14 days. Shoots were either in light [S(L)] or dark [S(D)] conditions, and roots were either in light [R(L)] or dark [R(D)] conditions also. Root tissue was harvested and the root phosphate content quantified using the malachite green method. No significant difference between WT and *hy5* was detected for any illumination regime (student's t-test, $p < 0.05$), error bars denote S.E.M, n = 6. The experiment was repeated independently 3 times with similar results.

This is particularly interesting because it confirms previous results [**Figure 43, Figure 46, Figure 53**] that differences in *hy5* Pi content appear to be restricted to the shoot tissue. *hy5* plants have altered root Pi transporter expression, and it has been reported that *hy5* plants have reduced Pi uptake rates (Sakuraba *et al.*, 2018). Since I have not found a significant difference in root Pi content between WT and *hy5* plants in a range of conditions (different illumination regimes, different Pi contents and different sucrose availabilities), this suggests that root-to-shoot phosphate transport is also altered in the *hy5* mutant, since root Pi content is maintained, and shoot Pi content reduced. This also suggests such a mechanism exists to maintain WT-levels of root Pi concentrations at the expense of shoot Pi content; future work should investigate this further.

Chapter 6: Discussion

It is important to understand the regulation of plant nutrient use if we are to improve the nutrient use efficiency of crop varieties, to reduce demand on heavy fertiliser application and achieve global food security (Godfray *et al.,* 2010; Veneklaas *et al.,* 2012). The research presented in this thesis aimed to explore the relationship between nutrient use and growth in Arabidopsis, in particular identifying new genetic components that modulate nitrate and phosphate metabolism. By utilising both a physiological approach (measuring enzyme activity, plant nutrient content and adaptive responses to nutrient deprivation) and a genetics approach (investigating how specific mutations in genes of interest alter such plant physiology), I have identified ethylene signalling as modulating Arabidopsis nitrogen metabolism, provided additional evidence that HY5 regulates phosphate metabolism, and shown that known components of phosphate signalling have additional roles in regulating nitrate assimilation. Together these findings further our understanding of plant nutrient metabolism, and offer potential new targets to alter plant nutrient use efficiency.

6.1 Understanding the role of CTR1 in regulating nitrogen metabolism

6.1.1 The *ctr1-1* mutation confers differences in nitrogen metabolism

As outlined in **Chapter 1**, the first objective of this thesis was to understand the role of ethylene signalling in regulating N metabolism. Ethylene signalling is known to be involved in plant nutrition, in particular phosphate nutrition, with ethylene biosynthesis and plant sensitivity to ethylene both altered in response to phosphate starvation (Song and Liu, 2015). Lines carrying mutations in components of ethylene biosynthesis and/or signalling have additionally been identified as having altered phosphate starvation induced gene expression and altered physiological and developmental adaptations to reduced phosphate availability

(Song and Liu, 2015). Whilst there are many studies investigating the role of ethylene and phosphate nutrition, the role of this phytohormone in regulating plant N metabolism is less well understood.

Previous studies have suggested that ethylene production is increased upon transfer of plants to high nitrate environments, and that this increase can upregulate, for example, the NRT1.1 nitrate transporter, and regulate root branching in response to high nitrate availability (Tian *et al.*, 2009). This would suggest that ethylene signalling positively promotes nitrate uptake, a theory consistent with findings that in high nitrate conditions applying ethephon (which induces ethylene release in plant tissues) to mustard increases NR activity (Khan *et al.*, 2008). However, this thesis suggests an alternative role for ethylene signalling. I show that the *ctr1-1* mutant, which displays constitutive ethylene signalling responses, has greatly increased chlorate resistance relative to WT plants, at a similar level to the strongly chlorate resistant *nrt1.1* loss-of-function mutant [**3.2.1**].

Chlorate resistance could also be due to altered signalling pathways involving the chlorate ion itself (LaBrie *et al.*, 1991), or wider changes to nutrient metabolism – as chlorate toxicity depends on other nutrients present (Steingrover and Feenstra, 1981). Whilst we cannot rule this out, subsequent results showing altered nitrate metabolism suggest in *ctr1-1* suggests this, at least in part, accounts for the chlorate resistant phenotype.

ctr1-1 has no difference in shoot nitrate accumulation [**3.2.4**], however, shoot NR activity is significantly reduced compared to WT [**3.2.2**]. The difference in shoot nitrate accumulation is perhaps not surprising – whilst chlorate is a structural analogue of nitrate, there are no reports in the literature of mutations affecting nitrate transporters other than NRT1.1

conferring chlorate resistance. Therefore, chlorate does not utilise all of the same influx, efflux and transport systems within the plant as nitrate.

As discussed in **1.3.6**, NR activity can be regulated at both the transcriptional and post-transcriptional level, with three mechanisms of post-translational control identified in Arabidopsis. Expression of the primary gene encoding NR is partially reduced [**3.2.12**], and subsequent work by colleagues using an anti-NR antibody reveals detectable NR protein abundance is reduced in *ctr1-1* also (Jamieson *et al.*, 2022). Altered regulation at both the transcriptional and post-transcriptional level may therefore contribute to the reduced NR activity, and increased chlorate resistance of *ctr1*. It is also possible that differences in post-translational modification of the NR enzyme can explain altered enzyme activity in *ctr1*. Interestingly, the *siz1* mutant, which lacks an E3 sumo ligase responsible for sumoylating NIA1 and NIA2 in Arabidopsis (Park *et al.*, 2011) has reduced NR activity and is also dwarfed, although unlike *ctr1-1* the growth phenotype of *Atsiz1* was recovered by exogenous supply of ammonium, but not nitrate. I have shown that the dwarfed growth phenotype of *ctr1-1* (at least in the seedling stage) persists regardless of N source [**3.2.5**], and is therefore not nitrate-dependent, although it would be interesting to test this on adult plants.

The finding that *ctr1-1* has reduced NR activity therefore appears to counteract that of previous studies that suggest ethylene signalling promotes nitrate uptake, although it is worth considering that these studies focussed on short-term bursts of ethylene application, rather than sustained long-term ethylene signalling as is found in the *ctr1-1* mutant. In addition, previous studies in Arabidopsis focus on the effect of ethylene in the root tissue (Tian *et al.*, 2009), whilst this thesis suggests that CTR1-dependent shoot NR activity may be of particular importance. It would be interesting to follow up these findings further, particularly

investigating whether short-term ethylene bursts can alter chlorate resistance, or whether it is long-term sustained alteration of ethylene signalling that is necessary for the *ctr1-1* phenotype.

Screening a variety of other mutants with altered ethylene signalling allows us to further understand the role of this phytohormone in promoting chlorate resistance. *ctr1-1* has constitutive ethylene signalling – accordingly *eto2* and *eto3* (which have increased ethylene signalling due to ethylene over production) also display increased chlorate resistance compared to WT [**3.2.7**]. However, neither line displays a difference in shoot NR activity [**3.2.9**], and chlorate resistance is undetectable in *eto1*. This is perhaps because ethylene-over-producing phenotypes are most prominent in seedlings; whilst *eto1* and *eto3* seedlings have significantly elevated ethylene levels relative to WT, there is no significant difference in the ethylene produced by leaves of soil-grown WT, *eto1* and *eto3* plants at the adult stage (Woeste *et al.*, 1999). Further work could investigate the nitrate metabolism of ethylene-over-producing lines over a series of time points during the seedling stage to determine if N metabolism is altered whilst these over-producing effects are still present.

In this study, neither the *ein2*, *ein3* nor *ein3* Δ *eil1* lines showed altered sensitivity to chlorate treatment compared to WT [**3.2.8**]. This suggests that below a certain threshold of ethylene signalling, there is no detectable alteration in chlorate resistance. Adult leaf tissue of WT Arabidopsis grown on soil under continuous illumination produce negligible amounts of ethylene (Woeste *et al.*, 1999); it is therefore likely that there is minimal difference in the ethylene signalling occurring in WT, and the ethylene-insensitive *ein2*, *ein3* and *ein3* Δ *eil1* lines used in this study. Future work should examine ethylene-insensitive lines (*ein2*, *ein3* and *ein3* Δ *eil1*) alongside controls under sustained ethylene (or ethephon) exposure, to

determine if these ethylene-insensitive lines phenocopy the WT response, or have an opposing phenotype to *ctr1-1* - specifically, whether they are more sensitive to chlorate treatment than WT, and whether they have elevated NR activity compared to WT, when plants are exposed to ethylene.

Whilst I found shoot nitrate content is unaltered in *ctr1*, which suggests that nitrate uptake is unchanged compared to WT, future work could confirm this by measuring the rate of nitrate uptake in the *ctr1-1* and ethylene-overproducing mutants relative to WT and *nrt1.1*. This would confirm whether ethylene signalling is affecting N metabolism by predominately altering the activity of the NR enzyme, or whether additional aspects of the nitrate assimilation pathway are affected. Additionally, reciprocal grafting experiments would determine whether the shoot *ctr1-1* genotype is sufficient to confer chlorate resistance in Arabidopsis, this would support the finding that altered shoot NR activity, rather than differences in nitrate uptake, are responsible for the *ctr1-1* chlorate phenotype.

6.1.2 Lack of EIN2 function correlates with suppression of chlorate resistance and NR activity reduction conferred by *ctr1*

It is plausible that the chlorate resistant phenotype of *ctr1-1* could be the result of the dwarfed phenotype this mutation confers (since smaller plants are likely to have lowered nutrition requirements), rather than a specific consequence of constitutive ethylene signalling. By screening EMS-treated *ctr1-1* seeds that contain additional mutations, I was able to isolate several lines of interest that maintained the chlorate-resistant phenotype of *ctr1-1* whilst losing the dwarfed characteristic that this line displays. The additional mutations present in these lines have therefore separated the chlorate resistance phenotype from the dwarfed phenotype of *ctr1*. Additionally, a colleague (Zhe Ji) has shown that a range of other

dwarf mutants (*min-1*; *cp3-1* and *dw1-1*), both taller and shorter than *ctr1*, show no detectable difference in chlorate resistance to that of WT (Jamieson *et al.*, 2022), suggesting dwarfism alone is insufficient to confer a chlorate resistant phenotype.

The *ctr1-1* phenotype can be suppressed by mutations in EIN2 (Alonso *et al.*, 1999), and previous work suggests the majority of "tall" mutants recovered would likely contain mutations at the EIN2 locus (Zhong Jie Ding, unpublished data). This suggested it was likely that the majority of 'tall' mutants I isolated contained mutations in EIN2 also. I therefore analysed a number of *ctr1-1* lines containing known mutations in EIN2 for altered chlorate sensitivity. Together, this work identified a number of mutagenized *ctr1-1* lines that display tall and chlorate-resistant (or partially chlorate-resistant) phenotypes. This supports the suggestion that chlorate resistance conferred by *ctr1-1* is specifically due to altered ethylene signalling, rather than a more general effect on chlorate metabolism or signalling.

This work offers plenty of scope for future experiments to further understand the mechanistic basis for the chlorate-resistant phenotype of *ctr1*. I have shown that it is possible to reverse both the *ctr1-1* dwarfed phenotype and the *ctr1-1* chlorate-resistant phenotype through the presence of additional mutations, a result that is unsurprising since any mutations in genes encoding downstream components of the ethylene signalling pathway that result in ethylene insensitivity would override the constitutive ethylene signalling phenotype of *ctr1*. It is particularly interesting that the chlorate-resistant phenotype of *ctr1-1* can persist even when the dwarfed phenotype is lost, and I have identified several lines of interest that offer scope to understand the mechanistic basis of this observation.

This work suggests that multiple independent loss-of-function mutations at EIN2 confer increased chlorate sensitivity on *ctr1.* However, EMS- treated *ctr1-1* seeds may contain a large

number of additional mutations located throughout the genome, and so the possibility that these lines contain additional mutations in genes encoding components of nitrate metabolic machinery cannot be ruled out. These lines therefore make excellent candidates for whole-genome sequencing, alongside *ctr1-1* controls, to understand the location of all new mutations that cannot currently be ruled out from producing this phenotype of interest. Whole-genome sequencing may also help identify new, unknown, regulators of ethylene-mediated modulation of N metabolism. Of particular interest is the role of EIN2, since I have identified lines containing known mutations in *EIN2* which retain chlorate sensitivity, although it is not yet clear whether these mutations are solely responsible for the altered height and chlorate sensitivity phenotypes. EIN2 is especially interesting since in addition to the "cleave and shuttle" mechanism of EIN2 signalling described in **1.5.3**, an additional cytoplasmic role for EIN2 signalling, independent of CTR1, has also been suggested (Qiu *et al.*, 2012). In addition to whole-genome sequencing, obtaining *ctr1-1* lines containing mutations within the EIN2 locus only, in a WT background, and measuring NR activity and chlorate resistance will confirm whether these mutations alone are sufficient to confer these traits or not. If so, this would suggest that EIN2 is of particular importance in regulating Arabidopsis N nutrition.

If specific mutations in EIN2 are responsible for the altered chlorate-resistant phenotype present in these lines, this will offer potential to understand further the role of this protein, in addition to CTR1, in modulating Arabidopsis nitrate metabolism, and may reveal new mechanisms for ethylene-mediated regulation of nitrate metabolism.

More broadly, ethylene has long been known to coordinate plant growth in response to environmental stress (Bleeker and Kender, 2000), but the involvement of ethylene signalling in metabolic regulation has been less clear. The phytohormone has been implicated in both

phosphate (Ma *et al.*, 2003) and potassium metabolism (Shin and Schachtman, 2004); this thesis provides further evidence that ethylene has a role in coordinating N metabolism as well.

6.2 Exploring phosphate as a regulator of nitrogen metabolism

Chapter 4 aimed to explore N metabolism in mutants lacking components of phosphate metabolism. As discussed in **Chapter 1**, there is a variety of evidence indicating that N and P metabolism must interact, and some recent findings have discovered genetic links between the two nutrient metabolism signalling pathways (Kant *et al.*, 2011; Lin *et al.*, 2013; Medici *et al.*, 2015; Maeda *et al.*, 2018). However there remains considerable scope to understand this further. In particular, I wanted to determine whether reduced Pi availability caused a reduction in Arabidopsis NR activity, as had previously been identified in the roots of bean plants (Gniazdowska and Rychter, 2000). Building on this finding, I aimed to determine whether actual plant Pi content, or genetic regulators of Pi starvation, were responsible for this result, and followed this up further by investigating how nitrate metabolism was altered in plants lacking components of Pi metabolism.

6.2.1 Phosphate availability alters nitrogen metabolism in Arabidopsis

A previous study demonstrated that Pi availability can alter NR activity in bean (Gniazdowska and Rychter, 2000). I have shown that this applies to Arabidopsis also: this thesis demonstrates that in Arabidopsis although the majority of NR activity occurs in the shoot, both shoot and root NR activity are reduced when phosphate availability is lowered [**4.2.1**]. I show that NR activity is not the only component of N metabolism affected, as shoot nitrate content is lowered in response to reduced Pi provision, and therefore nitrate uptake is also implicated [**4.2.2**]. This supports previous work identifying that Pi deficiency reduces nitrate

uptake in barley, maize and tobacco (Lee, 1982; De Magalhães *et al.*, 1998; Rufty *et al.*, 1990), and suggests that phosphate starvation causes a broad range of changes in Arabidopsis nitrate metabolism.

6.2.2 Mutations in regulatory components of phosphate signalling pathways confer differences in nitrogen metabolism

Having determined that lowered Pi availability reduces NR activity, I investigated N metabolism in a range of mutants lacking Pi signalling components, determining that genetic regulation, rather than shoot Pi content, is likely to regulate the observed changes in nitrate metabolism [**4.2.4**]. As described in **Chapter 1**, PHR1 is a MYB-CC transcription factor that is an important coordinator of the phosphate starvation response; with the *phr1* mutant lacking expression of many phosphate starvation-induced genes (Bari *et al.*, 2006). More recently PHR1 has been implicated in nitrate metabolism, regulating expression of NIGT1 genes, which encode nitrate-inducible transcriptional repressors (described in **1.4.1**). PHR1/PHL1-induced regulation of NIGT1 genes can downregulate nitrate uptake during phosphate starvation (Maeda *et al.*, 2018). This 2018 study identified the *P1BS* PHR1 binding sequence as overlapping with a NIGT1-recognition sequence, suggesting that PHR1 and PHL1 regulate expression of *NIGT1*-clade genes, a gene family strongly induced by nitrate (Maeda *et al.*, 2018). The authors further demonstrated that expression of *NIGT1*-clade genes is compromised in the *phr1* Δ *phl1* mutant, and that *nigt*Q-1 and *nigt*Q-2 quadruple mutants have enhanced nitrate uptake during Pi starvation. I add to this finding, showing that whilst in phosphate-replete conditions there is no difference in the shoot nitrate content of WT and the *phr1* mutant, under phosphate starvation conditions *phr1* shoot nitrate content is significantly increased, indicating that the failure of *phr1* to reduce shoot nitrate content

under phosphate starvation is another facet of the failed phosphate starvation phenotype of *phr1* mutants.

The role of PHR1 in regulating nitrate uptake is further supported by demonstrating that *pho2*, a mutation affecting a component of the PHR1 – miR399 – PHO2 signalling pathway induced during phosphate starvation (Bari *et al.*, 2006), confers an opposing phenotype to *phr1* in terms of nitrate content, with a significantly lowered shoot nitrate content compared to WT grown on high Pi concentrations, and no difference in shoot nitrate content compared to WT grown on low Pi concentrations [**4.2.5**]. The phenotype of *pho2* is matched by the *pht1;1* Δ *pht1;4* mutant which is deficient in phosphate uptake (Shin *et al.*, 2004), providing evidence that these results are independent of actual shoot Pi content.

I also demonstrate that in addition to nitrate uptake, additional steps in nitrate metabolism are affected in mutants lacking components regulating the low phosphate signalling pathway, notably NR enzyme activity which is reduced in *pho2* and the *pht1;1* Δ *pht1;4*. I show that the promoter of *NIA2*, which encodes the majority of Arabidopsis NR enzyme, does not contain a *P1BS* motif, however, putative NIGT1 binding sequences are present – future experiments should determine whether NIGT1 binds the *NIA2* promoter sequence A suggested hypothesis is therefore that NR activity could be mediated via PHR1-regulated NIGT1 transcriptional control; future work could utilise the *nigt*Q mutant previously described as having enhanced nitrate uptake during phosphate starvation (Maeda *et al.*, 2018). If WT levels of shoot nitrate content and shoot NR activity are restored in *pho2* Δ *nigtQ* and *pht1;1* Δ *pht1;4* Δ *nigtQ* lines, this would support the hypothesis that PHR1-mediated NIGT1 transcriptional control is responsible for the altered nitrate uptake and NR activity observed in *pho2* and *pht1;1* Δ *pht1;4.*

In this thesis I focus on the *phr1* single mutant, showing that despite the partially redundant effects of PHR1 and PHL1, the *phr1* mutation alone is sufficient to cause alterations in nitrate metabolism. Interestingly the rice *osphr3* mutant, which lacks functional *OsPHR3* (the rice homologue of *PHL1*), has been shown to have a reduced nitrate concentration compared to WT in both phosphate sufficient and phosphate depleted conditions (Sun *et al.*, 2018), therefore displaying an opposite phenotype to that found in the *phr1* Arabidopsis mutant used in this study. Investigating nitrate content and nitrate uptake in the *phl1* and *phr1* Δ *phl1* mutants would determine the role of Arabidopsis PHL1 further, establishing whether this has an additive effect to PHR1, and therefore a diverged role to rice *OsPHR3*, or not. This would be particularly useful to determine if additional Pi signalling mechanisms regulate nitrate metabolism in response to low phosphate. Although *phr1* has significantly higher shoot nitrate levels than WT in low phosphate conditions, the *phr1* shoot nitrate content in these conditions is still significantly lower than the *phr1* shoot nitrate content in phosphate-replete conditions, and so additional regulatory mechanisms must exist. Determining if this persists in the *phr1* Δ *phl1* double mutants would help to determine if PHR1/PHL1-independent phosphate signalling mechanisms are also involved in the regulation of N metabolism.

It was surprising that despite observed differences in nitrate content and NR activity, there is no obvious difference in chlorate resistance between WT, *phr1*, *pho2* and *pht1;1* Δ *pht1;4* genotypes [**4.2.7**]. This finding suggests that the observed changes in nitrate metabolism of the *pho2* and *pht1;1* Δ *pht1;4* genotypes are insufficient to confer an increase in chlorate resistance to these lines, at least at the concentration level tested. Since a reasonably high concentration of chlorate (2.5 mM) was used for treatment, it may be worth testing a range

of chlorate concentrations to determine if this observation persists under lower doses of chlorate treatment to better understand the biological significance of these findings.

6.2.3 Chlorate resistance of genotypes can vary according to the growth media used

An unexpected finding detailed in **Chapter 4** was that the chlorate resistance of certain genotypes can vary according to the growth media used [**4.2.11**]. I first demonstrate that, as with laboratory compost conditions, applying chlorate treatment to plants growing on ½ MS solidified with agarose produces symptoms of chlorate toxicity, in a dose-dependent manner. However, two genotypes that have a strong chlorate-resistant phenotype on compost do not retain this phenotype when treated using this agarose system. The *nrt1.1* mutant was first identified due to its strong chlorate-resistant phenotype (Tsay *et al.*, 1993), and has reduced high-affinity and low-affinity uptake of nitrate ions (Wang *et al.*, 1998), whilst I have shown the basis of the chlorate resistance phenotype seen in *ctr1-1* plants appears at least partially due to significantly reduced NR activity [**Chapter 3**; Jamieson *et al.*, 2022], although the mechanisms regulating this are not yet known.

Despite these genotypes not displaying a chlorate resistant phenotype as was initially expected, I do show that chlorate resistance can be altered using factors known to affect NR activity [**4.2.12**]. Light and sucrose have both been shown to cause accumulation of NR mRNA transcripts in dark-adapted Arabidopsis plants (Cheng *et al.*, 1992). I show that dark-grown plants retain chlorate resistance in this system, and that this resistance is removed upon the addition of sucrose to the media. Future work could do similar experiments with compost-grown plants to determine if the effects are similar or exacerbated by certain growth conditions. It does however, appear that susceptibility of Arabidopsis plants to chlorate treatment can still be modulated by external factors known to affect nitrate metabolism, and

it is unclear why *nrt1.1* and *ctr1-1* appear to lose their chlorate resistance when treated on agarose media. It would be interesting to test other known chlorate-resistant phenotypes in agarose conditions, for example *chl3* which has a deletion of the gene encoding NIA2 (Wilkinson *et al.*, 1991). This would enable any distinction in chlorate resistance caused by reduced chlorate uptake vs reduced chlorate reduction to be determined. It would also be interesting to determine if chlorate-hypersensitive mutants with enhanced nitrate & chlorate uptake (Wang *et al.*, 1986) maintain a hypersensitive phenotype, or whether the growth conditions override all differences in chlorate sensitivities observed on compost.

If treating plants on agarose does override genetic differences in chlorate sensitivity, it is possible that physiological differences caused by the growth conditions are influencing Arabidopsis chlorate sensitivity. One possible explanation is transpiration, since compost-grown plants kept in enclosed Magenta boxes appeared to show chlorate susceptibility, although plants in this system had clear signs of stress and so this result should be treated with caution. It is worth noting that chlorate treatment can induce a broad range of physiological changes in plants – chlorate treatment reduces photosynthetic rate, transpiration rate, and stomatal conductance in Longan trees (*Dimocarpus longan*), although the mechanistic basis for these observations is unclear (Lu *et al.*, 2017). It is likely that there at least some physiological differences in plants grown in enclosed vs open systems, since, for example, high humidity would reduce the transpiration rate. It is unclear how chlorate-induced changes in physiology could cause an opposing chlorate-resistance phenotype in enclosed vs open systems for *nrt1*.1 and *ctr1-1* but it is perhaps worth investigating further. Comparing physiological measurements (e.g. photosynthetic rate) of WT and chlorate-resistant genotypes on compost, and the same genotypes grown on Jiffy compost pellets

enclosed within Magenta boxes and/or agarose plates, in both the presence and absence of chlorate, would show whether growing plants in enclosed conditions is sufficient to override any differences in open systems, and whether chlorate treatment can influence these effects.

Whilst interesting, the biological significance of these findings is perhaps questionable, since laboratory compost conditions are closer to those of modern agriculture. However, it would be interesting to understand how nitrate metabolism of plants grown in enclosed systems (such as agarose and/or agar plates, widely used in Arabidopsis studies) differs compared to plants grown on open systems (such as compost), which are of more biological relevance when considering findings that may be applicable to crop development.

6.3 The role of HY5 in regulating phosphate metabolism

Chapter 5 investigated the role of HY5 in regulating Arabidopsis phosphate metabolism. HY5 has been described as a master regulator, and whilst first identified for its role in regulating plant growth in response to light (Osterlund *et al.*, 2000), has more recently been identified as a regulator of Arabidopsis nitrate metabolism, in particular coordinating the whole-plant carbon-nitrogen balance (Chen *et al.*, 2016). In 2018, research was published identifying the *hy5* null mutant as having reduced levels of ^{33}P-labelled uptake, whilst a HY5-overexpressor line had enhanced levels of ^{33}P-labelled uptake compared to WT (Sakuraba *et al.*, 2018). The same study showed that the *hy5* mutant had reduced expression of *PHT1;1* in both dark conditions and in seedlings exposed to either red light or far-red light, and that the HY5 protein could bind the *PHT1;1* phosphate transporter promoter region directly (Sakuraba *et al.*, 2018). Building on these findings, I show that the *hy5* mutant has impaired shoot phosphate accumulation and an altered subset of phosphate-starvation responses, and I investigate the role of HY5 in regulating phosphate metabolism in response to both sucrose

and light. An additional study published during the course of this research suggests that HY5 suppresses the transcriptional activation activity of FHY3 and EIN3 on *PHR1*, suggesting HY5 represses *PHR1* and PSI gene expression (Liu *et al.*, 2017). These findings included *the hy5-215* mutant having elevated seedling Pi content, and increased expression of *PHR1* in phosphate replete and starvation conditions. This somewhat contradicts the work of Sakuraba *et al.*, who showed the *hy5* null mutant had reduced phosphate uptake, although does partially support a subsequent publication by Yeh *et al*. who report the same *hy5* null mutant as having a reduced shoot phosphate content, but not root phosphate content, compared to WT in phosphate replete conditions. Chapter 5 therefore supports and builds upon these studies, to provide further evidence that *hy5* has altered Pi metabolism.

6.3.1 *hy5* has altered regulation of phosphate metabolism

I demonstrate that *hy5* plants have a reduced shoot Pi content compared to WT and that this is applicable in both phosphate-replete and phosphate-deficient environments [**5.2.2; 5.2.5**], contradicting Liu *et al.* I provide further evidence that HY5 modulates phosphate metabolism by showing that *hy5* has an altered subset of phosphate starvation responses, and the HY5 protein is therefore at least partially involved in regulating the Arabidopsis response to phosphate deprivation, in addition to shoot phosphate accumulation [**5.2.3; 5.2.4; 5.2.7**].

Liu *et al.* suggest that HY5 regulates the phosphate starvation response through repression of PHR1 activity (Liu *et al.*, 2017); PHR1 acts alongside PHL2 to regulate key components of the transcriptional response to phosphate starvation (Sun *et al.*, 2016). PHR1 has been shown to positively regulate a variety of phosphate starvation responses, including anthocyanin accumulation (Nilsson *et al.*, 2012; Liu *et al.*, 2022). If HY5 represses PHR1 activity, the *hy5* null mutant might be expected to have enhanced PHR1 activity, and a resulting increase in

phosphate starvation responses during conditions of phosphate starvation. However, I show that this is not the case – anthocyanin accumulation is impaired (rather than enhanced) in response to phosphate starvation in the *hy5* mutant [**5.2.4**]. Additionally acid phosphatase activity is reduced in the *phr1* mutant and enhanced in a *PHR1* overexpressor line (Sun *et al.*, 2016); yet acid phosphatase activity is unaltered in response to phosphate starvation in *hy5* [**5.2.7**]. This suggests the altered regulation of phosphate metabolism in *hy5* is more nuanced than being solely due to altered regulation of PHR1, and that HY5 has a role in modulating a subset of, but not all, phosphate starvation responses in Arabidopsis.

The research described in **Chapter 5** utilises the *hy5* loss-of-function mutant, and it would be interesting to further explore the role of HY5 in regulating phosphate acquisition by utilising HY5-overexpressor lines to determine if these display opposing phenotypes to those observed in this study. A HY5-overexpressor line has been shown to have enhanced ^{33}P-labelled Pi uptake (Sakuraba *et al.*, 2018) suggesting shoot Pi content is likely elevated in this line; it would be useful to determine whether the same line has enhanced primary root shortening in response to phosphate deprivation, and enhanced anthocyanin accumulation, therefore maintaining an opposing phenotype to the *hy5* mutant during phosphate starvation.

I show that *hy5* seedling biomass is unaffected by altered Pi provision [**5.2.6**], which suggests that *hy5* seedlings are able to maintain WT-levels of plant biomass despite reduced Pi accumulation in plant tissues, at least at the stage measured in this study. Investigating whether this result persists long-term would help determine whether HY5 is a candidate to alter nutrient use efficiency in plants, since reduced levels of Pi uptake do not appear to be causing a difference in growth. At present the effect of HY5 on altering nutrient use efficiency is unclear, since reducing external Pi concentration still caused the same extent of reduction

in seedling biomass in WT and *hy5* plants, despite the lowered internal phosphate concentration of *hy5* plants. Long-term, it would be interesting to extend this research to crop varieties, both to establish whether the role of HY5 as a regulator of phosphate nutrition is conserved across species, and also to investigate whether HY5 is a potential target for manipulation in order to improve crop nutrient use efficiency.

6.3.2 Shoot illumination is required for HY5-mediated changes in shoot phosphate accumulation

As described in **1.6.1**, HY5 is under the control of a variety of light signalling pathways (Osterlund *et al.*, 2000; Xu *et al.*, 2014; Huang *et al.*, 2012). I therefore investigated the effects of light, and specific tissue illumination regimes, on HY5-mediated phosphate metabolism. Growing plants on agarose plates allowed different tissue illumination regimes to be established, which indicated that HY5-dependent shoot phosphate accumulation was dependent on shoot illumination [**5.2.15**]. There was no observable difference in root phosphate content between WT and *hy5* in any condition tested, building upon results subsequently published by Yeh *et al.*, suggesting that shoot-to-root phosphate transport is altered in *hy5*, with root Pi contents maintained at the apparent expense of shoot Pi concentrations. Whilst Yeh *et al.* only looked at primary root length in different light conditions (and did not distinguish between root vs shoot illumination), the authors demonstrated that blue light (and not red light or far red light) was necessary to induce differences between *hy5* and WT primary root elongation. Using the light conditions of Yeh *et al.*, with the differential tissue illumination regimes presented here would be helpful to confirm that blue light-dependent shoot illumination is necessary for HY5-dependent shoot phosphate accumulation.

Shoot HY5 is mobile, and during shoot illumination has been proposed to travel to the roots to both promote root *HY5* expression, and root *NRT2.1* expression, thereby maintaining the C: N balance by increasing expression of genes encoding nitrate transporters, and therefore increasing nitrate uptake, during times of increased carbon fixation (Chen *et al.*, 2016). The finding described in this thesis, that shoot illumination is required to promote HY5-dependent shoot Pi accumulation, suggests that HY5 may perform a similar role in Arabidopsis Pi metabolism. To confirm this, future work could utilise the reciprocal grafting techniques used to determine the role of mobile shoot HY5 in regulating the Arabidopsis C: N balance (Chen *et al.*, 2016), to determine whether the depleted levels of ^{33}P-labelled uptake (Sakuraba *et al.*, 2018), or shoot Pi content [**5.2.2; 5.2.5**] seen in *hy5*, are restored in graft scions consisting of *hy5* roots with WT shoots, or whether a *hy5* root genotype is also affecting root-to-shoot phosphate transport.

Since I have determined that HY5 is necessary for a subset of Arabidopsis phosphate starvation responses [**5.2.3; 5.2.4; 5.2.7**] it would also be useful to determine whether these are dependent on shoot illumination also, and if these are dependent on blue light as suggested by Yeh *et al.*

hy5 plants have altered root Pi transporter expression, and it has been reported that *hy5* plants have reduced Pi uptake rates (Sakuraba *et al.*, 2018). Since I have not found a significant difference in root Pi content between WT and *hy5* plants in a range of conditions (different illumination regimes, different phosphate contents and different sucrose availabilities [**5.2.12, 5.2.18**]) this suggests that root-to-shoot phosphate transport may be altered in the *hy5* mutant, since root Pi content is maintained, and shoot Pi content reduced. This also suggests such a mechanism exists to maintain WT-levels of root Pi concentrations at the

expense of shoot Pi content, and it would be interesting to explore this further – for example measuring expression levels and accumulation in different tissues of phosphate transporters such as *AtPHT1;5* which has been shown to have a role in promoting source-to-sink Pi mobilisation, and comparing the *hy5* null mutant against WT and overexpression lines.

6.3.3 HY5 does not affect sucrose-mediated phosphate metabolism

Shoot illumination is necessary for photosynthesis, which results in carbon fixation. Fixed carbon is primarily transported as sucrose, and sucrose has a known effect on Arabidopsis Pi starvation responses. The presence of sucrose in Pi-deficient growth media increases the severity of Pi starvation symptoms in Arabidopsis (Karthikeyan *et al.*, 2007), and mutants impaired in sucrose transport have been shown to display phosphate-starvation symptoms even when Pi levels are replete (Lei *et al.*, 2011). I have shown that HY5 may coordinate phosphate metabolism with respect to shoot illumination (and therefore presumably to shoot carbon fixation), and *hy5* plants have been shown to have altered expression of genes affecting both sucrose metabolism and sucrose transport (Chen *et al.*, 2016). The sucrose sensor involved in Pi metabolism is unknown, and since HY5 influences sucrose metabolism and sucrose transport, it is possible that HY5 may play a role in this process. I therefore investigated whether HY5 was involved in sucrose-mediated increases in the severity of phosphate starvation symptoms in Arabidopsis, by investigating previously measured hallmarks of phosphate starvation in the *hy5* mutant under a range of sucrose concentrations, to determine if differences between WT and *hy5* were induced or exacerbated by the presence of sucrose in the media.

Despite the finding of Chen *et al.* that *hy5* has altered expression of genes encoding components of sucrose metabolism and sucrose transport, I have not found that increasing

sucrose concentrations exacerbate or relieve the altered Pi metabolism found in the *hy5* mutant. The shoot Pi content of *hy5* plants remains reduced in both phosphate-replete and phosphate-deficient conditions relative to WT, and this is not altered by the presence of sucrose in the growth media, with *hy5* shoot Pi content reduced by approximately 20% in all sucrose concentrations tested [**5.2.11**]. Root APase activity in WT and *hy5* plants was unchanged by sucrose in the media [**5.2.13**]. Whilst sucrose did reduce *hy5* seedling biomass at high concentrations, this was independent of the Pi concentration of the media [**5.2.10**], and no marked difference in the altered root system architecture of the *hy5* mutant, nor altered anthocyanin accumulation, in response to Pi starvation was observed by the addition of sucrose in the media [**5.2.13; 5.2.14**].

Therefore, although HY5 does appear to regulate Pi metabolism, it does not appear to be a significant contributor to the regulation of sucrose-dependent responses to low Pi in Arabidopsis. This result therefore differs from HY5's role in sucrose-mediated NO_3^- accumulation, where sucrose has been shown to enhance illumination-dependent increases in NO_3^- uptake, an effect that is reduced in the *hy5* mutant (Chen *et al.*, 2016). This thesis therefore suggests that a HY5-independent signalling pathway is responsible for sucrose-dependent changes in Arabidopsis Pi metabolism.

6.4 Conclusions and Implications

Taken together, Chapters 3, 4 and 5 therefore build on current understanding of the relationship between nutrient use and growth in Arabidopsis. I identify that ethylene signalling modulates Arabidopsis N metabolism, and further our understanding of the altered Pi metabolism of *hy5*. I also explore the interaction between NO_3^- and Pi metabolism, identifying that known genetic regulators of Pi metabolism alter NO_3^- uptake and NR activity,

rather than shoot Pi levels themselves. Key to these findings was the use of a genetics approach, utilising mutants that lack functional copies of genes of interest to reveal new insights into the regulation of plant nutrition. These findings emphasize the importance of considering how new regulators of Pi and/or NO_3^- metabolism alter plant nutrient use on a broader level and identify new targets for further research aimed at improving plant nutrient use efficiency.

Appendix 1: Jamieson *et al.*, 2022

Planta (2022) 255:94
https://doi.org/10.1007/s00425-022-03872-9

SHORT COMMUNICATION



Ethylene signaling modulates *Arabidopsis thaliana* nitrate metabolism

Fiona Jamieson[1] · Zhe Ji[1] · Eric J. Belfield[1] · Zhong Jie Ding[2] · Shao Jian Zheng[2] · Nicholas P. Harberd[1]

Received: 24 November 2021 / Accepted: 8 March 2022 / Published online: 26 March 2022
© The Author(s), under exclusive licence to Springer-Verlag GmbH Germany, part of Springer Nature 2022

Abstract

Main conclusion **Genetic analysis reveals a previously unknown role for ethylene signaling in regulating *Arabidopsis thaliana* nitrogen metabolism.**

Abstract Nitrogen (N) is essential for plant growth, and assimilation of soil nitrate (NO_3^-) and ammonium ions is an important route of N acquisition. Although N import and assimilation are subject to multiple regulatory inputs, the extent to which ethylene signaling contributes to this regulation remains poorly understood. Here, our analysis of *Arabidopsis thaliana* ethylene signaling mutants advances that understanding. We show that the loss of CTR1 function *ctr1-1* mutation confers resistance to the toxic effects of the NO_3^- analogue chlorate (ClO_3^-), and reduces the activity of the nitrate reductase (NR) enzyme of NO_3^- assimilation. Our further analysis indicates that the lack of the downstream EIN2 component (conferred by novel *ein2* mutations) suppresses the effect of *ctr1-1*, restoring ClO_3^- sensitivity and NR activity to normal. Collectively, our observations indicate an important role for ethylene signaling in regulating *Arabidopsis thaliana* NO_3^- metabolism. We conclude that ethylene signaling enables environmentally responsive coordination of plant growth and N metabolism.

Keywords *Arabidopsis* · Chlorate resistance · Ethylene · Nitrogen · Nitrate reductase · Signaling

Abbreviations

CTR1	Constitutive triple response
ctr1-1	*constitutive triple response 1* (Loss of function allele)
EIN2	Ethylene inensitive 2
EIN3	Ethylene insensitive 3
ETR1	Ethylene resistant 1 (Ethylene receptor)
N	Nitrogen
NR	Nitrate reductase
NRT1/NRT2	Nitrate transporters

Communicated by Dorothea Bartels.

✉ Shao Jian Zheng
sjzheng@zju.edu.cn

✉ Nicholas P. Harberd
nicholas.harberd@plants.ox.ac.uk

[1] Department of Plant Sciences, University of Oxford, Oxford OX1 3RB, UK

[2] College of Life Sciences, Zhejiang University, Hangzhou 310058, People's Republic of China

Introduction

Nitrogen (N) is essential for the synthesis of the amino and nucleic acids that underpin plant growth (Miller and Cramer 2005; Smith et al. 2010). There are two main routes through which plants acquire N. Some can acquire atmospheric N via symbiotic relationships with N-fixing bacteria (Smith et al. 2010). In contrast, many rely exclusively upon regulated processes of absorption of soil NO_3^- ions, ammonium ions or amino acids. For example, in *Arabidopsis thaliana*, soil NO_3^- is imported through root nitrate transporters (NRT1 and NRT2; Wang et al. 2012), processed via a dedicated metabolic assimilatory pathway that includes nitrate (NR) and nitrite (NiR) reductases (Smith et al. 2010), and then fed into amino and nucleic acid biosynthesis.

Because plant growth is profoundly influenced by the environment, environmental signals modulate N assimilation. For example, phytochrome-mediated light signaling regulates NR and NiR activities (Lillo 2008). Here we further investigate the environmental regulation of N metabolism by asking if the evolutionarily conserved ethylene environmental stress-signaling pathway (Smith et al. 2010; Binder 2020) regulates NO_3^- assimilation in *Arabidopsis thaliana*. This pathway begins with the ETR1

ethylene receptor, which, in the absence of ethylene, maintains activation of the downstream CTR1 kinase, which in turn represses downstream ethylene signaling via phosphorylation of EIN2 (Binder 2020). This phosphorylation prevents the proteolytic cleavage of EIN2. In contrast, in the presence of ethylene, hormone binding to ETR1 inactivates CTR1, resulting in dephosphorylation and cleavage of EIN2, with subsequent migration of the EIN2 C-terminal (CEND) fragment into the cytosol and nucleus. The CEND fragment stabilizes the EIN3 transcription factor, thus causing ethylene-promoted downstream gene activation (Binder 2020).

Whilst previous studies indicated a role for ethylene in regulating N assimilation (Khan et al. 2008; Tian et al. 2009), they focused primarily on the molecular effects of short-term ethylene bursts. We, therefore, undertook a systematic study at the whole-plant level, and over longer time scales. In particular, we used *Arabidopsis thaliana* mutants lacking CTR1 and EIN2. Lacking the CTR1 kinase, the *ctr1-1* mutant is dwarfed and displays constitutive ethylene responses (i.e., exhibits ethylene responses even in the absence of ethylene). First, using resistance to ClO_3^- as a proxy measure of altered NO_3^- metabolism, we found that the *ctr1-1* mutation confers increased ClO_3^- resistance, suggesting that *ctr1-1* confers a reduction in NO_3^- uptake or assimilation. Accordingly, we next found that *ctr1-1* confers a reduction in the activity of the NR enzyme of NO_3^- assimilation. Second, we mutagenized *ctr1-1* and screened for novel mutants carrying secondary mutations conferring suppression of *ctr1* phenotype. DNA sequencing of such mutants identified multiple independent mutations in the *EIN2* gene. Further analysis showed that these novel *EIN2* mutants displayed normal ClO_3^- resistance and NR activity, despite retaining *ctr1-1*. We conclude that ethylene signaling plays a role in modulating *Arabidopsis thaliana* NO_3^- metabolism.

Materials and methods

Plant materials and growth conditions

Arabidopsis thaliana (Col-0 genetic background unless stated otherwise) seeds were surface sterilised with 70% (*v*/*v*) ethanol and left to dry on filter paper, then sown on agar plates or the surface of sieved compost (ICL Levington Advanced F2 compost, particles < 1 cm) and subsequently stratified in the dark at 4 °C for 2–4 days. After stratification plants were moved to controlled environment rooms (CERs) with a long-day photoperiod (16 h light/8 h dark) at 22 °C, irradiance 120 µmol of photons m^{-2} s^{-1}.

ClO_3^- resistance assays and measurements of green shoot area

4–5-week-old *Arabidopsis thaliana* plants were left for ~ 7 days without watering, following which 2.5 mM $KClO_3$ was applied. Any solution not absorbed into the soil after 2 h was discarded. Control plants were treated with water. A second $KClO_3$ application occurred once the soil surface had become visibly dry (variable time between the two applications). Plants were imaged 7 days following the first application.

In quantitating susceptibility to $KClO_3$, photographic images were analyzed using imageJ (http://www.imagej.nih.gov/ij/) for determination of the proportion of each rosette displaying green versus yellow hues. Individual rosette images were cropped, and any leaves falling into the frame from other plants were manually removed by selecting and clearing that area. Using the Image > Adjust > Color Threshold command, all areas of green-hued tissue were selected by setting the following parameters: Hue 41–90; Saturation 0–255 and Brightness 60–255. This area was measured (Analyse > Measure), and compared to the yellow-hued area of tissue, measured by setting the parameters: Hue 1–40; Saturation 0–255; and Brightness 60–255. If necessary the brightness threshold was adjusted to ensure that no background, and all tissue, was captured. The proportion of the total area measured occupied by green hues gave an indication of resistance to ClO_3^-, and was calculated as follows:

$$\%\text{rosette tissue remaining green} = \frac{\text{Area of green tissue}}{\text{Area of green tissue} + \text{Area of yellow tissue}} \times 100.$$

NR activity assays, determination of NR mRNA and protein abundances

0.5 g rosette leaf was harvested, ground to a fine powder in liquid N_2 and homogenised in 5 ml/g extraction buffer [50 mM potassium phosphate (KH_2PO_4 pH 7.6), 1 mM EDTA, 5 mM 1,4-dithiothreitol (DTT), 0.5% Triton and 1 × HALT™ Protease Inhibitor Cocktail (ThermoFisher Scientific, Waltham, MA, USA)] until thawed. 2 ml of protein extract was transferred to a separate Eppendorf tube and centrifuged at 17,115*g* for 15 min before the supernatant was collected and centrifugation repeated. 1 ml of protein extract was collected and kept on ice for NR Activity Assays and protein quantification.

To determine NR activity, 200 µl protein extract was added to 800 µl reaction buffer (50 mM KH_2PO_4 (pH 7.6), 5 mM EDTA, 10 mM KNO_3 and 0.2 mM NADH). The reaction was allowed to proceed for 30 min in the dark at

room temperature, then stopped by adding 1 ml of 0.36 M zinc acetate (ZnAc), followed by centrifugation at 14,674*g* for 5 min. 500 µl of supernatant was transferred to a new tube, to which 1 ml of colour developer reagent (made up of equal volumes of 1% sulphanilamide in 3 M HCl and 0.02% N-(1-napthyl) ethylenediamine dihydrocholoride) was added. The reaction mixture was left in the dark for 30 min to allow colour development. The concentration of nitrite was determined by measuring the absorbance at 540 nm (OD_{540}) using an Evolution 260 BIO UV–Visible Spectrophotometer. Nitrate reductase activity was expressed as the absorbance of the reaction mixture at 540 nm (A540) relative to the sample protein concentration. Protein was quantified using the Bio-Rad DC colorimetric protein assay kit (Bio-Rad) according to the manufacturer's instructions.

RNA was extracted from 3rd and 4th youngest rosette leaves using Trizol (ThermoFisher) using the standard protocol. cDNA synthesis was performed using SuperScript III reverse transcriptase (Invitrogen). For semi-quantitative analysis of gene expression, RT-PCR reactions were set up using 1 µl of cDNA and 5 µM of intron-spanning primers for genes of interest in a 47 µl reaction mixture. The *CBP20* (At5g44200) gene was used as an internal normalisation and cDNA loading control. The amount of PCR product was quantified by measuring band intensities on 1% agarose gels stained with ethidium bromide and analysed using VisionWorksLS software.

For immunoblot analysis, total protein was extracted from WT and *ctr1* plants, either from rosette leaves of 5-week-old plants grown on soil or from 2-week-old seedling shoots grown on half-strength Murashige & Skoog salt (Merck Life Science, Dorset, UK) media (pH 5.8) containing 0.5% sucrose and 1% agarose, using extraction buffer containing 50 mM Tris–HCl (pH 7.5), 150 mM NaCl, 0.1% NP–40 detergent, 10% glycerol, 1 mM DTT and protease inhibitor cocktail (Roche LifeScience, Penzberg, Germany). Protein samples were heated at 70 °C for 10 min before being subjected to sodium dodecyl sulphate–polyacrylamide gel electrophoresis (SDS–PAGE) and transferred to a nitrocellulose membrane. The membrane was stained in Ponceau S solution (Sigma, St. Louis, MO, USA; P7170) following the manufacturer's instructions before blocking. Actin and NR proteins were detected using anti-Actin (Agrisera, Vännäs, Sweden; AS13 2640) and anti-NR (Agrisera; AS08 310) antibodies, respectively. The membranes were visualised on the iBright FL1500 Imaging System (ThermoFisher; A44241) and the band intensities were quantified with onboard image analysis.

Mutagenesis of *ctr1-1*

ctr1-1 seeds were initially bulked up from laboratory stocks in a CER, following which ~ 12,500 collected seeds were washed with 0.1% Tween-20 for 15 min. This solution was removed and the seeds rinsed three times with dH_2O prior to adding 50 ml of 0.4% ethyl methanesulfonate (EMS) solution, followed by mixing on a benchtop shaker for 8 h in darkness. Next, the seeds were washed 10 times with dH_2O, then soaked in 50 ml dH_2O and agitated on a benchtop shaker for 1 h to allow diffusion of residual EMS out of the seeds. The seeds were subsequently left to dry overnight on filter paper. The seeds were then mixed with ~ 130 g of sand, and 10 g of sand/ seed mixture sown on trays of Levington's F2 compost mix. Seeds were grown under standard conditions and allowed to self-fertilize. The resultant M_2 seeds were bulk harvested.

DNA sequence analysis

DNA fragments spanning *CTR1* were amplified using the primers (CTR1-F: 5'- AAAGTGGAGCAAGGGAGCAA and CTR1-R: 5'- ACCGCAGCTACAACCTATGG), and then sequenced by Sanger-sequencing to confirm the genetic background of each *ctr1-1* suppressor. Full-length *EIN2* gene fragments were amplified using the primers (EIN2-F: 5'-ATGGAAGCTGAAATTGTGAATGTGA and EIN2-R: 5'-TCAACCCAATGATCCGTACGC), and were also analysed with Sanger-sequencing.

Results and discussion

ctr1-1 confers ClO_3^- resistance and reduced NR activity

The *Arabidopsis thaliana ctr1-1* mutant maintains constitutive ethylene signaling, and displays a characteristic seedling ethylene 'triple response' phenotype (short root; short and thick hypocotyl; exaggerated apical hook) in the absence of ethylene (Kieber et al. 1993). Mature *ctr1-1* plants are dwarfed, have small rosette leaves, short stems, and delayed flowering (Achard et al. 2007). We first determined the possible effect of *ctr1-1* on NO_3^- metabolism, via the frequently used ClO_3^- resistance assay (treatment with $KClO_3$; see "Materials and methods"). Because the ClO_3^- ion is a structural analogue of NO_3^-, ClO_3^- is readily taken up by root NO_3^- uptake systems and then transported to the shoot. Here, NR converts ClO_3^- to chlorite (Cove 1976; Murphy and Imbrie 1981). Because chlorite is toxic, plants grown on $KClO_3$-treated soil display leaf chlorosis. This assay was previously used to screen for *Arabidopsis thaliana* mutants displaying increased ClO_3^- resistance, including *chl1*, subsequently identified as containing a loss of function *nrt1.1* mutation in *NRT1.1*, the gene encoding the NRT1.1 nitrate transporter (Ho et al. 2009).

Whilst ClO_3^- treatment of wild-type (WT) plants caused leaf chlorosis, treatment of control *nrt1.1* plants (where lack of the NRT1.1 impairs ClO_3^- uptake) did not (Ho et al. 2009; Fig. 1a). Interestingly, *ctr1-1* also confers ClO_3^- resistance (Fig. 1a): the vegetative rosette tissue of *ctr1-1* plants remained green following ClO_3^- treatment (Fig. 1a). We next quantitatively compared ClO_3^- resistances, using ImageJ (see "Materials and methods"). These comparisons revealed no significant differences between control-treated WT, *ctr1-1* and *nrt1.1* plants (Fig. 1b). In contrast, whilst the green tissue percentage of ClO_3^--treated *nrt1.1* plants was not detectably different from that of control, only ~ 25% of WT rosette tissue remained green following ClO_3^- treatment (Fig. 1b). ~ 80% of *ctr1-1* rosette tissue remained green following ClO_3^- treatment, indicating that *ctr1-1* confers relatively strong ClO_3^- resistance (albeit not as strong as conferred by *nrt1.1*; Fig. 1b), and hence that ethylene signaling might impact ClO_3 resistance.

We next studied a broader range of ethylene-related mutants, first using ethylene over-producing and receptor mutants. The ethylene over-producing *eto1*, *eto2* and *eto3* mutants all display enhanced ethylene production (Chae et al. 2003; Wang et al. 2004), whilst *etr1-1* contains a mutation in the gene encoding the ETR1 ethylene receptor, thus conferring ethylene insensitivity (Binder 2020). ImageJ analysis showed that whilst the percentage remaining green rosette tissue of ClO_3^--treated *eto1* and *etr1* was not significantly different to that of WT (~ 17%), thus indicating a relative lack of resistance, both *eto2* and *eto3* ClO_3^--treated rosettes retained ~ 40% green tissue (thus indicating partial resistance versus the stronger *ctr1* (~ 62%) and *nrt1.1* (~ 98%) resistances; Fig. 1c). Next, we assayed *ein2-1* and *ein3-1* mutants, which respectively lack the downstream EIN2 and EIN3 components of ethylene signaling, finding no significant difference between WT, *ein2-1* and *ein3-1*, in conditions where *ctr1-1* and *nrt1.1* exhibited obvious ClO_3^- resistance (Fig. 1d). These observations support the following conclusions. First, the constitutively active ethylene signaling of *ctr1-1* promotes ClO_3^- resistance. Accordingly, increased ethylene signaling in *eto2* and *eto3* (due to ethylene overproduction) also promotes ClO_3^- resistance. However, the ClO_3^- resistance of *eto2* and *eto3* is less than that of *ctr1-1* (and is undetectable in *eto1*), perhaps because their ethylene overproduction is largely a seedling (rather than adult plant) phenomenon (Chae et al. 2003). Second, the ethylene insensitivity conferred by *etr1-1*, *ein2-1* and *ein3-1* has no obvious effect on ClO_3^- resistance, suggesting that there is a threshold level of ethylene signaling below which further reductions do not detectably affect ClO_3^- resistance.

We next compared leaf extract NR activities, finding that *ctr1* plants retain ~ 50% of WT activity (Fig. 1e). To determine if this difference in NR activity was due to changes at transcriptional or post-transcriptional levels, we measured the relative abundances of mRNAs transcribed from the *NIA1* and *NIA2* genes that encode NR in *Arabidopsis thaliana*. As expected, *NIA2* mRNA was more abundant than *NIA1* (Fig. 1f), as it encodes ~ 90% of *Arabidopsis thaliana* NR (Yu et al. 1998). Whilst there was no detectable difference between *NIA1* mRNA abundances in WT and *ctr1-1*, NIA2 mRNA abundance was partially reduced (Fig. 1f). Furthermore, use of an anti-NR antibody revealed that detectable NR protein abundance was also reduced in *ctr1-1* versus WT (Fig. 1g). We conclude that reductions in NR-encoding transcript and NR protein abundances may contribute to the reduced NR activity and increased ClO_3^- resistance of *ctr1-1*. However, it is possible that CTR1 also regulates NR activity via post-translational mechanisms.

Lack of EIN2 function correlates with suppression of the ClO_3^- resistance and NR activity reduction conferred by *ctr1-1*

To further understand the role of CTR1 and the ethylene signaling pathway in regulating N metabolism, we next performed genetic suppression analysis of *ctr1-1*. Tall plants (in which the dwarfism conferred by *ctr1-1* was suppressed) were selected from an EMS-mutagenized *ctr1-1* M_2 population (see "Materials and methods"; Fig. 2a). Single tall plants were isolated, allowed to self-pollinate, shown to have 100% tall progeny (indicating homozygosity for new suppressing mutations; data not shown), and shown by DNA sequencing to retain the progenitor *ctr1-1* allele (indicating that they were not WT contaminants; data not shown). Four independent homozygous tall lines (9–11, 12–9, 16–3 and 22–10) were next selected for further analysis (Fig. 2b). For example, we found that line 22–10, despite retaining *ctr1-1*, lacked the ClO_3^- resistance conferred by *ctr1-1* (Fig. 2c). Furthermore, all of 9–11, 12–9, 16–3 and 22–10, again despite retaining *ctr1-1*, no longer displayed the reduced NR activity (Fig. 2d) conferred by *ctr1-1*. Therefore, each of lines 9–11, 12–9, 16–3 and 22–10 was carrying an unknown novel ('second-site') mutation suppressing the effects of *ctr1-1* on NO_3^- metabolism. Because mutations in *EIN2* have previously been shown to suppress *ctr1-1* phenotypes (Alonso et al. 1999), we determined the DNA sequences of *EIN2* in each of 9–11, 12–9, 16–3 and 22–10, finding independent *EIN2* nucleotide substitution mutations in each line (Fig. 2e).

A plausible potential explanation for the ClO_3^- resistance of *ctr1-1* was that this resistance was an inherent property of the dwarfism conferred, rather than a specific consequence of constitutive ethylene signaling. Accordingly, mutations at *EIN2* would suppress the ClO_3^- resistance conferred by *ctr1-1* because they suppress dwarfism, rather than because of an effect on ethylene-regulated N metabolism. To test

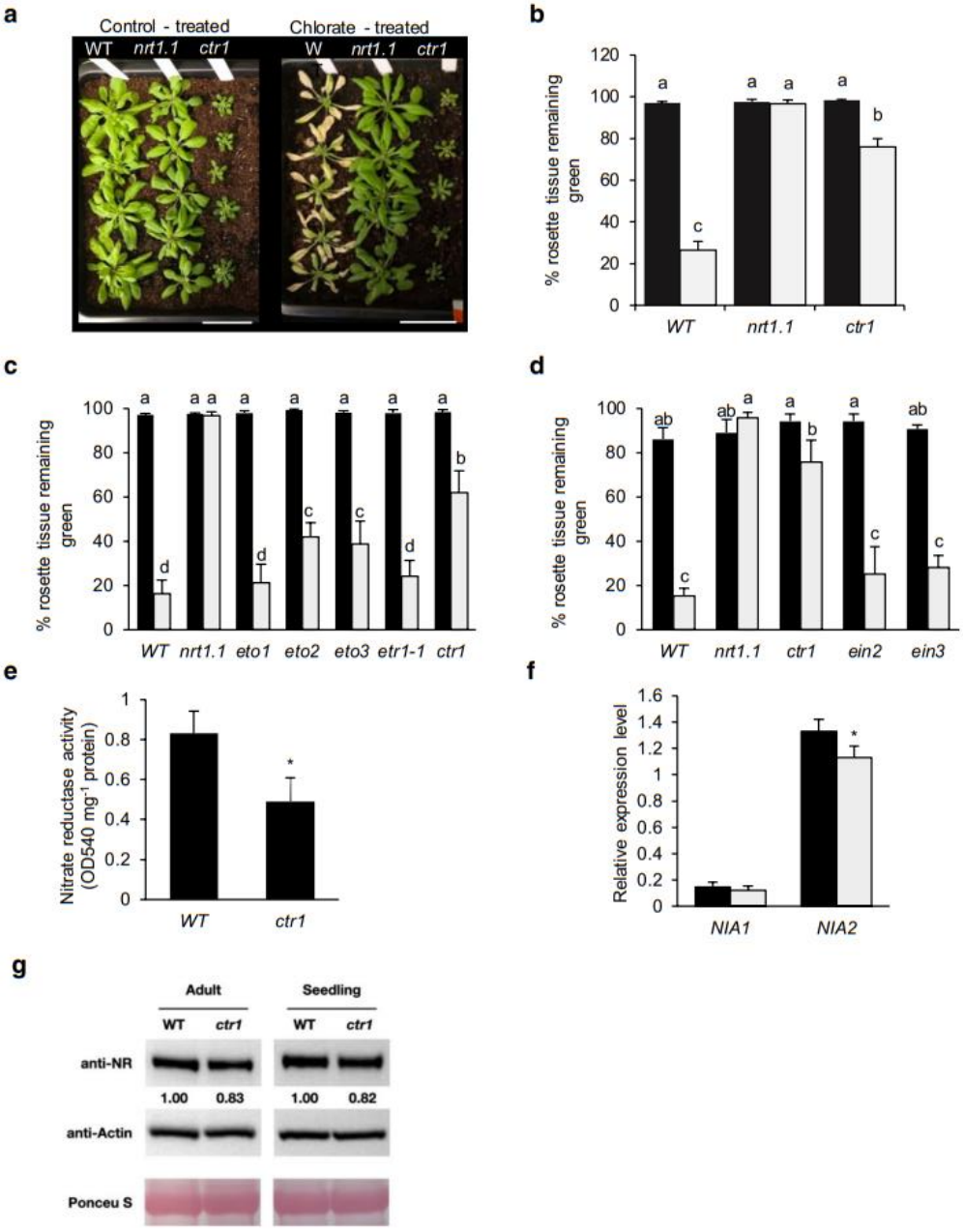


Fig. 1 The *ctr1-1* mutation confers chlorate resistance and reduced NR activity. **a** Soil-grown 6-week-old WT, *nrt1.1* and *ctr1-1* plants 8 days after treatment with water (control) or 2.5 mM $KClO_3$ (chlorate-treated), bolt-stems removed. Scale bars = 50 mm. **b–d** Proportion (%) of rosette tissue remaining green following treatment (as in **a**) with water (control, dark) or $KClO_3$ (chlorate-treated, light). Plant genotypes as indicated. Values are means ± SD. Different letters denote statistically significant differences (one-way ANOVA/Tukey HSD post hoc test, $P < 0.05$, $n = 4$). **e** NR activity in shoot tissue of 5-week-old WT and *ctr1-1* plants determined relative to protein content (* denotes statistically significant difference, student's *t*-test, $P < 0.05$, $n = 4$). **f** Semi-quantitative RT-PCR determined abundances of *NIA1* and *NIA2* mRNAs (relative to *CAP BINDING PROTEIN 20* (*CBP20*) control mRNA in WT (dark) and *ctr1-1* (light) shoots (* denotes statistically significant difference, student's *t*-test, $P < 0.05$, $n = 3$). **g** NR protein abundance in WT versus *ctr1-1*, with immunodetectable NR quantified against Actin control (arbitrarily set at 1.00 in WT), showing a reduction (0.82) in *ctr1-1*. A single representative of an experiment performed three times is shown

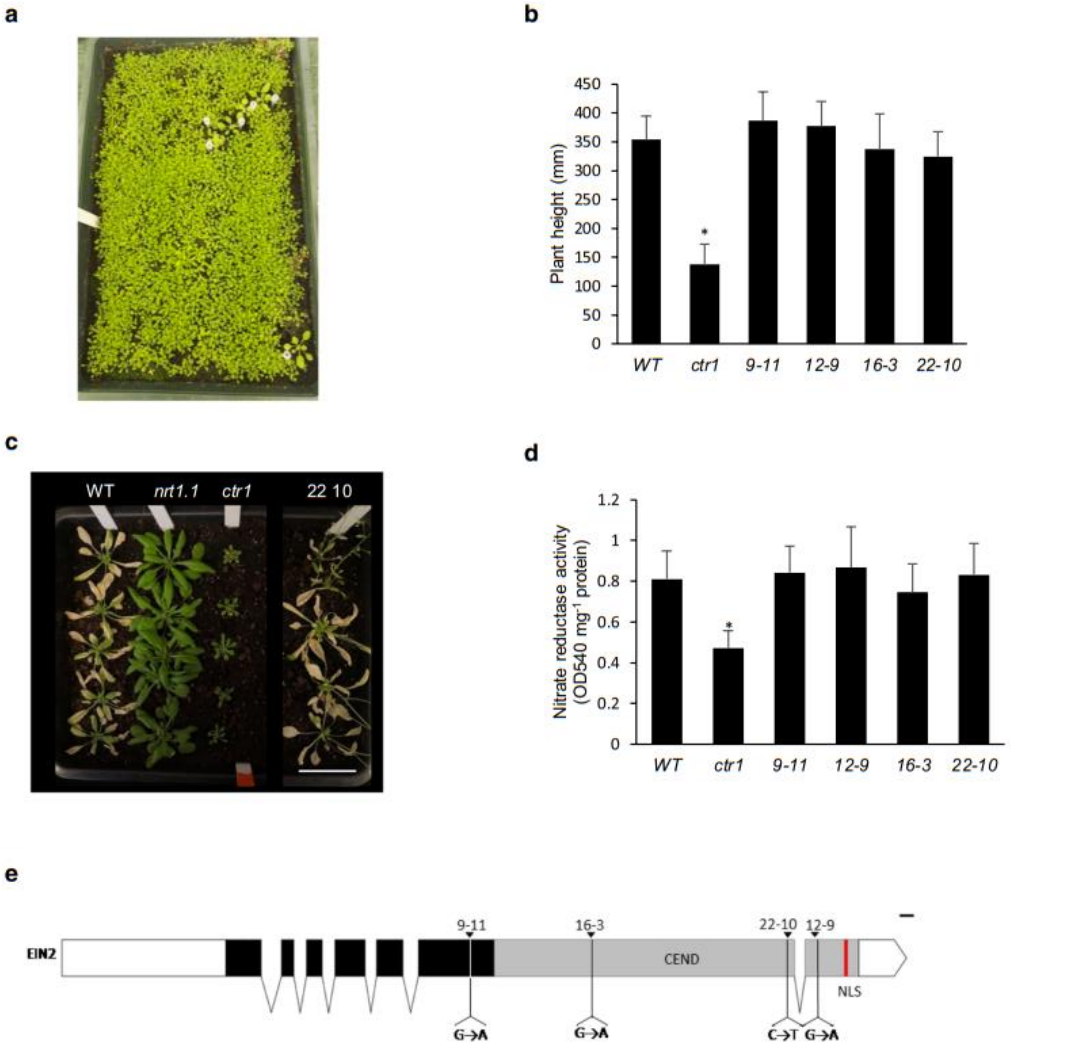


Fig. 2 Lack of EIN2 suppresses *ctr1-1*-conferred chlorate resistance and reduced NR activity. **a** Suppressor screen: tall plants putatively carrying novel mutations suppressing *ctr1-1* phenotype are marked with adjacent plastic pipette tips. **b** Heights of 5-week-old control (WT, *ctr1-1*) and suppressor line (9–11, 12–9, 16–3 and 22–10) plants. *Denotes statistically significant difference compared to WT (student's *t*-test, $P < 0.05$, $n = 10$). **c** 5-week-old WT, *nrt1.1*, *ctr1-1* and suppressor line 22–10 plants treated either with water (control, left panel) or with 2.5 mM $KClO_3$ (right panel). Plants were imaged 7 days after treatment. Scale bar = 50 mm. **d** NR activity (relative to protein content) in shoot tissue of 4-week-old control (WT, *ctr1-1*) and suppressor line (9–11, 12–9, 16–3 and 22–10) plants (*denotes statistically significant difference compared to WT, student's *t*-test, $P < 0.05$, $n = 4$). Error bars denote SD. **e** Diagram of the *Arabidopsis thaliana EIN2* gene structure: shaded bars denote exons, lines denote introns, unshaded bars denote untranslated regions. The grey region indicates the position of the EIN2 C-terminal (CEND) domain (Binder 2020), the red bar indicates the position of the predicted nuclear translocation sequence, and the black region the EIN2 N-terminus transmembrane domain (Binder 2020). Positions and nature of nucleotide substitution mutations in each of suppressor lines 9–11, 12–9, 16–3 and 22–10 are as indicated. Scale bar = 100 base pairs

this potential explanation we used a range of dwarf mutants (*min-1* is taller, whilst *cp3-1* and *dw1-1* are both shorter than *ctr1-1*; Fig. S1a; Fig. 2b). Nevertheless, all three of *min-1*, *cp3-1* and *dw1-1* exhibit a degree of ClO_3^- resistance not detectably different from that of WT (Supplemental Fig. S1b). We conclude that the ClO_3^- resistance conferred by *ctr1-1* is specifically due to constitutive ethylene signaling, rather than to a more generalized effect of dwarfism on ClO_3^- uptake or metabolism.

Whilst future analyses might benefit from mutant screens more directly assaying suppression of N-related (rather than plant height) phenotypes, our present initial observations

indicate that multiple independent loss-of-function mutations at *EIN2* confer increased ClO_3^--sensitivity on *ctr1-1*. These observations in turn suggest that lack of EIN2 function suppresses the effects of *ctr1-1* on NO_3^- metabolism, and that ethylene regulates plant N metabolism via the CTR1 and EIN2 ethylene signaling components. Being sessile organisms, plants need to respond to environmental variability by coordinating the regulation of growth and metabolism. Whilst ethylene signaling has long been known to coordinate growth in response to environmental stress, the involvement of this pathway in metabolic regulation has been less clear. Our results reveal that the ethylene signaling pathway enables regulatory coordination of plant growth, environmental response and N metabolism.

Author contribution statement FJ, ZJD and NPH conceived the project. FJ, ZJD and NPH designed the experiments. FJ, ZJ and ZJD performed the experiments. FJ, ZJ, EJB, SJZ, ZJD and NPH contributed to data analysis. FJ and NPH wrote the manuscript with input from all authors.

Supplementary Information The online version contains supplementary material available at https://doi.org/10.1007/s00425-022-03872-9.

Acknowledgements FJ was supported by the Biological and Biotechnological Sciences Research Council (BBSRC) Grant BB/M011224/1. This work was additionally supported by UK Biotechnology and Biotechnological Research Council Grants (BB/N013611/1 and BB/S013741/1) to EJB and NPH and Natural Science Foundation of Zhejiang Province Grant LY21C020001 to ZJD.

Declarations

Conflict of interest We declare that we have no financial and personal relationships with other people or organizations that can inappropriately influence our work; there is no professional or other personal interest of any nature or kind in any product, service and/or company that could be construed as influencing the position presented in, or the review of, the manuscript entitled.

References

Achard P, Baghour M, Chapple A, Hedden P, Van der Straeten D, Genschik P, Moritz T, Harberd NP (2007) The plant stress hormone ethylene controls floral transition via DELLA-dependent regulation of floral meristem-identity genes. Proc Natl Acad Sci USA 104:6484–6489. https://doi.org/10.1073/pnas.0610717104

Alonso JM, Hirayama T, Roman G, Nourizadeh S, Ecker JR (1999) EIN2, a bifunctional transducer of ethylene and stress responses in *Arabidopsis*. Science 284:2148–2152. https://doi.org/10.1126/science.284.5423.2148

Binder BM (2020) Ethylene signaling in plants. J Biol Chem 295:7710–7725

Chae HS, Faure F, Kieber JJ (2003) The *eto1*, *eto2*, and *eto3* mutations and cytokinin treatment increase ethylene biosynthesis in *Arabidopsis* by increasing the stability of ACS protein. Plant Cell 15:545–559. https://doi.org/10.1105/tpc.006882

Cove DJ (1976) Chlorate toxicity in *Aspergillus nidulans*: the selection and characterization of chlorate resistant mutants. Heredity 36:191–203. https://doi.org/10.1038/hdy.1976.24

Ho C-H, Lin S-H, Hu H-C, Tsay Y-F (2009) CHL1 functions as a nitrate sensor in plants. Cell 138:1184–1194. https://doi.org/10.1016/j.cell.2009.07.004

Khan NA, Mir MR, Nazar R, Singh S (2008) The application of ethephon (an ethylene releaser) increases growth, photosynthesis and nitrogen accumulation in mustard (*Brassica juncea* L.) under high nitrogen levels. Plant Biol 10:534–538. https://doi.org/10.1111/j.1438-8677.2008.00054.x

Kieber JJ, Rothenberg M, Roman G, Feldmann K, Ecker JR (1993) *CTR1*, a negative regulator of the ethylene response pathway in *Arabidopsis*, encodes a member of the Raf family of protein kinases. Cell 72:427–441. https://doi.org/10.1016/0092-8674(93)90119-b

Koornneef M, van Eden J, Hanhart CJ, Stam P, Braaksma FJ, Fenstra WJ (1983) Linkage map of *Arabidopsis thaliana*. J Hered 74:265–272. https://doi.org/10.1093/oxfordjournals.jhered.a109781

Lillo C (2008) Signalling cascades integrating light-enhanced nitrate metabolism. Biochem J 415:11–19. https://doi.org/10.1042/BJ20081115

Miller AJ, Cramer MD (2005) Root nitrogen acquisition and assimilation. Plant Soil 274:1–36. https://doi.org/10.1007/s11104-004-0965-1

Murphy TM, Imbrie CW (1981) Induction and characterization of chlorate-resistant strains of *Rosa damascena* cultured cells. Plant Physiol 67:910–916. https://doi.org/10.1104/pp.67.5.910

Quinn MH, Oliverio K, Yanovsky MJ, Casal JJ (2002) CP3 is involved in negative regulation of phytochrome A signalling in *Arabidopsis*. Planta 215:557–564. https://doi.org/10.1007/s00425-002-0784-7

Smith AM, Coupland G, Dolan L, Harberd N, Jones J, Martin C, Sablowski R, Amey A (2010) Plant biology. Garland Science, New York

Tian QY, Sun P, Zhang WH (2009) Ethylene is involved in nitrate-dependent root growth and branching in *Arabidopsis thaliana*. New Phytol 184:918–931. https://doi.org/10.1111/j.1469-8137.2009.03004.x

Wang KLC, Yoshida H, Lurin C, Ecker JR (2004) Regulation of ethylene gas biosynthesis by the *Arabidopsis* ETO1 protein. Nature 428:945–950. https://doi.org/10.1038/nature02516

Wang Y-Y, Hsu P-K, Tsay Y-F (2012) Uptake, allocation and signaling of nitrate. Trends Plant Sci 17:458–467. https://doi.org/10.1016/j.tplants.2012.04.006

Youn JH, Kim TW, Joo SH, Son SH, Roh J, Kim S, Kim TW, Kim SK (2018) Function and molecular regulation of DWARF1 as a C-24 reductase in brassinosteroid biosynthesis in *Arabidopsis*. J Exp Bot 69:1873–1886. https://doi.org/10.1093/jxb/ery038

Yu X, Sukumaran S, Marton L (1998) Differential expression of the Arabidopsis *Nia1* and *Nia2* genes: cytokinin-induced nitrate reductase activity is correlated with increased *Nia1* transcription and mRNA levels. Plant Physiol 116:1091–1096. https://doi.org/10.1104/pp.116.3.1091

Publisher's Note Springer Nature remains neutral with regard to jurisdictional claims in published maps and institutional affiliations.

References

Abel, S., Ticconi, C. A., & Delatorre, C. A. (2002) Phosphate sensing in higher plants. *Physiologia plantarum*, 115(1), 1–8.

Åberg, B. (1947) On the mechanism of the toxic action of chlorate and some related substances upon young wheat plants. *Kungl Lautbrukshogskolans Ann*, 15, 37–107.

ACCC (Australian Competition and Consumer Commission) (2008) ACCC Examination of Fertiliser Prices. Australian Competitor and Consumer Commission. GPO Box 3131, Canberra ACT 2601.

Achard, P., Baghour, M., Chapple, A., Hedden, P., Straeten, D. Van Der, Genschik, P., Moritz, T. and Harberd, N.P. (2007) The plant stress hormone ethylene controls floral transition via DELLA-dependent regulation of floral meristem-identity genes. *Proc. Natl. Acad. Sci. U. S. A.*, 104, 6484–6489.

Al-Sady, B., Ni, W., Kircher, S., Schäfer, E., & Quail, P. H. (2006) Photoactivated phytochrome induces rapid PIF3 phosphorylation prior to proteasome-mediated degradation. *Molecular cell*, 23(3), 439–446.

Andersson, M. X., Stridh, M. H., Larsson, K. E., Liljenberg, C., & Sandelius, A. S. (2003) Phosphate-deficient oat replaces a major portion of the plasma membrane phospholipids with the galactolipid digalactosyldiacylglycerol. *FEBS letters*, 537(1-3), 128–132.

Baker, A., Ceasar, S.A., Palmer, A.J., Paterson, J.B., Qi, W., Muench, S.P. and Baldwin, S.A. (2015) Replace, reuse, recycle: Improving the sustainable use of phosphorus by plants. *J. Exp. Bot.*, 66, 3523–3540.

Bari, R., Pant, B.D., Stitt, M. and Scheible, W.-R.R. (2006) PHO2, MicroRNA399, and PHR1 Define a Phosphate-Signaling Pathway in Plants. *Plant Physiol.*, 141, 988–999.

Bayle, V., Arrighi, J.-F., Creff, A., Nespoulous, C., Vialaret, J., Rossignol, M., Gonzalez, E., Paz-Ares, J. and Nussaume, L. (2011) Arabidopsis thaliana high-affinity phosphate transporters exhibit multiple levels of posttranslational regulation. *Plant Cell*, 23, 1523–35.

Bieleski, R. (1973) Phosphate Pools, Phosphate Transport, and Phosphate Availability. *Annual Review of Plant Physiology*, 24, 225-252.

Binder, B.M., Chang, C. and Eric Schaller, G. (2012) Perception of Ethylene by Plants - Ethylene Receptors. *The Plant Hormone Ethylene*. Wiley-Blackwell, pp. 117–145.

Binder, B.M., Mortimore, L.A., Stepanova, A.N., Ecker, J.R. and Bleecker, A.B. (2004) Short-term growth responses to ethylene in Arabidopsis seedlings are EIN3/EIL1 independent. *Plant Physiol.*, **136**, 2921–2927.

Bleecker, A. B., & Kende, H. (2000) Ethylene: a gaseous signal molecule in plants. *Annual review of cell and developmental biology*, 16, 1–18.

Braaksma, F.J., Feenstra, W.J. (1982) Isolation and characterization of nitrate reductase-deficient mutants of *Arabidopsis thaliana* . *Theoret. Appl. Genetics,* 64, 83–90.

Brenner, W.G., Romanov, G.A., Köllmer, I., Bürkle, L. and Schmülling, T. (2005) Immediate-early and delayed cytokinin response genes of Arabidopsis thaliana identified by genome-wide expression profiling reveal novel cytokinin-sensitive processes and suggest cytokinin action through transcriptional cascades. *Plant J.*, 44, 314–33.

Bridgeman, T.B., Chaffin, J.D. and Filbrun, J.E. (2013) A novel method for tracking western Lake Erie Microcystis blooms, 2002-2011. *J. Great Lakes Res.,* 39*,* 83-89.

Britto D.T., Kronzucker H.J. (2002) NH_4^+ toxicity in higher plants: a critical review. *Journal of Plant Physiology,* 159, 567–584.

Brodie, J.E., Devlin, M., Haynes, D. and Waterhouse, J. (2011) Assessment of the eutrophication status of the Great Barrier Reef lagoon (Australia). *Biogeochemistry*., 106, 281-302

Campbell, W.H. (1999) NITRATE REDUCTASE STRUCTURE, FUNCTION AND REGULATION: Bridging the Gap between Biochemistry and Physiology. *Annu. Rev. Plant Biol.,* 50, 277-303.

Castaings, L., Camargo, A., Pocholle, D., *et al.* (2009) The nodule inception-like protein 7 modulates nitrate sensing and metabolism in Arabidopsis. *Plant J.*, 57, 426–435.

Catarecha, P., Segura, M.D., Franco-Zorrilla, J.M., Garcia-Ponce, B., Lanza, M., Solano, R., Paz-Ares, J. and Leyva, A. (2007) A Mutant of the Arabidopsis Phosphate Transporter PHT1;1 Displays Enhanced Arsenic Accumulation. *Plant Cell*., 19, 1123–1133.

Chae, H.S., Faure, F. and Kieber, J.J. (2003) The *eto1*, *eto2*, and *eto3* mutations and cytokinin treatment increase ethylene biosynthesis in Arabidopsis by increasing the stability of ACS protein. *Plant Cell*, 15, 545–559.

Chang, C. and Stadler, R. (2001) Ethylene hormone receptor action in Arabidopsis. *BioEssays*, 23, 619–627.

Chang, K.N., Zhong, S., Weirauch, M.T., *et al.* (2013) Temporal transcriptional response to ethylene gas drives growth hormone cross-regulation in Arabidopsis. *Elife* , 2, e00675.

Chen, L.Q., Qu, X.Q., Hou, B.H., Sosso, D., Osorio, S., Fernie, A.R. and Frommer, W.B. (2012) Sucrose efflux mediated by SWEET proteins as a key step for phloem transport. Science., 335, 207–211.

Chen, X., Yao, Q., Gao, X., Jiang, C., Harberd, N.P. and Fu, X. (2016) Shoot-to-Root Mobile Transcription Factor HY5 Coordinates Plant Carbon and Nitrogen Acquisition. *Curr. Biol.*, 26, 640–646.

Chen, Y.F., Shakeel, S.N., Bowers, J., Zhao, X.C., Etheridge, N. and Schaller, G.E. (2007) Ligand-induced degradation of the ethylene receptor ETR2 through a proteasome-dependent pathway in Arabidopsis. *J. Biol. Chem*., 282, 24752–24758.

Chen, Y.-F., Wang, Y. and Wu, W.-H. (2008) Membrane Transporters for Nitrogen, Phosphate and Potassium Uptake in Plants. *J. Integr. Plant Biol*., 50, 835–848.

Cheng, C.L., Acedo, G.N., Cristinsin, M. and Conkling, M.A. (1992) Sucrose mimics the light induction of Arabidopsis nitrate reductase gene transcription. *Proc. Natl. Acad. Sci. U. S. A*., 89, 1861–1864.

Cooper, J., Lombardi, R., Boardman, D. and Carliell-Marquet, C. (2011) The future distribution and production of global phosphate rock reserves. *Resour. Conserv. Recycl*., 57, 7.

Cordell, D., Drangert, J.-O. and White, S. (2009) The story of phosphorus: Global food security and food for thought. *Glob. Environ. Chang*., 19, 292–305.

Cove, D. (1976) Chlorate toxicity in *Aspergillus nidulans*: The selection and characterisation of chlorate resistant mutants. *Heredity,* 36, 191–203.

Crawford, N.M. and Forde, B.G. (2002) Molecular and Developmental Biology of Inorganic Nitrogen Nutrition. *Arabidopsis book*., 1, e0011.

Dong, C.-H., Jang, M., Scharein, B., Malach, A., Rivarola, M., Liesch, J., Groth, G., Hwang, I. and Chang, C. (2010) Molecular Association of the Arabidopsis ETR1 Ethylene Receptor and a Regulator of Ethylene Signaling, RTE1. *J Biol Chem*. 285, 40706-40713

Duff, S. M., Plaxton, W. C., & Lefebvre, D. D. (1991) Phosphate-starvation response in plant cells: de novo synthesis and degradation of acid phosphatases. *Proceedings of the National Academy of Sciences of the United States of America*, 88(21), 9538–9542.

Duff, S.M.G., Sarath, G. and Plaxton, W.C. (1994) The role of acid phosphatases in plant phosphorus metabolism. *Physiol. Plant*., 90, 791–800.

Erisman, J.W., Sutton, M.A., Galloway, J., Klimont, Z. and Winiwarter, W. (2008) How a century of ammonia synthesis changed the world. *Nature Geosci.,* 1**,** 636–639

Essigmann, B., Güler, S., Narang, R. A., Linke, D., & Benning, C. (1998) Phosphate availability affects the thylakoid lipid composition and the expression of SQD1, a gene required for sulfolipid biosynthesis in Arabidopsis thaliana. *Proceedings of the National Academy of Sciences of the United States of America*, 95(4), 1950–1955.

FAO (1996) Rome Declaration on World Food Security and World Food Summit Plan of Action. World Food Summit 13-17 November 1996. Rome, Italy

FAO (2008) The State of Food Insecurity in the World 2008: High Food Prices and Food Security-threats and Opportunities. Food and Agricultural Organizations of the United Nations, Rome, Italy.

FAO (2011) Lessons from the world food crisis of 2006–08. Food and Agricultural Organizations of the United Nations, Rome, Italy.

FAO (2015) World Fertilizer Trends and Outlook to 2018. Food and Agricultural Organizations of the United Nations, Rome, Italy.

Forde, B.G. (2000) Nitrate transporters in plants: structure, function and regulation. *Biochim. Biophys. Act.* 1465, 219–235.

Gamble, R.L., Qu, X. and Schaller, G.E. (2002) Mutational analysis of the ethylene receptor ETR1. Role of the histidine kinase domain in dominant ethylene insensitivity. *Plant Physiol*., 128, 1428–1438.

Gao, Z., Chen, Y.-F., Randlett, M.D., Zhao, X.-C., Findell, J.L., Kieber, J.J. and Schaller, G.E. (2003) Localization of the Raf-like Kinase CTR1 to the Endoplasmic Reticulum of Arabidopsis through Participation in Ethylene Receptor Signaling Complexes. *J Biol Chem*., 278**,** 34725-34732.

Gniazdowska, A. and Rychter, A.M. (2000) Nitrate uptake by bean (Phaseolus vulgaris L.) roots under phosphate deficiency. *Plant and Soil*, 226, 79–85.

Godfray, H.C.J., Beddington, J.R., Crute, I.R., *et al.* (2010) Food security: the challenge of feeding 9 billion people. Science, 327, 812–818.

González, E., Solano, R., Rubio, V., Leyva, A. and Paz-Ares, J. (2005) PHOSPHATE TRANSPORTER TRAFFIC FACILITATOR1 is a plant-specific SEC12-related protein that enables the endoplasmic reticulum exit of a high-affinity phosphate transporter in Arabidopsis. *Plant Cell*, 17, 3500–3512.

Gruber, B.D., Giehl, R.F., Friedel, S. and von Wirén, N. (2013) Plasticity of the Arabidopsis root system under nutrient deficiencies. *Plant Physiol,* 163(1), 161-79.

Guo, H. and Ecker, J.R. (2003) Plant responses to ethylene gas are mediated by SCFEBF1/EBF2- dependent proteolysis of EIN3 transcription factor. *Cell*, 115, 667–677.

Ha, S. and Tran, L.-S. (2014) Understanding plant responses to phosphorus starvation for improvement of plant tolerance to phosphorus deficiency by biotechnological approaches. *Crit. Rev. Biotechnol.*, 34, 16–30.

Hermans, C., Hammond, J.P., White, P.J. and Verbruggen, N. (2006) How do plants respond to nutrient shortage by biomass allocation? *Trends Plant Sci.*, 11, 610–617.

Hinsinger, P. (2001) Bioavailability of soil inorganic P in the rhizosphere as affected by root-induced chemical changes: a review. *Plant and Soil* 237, 173–195

Ho, C.-H., Lin, S.-H., Hu, H.-C. and Tsay, Y.-F. (2009) CHL1 Functions as a Nitrate Sensor in Plants. *Cell*, 138, 1184–1194.

Hornitschek, P., Lorrain, S., Zoete, V., Michielin, O. and Fankhauser, C. (2009) Inhibition of the shade avoidance response by formation of non-DNA binding bHLH heterodimers. *EMBO J.*, 28, 3893–3902.

Hsieh, L.C., Lin, S.I., Shih, A.C.C., Chen, J.W., Lin, W.Y., Tseng, C.Y., Li, W.H. and Chiou, T.J. (2009) Uncovering small RNA-mediated responses to phosphate deficiency in Arabidopsis by deep sequencing. *Plant Physiol.*, 151, 2120–2132.

Huang, X., Ouyang, X., Yang, P., Lau, O.S., Li, G., Li, J., Chen, H. and Deng, X.W. (2012) Arabidopsis FHY3 and HY5 positively mediate induction of COP1 transcription in response to photomorphogenic UV-B light. *Plant Cell*, 24, 4590–4607.

Huber, S.C., MacKintosh, C. and Kaiser, W.M. (2002) Metabolic enzymes as targets for 14-3-3 proteins. *Plant Mol. Biol.*, **50**, 1053–1063.

Jamieson, F., Ji, Z., Belfield, E. J., Ding, Z. J., Zheng, S. J., & Harberd, N. P. (2022). Ethylene signaling modulates Arabidopsis thaliana nitrate metabolism. *Planta*, 255(5), 94.

Janes, G., von Wangenheim, D., Cowling, S., Kerr, I., Band, L., French, A. P., & Bishopp, A. (2018). Cellular Patterning of *Arabidopsis* Roots Under Low Phosphate Conditions. *Frontiers in plant science*, *9*, 735.

Jeong, S.W., Das, P.K., Jeoung, S.C., *et al.* (2010) Ethylene suppression of sugar-induced anthocyanin pigmentation in arabidopsis. *Plant Physiol.*, 154, 1514–1531.

Ji, Y. and Guo, H. (2013) From endoplasmic reticulum (ER) to nucleus: EIN2 bridges the gap in ethylene signaling. *Mol. Plant*, 6, 11–14.

Jiang, C., Gao, X., Liao, L., Harberd, N.P. and Fu, X. (2007) Phosphate Starvation Root Architecture and Anthocyanin Accumulation Responses Are Modulated by the Gibberellin-DELLA Signaling Pathway in Arabidopsis. *Plant Physiol.*, 145, 1460–1470.

Jonassen, E.M., Lea, U.S. and Lillo, C. (2008) HY5 and HYH are positive regulators of nitrate reductase in seedlings and rosette stage plants. *Planta*, **227**, 559–564.

Jonassen, E.M., Sévin, D.C. and Lillo, C. (2009) The bZIP transcription factors HY5 and HYH are positive regulators of the main nitrate reductase gene in Arabidopsis leaves, NIA2, but negative regulators of the nitrate uptake gene NRT1.1. *J. Plant Physiol.*, 166, 2071–6.

Jones, R.W. and Sheard, R.W. (1972) Nitrate reductase activity: Phytochrome mediation of induction in etiolated peas. *Nat. New Biol.*, 238, 221–222.

Ju, C., Poel, B. Van De, Cooper, E.D., Thierer, J.H., Gibbons, T.R., Delwiche, C.F. and Chang, C. (2015) Conservation of ethylene as a plant hormone over 450 million years of evolution. *Nat. Plants*, 1, 14004.

Ju, C., Yoon, G.M., Shemansky, J.M., *et al.* (2012) CTR1 phosphorylates the central regulator EIN2 to control ethylene hormone signaling from the ER membrane to the nucleus in Arabidopsis. *Proc. Natl. Acad. Sci. U. S. A.*, 109, 19486–19491.

Kaiser, W.M. and Huber, S.C. (2001) Post-translational regulation of nitrate reductase: Mechanism, physiological relevance and environmental triggers. *J. Exp. Bot*., 52, 1981-1989.

Kant, S., Peng, M. and Rothstein, S.J. (2011) Genetic Regulation by NLA and MicroRNA827 for Maintaining Nitrate-Dependent Phosphate Homeostasis in Arabidopsis. *PLoS Genet.*, 7, e1002021.

Karthikeyan, A.S., Varadarajan, D.K., Jain, A., Held, M.A., Carpita, N.C. and Raghothama, K.G. (2007) Phosphate starvation responses are mediated by sugar signaling in Arabidopsis. *Planta*, 225, 907–918.

Khan, N.A., Mir, M.R., Nazar, R. and Singh, S. (2008) The application of ethephon (an ethylene releaser) increases growth, photosynthesis and nitrogen accumulation in mustard (Brassica juncea L.) under high nitrogen levels. *Plant Biol.*, 10, 534–538.

Khanna, R., Huq, E., Kikis, E. A., Al-Sady, B., Lanzatella, C., & Quail, P. H. (2004) A novel molecular recognition motif necessary for targeting photoactivated phytochrome signaling to specific basic helix-loop-helix transcription factors. *The Plant cell*, 16(11), 3033–3044.

Kiba, T., Feria-Bourrellier, A.B., Lafouge, F., *et al.* (2012) The Arabidopsis nitrate transporter NRT2.4 plays a double role in roots and shoots of nitrogen-starved plants. *Plant Cell*, 24, 245–258.

Kim, H., Helmbrecht, E.E., Stalans, M.B., Schmitt, C., Patel, N., Wen, C.-K., Wang, W. and Binder, B.M. (2011) Ethylene Receptor ETHYLENE RECEPTOR1 Domain Requirements for Ethylene Responses in Arabidopsis Seedlings. *Plant Physiol*., 156, 417-429.

Kim, J., Yi, H., Choi, Goh, Shin, B., Song, P.S. and Choi, Giltsu (2003) Functional Characterization of Phytochrome Interacting Factor 3 in Phytochrome-Mediated Light Signal Transduction. *Plant Cell*, 15, 2399–2407.

Kircher, S. and Schopfer, P. (2012) Photosynthetic sucrose acts as cotyledon-derived long-distance signal to control root growth during early seedling development in Arabidopsis. *Proc. Natl. Acad. Sci. U. S. A.*, 109, 11217–21.

Konishi, M. and Yanagisawa, S. (2008) Ethylene signaling in Arabidopsis involves feedback regulation via the elaborate control of EBF2 expression by EIN3. *Plant J.*, 55, 821–831.

Konishi, M. and Yanagisawa, S. (2013) Arabidopsis NIN-like transcription factors have a central role in nitrate signalling. *Nat. Commun.*, 4, 1617.

Krapp, A., Berthomé, R., Orsel, M., *et al.* (2011) Arabidopsis roots and shoots show distinct temporal adaptation patterns toward nitrogen starvation. *Plant Physiol.*, 157, 1255–1282.

Krapp, A., David, L.C., Chardin, C., *et al.* (2014) Nitrate transport and signalling in Arabidopsis. *J. Exp. Bot.*, 65, 789–798.

Kronzucker, H., Siddiqi, M. & Glass, A. (1997). Conifer root discrimination against soil nitrate and the ecology of forest succession. *Nature*, 385, 59–61.

Krouk, G., Crawford, N.M., Coruzzi, G.M. and Tsay, Y.F. (2010) Nitrate signaling: Adaptation to fluctuating environments. *Curr. Opin. Plant Biol.*, 13, 265–272.

Labrie, S. T., Wilkinson, J. Q., & Crawford, N. M. (1991). Effect of Chlorate Treatment on Nitrate Reductase and Nitrite Reductase Gene Expression in Arabidopsis thaliana. *Plant physiology*, 97(3), 873–879.

Lambeck, I., Chi, J.C., Krizowski, S., Mueller, S., Mehlmer, N., Teige, M., Fischer, K. and Schwarz, G. (2010) Kinetic analysis of 14-3-3-inhibited arabidopsis thaliana nitrate reductase. *Biochemistry*, 49, 8177–8186.

Lark, R.M., Milne, A.E., Addiscott, T.M., Goulding, K.W.T., Webster, C.P. and O'Flaherty, S. (2004) Scale- and location-dependent correlation of nitrous oxide emissions with soil properties: An analysis using wavelets. *Eur. J. Soil Sci.*, 55, 611–627.

Lea, U.S., Leydecker, M.T., Quilleré, I., Meyer, C. and Lillo, C. (2006) Posttranslational regulation of nitrate reductase strongly affects the levels of free amino acids and nitrate, whereas transcriptional regulation has only minor influence. *Plant Physiol.*, 140, 1085–1094.

Lee, B.-R., Koprivova, A. and Kopriva, S. (2011) The key enzyme of sulfate assimilation, adenosine 5'-phosphosulfate reductase, is regulated by HY5 in Arabidopsis. *Plant J.*, 67, 1042–54.

Lee, J., He, K., Stolc, V., *et al.* (2007) Analysis of transcription factor HY5 genomic binding sites revealed its hierarchical role in light regulation of development. *Plant Cell*, 19, 731–749.

Lee, R.B. (1982) Selectivity and Kinetics of Ion Uptake by Barley Plants Following Nutrient Deficiency. *Ann. Bot.*, 50, 429–449.

Lei, M., Liu, Y., Zhang, B., Zhao, Y., Wang, X., Zhou, Y., Raghothama, K.G. and Liu, D. (2011) Genetic and genomic evidence that sucrose is a global regulator of plant responses to phosphate starvation in arabidopsis. *Plant Physiol.*, 156, 1116–1130.

Lei, M., Zhu, C., Liu, Y., Karthikeyan, A.S., Bressan, R.A., Raghothama, K.G. and Liu, D. (2011) Ethylene signalling is involved in regulation of phosphate starvation-induced gene expression and production of acid phosphatases and anthocyanin in Arabidopsis. *New Phytol.*, 189, 1084–1095.

Leivar, P., & Quail, P. H. (2011) PIFs: pivotal components in a cellular signaling hub. *Trends in plant science*, 16(1), 19–28.

Lejay, L., Gansel, X., Cerezo, M., Tillard, P., Müller, C., Krapp, A., Wirén, N. von, Daniel-Vedele, F. and Gojon, A. (2003) Regulation of Root Ion Transporters by Photosynthesis: Functional Importance and Relation with Hexokinase. *Plant Cell*. 15, 2218-2232.

Lejay, L., Wirth, J., Pervent, M., Cross, J.M.-F., Tillard, P. and Gojon, A. (2008) Oxidative Pentose Phosphate Pathway-Dependent Sugar Sensing as a Mechanism for Regulation of Root Ion Transporters by Photosynthesis. *Plant Physiol.,* 146, 2036-2053.

Lemaître, T., Gaufichon, L., Boutet-Mercey, S., Christ, A., and Masclaux-Daubresse, C. (2008) Enzymatic and metabolic diagnostic of nitrogen deficiency in *Arabidopsis thaliana Wassileskija* accession. *Plant Cell Physiol.* 49, 1056–1065.

Li, J.Y., Fu, Y.L., Pike, S.M., *et al.* (2010) The Arabidopsis nitrate transporter NRT1.8 functions in nitrate removal

from the xylem sap and mediates cadmium tolerance. *Plant Cell*, 22, 1633–1646.

Li, W., Ma, M., Feng, Y., Li, H., Wang, Y., Ma, Y., Li, M., An, F. and Guo, H. (2015) EIN2-directed translational regulation of ethylene signaling in Arabidopsis. *Cell*, 163, 670–83.

Lin, C. (2000) Plant blue-light receptors. *Trends Plant Sci.*, 5, 337–342.

Lin, S.I., Chiang, S.F., Lin, W.Y., Chen, J.W., Tseng, C.Y., Wu, P.C. and Chiou, T.J. (2008) Regulatory network of microRNA399 and PHO2 by systemic signaling. *Plant Physiol.*, 147, 732–746.

Lin, W.-Y., Huang, T.-K. and Chiou, T.-J. (2013) Nitrogen limitation adaptation, a target of microRNA827, mediates degradation of plasma membrane-localized phosphate transporters to maintain phosphate homeostasis in Arabidopsis. *Plant Cell*, 25, 4061–74.

Liu, J.Q., Allan, D.L. and Vance, C.P. (2010) Systemic signaling and local sensing of phosphate in common bean: Cross-talk between photosynthate and microRNA399. *Mol. Plant*, 3, 428–437.

Liu, K.H., Niu, Y., Konishi, M., *et al.* (2017) Discovery of nitrate-CPK-NLP signalling in central nutrient-growth networks. *Nature*, 545, 311–316.

Liu, T.-Y., Lin, W.-Y., Huang, T.-K. and Chiou, T.-J. (2014) MicroRNA-mediated surveillance of phosphate transporters on the move. *Trends Plant Sci.*, 19, 647–655.

Liu, Y., Xie, Y., Wang, H., Ma, X., Yao, W., & Wang, H. (2017) Light and Ethylene Coordinately Regulate the Phosphate Starvation Response through Transcriptional Regulation of *PHOSPHATE STARVATION RESPONSE1*. *The Plant cell*, 29(9), 2269–2284.

López-Arredondo, D. L., Leyva-González, M. A., González-Morales, S. I., López-Bucio, J., & Herrera-Estrella, L. (2014) Phosphate nutrition: improving low-phosphate tolerance in crops. *Annual review of plant biology*, *65*, 95–123.

López-Bucio, J., Cruz-Ramírez, A. and Herrera-Estrella, L. (2003) The role of nutrient availability in regulating root architecture. *Curr. Opin. Plant Biol*., 6, 280–287.

López-Bucio, J., Hernández-Abreu, E., Sánchez-Calderón, L., Nieto-Jacobo, M. F., Simpson, J., & Herrera-Estrella, L. (2002) Phosphate availability alters architecture and causes changes in hormone sensitivity in the Arabidopsis root system. *Plant Physiol.*, 129(1), 244–256.

Loudet, O., Chaillou, S., Merigout, P., Talbotec, J., and Daniel-Vedele, F. (2003) Quantitative trait loci analysis of nitrogen use efficiency in Arabidopsis. *Plant Physiol*., 1, 345–358.

Loth-Pereda, V., Orsini, E., Courty, P.E., *et al.* (2011) Structure and expression profile of the phosphate pht1 transporter gene family in mycorrhizal Populus trichocarpa1spi. *Plant Physiol.*, 156, 2141–2154.

Lu, J., Yang, R., Wang., H., Huang, X. (2017) Stress Effects of Chlorate on Longan (*Dimocarpus longan Lour.*) Trees: Changes in Nitrogen and Carbon Nutrition. *Horticultural Plant Journal*, 3(6), Pages 237 – 246.

Lucena, C., Waters, B.M., Romera, F.J., García, M.J., Morales, M., Alcántara, E. and Pérez-Vicente, R. (2006) Ethylene could influence ferric reductase, iron transporter, and H +-ATPase gene expression by affecting FER (or FER-like) gene activity. *J. Exp. Bot.*, 57, 4145–4154.

Ma, Z., Baskin, T.I., Brown, K.M. and Lynch, J.P. (2003) Regulation of root elongation under phosphorus stress involves changes in ethylene responsiveness. *Plant Physiol.*, 131, 1381–1390.

Maeda, Y., Konishi, M., Kiba, T., Sakuraba, Y., Sawaki, N., Kurai, T., Ueda, Y., Sakakibara, H. and Yanagisawa, S. (2018) A NIGT1-centred transcriptional cascade regulates nitrate signalling and incorporates phosphorus starvation signals in Arabidopsis. *Nat. Commun.*, 9, 1376.

Magalhães, J. V. De, Alves, V.M.C., Novais, R.F. De, Mosquim, P.R., Magalhães, J.R., Bahia Filho, A.F.C. and Huber, D.M. (1998) Nitrate uptake by corn under increasing periods of phosphorus starvation. *J. Plant Nutr.*, 21, 1753–1763.

Marchive, C., Roudier, F., Castaings, L., Bréhaut, V., Blondet, E., Colot, V., Meyer, C. and Krapp, A. (2013) Nuclear retention of the transcription factor NLP7 orchestrates the early response to nitrate in plants. *Nat. Commun.*, 4, 1713.

Marschner, H. (1995) Functions of Mineral Nutrients Micronutrients., Academic Press, San Diego, CA.

Mayerhofer, H., Panneerselvam, S. and Mueller-Dieckmann, J. (2012) Protein kinase domain of CTR1 from arabidopsis thaliana promotes ethylene receptor cross talk. *J. Mol. Biol.*, 415, 768–779.

McDaniel, B.K. and Binder, B.M. (2012) Ethylene receptor 1 (ETR1) is sufficient and has the predominant role in mediating inhibition of ethylene responses by silver in Arabidopsis thaliana. *J. Biol. Chem.*, 287, 26094–26103.

Medici, A., Marshall-Colon, A., Ronzier, E., *et al.* (2015) AtNIGT1/HRS1 integrates nitrate and phosphate signals at the Arabidopsis root tip. *Nat. Commun.*, 6, 6274.

Merchante, C., Alonso, J.M. and Stepanova, A.N. (2013) Ethylene signaling: Simple ligand, complex regulation. *Curr. Opin. Plant Biol.*, 16, 554–560.

Michalak, A.M., Anderson, E.J., Beletsky, D., *et al.* (2013) Record-setting algal bloom in Lake Erie caused by agricultural and meteorological trends consistent with expected future conditions. *Proc. Natl. Acad. Sci.* 110, 6448-6452

Mimura, T., Dietz, K. J., Kaiser, W., Schramm, M. J., Kaiser, G., & Heber, U. (1990) Phosphate transport across biomembranes and cytosolic phosphate homeostasis in barley leaves. *Planta*, 180(2), 139–146.

Minemakers Limited (2008) Rock Phosphate Price Rockets to Us$200/Tonne. Feasibility Planning Initiated on the Wonarah Project, Northern Territory. ASX and Press Release, January 09, 2008. Minemakers Limited (ABN 48116296541), Western Australia 6005.

Mudge, S.R., Rae, A.L., Diatloff, E. and Smith, F.W. (2002) Expression analysis suggests novel roles for members of the Pht1 family of phosphate transporters in Arabidopsis. *Plant J.*, 31, 341–353.

Muños, S., Cazettes, C., Fizames, C., Gaymard, F., Tillard, P., Lepetit, M., Lejay, L. and Gojon, A. (2004) Transcript profiling in the chl1-5 mutant of arabidopsis reveals a role of the nitrate transporter NRT1.1 in the regulation of another nitrate transporter, NRT2.1 W inside a box sign. *Plant Cell*, 16, 2433–2447.

Murashige, T. and Skoog, F. (1962) A Revised Medium for Rapid Growth and Bio Assays with Tobacco Tissue Cultures. Plant Physiology, 15**,** 473-497.

Murphy, T.M. and Imbrie, C.W. (1981) Induction and Characterization of Chlorate-resistant Strains of Rosa damascena Cultured Cells . *Plant Physiol.*, 67, 910–916.

Nguyen, G.N., Rothstein, S.J., Spangenberg, G. and Kant, S. (2015) Role of microRNAs involved in plant response to nitrogen and phosphorous limiting conditions. *Front. Plant Sci.*, 6, 629.

Nilsson, L., Lundmark, M., Jensen, P. E., & Nielsen, T. H. (2012). The Arabidopsis transcription factor PHR1 is essential for adaptation to high light and retaining functional photosynthesis during phosphate starvation. *Physiologia plantarum*, 144(1), 35–47.

Nussaume, L., Kanno, S., Javot, H., Marin, E., Nakanishi, T.M. and Thibaud, M.-C. (2011) Phosphate import in plants: focus on the PHT1 transporters. *Front. Plant Sci.*, 2, 83.

Oecking, C. and Jaspert, N. (2009) Plant 14-3-3 proteins catch up with their mammalian orthologs. *Curr. Opin. Plant Biol.*, 12, 760–765.

Osterlund, M.T., Hardtke, C.S., Ning, W. and Deng, X.W. (2000) Targeted destabilization of HY5 during light-regulated development of Arabidopsis. *Nature*, 405, 462–466.

Oyama, T., Shimura, Y., & Okada, K. (1997). The Arabidopsis HY5 gene encodes a bZIP protein that regulates stimulus-induced development of root and hypocotyl. *Genes & development*, 11(22**)**, 2983–2995.

Pant, B.D., Buhtz, A., Kehr, J. and Scheible, W.R. (2008) MicroRNA399 is a long-distance signal for the regulation of plant phosphate homeostasis. *Plant J.*, 53, 731–738.

Park, H.L., Seo, D.H., Lee, H.Y., Bakshi, A., Park, C., Chien, Y-C., Kieber, J., Binder, B and Yoon., G. (2023) Ethylene-triggered subcellular trafficking of CTR1 enhances the response to ethylene gas. *Nat Commun* 14, 365.

Park, B.S., Song, J.T. and Seo, H.S. (2011) Arabidopsis nitrate reductase activity is stimulated by the E3 SUMO ligase AtSIZ1. *Nat. Commun.*, 2, 400.

Peng, M., Bi, Y.-M., Zhu, T. and Rothstein, S.J. (2007) Genome-wide analysis of Arabidopsis responsive transcriptome to nitrogen limitation and its regulation by the ubiquitin ligase gene NLA. *Plant Mol. Biol.*, **65**, 775–797.

Penn, C.J., Camberato, J.J. (2019) A Critical Review on Soil Chemical Processes that Control How Soil pH Affects Phosphorus Availability to Plants. *Agriculture*, 9, 120.

Péret, B., Clément, M., Nussaume, L. and Desnos, T. (2011) Root developmental adaptation to phosphate starvation: better safe than sorry. *Trends Plant Sci.*, 16, 442–450.

Plaxton, W.C. and Tran, H.T. (2011) Metabolic adaptations of phosphate-starved plants. *Plant Physiol.*, 156, 1006–1015.

Pumplin, N. and Harrison, M.J. (2009) Live-cell imaging reveals periarbuscular membrane domains and organelle location in Medicago truncatula roots during arbuscular mycorrhizal symbiosis. *Plant Physiol.*, 151, 809–819.

Qiao, H., Chang, K.N., Yazaki, J. and Ecker, J.R. (2009) Interplay between ethylene, ETP1/ETP2 F-box proteins, and degradation of EIN2 triggers ethylene responses in Arabidopsis. *Genes Dev.*, 23, 512–521.

Qiao, H., Shen, Z., Huang, S.S.C., Schmitz, R.J., Urich, M.A., Briggs, S.P. and Ecker, J.R. (2012) Processing and subcellular trafficking of ER-tethered EIN2 control response to ethylene gas. *Science*, 338, 390–393.

Qiu, L., Xie, F., Yu, J. and Wen, C.K. (2012) Arabidopsis RTE1 is essential to ethylene receptor ETR1 amino-terminal signaling independent of CTR1. *Plant Physiol.*, 159, 1263–1276.

Raghothama K. G. (1999) PHOSPHATE ACQUISITION. *Annual review of plant physiology and plant molecular biology*, *50*, 665–693.

Reed, A.J., Canvin, D.T., Sherrard, J.H. and Hageman, R.H. (1983) Assimilation of [15N]Nitrate and [15N]Nitrite in Leaves of Five Plant Species under Light and Dark Conditions. *Plant Physiol.*, 71, 291.

Reisenauer H.M. (1966). Mineral nutrients in soil solution. In: ltman PL Ditter DS, *eds.Environmental biology*. Bethesda, MD: Federal American Society of Experimental Biology, 507–508.

Reymond, M., Svistoonoff, S., Loudet, O., Nussaume, L. and Desnos, T. (2006) Identification of QTL controlling root growth response to phosphate starvation in Arabidopsis thaliana. *Plant, Cell Environ.*, 29, 115–125.

Rizzini, L., Favory, J.J., Cloix, C., *et al.* (2011) Perception of UV-B by the arabidopsis UVR8 protein. *Science*, **332**, 103–106.

Rubio, V., Linhares, F., Solano, R., Martín, A.C., Iglesias, J., Leyva, A. and Paz-Ares, J. (2001) A conserved MYB transcription factor involved in phosphate starvation signaling both in vascular plants and in unicellular algae. *Genes Dev.*, 15, 2122–2133.

Rufty, T.W., MacKown, C.T. and Israel, D.W. (1990) Phosphorus stress effects on assimilation of nitrate. *Plant Physiol.*, 94, 328–333.

Saijo, Y., Sullivan, J. A., Wang, H., Yang, J., Shen, Y., Rubio, V., Ma, L., Hoecker, U., & Deng, X. W. (2003) The COP1-SPA1 interaction defines a critical step in phytochrome A-mediated regulation of HY5 activity. *Genes & development*, 17(21), 2642–2647.

Sakuraba, Y. and Yanagisawa, S. (2018) Light signalling-induced regulation of nutrient acquisition and utilisation in plants. *Semin. Cell Dev. Biol.*, **83**, 123–132.

Sakuraba, Y., Kanno, S., Mabuchi, A., Monda, K., Iba, K. and Yanagisawa, S. (2018) A phytochrome-B-mediated regulatory mechanism of phosphorus acquisition. *Nat. Plants*, 4, 1089–1101.

Sánchez-Calderón, L., López-Bucio, J., Chacón-López, A., Cruz-Ramírez, A., Nieto-Jacobo, F., Dubrovsky, J. G., & Herrera-Estrella, L. (2005). Phosphate starvation induces a determinate developmental program in the roots of Arabidopsis thaliana. *Plant & cell physiology*, 46(1), 174–184.

Sawaki, N., Tsujimoto, R., Shigyo, M., Konishi, M., Toki, S., Fujiwara, T. and Yanagisawa, S. (2013) A nitrate-inducible GARP family gene encodes an auto-repressible transcriptional repressor in rice. *Plant Cell Physiol.*, 54, 506–517.

Schachtman, D. P., Reid, R. J., & Ayling, S. M. (1998) Phosphorus Uptake by Plants: From Soil to Cell. *Plant physiology*, *116*(2), 447–453.

Schaller, G.E. and Bleecker, A.B. (1995) Ethylene-binding sites generated in yeast expressing the Arabidopsis ETR1 gene. *Science* 270, 1809-1811.

Scheible, W.R., Morcuende, R., Czechowski, T., *et al.* (2004) Genome-wide reprogramming of primary and secondary metabolism, protein synthesis, cellular growth processes, and the regulatory infrastructure of arabidopsis in response to nitrogen. *Plant Physiol.*, 136, 2483–2499.

Schindler, D.W., Hecky, R.E., Findlay, D.L., Stainton, M.P., Parker, B.R., Paterson, M.J., Beaty, K.G., Lyng, M. and Kasian, S.E.M. (2008) Eutrophication of lakes cannot be controlled by reducing nitrogen input: Results of a 37-year whole-ecosystem experiment. *Proc. Natl. Acad. Sci.*

Schlüter, U., Colmsee, C., Scholz, U., Bräutigam, A., Weber, A.P.M., Zellerhoff, N., Bucher, M., Fahnenstich, H. and Sonnewald, U. (2013) Adaptation of maize source leaf metabolism to stress related disturbances in carbon, nitrogen and phosphorus balance. *BMC Genomics*, 14.

Shane, M. W., McCully, M. E., & Lambers, H. (2004) Tissue and cellular phosphorus storage during development of phosphorus toxicity in Hakea prostrata (Proteaceae). *Journal of experimental botany*, 55(399), 1033–1044.

Shen, J., Yuan, L., Zhang, J., Li, H., Bai, Z., Chen, X., Zhang, W., & Zhang, F. (2011) Phosphorus dynamics: from soil to plant. *Plant physiology*, 156(3), 997–1005.

Shin, D.H., Choi, M., Kim, K., Bang, G., Cho, M., Choi, S.B., Choi, G. and Park, Y. Il (2013) HY5 regulates anthocyanin biosynthesis by inducing the transcriptional activation of the MYB75/PAP1 transcription factor in Arabidopsis. *FEBS Lett.*, 587, 1543–1547.

Shin, H., Shin, H.-S., Chen, R. and Harrison, M.J. (2006) Loss of At4 function impacts phosphate distribution between the roots and the shoots during phosphate starvation. *Plant J.*, **45**, 712–726.

Shin, H., Shin, H.-S., Dewbre, G.R. and Harrison, M.J. (2004) Phosphate transport in Arabidopsis : Pht1;1 and Pht1;4 play a major role in phosphate acquisition from both low- and high-phosphate environments. *Plant J.*, **39**, 629–642.

Shin, J., Park, E. and Choi, G. (2007) PIF3 regulates anthocyanin biosynthesis in an HY5-dependent manner with both factors directly binding anthocyanin biosynthetic gene promoters in Arabidopsis. *Plant J.*, 49, 981–994.

Shin, R. and Schachtman, D.P. (2004) Hydrogen peroxide mediates plant root cell response to nutrient deprivation. *Proc. Natl. Acad. Sci. U. S. A.*, 101, 8827–8832.

Shulman, Y., Cohen, S. and Loinger, C. (1985) Improved Maturation and Wine Quality of Carignane Grapes by Ethephon Treatments. *Am. J. Enol. Vitic.*, 36, 264-267.

Signora, L., Smet, I. De, Foyer, C.H. and Zhang, H. (2001) ABA plays a central role in mediating the regulatory effects of nitrate on root branching in Arabidopsis. *Plant J.*, 28, 655–62.

Smith, Barry E, Einsle, O., Smith, B. E., *et al.* (2002) Structure. Nitrogenase reveals its inner secrets. *Science*, 297, 1654–5.

Smithson, P. (1999) Special issue on phosphorus availability, uptake and cycling in tropical agroforestry, *Agroforestry Forum*, 9(4), 37–40.

Solano, R., Stepanova, A., Chao, Q. and Ecker, J.R. (1998) Nuclear events in ethylene signaling: A transcriptional cascade mediated by ETHYLENE-INSENSITIVE3 and ETHYLENE-RESPONSE-FACTOR1. *Genes Dev.*, 12, 3703–3714.

Solomonson, L. P., & Vennesland, B. (1972) Nitrate Reductase and Chlorate Toxicity in Chlorella vulgaris Beijerinck. *Plant physiology*, 50(4), 421–424.

Song, L. and Liu, D. (2015) Ethylene and plant responses to phosphate deficiency. *Front. Plant Sci.*, 6, 796.

Song, Y. H., Yoo, C. M., Hong, A. P., Kim, S. H., Jeong, H. J., Shin, S. Y., Kim, H. J., Yun, D. J., Lim, C. O., Bahk, J. D., Lee, S. Y., Nagao, R. T., Key, J. L., & Hong, J. C. (2008). DNA-binding study identifies C-box and hybrid C/G-box or C/A-box motifs as high-affinity binding sites for STF1 and LONG HYPOCOTYL5 proteins. *Plant*

physiology, 146(4), 1862–1877.

Steingröver E., Feenstra W.J. (1981) Resistance to low concentrations of chlorate on nitrate free medium. *Arabidopsis Inf Serv.*, 18, 143–145

Sun, L., Song, L., Zhang, Y., Zheng, Z., & Liu, D. (2016). Arabidopsis PHL2 and PHR1 Act Redundantly as the Key Components of the Central Regulatory System Controlling Transcriptional Responses to Phosphate Starvation. *Plant physiology*, 170(1), 499–514.

Sun, Y., Luo, W., Jain, A., *et al.* (2018) OsPHR3 affects the traits governing nitrogen homeostasis in rice. *BMC Plant Biol*., 18, 241.

Sutton, M.A., Oenema, O., Erisman, J.W., Leip, A., Grinsven, H. van and Winiwarter, W. (2011) Too much of a good thing. *Nature*, 472, 159–61.

Takei, K., Ueda, N., Aoki, K., Kuromori, T., Hirayama, T., Shinozaki, K., Yamaya, T. and Sakakibara, H. (2004) AtIPT3 is a key determinant of nitrate-dependent cytokinin biosynthesis in Arabidopsis. *Plant Cell Physiol.*, 45, 1053–1062.

Tian, Q.Y., Sun, P. and Zhang, W.H. (2009) Ethylene is involved in nitrate-dependent root growth and branching in Arabidopsis thaliana. *New Phytol.*, 184, 918–931.

Ticconi, C.A. and Abel, S. (2004) Short on phosphate: Plant surveillance and countermeasures. *Trends Plant Sci.*, 9, 548–555.

Tran, H.T., Hurley, B.A. and Plaxton, W.C. (2010) Feeding hungry plants: The role of purple acid phosphatases in phosphate nutrition. *Plant Sci.*, 179, 14–27.

Trull, M.C., Guiltinan, M.J., Lynch, J.P. and Deikman, J. (1997) The responses of wild-type and ABA mutant Arabidopsis thaliana plants to phosphorus starvation. *Plant, Cell Environ.*, 20, 85–92.

Tsay, Y.F., Schroeder, J.I., Feldmann, K.A. and Crawford, N.M. (1993) The herbicide sensitivity gene CHL1 of Arabidopsis encodes a nitrate-inducible nitrate transporter. *Cell*, 72, 705–13.

Veneklaas, E.J., Lambers, H., Bragg, J., *et al.* (2012) Opportunities for improving phosphorus-use efficiency in crop plants. *New Phytol.*, 195, 306–320.

Verly C, Djoman ACR, Rigault M, Giraud F, Rajjou L, Saint-Macary M-E and Dellagi A. (2020) Plant Defense Stimulator Mediated Defense Activation Is Affected by Nitrate Fertilization and Developmental Stage in *Arabidopsis thaliana*. *Front. Plant Sci.* 11, 583.

Vidal, J. (2008) Souring fertiliser prices threaten world's poorest farmers. Guardian, UK. Available at https://www.theguardian.com/environment/2008/aug/12/biofuels.food.

Vogel, J.P., Woeste, K.E., Theologis, A. and Kieber, J.J. (1998) Recessive and dominant mutations in the ethylene biosynthetic gene ACS5 of Arabidopsis confer cytokinin insensitivity and ethylene overproduction, respectively. *Proc. Natl. Acad. Sci.,* 95, 4766-4771.

Wagner, S. C. (2011) Biological Nitrogen Fixation. *Nature Education Knowledge,* 3(10), 15.

Walch-Liu, P. and Forde, B.G. (2008) Nitrate signalling mediated by the NRT1.1 nitrate transporter antagonises L-glutamate-induced changes in root architecture. *Plant J.*, 54, 820–828.

Walch-Liu, P., Neumann, G., Bangerth, F. and Engels, C. (2000) Rapid effects of nitrogen form on leaf morphogenesis in tobacco. *J. Exp. Bot.*, 51, 227–237.

Wang, K.L.C., Yoshida, H., Lurin, C. and Ecker, J.R. (2004) Regulation of ethylene gas biosynthesis by the Arabidopsis ETO1 protein. *Nature*, 428, 945–950.

Wang, L. and Liu, D. (2017) Analyses of Root-secreted Acid Phosphatase Activity in Arabidopsis. *BIO-PROTOCOL*, 7, e2202.

Wang, R., Liu, D. and Crawford, N.M. (1998) The Arabidopsis CHL1 protein plays a major role in high-affinity nitrate uptake. *Proc. Natl. Acad. Sci.*, 95, 15134-15139.

Wang, R., Tischner, R., Gutiérrez, R.A., Hoffman, M., Xing, X., Chen, M., Coruzzi, G. and Crawford, N.M. (2004) Genomic analysis of the nitrate response using a nitrate reductase-null mutant of arabidopsis. *Plant Physiol.*, 136, 2512–2522.

Wang, R., Xing, X., Wang, Y., Tran, A., & Crawford, N. M. (2009). A genetic screen for nitrate regulatory mutants captures the nitrate transporter gene NRT1.1. *Plant physiology,* 151(1), 472–478.

Wang, X., Feldmann, K.A. and Scholl, R.L. (1988), A chlorate-hypersensitive, high nitrate/chlorate uptake mutant of Arabidopsis thaliana. Physiologia Plantarum, 73, 305-310.

Wang, Y.Y. and Tsaya, Y.F. (2011) Arabidopsis nitrate transporter NRT1.9 is important in phloem nitrate transport. *Plant Cell*, 23, 1945–1957.

Wen, X., Zhang, C., Ji, Y., Zhao, Q., He, W., An, F., Jiang, L. and Guo, H. (2012) Activation of ethylene signaling is mediated by nuclear translocation of the cleaved EIN2 carboxyl terminus. *Cell Res.*, 22, 1613–1616.

White, P.J. and Brown, P.H. (2010) Plant nutrition for sustainable development and global health. *Ann. Bot.*, 105, 1073–1080.

Wilkinson, J.Q. and Crawford, N.M. (1991) Identification of the Arabidopsis CHL3 gene as the nitrate reductase structural gene NIA2. *Plant Cell*, 3, 461–471.

Wilkinson, J.Q., Crawford, N.M. (1993) Identification and characterization of a chlorate-resistant mutant of *Arabidopsis thaliana* with mutations in both nitrate reductase structural genes *NIA1* and *NIA2*. *Molec. Gen. Genet.* 239, 289–297

Wilkinson, K. A., & Henley, J. M. (2010) Mechanisms, regulation and consequences of protein SUMOylation. *The Biochemical journal*, *428*(2), 133–145.

Woeste, K.E., Ye, C. and Kieber, J.J. (1999) Two Arabidopsis mutants that overproduce ethylene are affected in the posttranscriptional regulation of 1-aminocyclopropane-1-carboxylic acid synthase. *Plant Physiol.*, 119, 521–529.

Wray J.L., Kinghorn J.R. (1989) Molecular and Genetic Aspects of Nitrate Assimilation. *Oxford Science Publications*, Oxford

Xu, H., Paerl, H.W., Qin, B., Zhu, G. and Gao, G. (2010) Nitrogen and phosphorus inputs control phytoplankton growth in eutrophic Lake Taihu, China. *Limnol. Oceanogr.*, 55, 420-432.

Xu, X., Paik, I., Zhu, L., Bu, Q., Huang, X., Deng, X.W. and Huq, E. (2014) PHYTOCHROME INTERACTING FACTOR1 enhances the E3 ligase activity of CONSTITUTIVE PHOTOMORPHOGENIC1 to synergistically repress

photomorphogenesis in Arabidopsis. *Plant Cell*, 26, 1992–2006.

Yanagisawa, S. (2014) Transcription factors involved in controlling the expression of nitrate reductase genes in higher plants. *Plant Sci.*, 229, 167–171.

Yeh, C-M., Kobayashi, K., Fujii, S., Fukaki, H., Mitsuda, N., and Ohme-Takagi, M. (2020) Blue Light Regulates Phosphate Deficiency-Dependent Primary Root Growth Inhibition in Arabidopsis. *Frontiers in plant science*, 10, 1803.

Yuan, H., & Liu, D. (2008) Signaling components involved in plant responses to phosphate starvation. *Journal of integrative plant biology*, 50(7), 849–859.

Zhang, H., He, H., Wang, Xuncheng, Wang, Xiangfeng, Yang, X., Li, L. and Deng, X.W. (2011a) Genome-wide mapping of the HY5-mediated genenetworks in Arabidopsis that involve both transcriptional and post-transcriptional regulation. *Plant J.*, 65, 346–358.

Zhang, Y., Zheng, S., Liu, Z., Wang, L. and Bi, Y. (2011b) Both HY5 and HYH are necessary regulators for low temperature-induced anthocyanin accumulation in Arabidopsis seedlings. *J. Plant Physiol.*, 168, 367–374.

Zhang, Z., Liao, H. and Lucas, W.J. (2014) Molecular mechanisms underlying phosphate sensing, signaling, and adaptation in plants. *J. Integr. Plant Biol.*, 56, 192–220.